Spectrochemical Study of Microscopic Crystals. X.[1] *The Absorption Spectra and Configuration of Bis(ethylenediamine)-copper(II) Complexes*

By Shoichiro YAMADA and Ryutaro TSUCHIDA

(Received October 13, 1955)

It is known that copper usually forms squareplanar complexes with ammonia and amines. Complexes of square-bipyramidal configuration, however, are also formed in some compounds involving water molecules of crystallization. For example, two molecules of water in the crystal of bis(ethylenediamine)-copper(II) nitrate dihydrate occupy positions comparatively close to the copper atom in the direction normal to the plane formed by one copper and four nitrogen atoms[2]. On the other hand, bis(ethylenediamine)-copper (II) perchlorate, which involves no water of crystallization, apparently has separate ions, $[Cu(en)_2]^{2+}$ [3], of planar configuration in the crystalline state. When molecules of ions approach the copper atom in the planar $[Cu(en)_2]$ group along the direction normal to the complex plane, the light absorption and its anisotropy usually undergo more or less distinct changes. Thus the measurement of the absorption spectra is expected to be of use to the elucidation of the problems on the configuration of the planar copper(II)-complexes. In the present paper polarized absorption spectra of bis(ethylenediamine)-copper(II) perchlorate, nitrate dihydrate, and tetrathiocyanato-mercurate have been determined in the crystalline state, and the above problems discussed using the results of the measurements.

Experimental

Materials.—Bis(ethylenediamine)-copper(II) perchlorate, $Cu(en)_2(ClO_4)_2$, was prepared in violet needles according to the method of Pfeiffer et al[4]. The crystal shows a striking dichroism on the prism face, that is, reddish purple and bluish purple. The measurement of polarized absorption spectra was made on the above face in the directions of extinction. The A- and B-absorption refer to the directions A and B as shown in the figure.

Bis(ethylenediamine)-copper(II) nitrate dihydrate, $Cu(en)_2(NO_3)_2 2H_2O$, was obtained in violet plates by the method of Grossmann et al[5]. The monoclinic crystals thus obtained show a marked dichroism on the well-developed (001)-face; it appears light purple with the electric vector along the b-axis and purplish blue with the electric vector along the a-axis. The dichroism measurement was made on the c-plane with polarized light vibrating along the a-axis and along the b-axis. The a- and b-absorption denote absorption with the electric vector along the a- and b-axis, respectively.

Bis(ethylenediamine)-copper(II) tetrathiocyanato-mercurate(II), $[Cu(en)_2][Hg(SCN)_4]$, was prepared in monoclinic plate-like crystals from aqueous solutions of $Cu(en)_2(NO_3)_2$ and of $K_2Hg(SCN)_4$. The crystals are deep purple, with the (010)-plane dominating. Dichroism is observed on the (010)[6]. The measurements of the absorption spectra were made on this plane with polarized light along α- and along β-direction of the crystal[7]. The a- and b-absorption refer to the absorption with the electric vector along the α- and β-direction, respectively.

Measurements.—Quantitative dichroism measurements of the crystals were made by Tsuchida-Kobayashi's microscopic method[8] with polarized light in the regions covering 7500 to 2400 Å. The notations used are the same as those in the previous papers of this series[1].

Results and Discussion

Dichroism of Bis(ethylenediamine)-copper (II) Perchlorate.—The results of the measurements are given in Fig. 1 and Table I. The crystal structure is unknown at present. But since the crystal has no water of crystallization, the perchlorate in the crystalline state involves the separate ions of $[Cu(en)_2]^{2+}$. Therefore, the absorption spectra obtained with this crystal are considered to represent the absorption of the separate planar complex ion, $[Cu(en)_2]^{2+}$, under rather small effect from external perchlorate ions. It is seen

1) Part IX of this series, S. Yamada and R. Tsuchida, This Bulletin, 28, 664 (1955).

2) T. Watanabe and M. Atoji, *Kagaku*, 21, 301 (1951) (in Japanese); read before the meeting of the Chemical Society of Japan, Osaka, May, 1950.

3) The notation, en, denotes a molecule of ethylenediamine.

4) P. Pfeiffer and H. Glaser, *J. Prakt. Chem.*, 151, 134 (1938).

5) H. Grossmann and B. Schück, *Z. anorg. allgem. Chem.*, 50, 1 (1906).

6) H. Scouloudi, *Nature*, 166, 357 (1950); *Acta Cryst.*, 6, 651 (1953).

7) The notations, α, β and γ, represent conventional symbols for optic elasticity axes of the crystal. The γ-direction corresponds with the b-axis. See ref. (6).

8) R. Tsuchida and M. Kobayashi, This Bulletin, 13, 619 (1938); "The Colours and the Structures of Metallic Compounds," Zoshindo, Osaka (1944), p. 180.

CHEMISTRY HALL LIBRARY

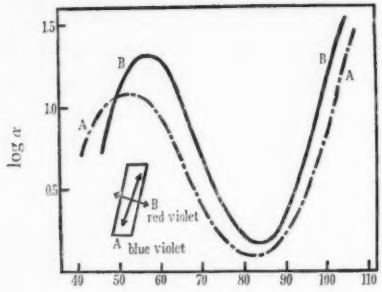

Frequency, ν, 10^{13}/sec.

Fig. 1. Absorption spectra of $[Cu(en)_2](ClO_4)_2$.

TABLE I

ABSORPTION MAXIMA OF BIS(ETHYLENEDIAMINE)-COPPER(II) PERCHLORATE IN THE CRYSTALLINE STATE

	ν, 10^{13}/sec.	log α	Half width
A-abs.	57.2	1.31	16.9
B-abs.	53.0	1.08	21.7

from the measurements that the crystal of the perchlorate shows absorption at about 50×10^{13}/sec. (band A) and at a wave-length shorter than 110×10^{13}/sec. (band B). The band at the longer wave-length is supposed to be due to the copper atom in combination with ligands. The absorption at the shorter wave-length may be considered as originating from the electron transfer between the copper atom and the ligand molecules, as will be discussed in the later part of this paper.

It was formerly established with planar complexes of copper(II)[9] that for the band A, absorption with the electric vector along the complex-plane, $\parallel$-absorption, has a larger absorption coefficient than $\perp$-absorption, absorption with the electric vector normal to the above. Therefore, it may be reasonable to suppose that the A- and B-absorption represent characteristics of the $\parallel$-absorption and those of the $\perp$-absorption, respectively. Thus the following relation on the dichroism may be derived. For the band A, the $\parallel$-absorption shows its maximum at a shorter wave-length than the $\perp$-absorption, and the absorption is much stronger with the $\parallel$-absorption than with the $\perp$-absorption. For the band B, the $\parallel$-absorption is bathochromic to the $\perp$-absorption.

Dichroism of Bis(ethylenediamine)-copper (II) Nitrate Dihydrate.—The results of the measurements are shown in Fig. 2 and Table II. According to the X-ray study of crystal

9) R. Tsuchida and S. Yamada, Read before the sixth annual meeting of the Chemical Society of Japan, Kyoto, April, 1953.

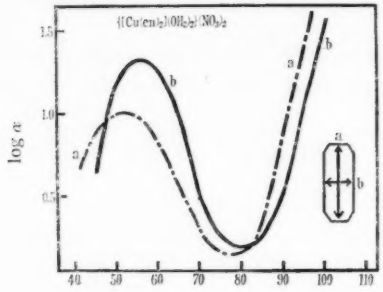

Frequency, ν, 10^{13}/sec.

Fig. 2. Absorption spectra of $\{[Cu(en)_2](OH_2)_2\}(NO_3)_2$.

TABLE II

ABSORPTION MAXIMA OF BIS(ETHYLENEDIAMINE)-COPPER(II) NITRATE DIHYDRATE IN THE CRYSTALLINE STATE

	ν, 10^{13}/sec.	log α	Half width
b-abs.	56.0	1.33	16.5
a-abs.	52.2	1.00	21.5

structure, the copper atom is bound with four nitrogen atoms of ethylenediamine molecules in planar configuration, with the neighbouring oxygen atoms of water molecules at a slightly greater distance in the direction normal to the plane formed by the copper and four nitrogen atoms. The planes of the complexes are inclined to the bc-plane at a small angle. Referring to absorption with the electric vector along the a-axis as a-absorption and absorption with the electric vector along the b-axis as b-absorption, then the crystal analysis indicates that the a-absorption corresponds roughly with the $\perp$-absorption of the planar complex ions and the b-absorption corresponds with the $\parallel$-absorption[2].

The crystals of bis(ethylenediamine)-copper (II) nitrate dihydrate exhibit in the region of the present measurement two bands at $50\text{–}60\times10^{13}$/sec. (band A), and at the wave-length shorter than 110×10^{13}/sec. (band B), both bands corresponding to the absorption bands of the perchlorate.

The band A of this crystal is seen to be slightly displaced bathochromically as compared with the crystal of the perchlorate. This seems to indicate that the complexes, in the crystal of the nitrate dihydrate undergo an effect from the two water molecules in the direction normal to the complex-plane.

From the present measurement are obtained the following relations on the dichroism of the complex ion. *For the band A, the $\parallel$-absorption has much greater intensity than the $\perp$-absorption, and the former is hypsochromic*

to the latter. The above rule about the intensity is the same as that formerly derived with other planar complexes of copper(II) as well as with the perchlorate[9]. For the absorption bands of planar complexes of platinum(II) and palladium(II) which are considered as due mainly to co-ordinate linkages, the ∥-absorption was found to have much greater oscillator strength than the ⊥-absorption[10]. The above relation with the cupric complexes seems to be in good agreement with the general rule for planar complexes of palladium(II) and platinum(II).

The second rule that the ∥-absorption is hypsochromic to the ⊥-absorption seems to indicate that the band A consists of two components having opposite polarization properties. This may be discussed later with reference to the absorption of the complex ion, $[Cu(en)_2]^{2+}$, in solution.

The present measurement also shows that, *for the band B, the ⊥-absorption is bathochromic to the ∥-absorption.* The fact that the nitrate dihydrate shows with the band A polarization property essentially similar to the perchlorate seems to indicate that the effect of the two water molecules on the band A is small and, at the same time, that the energy level associated with the band A is disturbed very little. On the contrary, their marked effect is observed with the absorption at the shorter wave-length. Thus the polarization property for the band B of the nitrate dihydrate is found to be reversed, as compared with the perchlorate. This reversal, which is ascribed to the effect of the two water molecules close to the copper atom, will be discussed in the later part of this paper.

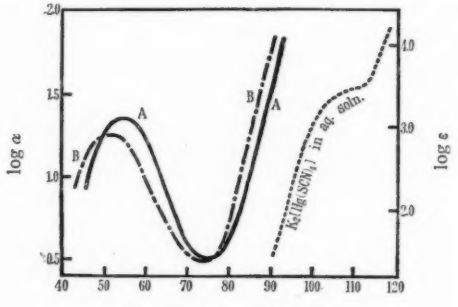

Frequency, ν, 10^{13}/sec.

Fig. 3. Absorption spectra of $[Cu(en)_2][Hg(SCN)_4]$. The spectrum of the solution (dotted curve) is taken from ref. 1.

10) S. Yamada, H. Yoneda and R. Tsuchida, *J. Chem. Soc. Japan*, **69**, 145 (1948); S. Yamada, *J. Am. Chem. Soc.*, **73**, 1182 (1951); S. Yamada and R. Tsuchida, This Bulletin, **26**, 489 (1953).

Bis(ethylenediamine)-copper(II) Tetrathiocyanato-mercurate(II).—The results of the present measurement are shown in Fig. 3 and Table III. According to the result of the

TABLE III

ABSORPTION MAXIMA OF BIS(ETHYLENEDIAMINE)-COPPER(II) TETRATHIOCYANATO-MERCURATE(II) IN THE CRYSTALLINE STATE

	ν, 10^{13}/sec.	log α	Half width
A-abs.	54.8	1.18	15.0
B-abs.	51.5	1.05	17.3

crystal analysis[5], it is seen that the B-absorption involves more ⊥-absorption of the $[Cu(en)_2]^{2+}$-ion than the ∥-absorption, and that the A-absorption involves more ∥-absorption. The crystal is found to show absorption bands at about 50×10^{13}/sec. and at a shorter wave-length than about 90×10^{13}/sec. The band at 50×10^{13}/sec. of the crystal clearly corresponds to the band A of the $[Cu(en)_2]^{2+}$-group, since the $[Hg(SCN)_4]^{2+}$-ion is expected to absorb at a much shorter wave-length region[1] (Fig. 3). For the $[Cu(en)_2]^{2+}$-ion in the crystal of $[Cu(en)_2][Hg(SCN)_4]$, the following relation is found on the dichroism. *For the band A, the ∥-absorption is hypsochromic to the ⊥-absorption the intensity being greater with the ∥-absorption than with the ⊥-absorption.* This relation is essentially similar to that with the crystal of $\{[Cu(en)_2](OH_2)_2\}(No_3)_2$.

The X-ray investigation showed that "two N atoms of the SCN-groups in the crystal of $[Cu(en)_2][Hg(SCN)_4]$ are co-ordinated to each copper atom at a distance of 2.58 Å in the direction perpendicular to the complex-plane, giving the copper atom a total of six-fold co-ordination"[5]. In the same report a value of 2.07 Å was obtained for the co-ordinate bond distance between the copper and nitrogen atoms in the plane formed from a copper and four nitrogen atoms of ethylenediamine molecules. The Cu-N distance of 2.58 Å seems to be too great for the ordinary co-ordinate linkage to be expected between the copper atom and the nitrogen atoms of the NCS-groups. The band A of $[Cu(en)_2][Hg(SCN)_4]$, however, is seen to be displaced slightly bathochromically, as compared with that of $[Cu(en)_2](ClO_4)_2$. This may be regarded as one effect by the interaction between copper and nirtogen atoms. The dichroism for the band A is the same as that with the perchlorate, as was found to be the case with the nitrate dihydrate.

Another absorption band in the ultra-violet may be considered as superposition of the

absorption bands of complex ions, $[Cu(en)_2]^{2+}$ and $[Hg(SCN)_4]^{2-}$. In any case, the absorption is seen to lie in the far longer wave-length regions than would be expected from the corresponding bands of either of the component complexes in solution. This bathochromic shift also may be taken as indicating that the complexes are subjected to the effect caused by the interaction between a copper and two nitrogen atoms of the NCS-groups. Judging from the absorption curves of the separate component complexes, the ascending curve at about $80-90\times10^{13}$/sec. may most probably be considered as due to the $[Cu(en)_2]^{2+}$-ion. *It is found for this band that the* $\parallel$*-absorption is hypsochromic to the* $\perp$*-absorption.* This dichroism, reverse to that of the $[Cu(en)_2](ClO_4)_2$, shows the effect of NCS^- ions on the $[Cu(en)_2]^{2+}$ group.

General Discussion

Inspecting the results presented above, we find the following rules about the effects on the absorption spectrum of the complex ion caused by the outer groups which come comparatively close to the copper atom. (1) *The band A is displaced bathochromically, its polarization property being unchanged.* (2) *The band B undergoes a large bathochromic shift, its polarization property being reversed.*

These changes, above all the reversal of the polarization property, are so definite that they may be used for determining whether or how close such molecules as water and ammonia in the crystalline state approach the copper atom in the direction normal to the square-planar complex.

The results stated above clearly indicate that water molecules in the nitrate dihydrate or thiocyanate ions in the tetrathiocyanato-mercurate(II) have considerable effects on the copper atom. But judging from the distance between the copper atom and the approaching groups, as revealed by the X-ray analysis[2,5], the effect may be mostly electrostatic, and the linkage between them may be different from the linkage between the copper atom and ethylenediamine molecules in the complex-plane. Furthermore, the typical sexa-co-ordinate copper(II) complex of octahedral configuration would show its absorption in the much longer wave-length region, as may be readily realized from the absorption maximum at $40-45\times10^{13}$/sec. for the $[Cu(en)_3]^{2+}$ in aqueous solution against about $52-57\times10^{13}$/sec. for the $[Cu(en)_2]^{2+}$ in the crystalline state[11]. This also seems to support the above conclusion.

The magnitude of the bathochromic change for the band A and band B may be supposed to depend upon the strength of the effect of the approaching groups on the copper atom. Thus, inspecting the results, we obtain with both the bands the decreasing order of the effect on the copper atom: tetrathiocyanato-mercurate(II) > nitrate dihydrate > perchlorate.

Formerly, one of the present authors (R. T.)[11] reported that the band A of planar quadri-co-ordinate complexes of copper(II) suffers large bathochromic change when taking up two more ligands to complete the sexa-co-ordination. This would indicate that the approach of the fifth or sixth group to the copper atom may cause bathochromic shift of the band. The general rule (1) seems to be in good agreement with it. This is also in qualitative agreement with the result obtained by Ballhausen[12] through quantum-theoretical treatment on the basis of the crystal field theory. It is to be noted that the polarization property for the band A is not changed on the approach of the fifth and sixth groups. This fact seems to show that the band A may originate from an electronic transition of the comparatively deeper part of the complex ion, favouring the interpretation that the absorption band A of copper (II)-complexes is due to transition of the *d*-electrons of the copper atom which is under the effect of the surrounding ligands.

The general rule (2) indicates that the effect of the approaching outer groups on the band B is seen to be quite large. One explanation for the general rule (2) may be that the same transition in the shorter wave-length that exist in the separate $[Cu(en)_2]^{2+}$-ion may have their polarization properties reversed due to the approach of the outer groups to the copper atom. But an alternative explanation may be that, as the groups come closer to the copper atom in a complex ion, a new transition polarized in the X-Cu-X direction, X being the approaching groups, is given rise to in the wave-length region slightly longer than the original transition. Assuming the latter interpretation, this new transition would most probably be due to the electron transfer from the copper atom to the ligands, as was assumed between the copper and ethylenediamine for the absorption band B of the separate complex ion without any specific effect from outside. Based on the electron transfer model on the supposed new band, we may consider that, when the outer groups come close enough to the copper atom, the electronic clouds on

11) R. Tsuchida and H. Ito, Read before the symposium on co-ordination compounds, Nagoya, November, 1953.

12) C. J. Ballhausen, *Kgl. Danske Videnskab. Selskab, Mat.-fys. Medd.*, **29**, No. 4 (1954).

the copper atom move to increase the electronic density toward the approaching groups, making the electron transfer easier with the electric vector along the L-Cu-L direction.

This mechanism of electron transfer provides the possibility of explaining the association band of planar complexes[13]. Thus when some anions in solution come very close to the metal atom in the centre of the planar complex ion, there would be electron transfer between the metal atom and the anions.

Now the absorption spectrum of $[Cu(en)_2]^{2+}$ in aqueous solution may be discussed using the above results. In aqueous solution, water molecules are considered to be located so close to the copper atom in the square-planar complex that the interaction of the above type may be expected between the copper atom and water molecules. In fact, the absorption maximum of $Cu(en)_2(NO_3)_2$ in aqueous solution lies at about 54×10^{13}/sec.[11], a much longer wave-length than the maximum of the perchlorate, and even longer than the nitrate dihydrate in the crystalline state. In consequence, the effect of water molecules on the $[Cu(en)_2]^{2+}$ ion may be greater in aqueous solution than in the crystals of the nitrate dihydrate. But, as is discussed in the preceding section of this paper, the approaching water molecules are not supposed to form strongly covalent bonds with the copper atom, since the supposed octahedral complex formed by strong bonds would show its absorption at a far longer wave-length.

It seems unusual that the absorption band A of the solution is quite symmetrical, since the simple superposition of the $\parallel$- and $\perp$-absorption, as obtained with the crystal, would yield unsymmetrical curve for the band A. It must be concluded, therefore, that the band A, which has only one component in the solution, is split in the crystalline state into two components having opposite polarization properties. The splitting of the band A in the crystal may be ascribed to the perturbation by the surrounding ions, and might be a kind of Davydov splitting[14].

A similar consideration applies to the absorption spectrum of $[Cu(en)_2]^{2+}$ in ammoniac solution, which exhibits the band A at about 48×10^{13}/sec.[15]. The bathochromic shift of the band A is seen to be much greater in ammoniac solution than in aqueous solution, and even than in the tetrathiocyanato-mercurate(II), suggesting that the effect of ammonia on the copper atom is greater than that of water molecules in the aqueous solution or that of thiocyanate ions in the latter. Judging from the remarkable, bathochromic shift, it may be reasonable to suppose that the linkage between ammonia molecules and the copper atom should have considerable covalent bond character.

Summary

Polarized absorption spectra of bis (ethylenediamine)-copper(II) perchlorate, nitrate dihydrate and tetrathiocyanato-mercurate(II) in the crystalline state have been determined by Tsuchida-Kobayashi's microscopic method in the region between 2400 and 7000Å. These compounds all show a band at about 50×10^{13}/sec. (band A) and another absorption at a wave-length shorter than 90×10^{13}/sec. (band B).

The band A of the latter two compounds suffers bathochromic effect, and the polarization property for the band B is reversed, as compared with the former. From these differences, it has been concluded that in the former two compounds, OH_2 or NCS^- causes a considerable effect upon the copper atom.

Using the results of the measurements, the nature of the absorption bands and absorption spectra of the complex ion in aqueous solution has been discussed.

The present author wish to thanks Mr. M. Atoji for his interest in this work and the Ministry of Education for a grant.

Department of Chemistry, Faculty of Science, Osaka University, Osaka

13) H. Yoneda, to be published soon.

14) A.S. Davydov, *Zhur. eksp. teor. Fiz.*, **18**, 210 (1948); *Akad. Nauk S.S.S.R., Pamyati S. I. Varilov*, **1952**, 197; *C.A.*, **43**, 4575 (1949).

15) F. Rosenblatt, *Z. anorg. Chem.*, **204**, 351 (1932).

Vapor Pressure of Germanium Monosulfide

By Ei-ichi SHIMAZAKI and Tsuguyasu WADA

(Received October 6, 1955)

Germanium monosulfide has a relatively high volatility, and hence it can be removed from germanite or other minerals containing germanium sulfide by vaporizing it in reducing atmosphere[1]. However, the quantitative value of vapor pressure has not yet been reported.

In the present work, the vapor pressure of germanium monosulfide is determined by means of Knudsen's effusion method over the temperature range from 338°C to 399°C, and the heat, free energy, and entropy of sublimation are calculated from the experimental results obtained.

As Kundsen has first derived[2], the weight of vapor G effusing in a time τ through an area A is related to the pressure p by

$$p=\sqrt{\frac{2\pi RT}{M}}\cdot\frac{G}{\tau}\cdot\frac{1}{A}, \qquad (1)$$

where R is the gas constant, T is the absolute temperature and M is the molecular weight of effusing vapor. The method based on the above relation is the most reliable one when the vapor pressure to be measured is lower than 10^{-2} mmHg.

It has been already confirmed that the dissociation of germanium monosulfide such as

$$GeS(s) \rightleftarrows Ge(s)+\frac{1}{2}S_2(g), \qquad (2)$$

does not practically occur at the temperature of this experiment. According to the recent study of Ono and Sudo[3], the dissociation pressure Ps_2 of the above reaction is only 10^{-13} atm. even at 415°C.

The molecular association in effusing vapor is not considered, regarding the molecular formula as GeS. Although there is no direct evidence, this assumption is supported by the measurement on the density of vapor at 1100°C and 1500°C[4], and by the spectroscopic information on the gaseous germanium monosulfide[5].

1) W.C. Johnson, L.S. Foster and C.A. Kraus, *J. Am. Chem. Soc.*, **57**, 1828 (1935).
2) M. Knudsen, *Ann. Phys.*, **28**, 75, 999 (1909); **29**, 179 (1909).
3) K. Ono and K. Sudo, *Bull. Res. Inst. Mineral Dressing and Metallurgy*, Tohoku Univ., **10**, 181 (1954).
4) L.F. Nilson and O. Pettersson, *Z. phys. Chem.*, **1**, 27 (1887).
5) V. Shapiro, R.C. Gibbs and A.W. Laubengayer, *Phys. Rev.*, **40**, 354 (1932).

Experimental

Apparatus and Procedure.—The apparatus used for determination of vapor pressure is the same as that used by Niwa in the studies on the vapor pressure of alkali halides[6]. It is essentially composed of a quartz cell having a small orifice from which the vapor is effused, and a microbalance by which the weight of effused vapor is determined. Details have been described in Niwa's original paper.

The original experimental procedure is modified in some respect: In the present work the decrease of weight during a certain time is measured by the microbalance which is calibrated in advance, whereas in the original paper the time required to effuse a certain quantity of a sample, a quantity corresponding to the rider, was measured. There is no essential difference, however, between these two procedures.

The accuracy of experiment is not greatly different from Niwa's, in which the maximum error is estimated as 2.6% at most.

Material.—Germanium monosulfide used was prepared by treating metallic germanium with hydrogen sulfide. Metallic germanium was obtained by reduction of germanium dioxide having a purity of 99.999% with hydrogen. The powder

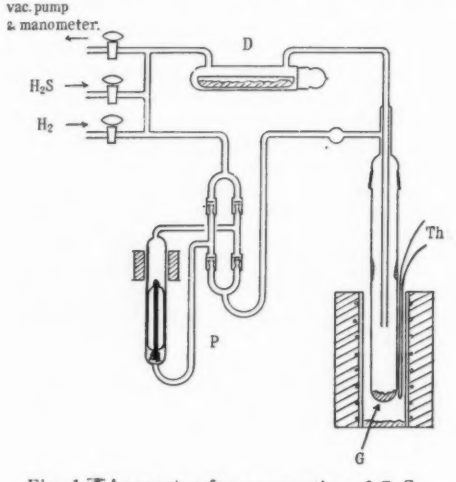

Fig. 1. Apparatus for preparation of GeS.
D; Phosphorous pentoxide.
P; Circulation pump.
Th; Pt-PtRh thermocouple.
G; Powder of germanium metal.

6) K. Niwa, *J. Fac. Sci. Hokkaido Imp. Univ.*, Ser. III, **2**, 202 (1938).

of germanium thus obtained was taken in a reaction tube of Telex glass with 2 cm. diameter and 20 cm. long, which is connected to vacuum pump, circulation pump, and storage bulbs of hydrogen sulfide and hydrogen, as shown in Fig. 1. Then, after the treatment with hydrogen at 600°C to remove completely the rest of oxygen, hydrogen sulfide was introduced up to about 100 mmHg and was circulated gently at 550°C. As reaction proceeded, germanium monosulfide was condensed on the cold part of reaction tube.

Germanium monosulfide thus prepared has the appearance of dark grey with metallic lustre, whereas it becomes reddish brown when it is finely powdered[7]. The X-ray powder pattern is consistent with the crystal structure of germanium monosulfide which is proposed by Zachariasen[8] such as orthorhombic with lattice parameters of a=4.29, b=10.42, and c=3.64 Å, as shown in Table I. The lines of metallic germanium, germanium dioxide, or germanium disulfide are not observed. Germanium disulfide may be the only possible impurity. But its vapor pressure is far less than that of monosulfide[9], so it does not markedly affect the results even if it is present.

TABLE I

X-RAY DIFFRACTION PATTERN OF GERMANIUM MONOSULFIDE

obs. d (A)	Intensity.	(hkl)	d (calc.)	Intensity observed by Zachariasen[8].
5.26	vvw	(020)	5.21	vvw
4.00	vw	(110)	3.97	vw
3.34	st	(120)	3.32	m
3.00	mw	(012)	2.97	m
2.79	mw	(101)	2.77	—
2.70	st	(111)	2.68	st
2.63	vst	(040)	2.61	vvst
2.18	m	(131)	2.17	st
2.11	w	(210)	2.10	mst
1.910	mw	(141)	1.899	st
1.888	vw	(150)	1.876	m⁻
1.824	m	(230)	1.826	m
1.746	vw	(060)	1.737	vw
1.669	m	(151)	1.689	st
1.639	vw	(231)	1.632	w
1.618	vw	(160)	1.610	m
1.598	vw	(122)	1.590	m
1.578	vw	(061)	1.568	m
1.497	w	(250)	1.496	m
1.386	w dif.			
1.311	w			

Ono and Sudo[3] have shown that the decomposition of germanium monosulfide to form disulfide and metal such as

$$2GeS(s) \rightleftarrows GeS_2(s)+Ge(s), \qquad (3)$$

is possible at the temperature below 388°C. After the measurement, however, the residue remaining in the cell was reexamined by X-ray diffraction, and it was confirmed that the decomposition like the above had not occurred.

Results

Vapor pressure.—The experimental results on G and τ for various temperatures, and vapor pressures calculated according to equation (1) are recorded in Table II.

TABLE II

RESULTS OF EXPERIMENTS AND VAPOR PRESSURE OF GERMANIUM MONOSULFIDE

Temp. °C	Decrease of weight, G, (mg.)	Duration, τ, (sec.)	Vapor pressure p, (mmHg)
399	5.48_0	3780	12.73×10^{-3}
387	2.73_5	3600	6.61 〃
382	3.38_4	5400	5.44 〃
378	1.88_0	3720	4.37 〃
375	1.95_2	5300	3.18 〃
368	0.95_4	3630	2.26 〃
364	1.76_4	7200	2.10 〃
361	0.63_6	3000	1.82 〃
356	0.54_9	3600	1.30 〃
348	0.65_1	6600	0.83 〃
338	0.34_7	6300	0.46 〃

The area of orifice is 4.94×10^{-3} cm.

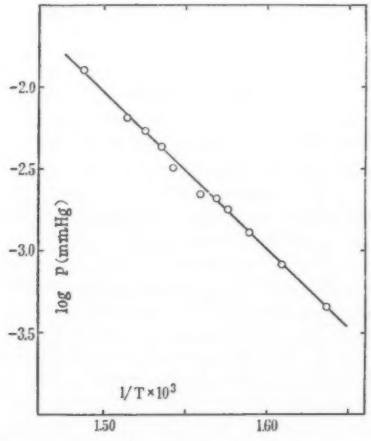

Fig. 2. Logarithms of vapor pressures of GeS, plotted against $1/T$.

As shown in Fig. 2, the logarithms of vapor pressures are linearly related against the reciprocals of the absolute temperature. This straight line is represented by the following equation;

$$\log p_{(mmHg)} = -\frac{9591}{T}+12.357. \qquad (4)$$

7) W.C. Johnson and A.C. Wheatley, *Z. anorg. allgem. Chem.*, **216**, 273 (1932).
8) W.H. Zachariasen, *Phys. Rev.*, **40**, 917 (1932).
9) N. Matsumoto and E. Shimazaki, *J. Chem. Soc. Japan (Pure Chem. Sect.)* (to be published).

Calculation of Thermodynamic Values.—The heat of sublimation ΔH_T, free energy change of sublimation ΔG_T, and entropy change of sublimation ΔS_T are calculated according to well-known thermodynamic relations:

From Clausius-Clapeyron's equation,

$$\Delta H_T = -R\frac{\mathrm{d}\ln p}{\mathrm{d}(1/T)}. \quad (5)$$

As to free energy change of sublimation,

$$\Delta G_T = -RT\ln p_{(\mathrm{atm.})}, \quad (6)$$

and as to entropy change of sublimation,

$$\Delta S = \frac{\Delta H_T - \Delta G_T}{T}. \quad (7)$$

The values of these thermodynamic functions are obtained as shown in Table III.

TABLE III

HEAT, FREE ENERGY, AND ENTROPY OF SUBLIMATION OF GERMANIUM MONOSULFIDE AT THE TEMPERATURE FROM 338° TO 399°C

ΔH_T, kcal./mol.	ΔG_T, cal./mol.	ΔS_T, cal./deg.mol.
43.9	43869–43.343T	43.3

The authors wish to express their thanks to Professor K. Niwa for his encouragement, and Professor Kenji Ono and Mr. Hideo Baba for the supply of germanium dioxide.

Department of Chemistry, Faculty of Science, Hokkaido University
Sapporo

*Studies on Dimethylglyoximato-cobalt (III) Complexes. IV. Intramolecular O-H-O Hydrogen Bonds in Bis-(dimethylglyoximato)-cobalt (III)-complexes**)

By Akitsugu NAKAHARA, Junnosuke FUJITA and Ryutaro TSUCHIDA

(Received October 6, 1955)

Introduction

It has been well-known for the last two decades that two dimethylglyoximate ions usually tend to coördinate to a metal atom with planar configuration[1,2]. The origin of this tendency, however, remained unclarified till last year[3]. In the former papers of this series[3,4], one of the present authors elucidated the tendency by taking intramolecular O-H-O hydrogen bonds into consideration. As far as the dimethylglyoximato-cobalt (III)-complexes are concerned, there has never been found any paper which dealt with direct confirmations of such hydrogen bonds. Although the first description of the subject was already published in the preceding paper[5], it seems to be desirable to perform further investigations in order to clear up some ambiguity which was concerned with the assignment of the infrared absorption band at 1725 cm^{-1}. In this work, we have measured infrared absorption spectra of hydrogen dichloro-bis-(dimethylglyoximato)-cobaltate (III) preparing with both normal and deuterated dimethylglyoxime and of several other dimethylglyoximato-cobalt (III)-complexes. Consequently, we have succeeded not only in justifying our previous conclusion but also in finding out a series of very short and symmetric O-H-O hydrogen bonds.

Experimental

Materials. Normal and Deuterated Dimethylglyoxime.—A convenient method was applied to prepare the deuterated dimethylglyoxime, dgD_2.

First of all, normal dimethylglyoxime was converted into dipotassium salt, dgK_2, by the action of an excessive amount of potassium hydroxide. 5g of dipotassium dimethylglyoximate which was perfectly free from moisture was mixed with 10 ml. of heavy water, and to this 10 ml. of concentrated deuterium chloride was added. After vigorous shaking of the mixture the insoluble

* Although in the former papers of this series the symbols, DH_2 and DH, were used for dimethylglyoxime and its ion, respectively, in the present paper the symbols, dgH_2 and dgH, are preferably chosen for the convenience of discrimination from deuterated dimethylglyoxime, dgD_2, and its ion, dgD.

1) L. Cambi and C. Coriselli, *Gazz. chim. ital.*, **66**, 91 (1936).
2) Y. Nakatsuka and H. Iinuma, This Bulletin, **11**, 48 (1936).
3) A. Nakahara, ibid., **27**, 560 (1954).
4) A. Nakahara, ibid., **28**, 207 (1955).
5) A. Nakahara, ibid., **28**, 473 (1955).

deuterated dimethylglyoxime was separated from liquor. It was heated to 110° in order to remove the moisture and adsorbed deuterium chloride. Pure normal dimethylglyoxime, dgH_2, was purified by the same procedure using normal water and hydrochloric acid instead of heavy water and deuterium chloride.

Normal and Deuterated Hydrogen Dichloro-bis-(dimethylglyoximato)-cobaltate (III).—The normal complex, $H[Co(dgH)_2Cl_2]$, was prepared by the method of Cambi et al.[6] as described in the former paper[4]. Deuterated complex, $D[Co(dgD)_2Cl_2]$, was prepared according to the following direction: 0.6 g of cobalt (II) chloride hexahydrate which was perfectly free from nickel (II) ion was dehydrated by heating until the color changed from red to blue. Instantly, it was dissolved in 10 ml. of heavy water and to this 0.6 g of deuterated dimethylglyoxime was added. The mixture was heated on a water bath and oxidized by a few drops of hydrogen peroxide. Then, the reaction mixture was filtered by suction. Dark green microscopic crystals of deuterated complex were precipitated from the filtrate by adding excess of concentrated deuterium chloride. On the other hand, partly deuterated complex, $H[Co(dgD)_2Cl_2]$, was obtained from the aqueous solution of the residual by adding excess of concentrated hydrochloric acid.

Concentrated solution of deuterium chloride was obtained by passing hydrogen chloride through **heavy water**, (specific weight $d_4^{20}=1.1049$) which was produced by Norsk Hydro Elektrisk Kvaelstofaktieselskab.

Hydrogen Dibromo-bis-(dimethylglyoximato)-cobaltate (III), $H[Co(dgH)_2Br_2]$; Hydrogen Dinitro-bis-(dimethylglyoximato)-cobaltate (III), $H[Co(dgH)_2(NO_2)_2]$; Sodium Dinitro-bis-(dimethylglyoximato)-cobaltate (III), $Na[Co(dgH)_2(NO_2)_2]$; Nitro-bis-(dimethylglyoximato)-aquo-cobalt (III), $[Co(OH_2)(dgH)_2(NO_2)]$; Nitro-bis-(dimethylglyoximato)-ammine-cobalt (III), $[Co(NH_3)(dgH)_2(NO)_2]$; Chloro-bis-(dimethylglyoximato)-ammine-cobalt (III), $[Co(NH_3)(dgH)_2Cl]$; Bis-(dimethylglyoximato)-diammine-cobalt (III) Chloride, $[Co(NH_3)_2(dgH)_2]Cl$; Hydrogen dinitro-bis-(mono-O-methyl-dimethylglyoximato)-cobaltate (III), $H[Co(dgCH_3{}^*)_2(NO_2)_2]$; Tris-(dimethylglyoximato)-cobalt (III), $[Co(dgH)_3]$.—These complexes were prepared by the direction described in the former paper[4].

Bis-(dimethylglyoximato)-nickel (II), $[Ni(dgH)_2]$.—This was recrystallized from chloroform solution as long acicular crystals.

Measurements. The spectra were obtained with a Perkin-Elmer Model 21 spectrophotometer using sodium chloride prisms and Nujol suspensions of the compounds. For optical measurements all the samples were freed from accompanying moisture including their own water of crystallization.

Results and Discussion

The Infrared Absorption Spectra of Normal and Deuterated Dimethylglyoxime.—The results of the measurements are shown in Fig. 1. Among many differences between the two curves, the one in the region from 3300 to 2300 cm^{-1} is the most significant, so far as this study is concerned.

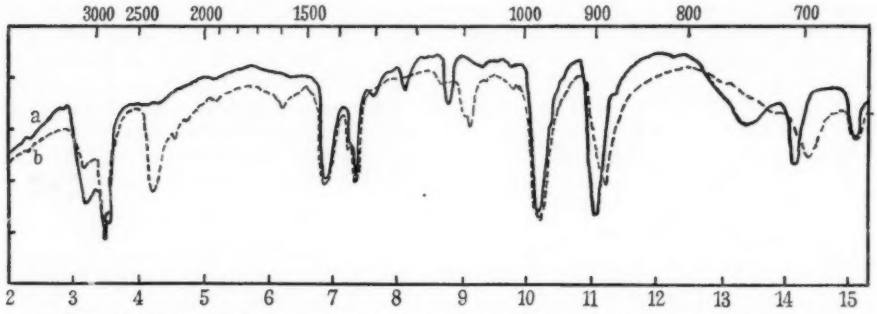

Fig. 1. Infrared absorption spectra of dimethylglyoxime: dgH_2, (a); dgD_2, (b).

In that region normal dimethylglyoxime, (a), has a strong absorption band at about 3170 cm^{-1}, which corresponds to the O-H fundamental stretching vibration frequencies. On the other hand, the curve of deuterated dimethlyglyoxime, (b), shows a rather weak band at the same wave-length in compensation for a new strong band at about 2360cm^{-1}, which is characteristic of O-D stretching vibration. This is the clear evidence for the success in substituting deuterium for hydrogen atom. Rundle et al.[7] obtained the deuterated dimethylglyoxime by recrystallizing the parent compound from heavy water. But the present method may be more effective than theirs.

The Spectra of Normal and Deuterated Hydrogen Dichloro-bis-(dimethylglyoximato)-cobaltate (III).—The spectra of normal

6) L. Cambi and C. Coriselli, *Gazz. chim. ital.*, **66**, 81 (1936).

7) L.E. Godycki, R.E. Rundle, R.C. Voter and C.V. Banks, *J. Chem. Phys.*, **19**, 1205 (1951).

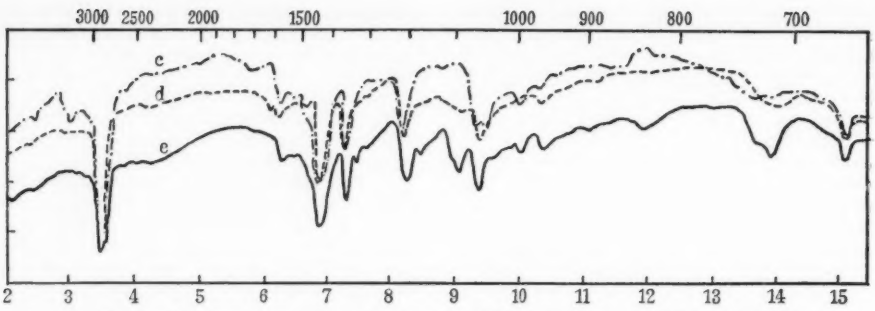

Fig. 2. Infrared absorption spectra of: (c), $H[Co(dgH)_2Cl_2]$; (d), $H[Co(dgD)_2Cl_2]$; (e), $D[Co(dgD)_2Cl_2]$.

complex, (c), partly deuterated complex, (d), and completely deuterated complex, (e), are shown in Fig. 2. In the former paper[5] the band at 1725 cm^{-1} on the curve of normal complex, $H[Co(dgH)_2Cl_2]$, was assigned to the O-H stretching frequency under the formation of strong intramolecular O-H-O hydrogen bond. (See, Fig. 3.) But the assignment

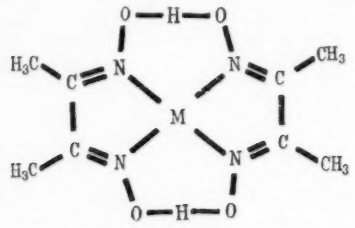

Fig. 3. Planar configuration of two dimethylglyoximate ions in bis-(dimethylglyoximato)-cobalt (III)-complexes.

was less reliable on account of the lack of decisive evidence. Now this ambiguity is perfectly swept off by the fact that the concerned band at about 1700 cm^{-1} have not been recognized on the curve of corresponding deuterated complexes, (b) and (e), as is clear from Fig. 2.

Thus, there is nodoubt in the conclusion that the absorption band at 1725 cm^{-1} of hydrogen dichloro-bis-(dimethylglyoximato)-cobaltate (III) is attributable to the O-H stretching frequency under the formation of intramolecular O-H-O hydrogen bonds.

Furthermore, it is also of interest to compare the curve of partly deuterated complex, $H[Co(dgD)_2Cl_2]$, with that of completely deuterated complex, $D[Co(dgD)_2Cl_2]$. The former complex was prepared, as described in the experimental part, through a procedure in which deuterated complex was dissolved in ordinary water. Nevertheless, there cannot be recognized on the curve, (d), any indication of such O-H stretching band as can be seen in the normal complex, (c). It is, therefore, clear that the deuterium atom in the complex is hardly affected by hyrogen atom of the solvent. It may be supposed that the deuterium atom situated between the two oxygen atoms is as hard to replace as that of hydrogen.

Spectra of Other Bis-(dimethylglyoximato)-cobalt (III)-complexes.—The infrared absorption spectra of several other complexes are shown in Fig. 4, not about the whole aspect

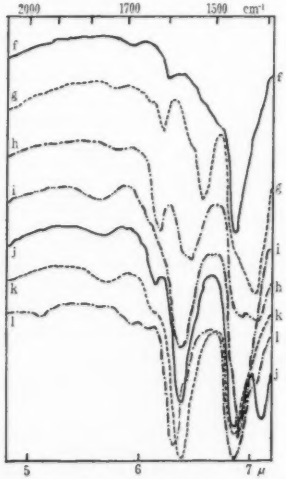

Fig. 4. Infrared absorption spectra of: (f), $H[Co(dgH)_2Br_2]$; (g), $H[Co(dgH)_2(NO_2)_2]$; (h), $Na[Co(dgH)_2(NO_2)_2]$; (i), $[Co(OH_2)(dgH)_2(NO_2)]$; (j), $[Co(NH_3)(dgH)_2(NO_2)]$; (k), $[Co(NH_3)(dgH)_2Cl]$; (l), $[Co(NH_3)_2(dgH)_2]Cl$.

but only about the concerned region.

All the bis-(dimethylglyoximato)-cobalt(III)-complexes show their respective O-H stretching band at about 1700 cm^{-1}. While in some

* $dgCH_3 = H_3C \cdot C(NOCH_3) \cdot C(NO) \cdot CH_3$

complexes the stretching bands are rather high in frequency and comparatively distinct in appearance, in other complexes they are the opposite. (Table I).

TABLE I

O-H STRETCHING FREQUENCIES OF BIS-(DIMETHYLGLYOXIMATO)-COBALT (III)-COMPLEXES

Complexes	O-H stretching frequencies cm^{-1}
$H[Co(dgH)_2Cl_2]$	1725
$H[Co(dgH)_2Br_2]$	1686
$H[Co(dgH)_2(NO_2)_2]$	1725
$Na[CO(dgH)_2(NO_2)_2]$	1740
$[Co(dgH)_2(NH_3)_2]Cl$	1695
$[Co(OH_2)(dgH)_2(NO_2)]$	1770
$[Co(NH_3)(dgH)_2Cl]$	1760
$[Co(NH_3)(dgH)_2(NO_2)]$	1766

hydrogen bonds in the series of above bis-(dimethylglyoximato)-cobalt (III)-complexes.

The Spectra of Hydrogen Dinitro-bis-(mono-O-methyl-dimethylglyoximato)-cobaltate(III), $H[Co(dgCH_3)_2(NO_2)_2]$, Tris-(dimethylglyoximato)-cobalt (III), $[Co(dgH)_3]$, and bis-(dimethylglyoximato)-nickel (II), $[Ni(dgH)_2]$. —The results of the measurements are shown in Fig. 5. The above described O-H stretching band at about 1700 cm^{-1} can be recognized neither on the curve of the first complex, (m), nor on that of the second complex, (n).

This fact may certify the previous conclusion[5] that the band at about 1700 cm^{-1} is characteristic of the bis-(dimethylglyoximato)-metal-complexes in which the two dimethylglyoximate ions coördinate to a metal atom with planar configuration. The infrared absorption spectrum of bis-(dimethylglyoximato)-nickel (II), (o), which was newly measured in the present work shows the characteristic band at 1775 cm^{-1}, agreeing with the results of the measurement by Rundle et al.

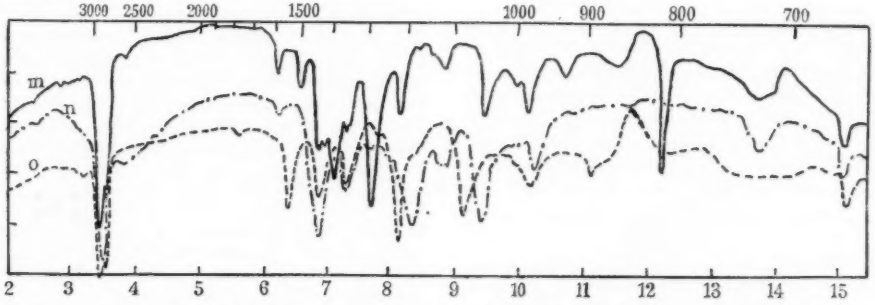

Fig. 5. Infrared absorption spectra of: (m), $H[Co(dgCH_3)_2(NO_2)_2]$, (n), $[Co(dgH)_3]$; (o), $[Ni(dgH)_2]$.

But the relations between those absorption bands and the chemical structures are probably complicated matters. At any rate, those data shown in Fig. 4 and Table I are a series of the same examples of O-H-O hydrogen bond as those of hydrogen dichloro-bis-(dimethylglyoximato)-cobaltate (III) and Bis-(dimethylglyoximato)-nickel (II). There are some reports of both theoretical and experimental investigations concerning the relation between the oxygen-oxygen distance and the fundamental optical vibration frequency of the hydrogen atom of an O-H-O hydrogen bond[7,8,9,10]. According to Rundle et al., the O-H-O hydrogen bond in bis-(dimethylglyoximato)-nickel (II) is a kind of very short and symmetric hydrogen bond. If it be the case, *there might be expected the same kind of examples of very short O-H-O*

Summary

Infrared absorption spectra of hydrogen dichloro-bis-(dimethylglyoximato)-cobaltate (III) prepared from both normal and deuterated dimethylglyoxime and of several other dimethylglyoximato-cobalt (III)-complexes were measured. It has been ascertained through the data of deuterated complexes that the absorption band at 1725 cm^{-1} of hydrogen dichloro-bis-(dimethylglyoximato)-cobaltate (III) is attributable to the O-H stretching frequency under the formation of intramolecular O-H-O hydrogen bonds.

All the bis-(dimethylglyoximato)-cobalt (III)-complexes show similar O-H stretching bands in the same region. It has been forecast that a series of examples of the very short and symmetric O-H-O hydrogen bond may be expected in the bis-(dimethylglyoximato)-cobalt (III)-complexes.

8) R.E. Rundle and M. Parasol, *J. Chem. Phys.*, **20**, 1487 (1952); L.E. Godycki and R.E. Rundle, *Acta Cryst.*, **6**, 487 (1953).

9) R.C. Lord and R.E. Merrifield, *J. Chem. Phys.*, **21**, 166 (1953).

10) A.N. Baker, Jr., ibid., **22**, 1625 (1954).

The authors are indebted to Mr. Naofumi Ooi of the Sumitomo Chemical Co. for obtaining most of the spectra. We also wish to thank the Ministry of Education for a grant which enabled us to carry out this investigation.

Department of Chemistry, Faculty of Science
Osaka University, Osaka

The Crystal Structure of Potassium Tetranitro-diammine-cobaltiate (III), $K[Co(NH_3)_2(NO_2)_4]$

By Yoshimichi KOMIYAMA (formerly, Y. TANITO)

(Received October, 12, 1955)

Introduction

Various attempts[1] have been made to determine the configuration of a complex anion, $[Co(NH_3)_2(NO_2)_4]^-$, because such a di-substituted complex should be capable of existing in two geometrically isomeric forms on the octahedral theory. In 1936, Wells[2] determined the crystal structure of the silver salt, $Ag[Co(NH_3)_2(NO_2)_4]$, and found that the two ammonia groups were co-ordinated to the central cobalt atom in *trans*-positions with respect to each other. On the other hand, in 1949 Kuroya and Yamasaki[3] examined very closely the oxalato-dinitrodiammine complex derived from the NH_4-salt or "Erdmann's salt". Namely they repeated fractional crystallizations and attempted to resolve each fraction into optical isomers. Finally they came to the conclusion that in the aqueous solution of the Erdmann's salt at room temperatures the *cis*- and *trans*-isomers should possibly coexist as an equilibrium mixture. It would be of interest to determine the configuration of the complex anion in the crystals of the Erdmann's salt itself, $NH_4[Co(NH_3)_2(NO_2)_4]$ and also the potassium salt. Since these two salts are isomorphous, their structures have been determined at the same time. In this paper the crystal structure of the potassium salt will be given; that of the Erdmann's salt will be treated in the next paper.

1) Y. Shibata and T. Maruki, *J. Chem. Soc. Japan*, 37, 1142 (1916); E.H. Riesenfeld and R. Klement, *Z. anorg. Chem.*, 124, 1 (1922). W. Thomas, *J.C.S.*, 123, 617 (1923); I.E. Knaggs, *J. C. S.* 121, 2074 (1922); B.C. Ray, *J. Indian Chem. Soc.*, 440 (1937); H. Sueda, *J. Chem. Soc. Japan*, 57, 406 (1936); E.A. Gilinskaya, *Ser. Fiz-Mat. i Estestven. Nauk*, 3, 133 (1953).

2) A.F. Wells, *Z. Krist.*, (A)., 95, 74 (1936).

3) Read at the annual meeting of Chem. Soc. Japan, (1949).

Experimental

Potassium tetranitro-diammine-cobaltiate (III) was prepared according to the method described by Jörgensen[4] and was recrystallized from water not exceeding 60°C. They belong to the orthorhombic bipyramidal class and are usually thin needles elongated along the *c*-crystal axis. Three crystal rods less than 0.2 mm. in diameter parallel to each principal axis were prepared. All the equatorial reflections were recorded by using Fe $K\alpha$ radiation ($\lambda=1.937$ Å). Usual multiple film technique was employed and the intensity of reflections were visually estimated by comparison with a standard scale. The usual correction factors were applied by means of the chart given by Cochran[5]. No correction for absorption was applied. A temperature factor and a scale factor for converting the observed values of $|F_{rel}|$ approximately to the absolute scale were calculated by Wilson's method[6]. The unit cell dimensions were obtained from high order reflections of the equatorial lines of the oscillation photographs.

The results are: $a=11.38\pm0.02$ Å, $b=12.95\pm0.02$ Å and $c=6.76\pm0.01$ Å, giving the axial ratio $a:b:c=0.879:1:0.522$, in agreement with those obtained morphologically, i.e., 0.8783: 1: 0.5192. From the density 2.107 g./cc. measured by the pyknometer method at 25.0°C, it was found that the unit cell contains four formula units of $K[Co(NH_3)_2(NO_2)_4]$, the calculated value being 2.106 g./cc. The space group is D_2^1-$P\ 2_12_12_1$. All the atoms are on the general positions: x, y, z; $\frac{1}{2}-x, \frac{1}{2}+y, \frac{1}{2}-z$; $\frac{1}{2}+x, \frac{1}{2}-y, \bar{z}$; $\bar{x}, \bar{y}, \frac{1}{2}+z$.

Determination of the Structure

Firstly the Patterson projections $P(X, Y)$ $P(Y, Z)$ and $P(X, Z)$ were evaluated.

Comparing these results with the corresponding Patterson maps of the Erdmann's salt, whose analysis has been carried out at

4) S.M. Jörgensen, *Z. anorg. Chem.*, 17, 477 (1898).

5) W. Cochran, *J. Sci., Inst.*, 25, 253 (1949).

6) A.J.C. Wilson, *Acta Cryst.*, 2, 318 (1949).

the same time, it was confirmed that these two crystals are isomorphous as expected, and moreover it was possible to identify Co–Co, K–K and K–Co vectors on each projection. Hence the positions of cobalt and potassium were fixed at once.

Preliminary Fourier projections of electron density upon the planes perpendicular to each principal axis were synthesized using observed F-values, whose sign was calculated from the parameter values of cobalt and potassium. From these projections it was possible to assign approximate parameters for nitrogen atoms which are co-ordinated nearly octahedrally around each cobalt atom. These were in good accord with the conclusion drawn from each Patterson projection. Though the Fourier prejections showed faint outlines of oxygen atoms they could not be located unequivocally. The c-crystal axis is as short as 6.76 Å, and it should be possible to obtain a clear projection of the whole structure in this direction, as any interleaving of the complex anion within this periodicity is probably ruled out. An attempt was made to determine the signs of $F(hk0)$ directly by taking the difference of the corresponding F-values observed for the ammonium and potassium salt, since both are isomorphous and the positions of potassium atoms are already known. The signs of 46 out of 120 observed reflections could be determined successfully. The projection thus obtained showed the outlines of the oxygen atoms more clearly than the previous one. A vector convergence map[7] was also made for this projection, by using the positions of cobalt atoms. Closer examination of this projection and vector convergence map enabled one to deduce the x- and y-parameters of all the atoms in the unit cell. $F(hk0)$ were then calculated. The agreement was reasonably good and enabled a start to be made with the process of refinement by means of Fourier syntheses. At this stage, all the z-parameter values of oxygen atoms were assumed using the data of interatomic distances and bond angles. Calculation of $F(0kl)$ and $F(h0l)$ values eliminated at once the possibility of the *cis*-configuration. Finally only one set of parameter values corresponding to the *trans*-configuration remained which could account for $F(0kl)$ and $F(h0l)$s. Then all the projections were refined by successive approximations as usual. The final parameters are listed in Table I. A final electron density projection along the c-crystal axis is shown in Fig. 1.

7) C.A. Beevers and J.H. Robertson, *Acta Cryst.*, 3, 164 (1950).

TABLE I

FINAL PARAMETERS

	x/a	y/b	z/c
Co	0.1690	0.1915	0.2500
K	0.117	0.473	0.695
$NH_3(1)$	0.278	0.265	0.064
$NH_3(2)$	0.062	0.118	0.436
N(1)	0.250	0.264	0.466
N(2)	0.056	0.305	0.234
N(3)	0.088	0.119	0.034
N(4)	0.281	0.078	0.266
O(1)	0.264	0.226	0.632
O(2)	0.293	0.350	0.442
O(3)	0.040	0.353	0.083
O(4)	−0.003	0.332	0.383
O(5)	−0.018	0.112	0.017
O(6)	0.150	0.072	−0.078
O(7)	0.257	0.005	0.376
O(8)	0.367	0.080	0.163

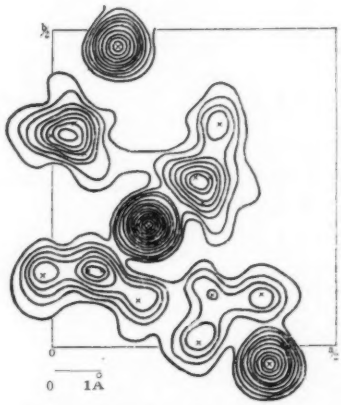

Fig. 1. Electron densities along the c-axis of $K[Co(NH_3)_2(NO_2)_4]$. Contours are at intervals of 2 e. A^{-2}.

The comparison of the observed structure factors with those calculated is given in Table II. The atomic scattering factors used for the calculation of the structure factors were those listed in the International Tables. A temperature factor of the form $\exp -B\left(\frac{\sin\theta}{\lambda}\right)^2$ was used, where B was given the value 2.5 $Å^2$. The value of B and the scale factor were estimated by plotting the values of $\log F_c/F_o$ versus $(\sin\theta)^2$ at the final stage. The reliability factor $R=\sum||F_o|-|F_c||/\sum|F_o|$ are 0.165, 0.185 and 0.235 for $(hk0)$, $(0kl)$ and $(h0l)$ respectively. The weighted mean value of R is 0.179, for which only observed reflections up to $\frac{\sin\theta}{\lambda}=0.501$ have been used.

TABLE II

OBSERVED AND CALCULATED STRUCTURE AMPLITUDES

ORIGIN OF CO-ORDINATE IS TAKEN AT A CENTER OF SYMMETRY ON EACH PROJECTION

hkl	$F_{obs.}$	$F_{cal.}$	*hkl*	$F_{obs.}$	$F_{cal.}$	*hkl*	$F_{obs.}$	$F_{cal.}$	*hkl*	$F_{obs.}$	$F_{cal.}$
200	17.8	−19.8	510	13.2	10.9	011	2.0	− 1.6	0121	12.2	13.0
400	1.8	3.8	520	16.3	15.5	012	12.9	13.1	0122	2.1	2.1
600	9.0	4.5	530	1.5	− 0.2	013	8.3	5.6			
800	4.0	7.1	540	16.5	−14.9	014	5.4	− 5.5	101	26.8	27.4
1000	3.6	− 4.6	550	11.7	11.3	015	2.0	1.4	102	4.8	− 0.1
020	12.3	−12.2	560	10.3	6.1	016	3.8	3.7	103	7.4	5.9
040	2.7	0.8	570	2.5	− 2.1				104	4.2	− 3.9
060	9.2	9.5	580	5.2	− 5.6	021	15.1	−16.2	105	17.2	16.6
080	6.5	− 4.4	590	—	0.1	022	1.8	1.5	106	6.0	− 7.1
0100	7.5	11.0	5100	9.1	− 8.9	023	19.5	21.7			
0120	—	− 1.0	5110	4.0	− 1.8	024	9.0	9.0	201	2.2	− 2.6
						025	6.5	− 6.0	202	6.8	11.6
110	4.8	− 4.9	610	3.2	4.2	026	8.6	− 9.3	203	16.2	13.2
120	19.3	−19.9	620	12.3	− 8.5				204	4.6	3.5
130	13.5	−13.9	630	5.8	3.8	031	7.0	−14.4	205	8.4	8.8
140	5.5	4.7	640	9.3	− 9.6	032	13.0	−18.0	206	5.0	4.8
150	13.5	−12.1	650	8.7	9.2	033	8.0	− 4.5			
160	7.1	− 7.7	660	6.6	6.8	034	—	4.7	301	8.2	9.5
170	6.3	− 5.3	670	3.9	3.1	035	—	2.2	302	6.0	0.4
180	10.5	14.1	680	16.5	−16.0	036	—	− 2.7	303	2.6	3.6
190	7.2	6.7	690	6.3	7.0				304	7.2	− 6.0
1100	13.0	11.3	6100	5.0	5.0	041	6.3	8.1	305	—	2.0
1110	3.6	1.9	6110	3.0	1.9	042	14.0	−16.3	306	1.4	− 1.3
1120	6.0	− 4.4				043	12.6	13.7			
1130	5.0	− 4.8	710	2.0	− 1.7	044	—	− 2.7	401	—	− 5.3
			720	2.4	− 2.3	045	8.1	− 8.8	402	23.0	−22.4
210	24.9	−24.4	730	6.0	− 1.9	046	2.2	2.1	403	—	− 0.2
220	11.1	11.0	740	5.8	4.3				404	8.0	− 7.8
230	—	− 3.2	750	4.2	3.0	051	—	− 0.5	405	3.2	− 0.2
240	27.0	−26.4	760	14.9	−14.0	052	6.3	4.6	406	2.6	1.1
250	1.8	0.1	770	9.0	− 7.8	053	4.7	4.1			
260	8.2	6.0	780	2.6	− 2.9	054	7.0	− 7.2	501	1.4	0.4
270	18.9	−18.5	790	—	0	055	7.4	− 7.2	502	8.6	5.6
280	5.2	4.0	7100	—	0.1	056	4.7	3.5	503	20.0	−16.4
290	2.5	1.3							504	6.0	5.8
2100	4.3	− 2.3	810	13.5	−13.8	061	15.7	−15.9	505	4.0	1.2
2110	12.3	−11.8	820	15.0	11.7	062	13.5	13.5	506	2.6	1.2
2120	2.9	− 3.6	830	4.0	6.3	063	16.2	16.4			
			840	6.2	9.3	064	7.3	− 2.3	601	3.2	− 5.4
310	1.2	− 0.9	850	4.5	0.9	065	2.2	− 2.6	602	15.0	−11.1
320	1.5	− 1.0	860	3.0	− 3.3	066	2.7	4.5	603	14.1	−13.4
330	36.0	35.3	870	6.3	− 5.2				604	8.0	− 8.0
340	5.0	1.2	880	6.6	5.6	071	9.0	8.8	605	7.8	− 4.6
350	20.5	−20.2	890	7.0	6.2	072	6.8	− 5.9			
360	14.2	13.7				073	1.8	− 4.0	701	17.6	−18.1
370	4.2	4.6	910	12.4	−11.8	074	4.3	5.4	702	4.8	− 4.4
380	10.8	7.1	920	4.0	2.1	075	4.0	4.6	703	15.2	−13.6
390	10.9	9.4	930	—	0.5				704	4.8	2.1
3100	3.0	1.9	940	1.2	− 1.4	081	2.9	1.9	705	5.2	− 5.5
3110	10.6	− 5.4	950	10.8	− 9.7	082	21.0	21.1			
3120	6.0	5.0	960	1.9	− 1.7	083	3.1	− 2.9	801	—	− 0.9
			970	4.0	4.1	084	9.0	− 8.0	802	2.5	− 2.4
410	—	− 3.8	1010	12.2	12.4	085	2.4	− 3.4	803	—	2.1
420	16.2	−19.7	1020	5.0	4.1	091	7.2	− 5.9	804	3.6	− 8.0
430	11.8	− 9.7	1030	2.1	− 2.8	092	2.5	2.1	805	—	− 1.7
440	6.7	− 1.7	1040	2.0	− 2.4	093	4.5	6.6			
450	3.9	1.4	1050	2.7	− 2.8	094	2.7	− 0.5	901	—	− 2.7
460	4.9	− 2.1	1060	3.7	1.8				902	5.0	− 1.6
470	8.1	9.4	1110	6.0	5.5	0101	—	0.7	903	—	− 2.8
480	10.2	10.7	1120	7.9	8.5	0102	10.3	10.3	904	3.6	− 2.9
490	13.4	−12.6	1130	3.3	− 3.2	0103	6.7	− 4.8	1001	2.4	2.0
4100	6.4	− 3.9	1140	1.4	− 1.6	0104	7.0	− 7.2	1002	2.6	1.1
4110	2.5	3.1	002	8.8	−12.5				1003	2.1	1.6
4120	4.2	4.5	004	13.7	11.6	0111	2.3	1.1			
			006	5.6	− 9.9	0112	—	0.2	1101	11.0	9.3
						0113	2.9	− 6.4	1102	—	0.4

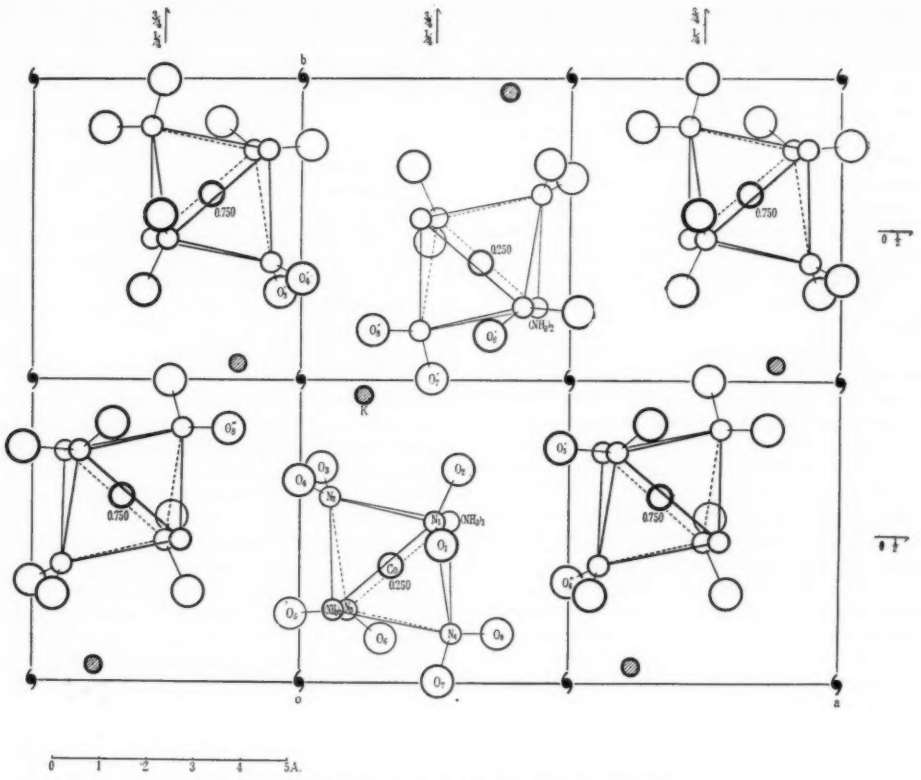

Fig. 2. Projectcion of the structure upon (001).

Description of the Structure

The structure projected upon a plane normal to the *c*-crystal axis is shown in Fig. 2, which corresponds to Fig. 1. The structure is built from potassium ions and complex anions $[Co(NH_3)_2(NO_2)_4]^-$, thus being essentially ionic.

Interatomic distances and bond angles calculated on the basis of the atomic parameters in Table I are listed in Table III. A perspective drawing of the complex anion is shown in Fig. 3.

TABLE III

INTERATOMIC DISTANCES AND INTERBOND ANGLES

Co.....$NH_3(1)$	2.00 Å	K		O(2)	3.08 Å
.....$NH_3(2)$	2.00 Å			O(3)	3.17 Å
.....N(1)	1.96 Å			O(4)	3.11 Å
.....N(2)	1.96 Å			O(3′)	2.97 Å
.....N(3)	1.96 Å			O(4′)	3.11 Å
.....N(4)	1.96 Å			O(7′)	3.26 Å
				O(8′)	2.79 Å
N(1).....O(1)	1.24 Å			O(8″)	3.08 Å
.....O(2)	1.23 Å				
O(1) O(2)	2.08 Å		$(NH_3)(1)$	O(1)(−)	2.97 Å
∠O(1)N(1)O(2)	115°			O(5′)	2.87 Å
N(2).....O(3)	1.21 Å		$(NH_3)(2′)$	O(5′)	3.07 Å
.....O(4)	1.26 Å				
O(3) O(4)	2.10 Å			O(1)	O(4″) 2.76 Å
∠O(3)N(2)O(4)	116°			O(2)	O(6′) 3.09 Å
				O(2)	O(7′) 2.99 Å
N(3).....O(5)	1.22 Å			O(3)	O(7′) 3.05 Å
.....O(6)	1.20 Å			O(3)	O(8″) 2.72 Å
O(5) O(6)	2.08 Å				
∠O(5)N(3)O(6)	118°				
N(4).....O(7)	1.23 Å				
.....O(8)	1.20 Å				
O(7) O(8)	2.14 Å				
∠O(7)N(4)O(8)	124°				

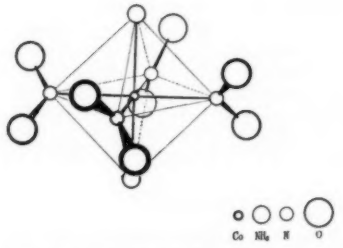

Fig. 3. A perspective drawing of a complex anion.

Two ammonia molecules are co-ordinated to a cobalt atom in *trans*-positions with respect to each other at a distance of 2.00 Å. Four nitrogen atoms of the nitro groups form a square around the cobalt atom within experimental errors, being 1.96 Å apart from it. Thus an octahedral co-ordination is completed around a cobalt atom. These interatomic distances are in good agreement with those found in the structures of various complex compounds of tervalent cobalt[8,9,10,11].

The size and shape of the nitro groups are also in agreement with our previous results.

The planes containing each nitro group are inclined at angles 58°, 56°, 42° and 86° respectively with the plane of four nitrogen atoms of the nitro groups in the same sense. Hence, the configuration of the complex anion is essentially similar to that found in crystals of the silver salt, $Ag[Co(NH_3)_2(NO_2)_4]$[2].

The distances of approach between N atom of ammonia molecule and O atom of nitro group of adjascent complex anion are found to be 2.87 Å, and 2.97 Å. They may be compared with those found in crystals of trinitro-triammine-cobalt (III). These short distances suggest hydrogen bonding between them. By these NH……O bonds the complex anions are held together, forming a network perpendicular to the *b*-crystal axis. Between these layers exist potassium ions.

A potassium ion is surrounded by eight oxygen atoms of the nitro groups with distances ranging from 2.79 Å to 3.26 Å. The co-ordination polyhedron around a potassium atom is rather distorted.

8) Y. Tanito, Y. Saito and H. Kuroya, This Bulletin, **25**, 188 (1952).
9) Y. Tanito, Y. Saito and H. Kuroya, This Bulletin, **25**, 328 (1952).
10) A. Nakahara, Y. Saito and H. Kuroya, This Bulletin, **25**, 331 (1952).
11) Y. Tanito, Y. Saito and H. Kuroya, This Bulletin, **26**, 420 (1953).

Summary

The crystal structure of potassium tetranitrodiammine-cobaltiate (III), $K[Co(NH_3)_2(NO_2)_4]$, prepared according to the method of Jörgensen, has been determined by two-dimensional Fourier method. The orthorhombic unit cell has the dimensions $a=11.38\pm0.02$ Å, $b=12.95\pm0.02$ Å and $c=6.76\pm0.01$ Å containing four formula units in it (Fe K_α, $\lambda=1.937$ Å), and the space group is D_2^1-$P2_12_12_1$. The shape and size of a complex ion was found to be similar to the one found in crystals of silver salt, $Ag[Co(NH_3)_2(NO_2)_4]$. Two ammonia molecules are co-ordinated to the central cobalt atom in *trans*-positions, with Co–N distance 2.00 Å.

The average dimensions of the nitro groups were: N–O=1.22 Å and ∠ONO=118°, in agreement with the results obtained for other nitro-complex compounds of cobalt. Each potassium atom is surrounded by eight oxygen atoms of the nitro-groups with distances ranging from 2.79 Å to 3.26 Å.

The author expresses his hearty thanks to Professor H. Kuroya and Dr. Y. Saito of this university for encouragement and invaluable discussions. Part of the cost of this study has been defrayed by a Grant of the Ministry of Education.

Institute of Polytechnics, Osaka City University, Osaka

*The Magnetic Susceptibility of Iodine in Various Solvents**

By Michio KONDO, Michihiko KISHITA, Masao KIMURA and Masaji KUBO

(Received October 25, 1955)

According to studies made by Bhatnagar and Lakra[1], iodine dissolved in cyclohexane has a much smaller diamagnetism than it has in other solvents, such as benzene. It seems rather peculiar that cyclohexane is abnormal as a solvent for iodine in view of the fact that both cyclic and aliphatic saturated hydrocarbons are quite normal in their general behavior as solvents. On the other hand, benzene is surely not an indifferent solvent for iodine. As Mulliken[2] has already clearly pointed out, iodine forms a molecular complex with benzene, the latter playing a role of a π donor ($b\pi$) while the former that of a halogenoid σ acceptor ($x\sigma$). By this conception, he could explain the finite electric moment of iodine in benzene and the charge-transfer spectra observed for a number of cases of similar complex formation.

The present writers have therefore undertaken to carry out the measurements of the magnetic susceptibility of iodine in various solvents in order to examine whether it depends upon the kinds of solvents to any appreciable degree, and if so, in what solvents iodine has an abnormal diamagnetism. The diamagnetism of differently colored solutions of iodine has already been studied by Courty[3], who believed that the magnetic susceptibilities of violet and brown solutions of iodine obey the additivity rule, while red and red-brown solutions do not. His results will be discussed critically in the present paper.

Apparatus and Experimental Procedure

A simple Gouy magnetic balance was employed for the determination of magnetic susceptibility at room temperature. The sample tube made of hard glass was symmetrical in form. It was 22 cm. long with a partition in the middle forming two compartments. The one compartment was filled with the solvent, while the solution under investigation was placed in the other compartment. The cross-sectional area of the liquid column amounted to 0.22 cm^2. The cell was suspended between the poles of a magnet from a semi-microbalance capable of determining weight changes as small as 0.01 mg. The electromagnet could be supplied with a direct current of up to 17 amp. taken from selenium rectifiers, ripples having been removed by means of a system of condensers. The rectifiers were fed from a 200-volt, three-phase alternating current source stabilized with an appropriate voltage stabilizer and led through suitable transformers before it was applied to the rectifiers. The total resistance of the coil of the electromagnet was less than 3 ohms. Each tip of the pole pieces separated by 1.2 cm. had a circular surface plane of 3 cm. in diameter. The resulting magnetic field could be raised up to about 24,000 oersteds.

The magnitude of the downward force f acting on the tube along its length is given by the expression,

$$f=\frac{1}{2}(\kappa-\kappa_a)AH^2=g\Delta w,$$

where κ and κ_a denote respectively the volume susceptibility of the liquid in one compartment and that of the air in the other compartment of the tube. A is the cross-sectional area of the liquid column, g the gravitational constant, and Δw the apparent increase in weight of the tube on application of the magnetic field. The magnetic balance was calibrated with distilled water and its magnetic susceptibility per cubic centimeter, which is practically identical with that per gram, was set equal to -0.720×10^{-6}. The susceptibility κ per unit volume of the solution under investigation was calculated from

$$\frac{\kappa-\kappa_a}{\kappa_o-\kappa_a}=\frac{\Delta w}{\Delta w_o},$$

where the suffix o refers to water used as the standard, and the volume susceptibility of air κ_a was put equal to $+0.0295\times10^{-6}$. For greater accuracy, a differential method was employed, viz., actual measurements were made of $\kappa-\kappa_o$ rather than $\kappa-\kappa_a$. Due correction was made of the force acting on the glass container because of its possible asymmetry by a blank test with the empty tube. The density of each solution was measured in order to convert the susceptibility per unit volume κ into that per unit weight $\chi=\kappa/\rho$.

Materials

Iodine was purified twice by sublimation. Hexane, benzene, toluene, ethyl alcohol, and carbon disulfide used as solvent were prepared according

* Read before a meeting of the Chemical Society of Japan held on October 14, 1955.

1) S.S. Bhatnagar and C.L. Lakra, *Indian J. Phys.*, 8, 43 (1933). See also P.W. Selwood, "*Magnetochemistry*," Interscience Publishers, Inc., New York, 1943, p. 66.

2) R.S. Mulliken, *J. Am. Chem. Soc.*, 72, 600 (1950); 74, 811 (1952); *J. Phys. Chem.*, 56, 801 (1952).

3) C. Courty, *Compt. rend.*, 204, 1248 (1937); *Bull. soc. chim. France*, 5, 84 (1938).

to the procedure given by Weissberger[4]. Special precaution was taken against the possible contamination of ferromagnetic impurities in the experimental materials.

Results

The diamagnetic susceptibilities of the solutions of iodine in various solvents are plotted against the weight fraction w of the solute in Fig. 1. It will be seen that the

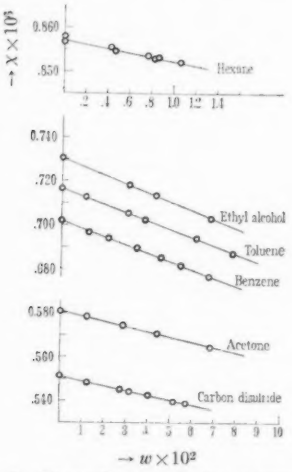

Fig. 1. Dependence of the diamagnetic susceptibilities per gram of solutions of iodine in various solvents upon the weight fraction of the solute.

experimental points lie on a straight line for each solvent over the whole range of concentrations investigated. In other words, the susceptibility of the solutions χ_{12} obeys a simple formula,

$$\chi_{12}=\chi_1(1-w)+\chi_2 w,$$

where suffixes 1 and 2 refer to the solvent and the solute respectively. The susceptibility of iodine in various solvents could be evaluated from the slope of the straight lines and are given in Table I.

TABLE I

MAGNETIC SUSCEPTIBILITY PER GRAM OF IODINE IN VARIOUS SOLVENTS

Solvent	$\chi \times 10^6$	Bhatnagar	Color
Hexane	−0.363		violet
Cyclohexane		−0.35	violet
Carbon disulfide	−0.337	−0.50	violet
Benzene	−0.334	−0.51	red
Toluene	−0.341		red
Ethyl alcohol	−0.329		brown
Acetone	−0.344		brown
(Iodine crystal)	−0.350~0.36		

4) A. Weissberger and E. Proskauer, "Organic Solvents", Oxford at the Clarendon Press, 1935.

The accuracy of the magnetic susceptibility of a solute depends upon the precision of the measurement of magnetic susceptibilities of the solutions as well as on the concentration range available. The probable error of the present data is estimated to be less than a few percent except that in hexane which may amount to several percent owing to the small solubility. The solubility of iodine in cyclohexane is almost as small as in hexane.

The susceptibility* of iodine in crystalline state is reported to be −0.36[5] or −0.350[6] at room temperature.

Discussion

The present authors have found no such remarkable dependence of the susceptibility upon solvents as has been reported by Bhatnagar and Lakra and by Courty. And yet a slightly lower value of susceptibility was observed for all employed solvents other than hexane in which iodine assumes a susceptibility value practically identical with that in a crystal.

Bhatnagar and Lakra[1] using a modified Quincke's method obtained the susceptibility values given in the third column of Table I. The striking difference between their results and the present writers' is that Bhatnagar and Lakra found a very high diamagnetism in benzene and in carbon disulfide while the present writers did not. As is mentioned later, one has good reason to believe it is unlikely that the diamagnetism of iodine in solutions is greater than that in pure phase.

Courty[2] used the following solvents for dissolving iodine: carbon tetrachloride, chloroform, and carbon disulfide (violet solutions), ethyl ether (brown solution), and benzene and toluene (red solutions). He found an increasing deviation from the additivity rule as the color changed from violet into red. The additivity of magnetic susceptibility implies two points, first the linear dependence of the susceptibility per unit weight of the solution upon the weight fraction of the solute and second the identity of the susceptibility of the solute in solutions with that of the pure phase. As regards the first, the present writers' data are in conformity for all the solvents employed. Courty's experimental points, on the other hand, are scattered about the respective straight lines to such a great extent that his conclusions concerning the additivity rule seem difficult to be accepted. As to the second point, the

* Susceptibility values are given in unit 10^{-6}.

5) International Critical Tables, VI.

6) S.R. Rao and H.S. Venkataramiah, *Current Sci.* (India), **14**, 195 (1945); *Chem. Abstr.*, **40**, 258 (1946).

diamagnetism of iodine which was found by the present writers in solutions other than hexane solution is slightly smaller than that in hexane or in pure phase. Even a violet-colored carbon disulfide solution gave a result nearly identical with that in benzene solution. The deviations found by Courty for brown and red solutions are of the same sign as in the present investigation but much greater in magnitude, whereas the deviations found by Bhatnagar and Lakra for benzene and carbon disulfide are of the opposite sign. They are also great, as has already been mentioned. In order to lend support to the present writers' results, the following theoretical calculation was carried out of the change of diamagnetism of iodine on dissolution in benzene.

Benesi and Hildebrand[7], using spectroscopic methods, have shown definitely that benzene and iodine form a 1:1 complex of considerable stability. They found that 60 percent of iodine dissolved in benzene is present in the complex. On the other hand, the close agreement in form and intensity between the spectrum of iodine in the vapor state and in violet solutions indicates that complexes are not formed in these.

Mulliken[2] developed a theory of molecular complexes based on the concept of charge-transfer. He discussed the structure of the complex of iodine with benzene (Bz) in terms of resonance between a predominant no-bond structure (Bz, I_2) and a small admixture of the type (Bz^+–I_2^-). From Fairbrother's[8] data of the moment of iodine in benzene and the overlap integral estimated for the most probable model of the complex, Mulliken calculated the ionic character of the complex in the ground state to be approximately 2.8 percent. The susceptibility of the complex in the hypothetical no-bond state may be assumed to be equal to the sum of the susceptibilities of its component parts. The diamagnetism of the dative structure was estimated in the following way. The principal susceptibility of benzene normal to the plane of the ring ($K_3=-91.2$) is more than twice that in the plane ($K_1=K_2=-37.3$)[9]. The loss of one out of six π-electrons of benzene to form Bz^+ will lead to the decrease of molal diamagnetism of the order of magnitude $(1/3)(1/6)\Delta K=3.0$, where the factor 1/3 was introduced to take into account all the possible orientations of the plane of the benzene ring in space. It would be more desirable to calculate the diamagnetic contribution of an electron in the highest occupied orbital of a benzene molecule by means of molecular orbital treatment. However, noticeable improvement is not to be expected in view of the uncertainty of other data[10]. The increase of diamagnetism of I_2 due to the gain of an electron to form I_2^- may be approximated by the difference between the diamagnetism of I^- and Pascal's constant for I, $50.6-44.6=6.0$*. Therefore with due regard to the constitutive correction constant ($+4.1$*) for C–I bond formation, the increase of molal susceptibility of the complex (Bz^+–I_2^-) over that of (Bz, I_2), i.e., the decrease of diamagnetism was calculated as $3.0-6.0+4.1=1.1$. It is doubtful whether this figure is really significant in view of the accumulated errors for a small difference. However, it would seem that the decrease of diamagnetism of iodine on dissolution in benzene should be very small, if at all, because the contribution of the dative structure is only 2.8 percent and in addition only 60 percent of iodine is present in the complex.

Summary

The diamagnetic susceptibility per gram of iodine in solutions of various solvents was measured with a Gouy magnetic balance at room temperature. The value -0.363×10^{-6} in hexane solution was practically identical with that of iodine in pure phase. The values of diamagnetism of iodine in carbon disulfide, benzene, toluene, ethyl alcohol, and acetone ranging from -0.329 to -0.341 are only slightly smaller than the value in hexane, in disagreement with the data found in literatures. A qualitative support for the present writers' result was afforded by theoretical considerations based on Mulliken's theory of complexes formed in accordance with the mechanism of electron transfer from a donor molecule to an acceptor.

We express our appreciation to the Ministry of Education for the financial support of this research.

Chemical Department, Faculty of Science
Nagoya University, Nagoya

7) H.A. Benesi and J.H. Hildebrand, *J. Am. Chem. Soc.*, **70**, 2382 (1948); **71**, 2703 (1949).
8) F. Fairbrother, *Nature*, **160**, 87 (1947); *J. Chem. Soc.*, **1948**, 1051.
9) K. Lonsdale and K.S. Krishnan, *Proc. Roy. Soc. London*, A **156**, 597 (1936).
10) S. Fujii and S. Shida, This Bulletin, **24**, 242 (1951).
* These numerical data were taken from Selwood. loc. cit.

Magnetochemical Study of Hydroxyazobenzenes

By Yoshio MATSUNAGA

(Received October 21, 1955)

Introduction

Zincke[1] showed in 1884 that the product of the condensation of phenylhydrazine with α-naphthoquinone is identical with 4-benzeneazo-1-naphthol which is prepared by the coupling of diazotized aniline with 1-naphthol, so that the problem of structure immediately presented itself. Although the physical and chemical properties of 4-hydroxyazobenzenes indicate that they exist in the azophenol form, Borsche[2] succeeded to show that "2'-nitro-4-hydroxyazobenzene" (I or II) can be prepared by the following distinct methods similarly.

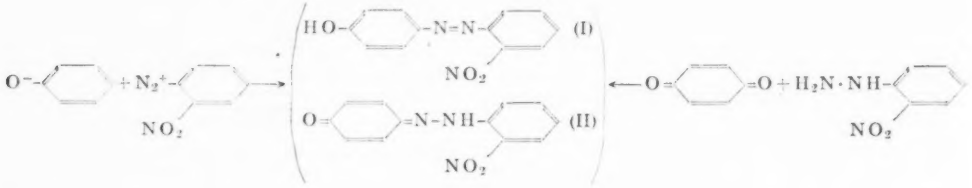

Furthermore, evidence of the quinonoid character of 2', 4'-dinitro-4-hydroxyazobenzene was provided by its ability to undergo the Diels-Alder reaction[3]. In spite of many researches, the investigators came to the different conclusions in regard to the structure of 2-hydroxyazobenzene; e. g. Kuhn and Bär[4] believed that the spectroscopic evidence favors the benzenoid structure, but on the other hand, Burawoy and Markowitsch[5] suggested that the same evidence favors the quinonoid structure.

These studies are merely concerned with the dissolved state of hydroxyazobenzenes. We can not decide conclusively the structure in the solid state. Diamagnetic susceptibility measurements seem to be of great service in deciding the forms of these compounds, as the azophenol form is made of the benzenoid structures, while the quinonehydrazone form contains the quinonoid structure. In such a case, a large difference between the susceptibilities of these two forms is expected. From this point of view, Pascal[6] examined the molar susceptibilities of some compounds, and compared them with the ones calculated from his own empirical constants. But his results quoted in Table I seem to be unplausible, as they are not consistent with the other evidences, and allowed the equilibrium between two forms in the solid state, and the migration of alkyl groups. Namely he concluded that 4-hydroxyazobenzene is quinonehydrazone form, and 4-methoxyazobenzene and 1-benzeneazo-2-naphthol are mixture of tautomers.

TABLE I

MOLAR SUSCEPTIBILITIES OF HYDROXYAZOBENZENES AND THEIR RELATED COMPOUNDS GIVEN BY PASCAL

Substance	Molar Suscept. $(-\chi_M)$*		
	obs.	calcd. (a)**	calcd. (b)**
4-Hydroxyazobenzene	99.6	117.3	95.0
4-Methoxyazobenzene	118.8	129.1	107.6
1-Benzeneazo-2-naphthol	140.7	153.7	124.8
4, 4'-Dimethoxyazobenzene	147.5	146.9	117.8
4, 4'-Diethoxyazobenzene	171.4	170.6	141.3
4-Aminoazobenzene	118.4	118.8	103.7

* Susceptibility values have been multiplied by 10^6 throughout this paper.

** (a) Azophenol form, (b) Quinonehydrazone form.

For the determination of the structures of hydroxyazobenzenes from the susceptibility measurement, it is necessary to reexamine the molar susceptibilities of azobenzene and its derivatives which have no tautomeric forms, and establish the empirical method to estimate them correctly.

1) T. Zincke and H. Bindewald, *Ber.*, **17**, 3026 (1884).
2) W. Borsche, *Ann.*, **357**, 171 (1907).
3) W.M. Lauer and S.E. Miller, *J. Am. Chem. Soc.*, **57**, 180 (1933).
4) R. Kuhn and F. Bär, *Ann.*, **516**, 143 (1935).
5) A. Burawoy and I. Markowitsch, ibid., **503**, 180 (1933).
6) P. Pascal, *Compt. rend.*, **150**, 1167 (1910), *Bull. soc. chim. France*, **9**, 868 (1911), *Ann. chim. phys.*, **25**, 289 (1912).

Experimental

Materials.—No. 1–10, 19 and 30 were kindly provided by Drs. F. Iimura and M. Kobayashi. No. 11–18 and 20–27 were prepared by the coupling of diazotized aniline or its substituted derivatives with phenol or *p*-cresol, and purified by recrystallization from aqueous ethanol or benzene, and finally by distillation or sublimation in vacuo. No. 28 and 29 were synthesized by the alkali fusion of nitrophenol[7] and recrystallized from aqueous ethanol. No. 28 was sublimed finally in vacuo. Their melting points are presented in Tables II and III.

Magnetic Measurement.—The susceptibilities were measured using a Gouy balance as previously described[8].

Results and Discussion

The results are shown in Table II for azobenzene and its derivatives which have unquestionable form and in Table III for hydroxyazobenzenes. The molar susceptibility of azobenzene has been found to be -111.3 by Pascal[9], while it is -105.0 by Banerjee[10]. Our result supports the latter value, so that Pascal's constitutive correction constant for azo-group 1.8 is not appropriate for the estimation of molar susceptibilities of the other compounds of which the structures will be discussed in this paper. We assumed that the molar susceptibilities are given by the sum of those of constitutional fragments of the molecules. For instance, we assumed that the azophenol form of 4-hydroxyazobenzene is built up from benzene, phenol, and azo-group by the loss of two atoms of hydrogen, and the molar susceptibility is given by the same relation too. Similar computations have been done for the compounds shown in Table II, and the mean value -0.4 has been obtained for the contribution of azo-group. Then the calculated values in Tables II and III have been estimated by the combination of this constant for azo-group and the molar susceptibilities of benzene and its derivatives; the following values were used, benzene -55.2[11], toluene -65.8[12], anisol -72.6[13], dimethylaniline -85.0[13], chlorobenzene -70.0[14], acetophenone -71.6[13], ethyl benzoate -93.3[15], nitrobenzene -61.8[12], phenol -60.8[13], *p*-cresol -71.4[16], resorcinol -67.9[17]. The accordance between the observed and the calculated molar susceptibilities is satisfactorily good within the limit of experimental errors. As the effect of substituents to single benzene nucleus is taken into consideration in our estimations, our calculated values are more compromising for these compounds than the ones obtained by the direct summation of Pascal's constants. For instance, Angus[15] and Trew[18] showed that methyl substitution in the aromatic nucleus gives a diamagnetic increment about one unit lower than the normal CH_2 increment of -11.7; furthermore, French[17] deduced that the isomerides of disubstituted benzenes possess different susceptibilities respectively. Even in our case, the interaction of substituents through an azo-group is not considered, so the results in Table show that the method is not adequate in a few cases.

Table II

Susceptibilities of Azobenzene and Its Derivatives

No.	Substance	M. p.	Suscept. ($-\chi$)	Molar Suscept. ($-\chi_M$) obs.	calcd.
1	Azobenzene	67.5–68.5	0.578	105.3	104.9
2	4-Methyl-	69–69.5	0.590	115.8	115.5
3	2-Methoxy-	39–40	0.574	121.9	122.3
4	4-Methoxy-	55	0.575	122.0	122.3
5	4-Dimethylamino-	115–115.5	0.594	133.8	134.7
6	4-Chloro-	87	0.551	119.4	119.7
7	4-Acetyl-	113–114	0.535	122.1	121.3
8	4-Carboethoxy-	86	0.568	144.4	143.0
9	4-Nitro-	133–134	0.492	111.7	111.5
10	4,4'-Dimethoxy-	162	0.574	139.0	139.7

For the quinonehydrazone form of 4-hydroxyazobenzene, the molar susceptibility

7) R. Willstätter and M. Benz, *Ber.*, **39**, 3492 (1906).
8) H. Akamatu and Y. Matsunaga, This Bulletin, **26**, 364 (1953).
9) P. Pascal, *Bull. soc. chim. France*, **9**, 79 (1911).
10) S. Banerjee, *Z. Krist.*, **A 100**, 316 (1939).
11) B.C. Eggleston et al., *J. Chem. Soc.*, **1954**, 941.
12) F.G. Baddar and S. Sugden, ibid., **1950**, 308.
13) "International Critical Tables", Vol. 6, McGraw-Hill Book Co. Inc., New York, 1929, p. 362.
14) C.M. French and V.C.G. Trew, *Trans. Faraday Soc.*, **41**, 439 (1945).
15) W.R. Angus, *Bull. soc. chim. France*, **1949**, D 483.
16) estimated.– 65.8 (toluene) – 60.8 (phenol) + 55.2 (benzene).
17) C.M. French, *Trans. Faraday Soc.*, **41**, 676 (1945).
18) V. C. G. Trew, ibid., **49**, 604 (1953). See also, C.M. French, ibid., **50**, 1329 (1954).

is estimated as −102.2 by the following schematic chemical equation,

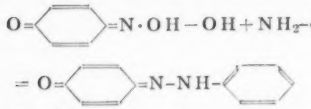

The values used in the above equation are −50.3 for *p*-benzoquinonemonoxime[13], −62.4 for aniline[12], and Pascal's constants for hydrogen and oxygen in alcohol. Consequently the difference of susceptibility between these two forms is expected to be 8.3 in 4-hydroxyazobenzene. Our calculated difference is remarkably smaller than that expected from the calculated molar susceptibilities for two isomeric forms given by Pascal. Although there is no experimental result which can compare with these two expected differences, comparison will be drawn in the later paper on the azo-derivatives of naphthols. For the other compounds, the data on substituted anilines and quinonemonoximes required by the estimation of molar susceptibility for the quinonehydrazone form are not always available, but the susceptibility difference between these two forms may be nearly constant.

The observed molar susceptibilities of all compounds in Table III are in accordance with the calculated values for the azophenol form, so that there can be no doubt that these hydroxyazobenzenes are in the azophenol form in the solid state. At first glance, the discrepancy in 2,2′-dihydroxyazobenzene is seriously large, but molar susceptibility of this compound is only 3.3 units higher than that of 4,4′-dihydroxyazobenzene. In the isomerides of dihydroxybenzene, molar susceptibility of catechol is 2.3 units more diamagnetic than the value for hydroquinone, so the difference between these two dihydroxyazobenzenes may be of probable magnitude, and the calculated values seem to be too small in these cases.

In the *ortho*-compounds, hydrogen bond undoubtedly exists between the nitrogen and oxygen atoms, but the effect of hydrogen bond to the molar susceptibility is not detectable in these compounds either[19]. Furthermore, the position of the proton between the nitrogen and oxygen atoms may not be the same in the tautomeric forms[20], because the observed susceptibility does not deviate so much from the value calculated for azophenol form.

TABLE III

SUSCEPTIBILITIES OF HYDROXYAZOBENZENES

No.	Substance	M. p.	Suscept.	Molar Suscept. ($-\chi_M$)	
			($-\chi$)	obs.	calcd
11	4-Hydroxy-	152	0.555	110.0	110.5
12	4′-Methyl-4-hydroxy-	150	0.569	120.8	121.1
13	2′-Methoxy-4-hydroxy-	145–146	0.558	127.4	127.9
14	4′-Methoxy-4-hydroxy-	137–139	0.559	127.6	127.9
15	4′-Chloro-4-hydroxy-	153–155	0.537	125.0	125.3
16	2′-Nitro-4-hydroxy-	160–161	0.478	116.2	117.1
17	3′-Nitro-4-hydroxy-	157.5–158.5	0.483	117.4	117.1
18	4′-Nitro-4-hydroxy-	213	0.477	116.0	117.1
19	2-Hydroxy-	81–82	0.559	110.8	110.5
20	5-Methyl-2-hydroxy-	105–107	0.569	120.8	121.1
21	2′,5-Dimethyl-2-hydroxy-	97–98	0.594	134.4	131.7
22	4′,5-Dimethyl-2-hydroxy-	111–112	0.582	131.7	131.7
23	2′-Methoxy-5-methyl-2-hydroxy-	119	0.577	139.8	138.5
24	4′-Methoxy-5-methyl-2-hydroxy-	94–95	0.577	139.8	138.5
25	4′-Chloro-5-methyl-2-hydroxy-	152	0.551	135.9	135.9
26	3′-Nitro-5-methyl-2-hydroxy-	162–163	0.496	127.6	127.7
27	4′-Nitro-5-methyl-2-hydroxy-	181–183	0.503	129.4	127.7
28	2.2′-Dihydroxy-	165–167	0.568	121.7	116.1
29	4,4′-Dihydroxy-	decomp.	*	118.4**	116.1
30	2,2′,4,4′-Tetrahydroxy-	decomp.	0.537	132.2	130.3

* Monohydrate 0.566.

** 131.4 (Monohydrate)−13.0 (water).

19) P. Rumpf and M. Séguin, *Bull. soc. chim. France*, 1949, D366, 1950, 177, 542.

20) G.W. Wheland, "Advanced Organic Chemistry" John Wiley & Sons, Inc., New York, 1949, p. 628.

The observed molar susceptibilities of azo-derivatives of phenol are smaller than the calculated values in many cases. This decrease of diamagnetism will be interpreted by the resonance effect indicated in the structure (III).

(III)

Such an effect will be strengthened by the electron withdrawing substituents, and 2′- and 4′-nitro-derivatives are examples of this. In the azo-derivatives of *p*-cresol, methyl group will perturb such an effect to some extent, so that in some cases the observed values are more diamagnetic than the calculated ones. But we will not discuss in detail these apparent discrepancies on accounts of the complicated influence of substituents and the rather large experimental errors.

Summary

The magnetic susceptibilities of azobenzene and its nine derivatives were measured by the Gouy method. The procedure to estimate the molar susceptibility from the values observed for constitutional fragments of the molecule was applied to these compounds, and the empirical constant for azo-group −0.4 was determined. Twenty hydroxyazobenzenes, mainly derivatives of phenol and *p*-cresol, were also measured, and their molar susceptibilities were compared with the calculated values for the azophenol form and the quinonehydrazone one. The author concluded that they are all in the azophenol form in the solid state.

The author expresses his hearty thanks to Prof. H. Akamatu for his interest and to Drs. F. Iimura and M. Kobayashi for samples of many substances investigated. The cost of this research has been defrayed by the Grant in Aid for Scientific Research from the Ministry of Education, to which the author's thanks are due.

Department of Chemistry, Faculty of Science, The University of Tokyo
Tokyo

Absorption Spectra of Co(III) Complexes. II. Redetermination of the Spectrochemical Series

By Yoichi SHIMURA and Ryutaro TSUCHIDA

(Received October 27, 1955)

In the course of our studies on thec urve analyses of absorption spectra[1], the absorption curves of many Co(III) complexes have been determined. In the present paper, experimental details will be given for the cobaltic ammine, oxalato, carbonato and amino-acido complexes. Moreover, the "spectrochemical series" will be redetermined on the basis of the new data.

Experimental

Absorption measurements were made in aqueous solutions by a Beckman DU spectrophotometer, or by a spectrograph with a sector photometer. The concentration of the solutions varied from 1.0×10^{-2} to 3.3×10^{-5} gram complex-ion per litre. All measurements were made at room temperature. The complex perchlorates were used to minimize interaction between the complex ion and anions. The complexes were analyzed for water of crystallization and for perchlorate ion[2]. The results of the measurements are shown in

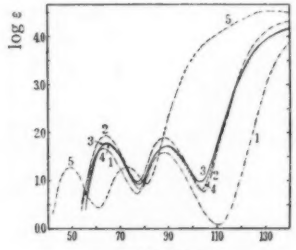

Fig. 1. Absorption curves of:
1, $[Co(NH_3)_6](ClO_4)_3$;
2, $[Co\ en_3](ClO_4)_3$;
3, *cis*-$[Co\ en_2(NH_3)_2](ClO_4)_3\cdot H_2O$;
4, *trans*-$[Co\ en_2(NH_3)_2](ClO_4)_3\cdot H_2O$;
5, $[Co(O_6Mo_6O_{18}H_6)](NH_4)_3\cdot 7H_2O$.

1) Part I of this series: Y. Shimura and R. Tsuchida, This Bulletin, 28, 572 (1955).

2) M. Linhard and G. Stirn, *Z. anorg. Chem.*, 268, 105 (1952).

Figs. 1-5. The numerical data for the first and the second absorption bands were previously reported[1].

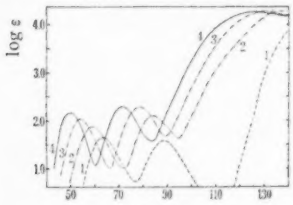

Fig. 2. Absorption curves of Co (III) ammine-oxalato series:
1, $[Co(NH_3)_3](ClO_4)_3$;
2, $[Co(NH_3)_4\ ox]\ ClO_4 \cdot H_2O$;
3, $[Co(NH_3)_2\ ox_2]\ NH_4 \cdot H_2O$;
4, $[Co\ ox_3]\ K_3 \cdot 3H_2O$.

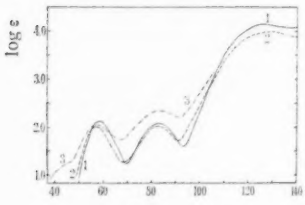

Fig. 3. Absorption curves of Co(III) carbonato complexes:
1, $[Co\ en_2\ CO_3]\ ClO_4$;
2, $[Co(NH_3)_4\ CO_3]\ ClO_4$;
3, $[Co(NH_3)_4\ CO_3]\ ClO_4$ (solution after standing three hours at room temperature).

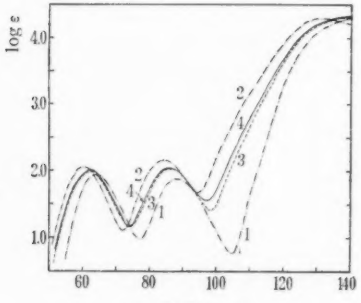

Fig. 4. Absorption curves of:
1, $[Co\ en_3]\ (ClO_4)_3$;
2, $[Co\ en_2\ ox]\ Cl \cdot 3H_2O$;
3, $[Co\ en_2\ glycine']\ (ClO_4)_2$;
4, $[Co\ en_2\ leucine']\ (ClO_4)_2$.

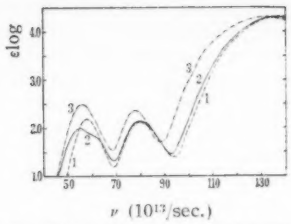

Fig. 5. Absorption curves of amino-acido complexes of Co(III);
1, β-$[Co\ glycine'_3] \cdot H_2O$;
2, α-$[Co\ glycine'_3] \cdot 2H_2O$;
3, [Co edta] $Na \cdot 4H_2O$.

Description of the Individual Complexes

α-$[Co(glycine')_3] \cdot 2H_2O$ and β-$[Co(glycine')_3] \cdot H_2O$.—For the preparations, the method of Ley and Winkler[3] was followed. The α-form has purple color and the β-form red. These two forms correspond to geometric isomers, *cis-cis* and *cis-trans* forms. The β-isomer was insoluble in water and the spectrum of the isomer was measured in 60% $HClO_4$. As will be seen in Fig. 5, the main difference between the curves of the two isomers occurred in the region of the first band: the first band of the β-form is normal but the α-form shows distinct indication of splitting of the first band. This splitting may be considered as a proof for the *cis-trans* structure of the α-form. since the similar splitting was reported for the first band of *trans*-$[Co(NH_3)_4(OCOCH_3)_2]\ ClO_4$ and not for the first band of the corresponding *cis* isomer[4].

$[Co\ en_2 glycine'](ClO_4)_2$ and $[Co\ en_2\ leucine'](ClO_4)_2$.—These perchlorates were prepared by adding concentrated aqueous solution of $NaClO_4$ and alcohol to the solutions of the corresponding chlorides[5]. They were twice recrystallized from water-alcohol mixture, and washed by alcohol and dried in air. The absorption curves of the two complexes have almost the same features.

$[Co(NH_3)_4CO_3]ClO_4$[6].—The tetrammine complex was unstable in aqueous solutions. The decomposition intermediates have more hyperchromic and more diffuse bands than the original tetrammine complex (see Fig. 3). The bisethylenedaimine complex was very stable in aqueous solutions

cis- and trans-$[Co\ en_2(NH_3)_2](ClO_4)_3 \cdot H_2O$.—These were precipitated from the concentrated

3) H. Ley and H. Winkler, *Ber.*, **42**, 3894 (1909); H.F. Holtzclaw, Jr. and D.P. Sheetz, *J. Am. Chem. Soc.*, **75**, 3053 (1953).
4) M. Linhard and M. Weigel, *Z. anorg. Chem.*, **264**, 321 (1951).
5) J. Meisenheimer, L. Angermann and H. Holsten, *Ann.*, **438**, 261 (1924); I. Lifschitz, *Rec. trav. chim.*, **58**, 785 (1939).
6) M. Linhard and M. Weigel, *Z. anorg. Chem.*, **260**, 65 (1949).

solutions of the corresponding chlorides[7] by addition of 60% $HClO_4$, and were recrystallized twice from water and dried in air. The freshly dried crystals were analyzed since they effloresced on exposure to the air.

[Co $(NH_3)_5$]$(ClO_4)_3$, [Co en_3]$(ClO_4)_3$, [Co en_2 CO_3] ClO_4 [Co en_2 ox] $Cl \cdot 3H_2O$, NH_4[Co ox_2 $(NH_3)_2$]$\cdot H_2O$, K_3[Co ox_3]$\cdot 3H_2O$ and Na [Co edta]$\cdot 4H_2O$ were prepared essentially by the method described in literature.

Spectrochemical Series for the Ligands of Co (III) Complexes

The spectrochemical series represents the order of hypsochromic effects of ligands on the first or second absorption band of metallic complexes. During about the two decades which have elapsed since the first determination of the series by Tsuchida[8], a great deal of new measurement has been made by many authors. Examining the data found in literature as well as in the author's measurements, revision of the series for the ligands of Co(III) complexes has been attempted.

In Table I to VI, the ligands have been arranged in the order of frequencies of the first bands of their comlexes.

Abbreviations and Conventions i) An unidentate ligand is designated by the full formula. The atom which is attached directly to the central cobalt atom takes precedence of the other atoms; for example, chromate ion, $OCrO_3^=$; unidentate oxalate ion, $OCOCO_2^=$.

TABLE I

PENTAMMINE SERIES, [Co $(NH_3)_5$ A]

Ligand, A	First band ν (log ε)	Second band ν (log ε)	Ref.	Supplementary refs.
NO_2^-	65.5 (2.00)	(( ))	Linhard (1951)[9]	10, 11, 16)
$SO_3^=$	63.6 (2.15)	(( ))	Kiss (1938)[10]	17)
NH_3	62.9 (1.68)	88.3 (1.60)	12)	10, 11, 13, 14, 15)
OH_2	61.6 (1.62)	87.5 (1.62)	Kuroya (1950)[11]	10, 15)
ONO^-	61.1 (1.86)	(( ))	Linhard (1955)[18]	11, 16)
NCS^-	60.5 (2.24)	(( ))	19)	10, 18, 20, 21)
ONO_2^-	60.0 (1.77)	86.6 (1.77)	19)	10)
$OSO_3^=$	60.0 (1.70)		8)	
$OCHO^-$	59.7 (1.77)	85.3 (1.65)	Linhard (1951)[4]	
OH^-	59.6 (1.80)	81.1 (1.85)	Kiss (1938)[10]	
$OCOCH_3^-$	59.6 (1.82)	85.2 (1.70)	Linhard (1951)[4]	
$OCONH_2^-$	59.4 (1.85)	84.9 (1.70)	Linhard (1951)[4,22]	
$OCOCO_2^=$	59.2 (1.87)	(( ))	8)	17)
$OCO_2^=$	59.2 (1.92)	(( ))	Kiss (1938)[10]	17)
$SSO_3^=$	58.8 (1.82)	(( ))	19)	10, 23)
F^-	58.4 (1.70)	84.8 (1.63)	Linhard (1951)[22]	
N_3^-	57.8 (2.41)	(( ))	Linhard (1951)[24]	
Cl^-	56.2 (1.71)	82.5 (1.72)	Linhard (1951)[22]	10, 11, 14, 15)
$OCrO_3^-$	55.6 (2.14)	(( ))	8, 25)	17)
Br^-	54.7 (1.77)	(( ))	Linhard (1951)[22]	
I^-	51.8 (1.90)	(( ))	Linhard (1951)[22]	

7) A. Werner, *Ann.*, **386**, 1 (1912); A. Werner, F. Bräunlich, E. Rogowina and C. Kreutzer, ibid., **351**, 65 (1907).
8) R. Tsuchida, This Bulletin, **13**, 388, 436 (1938).
9) M. Linhard and M. Weigel, *Z. anorg. Chem.*, **267**, 113 (1951).
10) A. Kiss and D. Czeglédy, *Z. anorg. Chem.*, **235**, 407 (1938).
11) H. Kuroya, *J. Inst. Polytech. Osaka City Uuiv.*, C **1**, No. 1, 29 (1950).
12) This paper.
13) M. Linhard, *Z. Elektrochem.*, **50**, 224 (1944).
14) H. Kuroya and R. Tsuchida, This Bulletin, **15**, 427 (1940).
15) R. Tsuchida, *J. Chem. Soc. Japan*, **59**, 731 (1938).
16) B. Adell, *Z. anorg. Chem.*, **271**, 49 (1952).
17) H. Yoneda and M. Kobayashi, *J. Chem. Soc. Japan*, **75**, 1192 (1954).
18) M. Linhard, H. Siebert and M. Weigel, *Z. anorg. Chem.*, **278**, 287 (1955).
19) Y. Shimura, unpublished data.
20) R. Tsuchida, *J. Chem. Soc. Japan*, **59**, 586 (1938).
21) Y. Shimura, *J. Am. Chem. Soc.*, **73**, 5079 (1951).
22) M. Linhard and M. Weigel, *Z. anorg. Chem.*, **266**, 49 (1951).
23) A. Kiss, G. Auer and E. Major, *Z. anorg. Chem.*, **246**, 28 (1941).
24) M. Linhard and M. Weigel, *Z. anorg. Chem.*, **267**, 121 (1951).
25) R. Tsuchida and M. Kobayashi, This Bulletin, **13**, 471 (1938).

TABLE II

Cis SERIES OF TETRAMMINE COMPLEXES

Ligand	First band ν (log ε)	Second band ν (log ε)	Ref.	Supplementary refs.
NO_2^-	67.5 (2.20)	(( ))	Linhard (1951)[9]	11, 14, 26)
$SO_3^=$	65.9 (2.26)	(( ))	27)	
NH_3	62.9 (1.68)	88.3 (1.60)	12)	
OH_2	60.0 (1.40)	84.0 (1.49)	28)	10)
ONO^-	58.8	(( ))	Yalman[53]	
ox	58.7 (1.91)	84.0 (2.11)	12)	10, 11, 14, 17)
ONO_2^-	58.5 (1.7)	85 (1.6)	19)	
$OCHO^-$	58.2 (1.94)	82.5 (1.69)	Linhard (1951)[4]	
carb	57.4 (2.01)	82.6 (2.02)	12)	10, 11, 14)
$OCOCH_2^-$	57.3 (2.01)	82.0 (1.77)	Linhard (1951)[4]	
F^-	57.3 (1.74)	81.9 (1.51)	Linhard (1952)[29]	
N_3^-	55.7 (2.42)	(( ))	Linhard (1951)[24]	

TABLE III

Cis SERIES OF BISETHYLENEDIAMINE COMPLEXES

Ligand	First band ν (log ε)	Second band ν (log ε)	Ref.	Supplementary refs.
NO_2^-	69.0 (2.26)	(( ))	Adell (1951)[30]	14, 26)
$SO_3^=$	67.1 (2.35)	(( ))	19)	
ONO^-	65.9 (2.13)	(( ))	Adell (1951)[30]	
NH_3	64.4 (1.79)	89.4 (1.74)	12)	26)
en	63.9 (1.94)	88.4 (1.90)	12)	
gly	61.3 (2.00)	86.4 (2.04)	12)	
NCS^-	61.1 (2.53)	(( ))	19)	21, 26)
OH_2	60.6 (1.85)	84.5 (1.82)	Basolo (1950)[25]	32)
ox	60.1 (2.05)	84.3 (2.16)	12)	11, 14, 31)
$OCOC_2H_5^-$	59.4 (2.16)	82.7 (1.91)	Linhard (1951)[4]	
carb	58.4 (2.13)	83.0 (2.09)	12)	14)
OH^-	58* (1.97)*	81* (2.01)*	Bjerrum (1952)[32]	
Cl^-	55.9 (1.95)	76.6 (1.84)	Linhard (1952)[29]	26)
Br^-	54.3 (2.04)	(( ))	Linhard (1952)[29]	

TABLE IV

Trans SERIES OF TETRAMMINE COMPLEYXES

Ligand	First band Ia ν (log ε)	First band Ib ν (log ε)	Second band ν (log ε)	Ref.	Supplementary refs.
NO_2^-	68.2 (2.37)		(( ))	Linhard (1951)[9]	11, 14, 26, 43)
$SO_3^=$	66.6 (2.32)		(( ))	27)	
NH_3	62.9 (1.68)		88.3 (1.60)	12)	
OH_2	58.6		84.0	Yalman[53]	
$OCOCH_3^-$	54.4 (1.76)	64* (1.37)*	82.1 (1.76)	Linhard (1951)[4]	
N_3^-	52.8 (2.57)		(( ))	Linhard (1951)[24]	
Cl^-	47.7 (1.63)	63.0 (1.38)	74.8 (1.54)	Linhard (1952)[29]	28)

26) F. Basolo, *J. Am. Chem. Soc.*, **72**, 4393 (1950).
27) Y. Shimura, This Bulletin, **25**, 46 (1952).
28) R. Tsuchida, This Bulletin, **11**, 721 (1936).
29) M. Linhard and M. Weigel, *Z. anorg. Chem.*, **271**, 101 (1952).
30) B. Adell, *Acta Chem. Scand.*, **5**, 54 (1951).
31) A. Mead, *Trans. Farad. Soc.*, **30**, 1052 (1934).
32) J. Bjerrum and S. E. Rasmussen, *Acta Chem. Scand.*, **6**, 1265 (1952).

TABLE V

Trans SERIES OF BISETHYLENEDIAMINE COMPLEXES

Ligand	First band Ia ν (log ε)	First band Ib ν (log ε)	Second band ν (log ε)	Ref.	Supplementary refs.
NO_2^-	69.8 (2.27)		(( ))	Adell (1951)[33]	
NH_3	64.2 (1.77)		89.2 (1.73)	12)	11, 14, 26)
NCS^-	59.4 (2.44)		(( ))	19)	21, 26)
ONO^-	58.3 (1.72)		(( ))	Adell (1951)[33]	
$ONO_2^=$	58 (1.8)	66 (1.6)	85 (1.9)	19)	
OH^-	57* (1.72)*		79* (1.73)*	Bjerrum (1952)[32]	
$OCOC_2H_5^-$	55.7 (1.73)	67* (1.40)*	84.1 (1.80)	Linhard (1951[4])	
OH_2	55* (1.52)*	68* (1.57)*	86* (1.73)*	Bjerrum (1952)[32]	26)
$SSO_3^=$	54.9 (1.93)		(( ))	19)	23)
F^-	51.6 (1.35)	67.9 (1.49)	82.8 (1.67)	Linhard (1952)[29]	
Cl^-	48.8 (1.58)	64.9 (1.41)	77.5 (1.68)	1)	26, 29)
Br^-	45.6 (1.73)	(( ))	(( ))	Linhard (1952)[29]	
I^-	44.8	(( ))	(( ))	Ernsberger (1934)[34]	

TABLE VI

COMPLEXES CONTAINING ONLY ONE SPECIES OF LIGAND

Complex Ion	First band ν (log ε)	Second band ν (log ε)	Ref.	Supplementary refs.
$[Co(CN)_5]^{3-}$	?	?		10, 23, 26)
$[Co(C_5H_5)_2]^+$	74* (2.38)*	99* (3.04)*	Wilkinson (1952)[37]	
$[Co\ dg_3]$	(( ))	(( ))	Nakahara (1954)[38]	
$[Co\ dip_3]^{3+}$	66.7	(( ))	Yamasaki (1940)[39]	
$[Co\ phen_3]^{3+}$	66.5 (2.49)	(( ))	Yamasaki (1953)[40]	
$[Co\ pn_3]^{3+}$	64.5 (1.95)		Mathieu (1936)[41]	
$[Co\ dien_2]^{3+}$	64.2	88.0	Brigando (1953)[42]	
$[Co\ en_3]^{3+}$	63.9 (1.94)	88.4 (1.90)	12)	10, 11, 13, 14, 31)
$[Co(NH_3)_6]^{3+}$	62.9 (1.68)	88.3 (1.60)	12)	10, 11, 13, 15)
$[Co(ONO)_6]^{3-}$	62.8 (2.41)	(( ))	Kuroya (1950)[11]	10, 43)
β-$[Co\ gly_3]$	57.7 (2.20)	80.2 (2.14)	12)	
$[Co\ edta]^-$	55.9 (2.51)	78.1 (2.36)	12)	
$[Co\ acac_3]$	51.0 (2.04)	74.0 (2.47)	Sone (1948)[44]	45)
$[Co\ ox_3]^{3-}$	49.7 (2.17)	70.9 (2.30)	12)	10, 31, 46, 47)
$[Co(O_7Mo_6O_{18}H_3)]^{3-}$	49.2 (1.29)	72.8 (1.30)	1, 12, 35)	
$[Co(OH_2)_6]^{3+}$	49 (1.6)	75 (1.7)	Topp (1928)[48]	
$[Co(S_2COC_2H_5)_3]$	48.5 (2.43)	62.5 (2.56)	Kida (1955)[52]	
$[Co(S_2CNH_2)_3]$	47.2 (2.45)	62.0 (2.80)	Kida (1955)[52]	
$[Co\ carb_3]^{3-}$	46.5 (2.19)	68.2 (2.22)	Mori (1954)[47]	

33) B. Adell, *Acta Chem. Scand.*, **5**, 941 (1951).
34) M.L. Ernsberger and W.R. Brode, *J. Am. Chem. Soc.*, **56**, 1842 (1934).
35) Y. Shimura, H. Ito and R. Tsuchida, *J. Chem. Soc. Japan*, **75**, 560 (1954).
36) H. Kuroya and R. Tsuchida, *J. Chem. Soc. Japan*, **61**, 597 (1940).
37) G. Wilkinson, *J. Am. Chem. Soc.*, **74**, 6148 (1952).
38) A. Nakahara, This Bulletin, **27**, 260 (1954).
39) K. Yamasaki, This Bulletin, **15**, 130 (1940).
40) K. Yamasaki, T. Hara and M. Yasuda, *Proc. Japan Acad.*, **29**, 337 (1953).
41) J.-P. Mathieu, *Bull. soc.chim.* [5] **3**, 463 (1936).
42) J. Brigando, *Compt. rend.*, **236**, 708 (1953).
43) R. Tsuchida and S. Kashimoto, This Bulletin, **11**, 785 (1936).
44) K. Sone, I. Miyake, H. Kuroya and K. Yamasaki, *J. Chem. Soc. Japan*, **69**, 70 (1948).
45) I. Lifschitz, *Rec. trav. chim.*, **69**, 1495 (1950).
46) S. Kashimoto and M. Kobayashi, This Bulletin, **12**, 350 (1937).
47) M. Mori and M. Shibata, *J. Chem. Soc. Japan*, **75**, 1044 (1954).
48) J. Topp, Dissertation, Münster (1928): quoted in "Handbuch der Physik" XXI, p. 59 (1929).
49) K. Nakamoto, M. Kobayashi and R. Tsuchida, *J. Chem. Phys.*, **22**, 957 (1954).
50) F. Basolo, *J. Am. Chem. Soc.*, **75**, 227 (1953).
51) M. Martinette and J.C. Bailar, Jr., *J. Am. Chem. Soc.*, **74**, 1054 (1952).
52) S. Kida and H. Yoneda, *J. Chem. Soc. Japan*, **76**, 1059 (1955).
53) R.G. Yalman and T. Kuwana, *J. Phys. Chem.*, **59**, 298 (1955).

ii) Chelate and polydentate ligands are abbreviated as follows: acac, acetylacetonate ion; carb, chelate carbonate ion; dg, univalent ion of dimethylglyoxime; dien, diethylenetriamine; dip, 2, 2′-dipyridyl; edta, ethylenediaminetetraacetate ion (quadrivalent); en, ethylenediamine; gly, glycinate ion; ox, chelate oxalate ion; phen, 1, 10-phenanthroline; pn, propylenediamine.

iii) Frequency values are given by the unit of 10^{13}/sec.

iv) The bands hidden under the specific absorption bands of the ligands are indicated as (( )).

v) The data asterisked were roughly estimated from the figures of absorption curves in literature.

vi) The references collected under the column, "Supplementary Refs.", are not exhaustive or complete but may provide some information for the details.

Conclusion

From the Tables I–VI, the following series are obtained for the simple ligands:

NO_2^- $SO_3^=$ en NH_3 (ONO^-, NCS^-, OH_2) ox (ONO_2^-, $OSO_3^=$) ($OCHO^-$, OH^-, carb, $OCOR^-$) ($OCOCO_2^=$, $OCO_2^=$) $SSO_3^=$ F^- N_3^- Cl^- $OCrO_3^=$ Br^- I^- (1)

where the ligands in parentheses stand in almost the same positions. For more complicated ligands, the following series are obtained:

CN^- $C_5H_5^-$ dg (dip, phen) (dien, pn, en) NH_3 gly edta acac ox polymolybdate-ion $S_2COC_2H_5$ S_2CNH_2 carb. (2)

Miscellaneous notes

(A) Cyanate Ion.—Two broad absorption bands were reported for $K_3[Co(CN)_3]$ at 97.2 ($\log \varepsilon_{max}=2.37$) and at 117.0 ($\log \varepsilon_{max}=2.08$). Kiss and Czeglédy[10] assigned the two bands to the first and the second bands, but later Kuroya and Tsuchida[35] to the second and the third bands. More recently, Nakamoto, Kobayashi and Tsuchida[49] interpreted the effects of polar solvents no these two bands assuming that the bands are equally the specific bands due to the coordinated cyanate radicals. In view of the above condition, $[Co(CN)_3]^{3-}$ was marked by a question mark in Table VI. But it is very likely that the cyanate ion has an extraordinary high position on the spectrochemical series.

(B) Carbonate and Oxalate Ions.—The unidentate carbonate ion has a lower position on the spectrochemical series than the chelate carbonate ion. This is also true for oxalate radical. In accordance with this fact, carbonato- or oxalato- pentammine Co(III) salts are more unstable than the corresponding tetrammine salts.

(C) Methylamine.—Brigando[42] reported the following data:

	First band	Second band
$[Co(NH_3)_4(NH_2CH_3)_2]Cl_3$	61.9	86.7
$[Co(NH_3)_5]Cl_3$	62.5	88.2

The data show that methylamine stands immediately behind NH_3.

(D) Substituted Ethylenediamines.—Basolo[50] measured the absorption spectra of *trans*-dichlorobis(N- or C-alkylethylenediamine)-cobalt(III) chlorides. From the curves reported by him, it is shown that the first bands of these complexes are displaced towards the longer wave-lengths in the order of

en (C-dimethyl)-en (C, C′-tetramethyl)-en (N-methyl)-en (N-ethyl)-en (N-*n*-propyl)-en. (3)

The absorption data reported for some of the propylenediamine complexes[41,23,51] show that propylenediamine has almost the same position in relation to ethylenediamine.

(E) Pyridin.—Few data published for absorption spectra of Co(III) pyridin complexes. But judging from the data on $[Co\ py_4\ NH_3\ Cl]\ Cl_2$[14], it is certain that pyridin comes behind NH_3.

(F) Organic Acids.—Linhard[4] reported that many organic mono-acid-radicals have almost the same positions on the spectrochemical series, but that in the case of mono-, di- or tri-chloro acetic acid some blue shifts occurred in the first and second bands of the acido-pentammine or *cis*-diacido-tetrammine complexes. From the order of the blue shifts, the spectrochemical series of $OCOR^-$ is determined as follows:

$OCOR^-$: $R=CCl_3$, $CHCl_2$, CH_2Cl, CH_3 and others. (4)

Summary

The visible and ultra-violet absorption spectra of many cobaltic ammine, oxalato, carbonato and amino-acido complexes have been determined in solution.

The spectrochemical series for the ligands of Co(III) complexes has been redetermined.

Department of Chemistry, Faculty of Science, Osaka University
Nakanoshima, Osaka

Sterols and Other Unsaponifiable Substances in the Lipids of Shell Fishes, Crustacea and Echinoderms. XVII. Mono-unsaturated Sterol Components of the Starfish, Asterina Pectinifera

By Yoshiyuki TOYAMA and Toru TAKAGI

(Received November 15, 1955)

In the 16th report[1] of this series, hitodesterol, which was first separated from *Asterina pectinifera* by Matsumoto and Toyama[2], was re-examined with the result that this sterol was found to be identical with α-spinasterol. It was further indicated that a di-unsaturated C_{28}-sterol, possibly of the $\Delta^{7,22}$-type, is also present in a lesser amount in this starfish.

The present study is concerned with mono-unsaturated sterol components of this starfish. As described in the 16th report, the steryl acetate mixture of this starfish was subjected to repeated recrystallizations by which hitodesteryl acetate was eventually separated as the highest melting fraction. In the present study, the steryl acetate mixture recovered from mother liquors of these recrystallizations was fractionally crystallized, and two fractions, the fraction I of m.p. 157–158°C and the fraction II of m.p. 118–119°C, were separated. The acetate fraction I and its free sterol and benzoate were found to agree with the corresponding derivatives of Δ^7-spinastenol in their properties. Also the properties of the $\Delta^{8(14)}$-and Δ^{14}-isomers prepared from the fraction I were found to accord with those of the corresponding isomers of Δ^7-spinastenyl acetate. Accordingly the sterol of the fraction I was recognized as Δ^7-spinastenol. Regarding the sterol of the fraction II, the results of our examination of the properties of the acetate, free sterol, benzoate and two isomers ($\Delta^{8(14)}$- and Δ^{14}-isomers) showed its identity with Δ^7-cholestenol, which was previously found in *Asterias amurensis*[3]. Thus it is indicated that Δ^7-spinastenol and Δ^7-cholestenol are present in the mono- unsaturated sterol components of *Asterina pectinifera*. It should, however, be noted that the possibility of the presence of Δ^7-sterols of the C_{28}-series is not excluded, though such sterols of the C_{28}-series could not be separated in the present study. Although Δ^7-spinastenol has recently been found in oats[4] and wheat[5], the present study is the first instance in which the occurrence of this sterol in the animal kingdom is demonstrated.

It was reported in previous studies by the authors that sterols of *Coscinasterias acutespina*[6] as well as of *Luidia quinaria*[7] consist mainly of mono-unsaturated Δ^7-sterols of the C_{28}- or C_{29}-series. A steryl acetate fraction,

TABLE I

PROPERTIES OF Δ^7-SPINASTENOL

	Fraction from *Asterina pect.*		Fraction from *Luidia quinaria*		Δ^7-Spinastenol[8]	
	m.p. (°C)	$[\alpha]_D^\circ$	m.p. (°C)	$[\alpha]_D^\circ$	m.p. (°C)	$[\alpha]_D^\circ$
Free sterol	145–147	+8.4	145–147	+9	144–145	+11
Acetate	157–158	+6.1	157	+6	156–157	+ 8
Benzoate	178–180	+15	177	——	180.5	+13
$\Delta^{8(14)}$-Isomer	112–113	+20	115	——	112–113	+23
Acetate of $\Delta^{8(14)}$-Isomer	113–114	+14	111–112	+18	116–117	+12
Δ^{14}-Isomer	123–124	——	——	——	127.5	+36.5
Acetate of Δ^{14}-Isomer	86– 87	+26	——	——	86.5	+24.3

1) Y. Toyama and T. Takagi, This Bulletin, **28**, 469 (1955).
2) T. Matsumoto and Y. Toyama, *J. Chem. Soc. Japan*, **64**, 1069 (1943).
3) T. Matsumoto and T. Wainai, *J. Chem. Soc. Japan, Pure Chem. Sect.*, **75**, 756 (1954); Y. Toyama and T. Takagi, This Bulletin, **27**, 421 (1954).
4) D.R. Idler et al., *J. Am. Chem. Soc.*, **75**, 1712 (1953).
5) D.R. Idler, A.A. Kandutsch and C.A. Baumann, *J. Am. Chem. Soc.*, **75**, 4325 (1953).
6) Y. Toyama and T. Takagi, *J. Chem. Soc. Japan, Pure Chem. Sect.*, **76**, 243 (1955).
7) Y. Toyama and T. Takagi, This Bulletin, **27**, 39 (1954).
8) D. Larsen and F.W. Heyl, *J. Am. Chem. Soc.*, **56**, 2663 (1934); D.H.R. Barton and J.D. Cox, *J. Chem. Soc.*, **1948**, 783.

m.p. 157°C, obtained in the previous study on *Luidia quinaria* was not closely studied at that time due to the scarcity of the material, but this fraction is very likely to consist mainly of Δ^7-spinastenyl acetate. In Table I, the melting points and specific rotations of the free sterol and its derivatives of the Δ^7-spinastenol fractions from *Asterina pectinifera* and *Luidia quinaria* are compared with those reported for Δ^7-spinastenol by previous authors.

Experimental

1. Δ^7-Spinastenyl Acetate Fraction.—As described in the 16th report, the solid material (49 g.) separated from the unsaponifiable matter of the acetone-soluble oil extracted from the starfish, *Asterina pectinifera*, was refluxed with acetic anhydride. The acetylated product was then recrystallized from 200 cc. of acetone-ether, yielding 26.5 g. of crystalline solid (crude steryl acetate). This was subjected to repeated recrystallizations from acetone until eventually a crude hitodesteryl acetate fraction (2.2 g.) of m.p. 182–183°C was obtained after thirteen recrystallizations. In the present study, a steryl acetate fraction (4.8 g.), m.p. 153–156°C, recovered from the mother liquors of the 5th–9th recrystallizations was fractionally crystallized from acetone, and the main fraction obtained was fractionated further. After several repetitions of fractionation, a fraction (1.6 g.) of m.p. 157–158°C was obtained. The melting point of this fraction was unaltered by further recrystallizations, and all fractions obtained by a further fractionation had the same melting point.

The fraction, m.p. 157–158°C, had $[\alpha]_D^{22}=+6.1°$, saponification value 123.9 and iodine value by the perbenzoic acid method 58.7 (calcd. for $C_{71}H_{52}O_2$: saponification value 122.8; iodine value 55.6). The change of color developed in the Liebermann-Burchard reaction for this fraction with the period of reaction is shown by the curve A in Fig. 1 in which the absorption at 620 mμ is plotted against the period of reaction. The curve A is quite similar to the curve for a typical Δ^7-sterol. Saponification of this fraction gave free sterol which had m.p. 145–147°C and $[\alpha]_D^{22}=+8.4°$ after recrystallization from acetone. Benzoate prepared from the free sterol had m.p. 178–180°C, $[\alpha]_D^{24}=+15°$ and saponification value 108.9 (calcd. for $C_{35}H_{54}O_2$: 108.1).

The acetate fraction of m.p. 157–158°C was dissolved in glacial acetic acid, palladium catalyst was added to the solution, and the mixture was shaken in an atmosphere of hydrogen for seven hours. Absorption of hydrogen did not occur, but an isomerization product was obtained, which showed m.p. 113–114°C and $[\alpha]_D^{21}=+14°$ after recrystallization from methanol. The change of color vs. the period of reaction in the L. B. reaction for this product is shown by the curve B in Fig. 1 which closely resembles the curve for a $\Delta^{8(14)}$-sterol. Saponification of this product gave free sterol which had m.p. 112–113°C and $[\alpha]_D^{25}=+20°$ after recrystallizations from methanol and acetone.

The $\Delta^{8(14)}$-isomer (acetate) obtained above was dissolved in chloroform, and dry hydrogen chloride was passed through the solution for two hours. The product obtained had m.p. 86–87°C and $[\alpha]_D^{27}=+26°$ after recrystallization from ethanol. Saponification of this product gave free sterol which, recrystallized from methanol, had m.p. 123–124°C. The change of color vs. the period of reaction in the L. B. reaction for this sterol is shown by the curve C in Fig. 1 which is similar to the curve for a typical Δ^{14}-sterol.

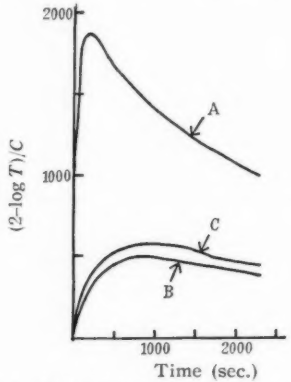

Fig. 1. Liebermann-Burchard reaction for Δ^7-spinastenyl acetate fraction.
T: Transmittance, *C*: Concentration (10^{-3} mol.)
Curve A for Δ^7-spinastenyl acetate fraction.
Curve B for $\Delta^{8(14)}$-isomer (acetate)
Curve C for Δ^{14}-isomer (free sterol)

2. Δ^7-Cholestenyl Acetate Fraction.—The acetone-ether filtrate separated from the crude steryl acetate (26.5 g.) was concentrated, and a further quantity (2.5 g.) of crude steryl acetate fraction was obtained. This fraction and the fractions recovered from the mother liquors of the 1st and 2nd recrystallizations of the crude steryl acetate (26.5 g.) were united. The united material (9.3 g.), m.p. 105–126°C, was fractionally crystallized from methanol, yielding the 1st crop (1.3 g.) of m.p. 130–132°C and the 2nd crop (6.0 g.) of m.p. 119–123°C. The 2nd crop was separated further into the following fractions by fractional crystallization from methanol: the 1st fraction (0.9 g.) of m.p. 125–127°C; the 2nd fraction (0.5 g.) of m.p. 123–124°C; the 3rd fraction (0.6 g.) of m. p. 120–121°C; the 4th fraction (0.8 g.) of m.p. 119–120°C; the 5th fraction (0.6 g.) of m.p. 119–120°C; the 6th fraction (2.6 g., recovered from the final filtrate) of m.p. 118–119°C. A further fractional crystallization of the 6th fraction gave fractions of the same melting point, 118–119°C. This frac-

tion had $[\alpha]_D^{28}=-2.0°$, saponification value 130.0 and iodine value by the perbenzoic acid method 62.0 (calcd. for $C_{29}H_{48}O_2$: saponification value 130.8; iodine value 59.2). The L. B. reaction for this fraction is shown by the curve A in Fig. 2. Free sterol obtained by saponification of this fraction had m.p. 122–123°C and $[\alpha]_D^{19}=\pm 0$ after recrystallization from methanol. Benzoate prepared from the free sterol had m.p. 153–155°C, $[\alpha]_D^{19}=+4°$ and saponification value 112.6 (calcd. for $C_{34}H_{50}O_2$; 114.3) after recrystallization from acetone.

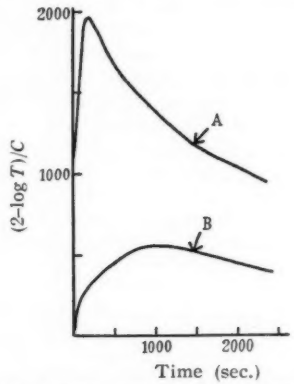

Fig. 2. Liebermann-Burchard reaction for Δ^7-cholestenyl acetate fraction.
T: Transmittance, C: Concentration (10^{-3} mol.)
Curve A for Δ^7-cholestenyl acetate fraction.
Curve B for $\Delta^{8(14)}$-isomer (acetate)

The isomerization product obtained by shaking a solution of this fraction (acetate) in an atmosphere of hydrogen for five hours in the presence of palladium catalyst showed m.p. 77–78°C and $[\alpha]_D^{21}=+9°$ after recrystallization from methanol. The L. B. reaction for this product is shown by the curve B in Fig. 2. Saponification of this product gave free sterol of m.p. 119–120°C and $[\alpha]_D^{21}=+20°$ after recrystallization from methanol.

Summary

In a continuation of the study on sterol components of *Asterina pectinifera*, the present study is concerned with mono-unsaturated sterol components. The steryl acetate fraction recovered from the mother liquors of the recrystallizations, which were carried out for the separation of hitodesteryl (α-spinasteryl) acetate in a previous study, was subjected to fractional crystallizations by which two fractions, Δ^7-spinastenyl acetate fraction and Δ^7-cholestenyl acetate fraction, were eventually separated. Accordingly it has been found that the sterol mixture of *Asterina pectinifera* contains Δ^7-spinastenol and Δ^7-cholestenol besides hitodesterol.

Department of Applied Chemistry
Faculty of Engineering
Nagoya University, Nagoya

Spectrochemical Investigations of the Interaction between Simple Salt Anions and Transition Metal Cations. III. Association between Cupric Alaninate Complex and Sulphite Anion

By Hayami YONEDA

(Received October 25, 1955)

Introduction

In the previous report[1] the author studied the absorption due to association between bisethylenediamine cupric complex and several anions, which had strong reducing power against cupric aquo ion, and concluded from comparison of the equilibrium constants of association that the special polarising power of the central cupric ion and the large polarisability of anions played an important role in association. If such a conclusion is appropriate, we can expect that there should exist the similar absorption due to association between the electrically neutral complex and the very easily polarisable anion and that we could determine the equilibrium constant of association by analyzing the absorption data.

In the present investigation, marked absorption due to association was found between cupric alaninate complex and sulphite and thiosulphate anions, and the estimation of the equilibrium constant was performed in the case of sulphite anion.

1) This Bulletin, 29, 68 (1956).

Experimental

Cupric alaninate $Cu(CH_3CHNH_2\cdot COO)_2\cdot H_2O$ was prepared by dissolving freshly precipitated cupric hydroxide into the boiling solution containing an equivalent amount of alanine and was recrystallized twice from hot water.

Optical densities were measured by means of Shimadzu the spectrophotometer using tungsten and hydrogen lamps and 1 cm. quartz cells. All measurement was done at room temperature 20°C.

Results

In the preliminary experiment the following measurement was made. Na_2SO_3 and $Na_2S_2O_3$, were dissolved to make 1 M solutions. In each solution cupric alaninate complex was dissolved to the concentration of 0.01 M. Such solutions of the complex were measured in their optical densities. In order to cancel the absorption due to the unassociated free anions, the corresponding salt solution was used as a standard. The results are shown in Fig. 1 with the results obtained in the

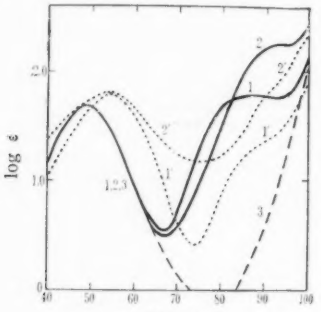

ν, 10^{13} sec^{-1}

Fig. 1.

1. ——— [Cu alanine$_2$] in 1 mol./l. Na_2SO_3
2. ——— [Cu alanine$_2$] in 1 mol./l. $Na_2S_2O_3$
3. - - - - [Cu alanine$_2$] in water
1′. ----- [Cu en$_2$]$(ClO_4)_2$ in 1 mol./l. Na_2SO_3
2′. ----- [Cu en$_2$]$(ClO_4)_2$ in 1 mol./l. $Na_2S_2O_2$

(Curves 1′ and 2′ were cited from the previous work.)

ethylenediamine complex. It is interesting to find that the absorption due to association appears more distinctly here than in the case of the cupric ethylenediamine complex. In the present case too, the characteristic absorption band proper to the complex remains constant.

In addition, it is noteworthy that the solution was photosensitive in the case of thiosulphate and that the reduction of cupric ion to cuprous ion proceeded at a measurable rate during measurment, and that the characteristic blue color of the complex faded gradually. In the sulphite solution such reduction was not observed during measurement. Accordingly, the determination of the equilibrium constant was done only in the case of sulphite. In order to estimate the equilibrium constant, optical densities of the following solutions were measured in the wavelength regions 400–320 mμ.

1) The solution which contains both [Cu alanine$_2$] and Na_2SO_3 at 0.01 M concentration.

2) The solution which contains both the complex and sulphite at 0.0075 M concentration.

3) The solution which contains both the complex and sulphite at 0.0050 M concentration.

4) The solution which contains only the complex at 0.01 M concentration.

The slight absorption which originated from Na_2SO_3 was canceled by taking the sulphite solutions of the corresponding concentration as a standard in the measurement. The results are shown in Fig. 2. In the figure, the full

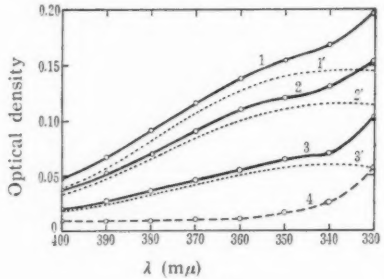

Fig. 2.

lines 1, 2, 3 correspond to the absorption of 0.01, 0.0075, 0.0050 M solutions and a broken line 4 to that of the complex only solution. The dotted lines 1′, 2′, 3′ are the results of subtraction from the absorption 1, 2, 3 by the absorption of the complex of the corresponding concentrations.

Determination of the Equilibrium Constant.—In the following equilibrium

$$Cu\ alanine_2 + SO^2{}_3 \rightleftarrows (Cu\ alanine_2\cdot SO_3)$$

the equilibrium constant of association is represented by

$$K=\frac{[(Cu\ alanine_2\cdot SO_3)]}{[Cu\ alanine_2]\cdot[SO_3{}^{2-}]}$$

As the total concentrations of the complex and the anion in the solution are always the same in the present case, we put them as u. If we represent the concentration of the association product in equilibrium with x, then the concentrations of the complex and the anion in equilibrium are both represented with $u-x$, and the equilibrium constant K is expressed by

$$K=\frac{x}{(u-x)^2} \qquad (1)$$

where u takes the values of 0.01, 0.0075, and 0.0050. If we represent x corresponding to $u=0.01$, 0.0075, 0.0050 with x_1, x_2, x_3, and then these x_1, x_2, and x_3 take the definite values against the definite value of K. Consequently, x_2/x_1 and x_3/x_1 are also definite against the definite value of K. The values of x_2/x_1 and x_3/x_1 against K were calculated and plotted in Fig. 3.

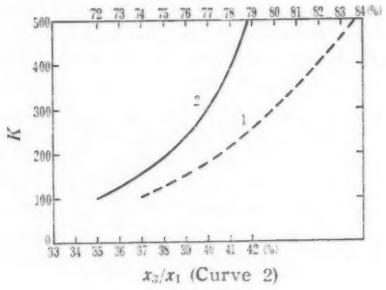

Fig. 3.

On the other hand, the measured optical density D is represented by

$$D=\varepsilon_c(u-x)+\varepsilon_a x \qquad (2)$$

This relation is modified to

$$D-\varepsilon_c u=(\varepsilon_a-\varepsilon_c)x=y \qquad (3)$$

where ϵ_c and ϵ_a are the molar extinction coefficients of the complex and the association product, and y represents the absorption due to association. If we represent y in the cases of x_1, x_2, x_3 with y_1, y_2, y_3 respectively, then $x_2/x_1=y_2/y_1$ and $x_3/x_1=y_3/y_1$. The values of y_2/y_1 and y_3/y_1 in each wave-length were calculated from the observed values of D, and the corresponding values of K were read from the graph. The results thus obtained are listed in Table I.

Discussion

We have obtained $K=240$ as the value of the equilibrium constant of association between [Cu alanine$_2$] and SO_3^{2-}. This value is almost ten times as large as that between [Cu en$_2$]$^{2+}$ and SO_3^{2-}($K=25$). This surprising fact can be interpreted only by assuming that the electronic configuration of the central cupric ion plays an important role in association. In other words, in the ethylenediamine complex the charge of the central cupric ion is considerably neutralized by the lone pair electrons of the coordinating N atoms of the ethylenediamine molecules and as the result it has only the small polarising power against the outer anion. In contrast to this, in the alanine complex, though the charge neutralization as a whole complex radical is complete, the charge of the cupric ion is incompletely canceled, so that the cupric ion has enough polarising power against the outer anion.

As reported previously, $S_2O_3^{2-}$ associates much more firmly with [Cu en$_2$]$^{2+}$ than SO_3^{2-}. This fact suggests the much greater polarisation of $S_2O_3^{2-}$. Such polarisation is to be strengthened in the association with [Cu alanine$_2$]. As the result $S_2O_3^{2-}$ excited by a photon easily transfers its electron to the central cupric ion. The photochemical reduction of [Cu alanine$_2$] in the thiosulphate solution can be thus explained.

Conclution

Marked association absorption was found between electrically neutral [Cu alanine$_2$] and SO_3^{2-}, and $S_2O_3^{2-}$ and the equilibrium constant of association was determined spectrophotometrically in the case of [Cu alanine$_2$] and SO_3^{2-}. The value of K was found to be 240.

This value is much larger than that obtained in the corresponding case of [Cu en$_2$]$^{2+}$ and SO_3^{2-} ($K=25$). This result can be explained by assuming that the central

TABLE I

VALUES OF y AND K

λ(mμ)	y_1	y_2	y_3	y_2/y_1	K	y_3/y_1	K
390	0.058	0.045	0.023	77.5%	200	39.7%	285
380	.084	.065	.033	77.4%	195	39.8%	290
370	.106	.083	.042	78.5%	235	39.6%	280
360	.127	.099	.049	77.8%	210	39.0%	245
350	.141	.109	.057	77.7%	205	39.0%	245
340	.145	.113	.057	78.0%	215	39.3%	260
330	.143	.112	.056	78.7%	245	39.2%	255
320	.145	.114	.056	78.6%	240	39.0%	245
				Mean	218	Mean	263

Probable value of $K=240$

cupric ion in [Cu alanine$_2$] has much stronger polarising power than in [Cu en$_2$]$^{2+}$. The assumption of such strong polarising power can explain the photochemical reduction of Cu alanine$_2$·S_2O_3 system.

The author wishes to express his sincere thanks to Prof. R. Tsuchida and Prof. M. Kobayashi, Osaka University for their kind advice and encouragement during this work.

Chemistry Department, Wakayama University, Wakayama

Cyanoethylation of Trichlorosilane. I. β-Addition.[1]

By Shunichi NOZAKURA and Shiro KONOTSUNE

(Received October 20, 1955)

Since Sommer and coworkers[2] discovered the peroxide-catalyzed addition of trichlorosilane to 1-octene in 1947, a number of olefins have been found to react in the following manner[3]:

$$HSiCl_3 + CH_2=CHR \longrightarrow Cl_3SiCH_2CH_2R$$

Wagner and Strother[4] also reported the preparation of vinyltrichlorosilane from acetylene and trichlorosilane in the presence of catalysts such as peroxide and platinized asbestos. Thus the method gained its importance in the industrial production of vinyltrichlorosilane.

However, the olefins which have hitherto been used were generally simple olefins, and only a few reactive vinyl compounds were tried. In an attempt to effect the addition of trichlorosilane with styrene, Burkhark[3] was only able to isolate a nonvolatile telomeric product. Quite recently, in the midst of our experiments, butadiene[5] and vinyltrimethylsilane[1] were reported to react with trichlorosilane.

In this paper we describe the addition reaction of trichlorosilane and acryronitrile. Acrylonitrile among the various vinyl compounds was tried first, as we expected that the addition might take place readily and the identification of its products might also be easy.

TABLE I

CYANOETHYLATION OF TRICHLOROSILANE IN THE PRESENCE OF BENZOYLPEROXIDE AND PLATINIZED ASBESTOS

No.	Trichlorosilane, g.	Acrylonitrile, g.	Catalyst, g.	Reaction[a] temp. °C	Reaction time, hr.	Yield,[b] %
1	19.1	7.6	—	160	5.0	9.7
2	19.9	7.8	—	180	5.0	10
3	18.5	8.0	benzoylperoxide, 0.05	160	5.0	46[c]
4	19.9	7.8	〃 0.05	130	5.0	0[d]
5	19.9	7.8	〃 0.05	100	5.0	0[e]
6	19.6	7.8	benzoic acid 0.05	160	5.0	0
7	19.7	7.8	platinized asbestos 0.1	160	5.5	11
8	19.3	7.6	〃 0.1	180–200	5.8	61

a) Reaction temperatures fluctuated within ±3°C.
b) The yields are based on trichlorosilane used.
c) A pale yellow precipitate weighed 3.2 g. (Si, 5.3%)
d) Precipitate, 1.1 g. (Si, 4.01%)
e) Precipitate, 2.8 g. (Si, 1.69%)

1) Paper IV in a series on the study of organosilicon compound.
2) L.H. Sommer, et. al., *J. Am. Chem. Soc.*, **69**, 188 (1947).
3) C.A. Burkhard and R.H. Krieble, ibid., **69**, 2687 (1947); W. Pietrusza, et. al.; ibid., **70**, 484 (1948); C.L. Agre, ibid., **71**, 300 (1949); C.A. Burkhard, ibid., **72**, 1402 (1950).
4) G.H. Wagner and C.O. Strother, *Brit.*, 670, 617, Apr. 23, 1952; C.A. **46**, 8894c.
5) D.L. Bailey and A.N. Pines, *Ind. Eng. Chem.*, **46**, 2363 (1954).
6) D. Seyferth and E.G. Rochow, *J. Org. Chem.*, **20**, 250 (1955).

Cyanoethylation of Trichlorosilane in the Presence of Benzoylperoxide and Platinized Asbestos

Table I shows the catalytic effects of benzoylperoxide and platinized asbestos. Benzoylperoxide was effective at above 160°C., and it produced simultaneously a considerable amount of an insoluble pale yellow precipitate which appeared to be either polyacrylonitrile or tellomeric product. Although such an insoluble precipitate was also produced at 130°C or at lower temperatures, no addition product, except the polymer, was obtained. Experiment with benzoic acid alone, which is a possible decomposition product of benzoylperoxide, had no catalytic action at all. On the other hand, platinized asbestos, which has been known to be effective in the addition of trichlorosilan to acetylene, catalyzed effectively and gave cyanoethylation product without accompanying the precipitate.

Cyanoethylation of Trichlorosilane in the Presence of Organic Bases

Organic and inorganic bases are known to be effective catalysts in the usual case of cyanoethylation. However, in our cases inorganic bases such as metal hydroxides were inadequate because of their strong reactivity towards trichlorosilane, and this led us to turn our attention to tertiary organic bases. The results obtained with the addition of organic bases are given in Table II. The reaction mixtures were clear in almost all the cases and colored from a light yellow to a light orange. The addition product obtained here was the same as that from peroxidecatalysed. In contrast to the latter case, there occurred no precipitate. Pyridine was also effective at a temperature as low as 130°. Catalytic activities of the bases increased in the order, dimethylaniline$\ll$quinoline$<$pyridine, piperidine$<$triethylamine.

It is also of interest to note that pyridine hydrochloride, benzyltriethylammonium chloride, and piperidine have shown a moderate catalytic activity. Since piperidine has an active hydrogen, it may react with trichlorosilane to form piperidylsilicon bonds and piperidine hydrochloride. The catalytic activity of piperidine may possibly be due to the effect of the latter two compounds.

It must be taken into consideration that tertiary amine may have also changed to its hydrochloride to a certain extent prior to heating by a small amount of moisture which inevitably adhered to the sealed tube and the resulting hydrochloride acted as a catalyst. However, this is not very serious in view of the fact that the catalytic activity of pyridine was found to be higher than its hydrochloride as clearly demonstrated in the experiment No. 8 and 9 (Table II).

Structural Proof of Addition Products

The addition product was proved to consist almost exclusively of β-cyanoethyltrichlorosilane, which was identified by the process described below. Cyanoethyltrichlorosilane was converted to the corresponding trimethylsilylpropionic amide (IV), m.p. 95–6°C.

Table II

Cyanoethylation of trichlorosilane in the presence of organic bases

No.	Trichlorosilane, g.	Acrylonitrile, g.	Catalyst, g.	Reaction temp. °C	Reaction time, hr.	Yield,[b] %
1	19.9	8.7	pyridine, 0.1	185	5.0	67
2	27.8	13.0	〃 0.1	160	5.0	69
3	19.9	8.7	〃 0.1	130	6.0	14
4	18.6	8.0	triethylamine, 0.1	160	5.0	76
5	20.1	8.7	piperidine, 0.1	160	5.0	69
6	20.2	8.7	quinoline, 0.1	160	5.0	40
7	20.5	7.9	dimethylaniline, 0.1	160	5.0	0
8	20.0	7.8	pyridine, 0.05	160	5.0	59
9	19.8	7.8	pyridine hydrochloride[a]	160	5.0	35
10	20.5	8.9	benzyltriethylammonium chloride, 0.1	160	5.0	70

a) The pyridine hydrochloride was prepared in the reaction tube by interacting 0.05 g. of pyridine and an excess of concd. hydrochloric acid and by drying in vacuo.
b) The yields are based on trichlorosilane used.

The structure of the latter compound was already proved by Sommer[7] through a series of reactions. Mixed melting point test of our addition product with that synthesized showed no depression. Therefore, the compound (I) was assigned to be β-cyanoethyltrichlorosilane.

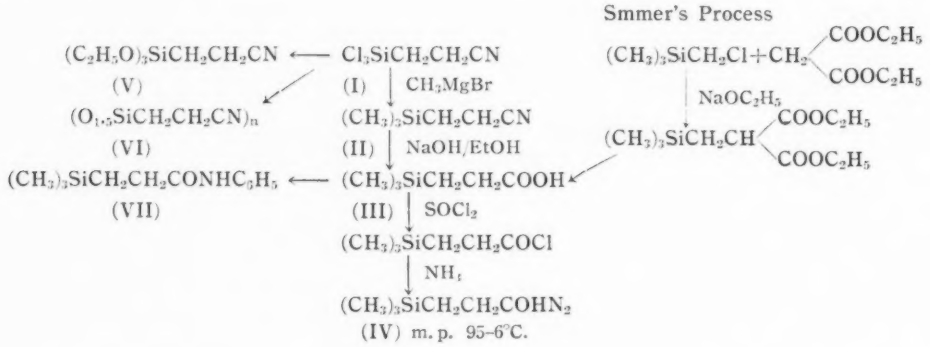

The examination of the compound (II) by infra red spectrum proved it to be identical with that derived from β-trimethylsilylpropionic amide according to Sommer's method.

The following new compounds were prepared and characterized; β-cyanoethyltriethoxysilane (V), β-cyanoethylpolysiloxane (VI), and β-trimethylsilylpropionic anilide (VII).

The Effect of Solvent on the Base-catalyzed Cyanoethylation of Trichlorosilane

Although a more accurate measurement of reaction rate must be done for a detailed discussion, we carried out here an approximate comparison of three solvents, acetonitrile, chlorobenzene, and benzene, dielectric constants of which being 37.5, 5.61, and 2.29 respectively. The effect of the solvents on the base-catalyzed addition reaction are summarized in Table III. When the reactions were carried out in the presence of the strongest catalyst such as triethylamine, there were no detectable differences among the solvents studied. However, when a weaker base catalyst such as pyridine was used, a marked difference was observed among them.

Discussion of Reaction Mechanisms

The peroxide-catalyzed cyanoethylation may be regarded as a radical chain reaction as Sommer and others have suggested in the case of other olefins. Tne base-catalyzed cyanoethylation of trichlorosilane does not seem to be a radical reaction. Although there

TABLE III

CYANOETHYLATION OF TRICHOLOROSILANE IN VARIOUS SOLVENTS AT 160°C

No.	Trichlorosilane, g.	Acrylonitrile, g.	Catalyst, g.	Solvent, ml.	Reaction time, hr.	Yield[b] %
1	22.2	9.6	triethylamine, 0.1	acetonitrile, 26	5.0	64
2	21.8	9.4	〃, 0.1	benzene, 45	5.0	59
3	20.4	8.8	pyridine, 0.1	acetonitrile, 40	1.0	39
4	16.8	7.3	〃, 0.07	〃 34	2.0	59
5	20.4	8.8	〃, 0.1	benzene, 40	1.0	0
6	17.1	7.5	〃, 0.07	〃, 34	2.0	0
7	18.8	8.1	〃, 0.1	〃, 38	5.0	0
8	20.0	8.7	〃, 0.1	chlorobenzene, 40	5.0	0
9	16.8	7.3	〃, 0.07	nitrobenzene, 34	2.0	—[a]

a) The colour of the reaction mixture was brownish black and its distillation was difficult due to decomposition.

b) The yields are based on trichlorosilane used.

7) L.H. Sommer, et. al., *J. Am. Chem. Soc.*, 73, 5130 (1951); 76, 1609 (1954).

has not yet been reported an example in which the fission of silicon-hydrogen bond and addition of it to a double bond may be explained in terms of ionic mechanism, we believe that ionic mechanism involved in our case. The following three pieces of evidence may support such an ionic mechanism. First, base catalysts are effective. Second, no appreciable amount of precipitates of polyacrylonitrile is produced in the base-catalyzed reactions in contrast to the case of peroxide-catalyzed. Third, solvents give a considerable effect in some cases as mentioned above. The deficiency of the influence of the solvents in the case of triethylamine catalyst is probably due to the much higher catalytic activity of triethylamine than that of pyridine.

In view of these facts we may suggest the following reaction mechanism, which is similar to the ordinary cyanoethylation:

$$Cl_3SiH + B \longrightarrow Cl_3Si^- + HB^+$$
$$Cl_3Si^- + CH_2=CHCN \longrightarrow Cl_3SiCH_2CH^-CN$$
$$Cl_3SiCH_2CH^-CN + HB^+ \longrightarrow Cl_3SiCH_2CH_2CN + B$$

where B represents organic bases.

Organic salts, such as pyridine hydrochloride and benzyltriethylammonium chloride, are soluble in the reaction mixture and we considered that their catalytic effect is probably due to a salt effect.

Experimental

General Procedure for Cyanoethylation of Trichlorosilane.—Trichlorosilane (b.p. 31.5–32.0°C) and freshly distilled acrylonitrile) b.p. 76.5–77°C) were charged into a hard glass reaction ampule of about a 100 ml. capacity and cooled in an ice-salt bath, and the open end of the ampoule was sealed after the air had been replaced by dry nitrogen. Heating was carried out in an electric furnace equipped with an automatic controller. After cooling, the reaction tube was opened and the precipitate if any was filtered. The precipitate was washed with dry benzene and absolute alcohol, dried in a desiccater, and analyzed for silicon.

A mixture of the solvent and the unreacted starting material of the filtrate was distilled under atmospheric pressure, and then the product was distilled from a Claisen flask under reduced pressure.

Catalyst.—Platinized asbestos was prepared according to the following directions. Three grams of purified asbestos was mixed with 0.06 g. of chloroplatinic acid, H_2PtCl_6, and an appropriate quantity of water. After being dried on the water bath, the mixed asbestos was heated in a glass tube at 200°C in a stream of air for one hour and then reduced with dry hydrogen at 200°C for three hours.

β-Cyanoethyltrichlorosilane (I).—After the purification by redistillation, the physical constants of β-cyanoethyltrichlorosilane were determined. B.p. 109° (30 mmHg), m.p. 34.6–35.1°C.

Anal. Found: Cl, 56.25. Calcd. for $C_3H_4NSiCl_3$: Cl, 56.43%.

β-Cyanoethylpolysiloxane (VI).—β-cyanoethyltrichlorosilane (I) was poured into a large quantity of water to give a homogeneous solution. When the solution was neutralized with 6N aqueous ammonia, β-cyanoethylpolysiloxane (VI) precipitated as a white amorphous powder. After filtration and washing with water the precipitate was dried at 100°C over phosphorous pentoxide.

Anal. Found: Si, 26.38; N, 13.22. Calcd. for $C_3H_4NO_{1.5}Si$: Si, 26.42; N, 13.21%.

β-Cyanoethyltriethoxysilane (V).—In a 200 ml. three-necked flask equipped with a mercury-sealed stirrer, a dropping funnel, and a calcium chloride tube, a mixture of 9.8 g. of absolute ethanol and 9.8 g. of dry benzene was placed. A solution of 12 g. of β-cyanoethyltrichlorosilane in an equal quantity of dry benzene was added dropwise through the dropping funnel under vigorous stirring. The temperature of the reaction mixture was kept below 0°C by the external cooling with ice-salt bath. After the addition was completed stirring was continued for one and a half hours. Then a slight excess of dry ammonia was introduced into the reaction mixture under cooling. An excess amount of ammonia was driven off by dry air, and the resulting ammonium chloride was filtered off. Vacuum distillation of the filtrate gave 9.0 g. of the crude β-cyanoethyltriethoxysilane (V), b.p. 121–130°C (20 mmHg) (65%). Redistillation yielded the pure compound, b.p. 111.5–112.5° (10 mmHg), d_4^{25}, 0.9699; n_D^{25}, 1.4103.

Anal. Found: Si, 12.58; N, 5.8; MR_D, 55.55. Calcd. for $C_9H_{19}NO_3Si$: Si, 12.92; N, 6.4%; MR_D, 55.26.

β-Cyanoethyltrimethylsilane (II).—Eleven gram (0.058 Mol.) of β-cyanoethyltrichlorosilane (I) was methylated in the usual manner with the ether solution of methylmagnesiumbromide prepared from 6.2 g. (0.25 Atom) of magnesium and the reaction gave 5.8 g. of β-cyanoethyltrimethylsilane (II)., b.p. 98.5–101.8° (75 mmHg) (78%).

In order to remove a possible impurity of β-trimethylsilylmethylketone, the crude product was shaken with a saturated solution of sodium bisulfite. After washing with the water and drying over calcium chloride, it was subjected again to vacuum distillation, b.p. 98°–97.5° (65–64 mmHg), d_4^{25}, 0.8226; n_D^{25}, 1.4202.

The infra red spectrum of the compound (II) was identical with that of the standard sample prepared according to the method described by Sommer[7].

Anal. Found: Si, 21.67; N, 10.7; Mol. Wt. (in benzene), 127; MR_D, 39.09. Calcd. for $C_5H_{13}NSi$: Si, 21.92; N, 11.0%; Mol. Wt., 127; MR_D, 39.07.

β-Trimethylsilylpropionic Acid (III).—A mixture of 3.0 g. of β-cyanoethyltrimethylsilane, 10 ml. of 50% aqueous sodium hydroxide and 10 ml. of alcohol was refluxed for three and half hours until the evolution of ammonia ceased. The reac-

tion mixture was concentrated by an aspirator on a water bath to a slushy state. It was dissolved in a small portion of water and extracted with ether in order to remove the unreacted nitrile. The water layer was acidified with concentrated hydrochloric acid and the separating oil was extracted again with ether. The ether solution was dried with sodium sulfate, filtered, and distilled under vacuum to yield 1.0 g. of β-trimethylsilylpropionic acid. (III), b.p. 114–6° (20 mmHg) (49%). n_D^{25}, 1.4257 (in literature[7]); n_D^{20}, 1.4282).

Anal. Found: Si, 18.85; Mol. Wt., (from titration), 142. Calcd. for $C_5H_{14}O_2Si$: Si, 19.19%; Mol. Wt., 145.

β-Trimethylsilylpropionic Amide (IV) and Anilide (VII).—When 0.9 g. of thionylchloride was added to 0.2 g. of β-trimethylsilylpropionic acid (III), a vigorous reaction took place instantly. After refluxing for a half hour, an excess of thionylchloride was evaporated in vacuo. To the ice-cold residual oil 20 ml. of ether saturted with dry ammonia was poured in. After standing for about a half hour, an excess ammonia was driven off with a stream of dry air. The precipitating ammonium chloride was separated by filtration and the filtrate was evaporated to yield 0.2 g. of β-trimethylsilylpropionic amide (IV), m.p. 95–6°C (recrystallised from petroleum benzine).

Anal. Found: Si, 19.23. Calcd. for $C_5H_{15}NOSi$: Si, 19.34%.

The mixed melting point test of the compound (IV) with the standard sample prepared according to Sommer[7] showed no depression.

β-Trimethylsilylpropionic anilide (VII) was prepared by heating in a sealed tube the mixture of 0.1 g. of the acid (III) and 0.2 g. of aniline at 180°C for eight hours. The reaction mixture was digested with 4 ml. of 2N hydrochloric acid and the insoluble oil crystallised in large needles after standing for a long time, m.p. 87–8°C. (recrystallised from alcohol)

Anal. Found: Si, 12.99. Calcd. for $C_{12}H_{19}NOSi$: Si, 12.68%.

Summary

1. Cyanoethylation of trichlorosilane was found to be catalysed by organic bases, benzoylperoxide, or platinized asbestos at about 160°C. The catalytic activities of organic bases increased in the order, dimethylaniline ≪ quinoline < pyridine, piperidine < triethylamine. Pyridine hydrochloride and benzyltriethylammonium chloride has also catatytic effects.

2. The orientation of the addition reaction was found to be almost exclusively of the β-position.

3. An ionic mechanism was suggested for the organic base-catalysed addition reaction.

The authors are much indebted to Profs. S. Murahashi and H. Tani for their many helpful suggestions. Appreciation is also expressed to Nihon Silicon Resin Co. for their kindness of supplying the trichlorosilane.

Department of Chemistry, Faculty of Science, Osaka University, Osaka

---

Cyanoethylation of Trichlorosilane. II. α-Addition[1]

By Shunichi NOZAKURA and Shiro KONOTSUNE

(Received October 20, 1955)

In the previous paper[2] the authors reported the cyanoethylation of trichlorosilane in the presence of organic bases, benzoyl peroxide, or of platinized asbestos. These addition reactions which were carried out in sealed glass tubes gave exclusively the β-adduct, β-cyanoethyltrichlorosilane.

In an attempt to bring about this reaction in a large scale with an autoclave made from 18-8 stainless steel in the presence of pyridine or platinized asbestos, there was obtained, curiously enough, an α-addition product instead of the expected β-adduct:

$$Cl_3SiH + CH_2{=}CHCN \begin{cases} \xrightarrow{\beta\text{-addition}} Cl_3SiCH_2CH_2CN \quad \text{b.p. } 117\text{–}8^\circ \text{ (41 mmHg)} \\ \xrightarrow{\alpha\text{-addition}} Cl_3SiCHCN \quad \text{b.p. } 96\text{–}8^\circ \text{ (41.5 mmHg)} \\ \qquad\qquad\quad | \\ \qquad\qquad\quad CH_3 \end{cases}$$

1) Paper V in a series on the study of organosilicon compound.

2) S. Nozakura and S. Konotsune, This Bulletin 29, 322, (1956).

Since this is a new example where trichlorosilane reacted with olefin according to the Markownikow's rule, we performed a more detailed research concerning this unusual reaction. In this paper, we describe the details of the characteristic features of the above reaction, the structural proof of the product, and some discussions on the reaction mechanisms.

Cyanoethylation of Trichlorosilane in an Autoclave

The typical experiment of the cyanoethylation which was carried out in an autoclave is shown in Fig. 1. The reaction started at a temperature ranging from 150 to 170°C. As the reaction was exothermic, the pressure rose rapidly with the simultaneous elevation of the temperature, and dropped also very quickly, and at last settled on a constant value in the course of about ten minutes.

In the absence of the catalyst, the initiation of a reaction could be observed at a somewhat higher temperature than that of the reaction using catalyst, but no distillable product was obtained.

Another feature was a yield of a considerable amount of nonvolatile distillation residue. It was also noticeable that any fraction which distilled in the range of boiling point of the β-isomer was not obtained at all.

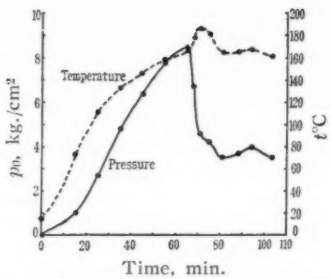

Fig. 1. An example of the cyanoethylation of trichlorosilane in an autoclave. (Trichlorosilane, 32.5 g., acrylonitrile, 19.1 g., and pyridine, 0.2 g.)

The Structural Proof of the Product obtained in an Autoclave

Several derivatives of the addition product was prepared, and their chemical and physical properties were compared with those of the derivatives of the known β-cyanoethyltrichlorosilane. The reactions involved are as follows:

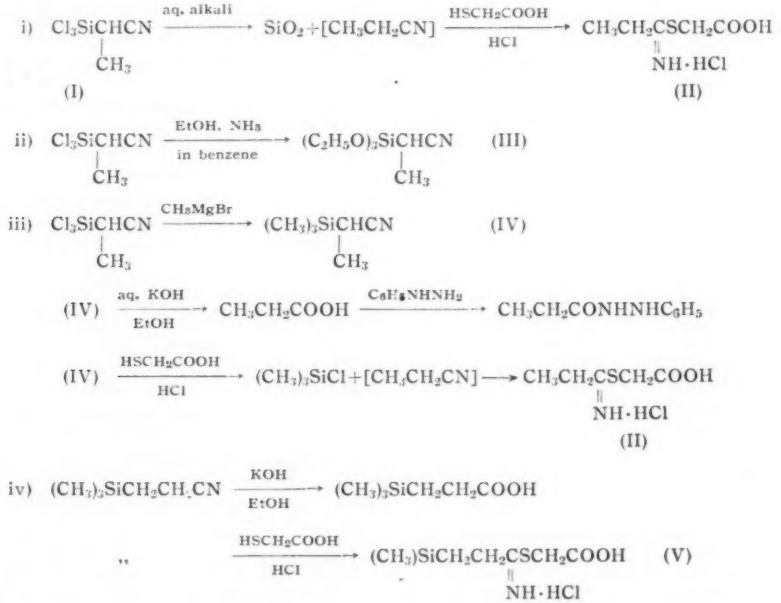
i) Cl3SiCHCN | CH3 (I) —aq. alkali→ SiO2 + [CH3CH2CN] —HSCH2COOH, HCl→ CH3CH2CSCH2COOH ‖ NH·HCl (II)
ii) Cl3SiCHCN | CH3 —EtOH, NH3 in benzene→ (C2H5O)2SiCHCN | CH3 (III)
iii) Cl3SiCHCN | CH3 —CH3MgBr→ (CH3)2SiCHCN | CH3 (IV)
(IV) —aq. KOH, EtOH→ CH3CH2COOH —C6H5NHNH2→ CH3CH2CONHNHC6H5
(IV) —HSCH2COOH, HCl→ (CH3)3SiCl + [CH3CH2CN] → CH3CH2CSCH2COOH ‖ NH·HCl (II)
iv) (CH3)2SiCH2CH2CN —KOH, EtOH→ (CH3)3SiCH2CH2COOH
,, —HSCH2COOH, HCl→ (CH3)SiCH2CH2CSCH2COOH ‖ NH·HCl (V)

i) When the product (I) was hydrolyzed in a large excess of water and neutralized with an aqueous solution of ammonia, there was precipitated an amorphous silica as the result of the cleavage of the silicon-carbon bond. The organic fragment, propionitrile, was separated out and identified as the

thioglycolic acid adduct (II). In contrast with this, the β-isomer did not result in the cleavage of the silicon-carbon bond but gave the corresponding β-cyanoethylpolysiloxane.

ii) The alcoholysis of the compound (I) was carried out according to an usual manner which contains the treatment with absolute alcohol in benzene and with dry ammonia. The low yield (37%) of the alcoholysis may be partly due to the cleavage of the silicon-carbon bond during the reaction. The physical constants of the compound (III) were also quite different from that of the β-isomer.

iii) The hydrolysis of α-cyanoethyltrimethylsilane (IV) by an aqueous solution of alkali resulted in the cleavage of the silicon-carbon bond. The fission product, propionic acid, was identified as its phenylhydrazide. The reaction of the compound (IV) with thioglycolic acid in the presence of dry hydrogen chloride also gave the fission product (II).

iv) On the other hand, the hydrolysis and the reaction with thioglycolic acid of the β-cyanoethyltrimethylsilane yielded β-trimethylsilylpropionic acid and silicon-containing thioglycolic acid adduct (V), respectively. This is the marked difference from the case of the α-isomer.

The fission of the silicon-carbon bonds shown in these reactions is reasonably explainable by assigning α-cyanoethyltrichlorosilane to the structure of this addition product. Sommer and Marans[3] also reported the fission of ethyltrimethylsilylacetate by acid or alkali:

$$(CH_3)_3SiCH_2COOC_2H_5 \xrightarrow{HCl} (CH_3)_3SiCl + CH_3COOC_2H_5$$
$$(CH_3)_3SiCH_2COOC_2H_5 \xrightarrow{OH^-} (CH_3)_3SiOH + CH_3COOC_2H_5$$

The ease of fission of α-cyanoethylsilyl derivatives may be interpreted by the similar situation of its electronic configuration to that of ethyltrimethylsilylacetate, that is, in both cases an electronically negative atom

TABLE I

α-CYANOETHYLATION OF TRICHLOROSILANE IN SEALED TUBES AT 160°C[a]

No.	Catalysts, g.		Reaction time, hr.	Yield of α-adduct, %[b]	Appearance after heating
1	$AlCl_3$,	0.1	5.0	0	light brown
2	$FeCl_3$,	0.1	5.0	0	light yellow
3	stainless foil, pyridine	2.0 0.1	5.0	0	characteristic deep brownish black
4	Fe powder pyridine,	1.5 0.1	5.0	trace	light brown
5	Ni powder pyridine,	2.0 0.1	5.0	7	characteristic deep brownish black
6	Cr powder pyridine,	2.0 0.1	5.0	12	brown, mainly β-addition[c]
7[d]	stainless foil, pyridine,	2.0 0.1	3.0	0	light yellow
8[e]	stainless foil, pyridine,	2.0 0.1	5.0	31	characteristic deep brownish black
9	$NiCl_2$,	0.2	5.0	trace	colorless
10	$NiCl_2 \cdot C_5H_5N \cdot HCl$,	0.2	5.0	22	characteristic deep brownish black[f]
11	$NiCl_2 \cdot C_5H_5N$,	0.1	2.0	17	,, [g]
12	$NiCl_2 \cdot 4C_5H_5N$,	0.1	5.0	7	,, [h]

a) About 20 g. of trichlorosilane and 1.1 times equivalents of acrylonitrile were used.
b) Considering from their boiling points, the contamination by β-adduct if any is probably very small. The yields are based on trichlorosilane.
c) b.p. 97–101° (30 mmHg).
d) Benzene (40 ml.) was used as solvent.
e) Acetonitrile (40 ml.) was used as solvent.
f) Distillation residue, 5 g.
g) Residue, 7 g.
h) Reaction temp., 160–70°C. Residue, 8 g. Hydrolyzable Cl, 32.1%.

3) L.H. Sommer and N.S. Marans, *J. Am. Chem. Soc.*, **72**, 1935 (1950).

(oxygen or nitrogen) having the unshared electrons is situated at the β-position to silicon by an unsaturated bond.

$$\equiv Si-CH_2-\overset{OC_2H_5}{\overset{|}{C}}=\ddot{O}: \qquad \equiv Si-\overset{CH_3}{\overset{|}{CH}}-C\equiv N:$$

Cyanoethylation of Trichlorosilane in sealed Tubes

In order to find out what catalysed the α-cyanoethylation in an autoclave, we carried out the reaction in a sealed glass tube in the presence of one of several possible catalysts taking it into consideration that the wall of the autoclave might have some catalytic influences. Experimental results are given in Table I. The Friedel-Crafts type catalyst, anhydrous ferric chloride and aluminum chloride, showed no effect. Only nickel metal among the constituent metals of 18-8 stainless steel of the autoclave seemed te be responsible for a catalytic effect for the α-addition in the presence of pyridine, but in this case the yield of the product was very low and the distillation residue amounted to a considerable quantity. Anhydrous nickel (II) chloride also showed only a poor catalytic activity. Mono- and tetrapyridine nickel (II) chloride, $NiCl_2 \cdot C_5H_5N$, $NiCl_2 \cdot 4C_5H_5N$, and nickel chloride pyridine hydrochloride complex compound, $NiCl_2 \cdot C_5H_5N \cdot HCl$, were found to show the marked catalytic effect for the α-addition.

In all the α-addition reactions, as we mentioned above, the comparatively large amount of distillation residue was observed. This may have a close correlation with the fact that α-cyanoethyltrichlorosilane was found to be easily decomposed by heating in the presence of tetrapyridine nickel chloride. When α-cyanoethyltrichlorosilane was heated along with a catalytic amount of tetrapyridine nickel chloride in a sealed tube at 160°C., only 43% of the starting chlorosilane was recovered from the deep brownish black reaction mixture by distillation in vauco. The distillation residue was about 19% of the starting material, and therefore the total weight loss during the procedure amounted to about 38% of the starting material. Thus, the large weight loss and the considerable amount of the residue suggest us the decomposition of the α-adduct. Therefore, it seems to be probable that the low yield of the α-cyanoethyltrichlorosilane is partly due to the secondary degradation reaction, and the yield of the primary addition product may be much higher than the observed value.

Reaction Mechanism

In view of the above results it appears to be that either nickel chloride pyridine hydrochloride complex, mono- or tetrapyridine nickel chloride is one of the probable catalyst for the reaction in an autoclave. The mechanism of the catalytic action of these compounds still remains to be ambiguous.

As both the peroxide- and base-catalyzed additions are known to lead to the β-addition, one of the possible interpretations of the α-addition is the intermediate ionization of a silicon-hydrogen bond to a siliconium cation and a hydride anion.

$$Cl_3Si-H+\overset{\delta+}{C}H_2=\overset{\delta-}{C}HCN \longrightarrow CH_2\underset{SiCl_3}{\underset{|}{C}}HCN$$

These ionic mechanism is supported in part by the effect of solvents, which is shown in experiment No. 7 and 8 in Table I.

Experimental

Catalysts.—The preparation of the platinized asbestos was described in the preceding paper[2].

Mono- and tetra-pyridine nickel chlorides and nickel chloride pyridine hydrochloride complex were prepared according to the method of Reizenstein[4].

Iron powder was the commercial product, and nickel and chrom powder were prepared from the electrolyzed metals.

The Reaction of Trichlorosilane and Acrylonitrile.—A mixture of trichlorosilane, acrylonitrile, and a catalyst was charged into a 18-8 stainless steel autoclave of 100 ml. capacity. The air in the autoclave was replaced by nitrogen, and then the gradual heating was applied. (Fig. 1). A sudden exothermic reaction started at a temperature between 150 and 170°C in the presence of either pyridine or platinized asbestos. The heating was stopped in about thirty minutes after the rapid decrease of the pressure had ceased. The color of the reaction mixture was always a deep brownish black which was characteristic to the α-cyanoethylation of trichlorosilane. The reaction mixture was then washed out by benzene, and after the removal of benzene by distillation at an atmospheric pressure, the remaining product was distilled in vacuo. The yield of α-cyanoethyltrichlorosilane was 21-39% (to trichlorosilane used) and approximately equal volume of non-volatile distillation residue was produced.

Without catalyst, the reaction started at about 190°C, the yield of addition product was null, and a resin-like distillation residue of about 30 weight % was obtained.

The purified α-cyanoethyltrichlorosilane boils at 96-8° (41.5 mmHg).

Anal. Found: Hydrolyzable Cl, 56.3. Calcd. for $C_3H_4NSiCl_3$: Cl, 56.5%.

4) F. Reizenstein, *Z. anorg. Chem.*, **11**, 254 (1896); **18**, 264 (1898).

The procedure for the reaction of trichlorosilane and acrylonitrile in sealed glass tubes was similar to that of the preceding paper.

Degradation of α-Cyanoethyltrichlorosilane.—A mixture of 27 g. of α-cyanoethyltrichlorosilane (b.p. 99–102° (50 mmHg)) and 0.1 g. of tetrapyridine nickelchloride sealed in glass reaction tube was heated at 160°C. for six hours. The reaction mixture was colored to a deep brownish-black. Distillation gave 11.6 g. (43%) of the recovered chlorosilane (b.p. 101–5° (51 mmHg)), and 5.0 g. of a resin-like distillation residue (hydrolyzable Cl, 32.3%).

Hydrolysis of α-Cyanoethyltrichlorosilane (I).—When a small portion of α-cyanoethyltrichlorosilane was poured onto a large amount of water, it dissolved clearly with the evolution of heat. By neutralizing the acidic solution with an excess of 6 N aqueous solution of ammonia, the gellation took place. The gelled silica was filtered, washed with water, and dried in vacuo at 100°C.

Anal. A qualitative test for N was negative. Found: Si, 44.15. Calcd. for SiO_2: Si, 46.65%.

When 2.5 g. of trichlorosilane (I) was added dropwise to 10 ml. of 6 N aqueous sodium hydroxide, the once precipitated silica dissolved clearly into the solution. The alkaline solution was extracted twice with 20 ml. of ether. The ether layer was dried with calcium chloride, filtered, 1.0 g. of thioglycolic acid was added, and it was saturated with dry hydrogen chloride under the ice-cooling. After standing over night in ice-water, the thioglycolic acid adduct of propionitrile (II) crystallised in fine needles. The crystal was filtered, washed with ether, and dried in desiccater over phosphorous pentoxide, the yield was 0.5 g. (20%), m.p. 124°.

Anal. Found: Cl, 19.38. Calc. for $C_5H_{10}NO_2SCl$: Cl, 19.33%.

α-Cyanoethyltriethoxysilane (III).—The reaction procedure was analogous to that of β-cyanoethyltriethoxysilane in the preceding paper. From 16.6 g. (0.088 mol.) of α-cyanoethyltrichlorosilane and 13.0 g. (0.28 mol.) of absolute alcohol, 1.4 g. of ethylorthosilicate (b.p. 76–8° (26 mmHg)) and 7.1 g. of the crude α-cyanoethyltriethoxysilane (III) (b. p. 115–9° (26 mmHg)) was obtained. (37%). The compound (III) was purified by redistillation, b.p. 119–120° (26.5 mmHg) d_4^{25}, 0.9630; n_D^{25}, 1.4070.

Anal. Found: N, 6.45; Si, 12.73. MR_D, 55.46. Calcd. for $C_9H_{19}NO_3Si$: N, 6.45; Si, 12.91%. MR_D, 55.26.

α-Cyanoethyltrimethylsilane (IV).—When 19g. (0.10 mol.) of α-cyanoethyltrichlorosilane (I) was methylated in a usual manner with the ether solution of methylmagnesium bromide prepared from 10.7 g (0.44 Atom) of magnesium, 6.4 g. of crude α-cyanoethyltrimethylsilane (IV) was obtained, b.p. 95–9° (66 mmHg) (50%). In order to remove the possible impurity of α-trimethylsilylethylmethylketone, the crude product was shaken with the saturated solution of sodium bisulfite, washed with water, dried with sodium sulfate, and distilled again in vacuo, yielding 4.1 g. of pure α-cyanoethyltrimethylsilane (IV), b.p. 91.5–92.5° (58 mmHg); d_4^{25}, 0.8254; n_D^{25}, 1.4232.

Anal. Found: N, 10.50; Si, 21.09. MR_D, 39.19. Calcd. for $C_5H_{13}NSi$: N, 11.02; Si, 22.05%. MR_D, 39.09.

Reactions of β- and α-Cyanoethyltrimethylsilane (IV) with Thioglycolic Acid.—When a mixture of 0.2 g. of α-cyanoethyltrimethylsilane (IV), 0.3 g. of thioglycolic acid, and 1 ml. of dry ether, was saturated with dry hydrogenchloride under the cooling with ice water, a needlelike crystal began to appear within a half hour. After standing for one hour, the crystal was filtered and washed with ether, dried in desiccater. The yield of the thioglycolic acid adduct of propionitrile was 0.1 g., m.p. 119–120°.

Anal. Found: Cl, 19.23; Si, 0.00. Calcd. for $C_5H_{10}NO_2SCl$: Cl, 19.33; Si, 0.00%.

A mixture of 0.2 g. of β-cyanoethyltrimethylsilane, 0.3 g. of thioglycolic acid, and 1 ml. of ether was similarly treated with dry hydrogen chloride. The crystallization was completed in half an hour and 0.2 g. of the needle-like adduct was obtained, m.p. 143°.

Anal. Found: Cl, 13.98; Si, 11.03. Calcd. for $C_8H_{18}NO_2SClSi$: Cl, 13.87; Si, 10.95.

Alkaline Hydrolysis of α-Cyanoethyltrimethylsilane (IV).—When a solution of 4.0 g. of potassium hydroxide in 4 ml. of water was added to 3.1 g. of α-cyanoethyltrimethylsilane, a vigorous reaction took place. Then 10 ml. of alcohol was added to the solution and it was refluxed for five hours until the evolution of ammonia ceased. To the reaction mass 40 ml. of water was added after cooling, and extracted with 10 ml. of ether to remove the unreacted nitrile. The aqueous layer was acidified with hydrochloric acid and extracted again with ether. The ether layer, which contained the produced carboxylic acid, was dried with sodium sulfate, filtered, and distilled. The carboxylic acid thus obtained was identified as its phenylhydrazide as follows; the distillate (b.p. 65–145°, 1.3 g.) and 2.0 g. of phenylhydrazine were refluxed for a half hour on a free flame. After cooling, the crystalline mass was filtered and washed thoroughly with benzene to yield 1.0 g. of propionic phenylhydrazide as a scaly crystal, m.p. 154–5°. After recrystallization from benzene, it melted at 155–6°C (157° in literature).

Summary

Contrary to the case of β-cyanoethylation, α-cyanoethylation of trichlorosilane was found to take place in an autoclave in the presence of either pyridine or platinized asbestos.

In the reactions in sealed glass tubes, on the other hand, stainless steel and pyridine, mono- and tetrapyridine nickel chloride, and nickel chloride pyridine hydrochloride complex were effective for the α-addition. An ionic mechanism was suggested for the α-cyanoethylation.

The structural proof of α-cyanoethyltrichlorosilane was given from the comparison

of the physical constants and chemical behaviour of it to those of the β-isomer. α-Cyanoethyl-triethoxysilane and -trimethylsilane were prepared from α-cyanoethyltrichlorosilane and characterised.

The authors are much indebted to Profs. S. Murahashi and H. Tani for their many helpful suggestions. Appreciation is also expressed to Nihon Silicon Resin Co. for their kindness of supplying the trichlorosilane.

Department of Chemistry
Faculty of Science
Osaka University, Osaka

Electronic States of the C_2 Radical

By Kenji FUEKI and Jiro HIGUCHI

(Received October 25, 1955)

Introduction

The investigation of the electronic properties for the carbon-carbon bond have generally been performed on the interactions between the π-electrons. For the precise study of charge distribution, hyperconjugation and so on, it is very desirable to take into consideration the mutual interactions between all the electrons, at least between all the valence electrons. Nevertheless, only a few investigations have been carried out in such a way, because of the complicated procedure required, in comparison with that for the π-electrons only. Moreover, it is very difficult to appraise the effect of the errors accompanying the calculation for the σ-electrons, since there are, in general, few experimental data except for the π-orbitals. From this point of view, the C_2 radical is one of the most suitable examples, because it is the simplest molecule and there are abundant experimental data on it.

The Swan bands and the Mulliken bands of the C_2 radical have been detected in flames, explosions and electric discharges of hydrocarbons, and recently also in flash photolysis; the other bands have also been observed by spectroscopic technique. On the other hand, theoretical investigations were qualitatively made by Mulliken[1], who predicted many unobserved states. A quantitative calculation was carried out by Araki, Tutihasi and Watari[2] using the AO method, but the results were not sufficiently satisfying to explain the observed electronic states. In the present work, therefore, the LCAO-SCF method was adopted and the interactions between all the electrons were included.

Outline of Calculation

The calculation was carried out by taking ten atomic orbitals c, s, σ, π_+, π_-, c', s', σ', π_+' and π_-' into consideration, which mean $1s$, $2s$, $2p\sigma$, $2p\pi_+$, $2p\pi_-$ orbitals of each carbon atom. The $1s$ AO's were regarded as the inner shells, since the overlap integrals between c or c' and the other AO's are fairly small in comparison with the others[3]. The internuclear distance was taken as 1.33 Å, nearly equal to the equilibrium internuclear distance of the observed lowest state $^3\Pi_u$, i. e., 1.31 Å[4].

The atomic orbitals used were the Hartree SCF AO's for the s^2p^2 configuration of carbon atom[5] as in the case of the CH radical[6], assuming that they satisfy the following Fock equations for the valence state $V_2(\sigma\pi)$ in the s^2p^2 configuration.

$$(I+2J_c-K_c+2J_s-K_s+J_\sigma-\frac{1}{2}K_\sigma+J_\pi-\frac{1}{2}K_\pi)s$$
$$=(I_s+2J_{cs}-K_{cs}+J_{ss}+J_{s\sigma}-\frac{1}{2}K_{s\sigma}+J_{s\pi}-\frac{1}{2}K_{s\pi})s, \quad (1)$$

$$(I+2J_c-K_c+2J_s-K_s+J_\pi-\frac{1}{2}K_\pi)\sigma$$
$$=(I_\sigma+2J_{c\sigma}-K_{c\sigma}+2J_{s\sigma}-K_{s\sigma}+J_{\sigma\pi}-\frac{1}{2}K_{\sigma\pi})\sigma, \quad (2)$$

1) R.S. Mulliken, *Phys. Rev.*, **41**, 751 (1932); **56**, 778 (1939).

2) G. Araki, S. Tutihashi and W. Watari, *Prog. Theor. Phys.*, **6**, 135 (1951); G. Araki and W. Watari, *Prog. Theor. Phys.*, **6**, 945 (1951).

3) $S_{cc'}=0.00005$, $S_{sc'}=0.05086$, $S_{\sigma c'}=0.08619$, while $S_{ss'}=0.45626$, $S_{s\sigma'}=0.44413$.

4) G. Herzberg, "Molecular Spectra and Molecular Structure", D. Van Nostrand Company, Inc., New York (1950), Second Edition, Vol. 1, p. 518.

5) C.C. Torrance, *Phys. Rev.*, **46**, 388 (1934). The Hartree-Fock SCF AO's for the V_4 $(\sigma\pi)$ have not yet been obtained, and therefore the Hartree SCF AO's were used.

6) J. Higuchi, *J. Chem. Phys.*, **22**, 1339 (1954).

$$(I+2J_c-K_c+2J_c-K_s+J_\sigma-\frac{1}{2}K_\sigma)\pi_\pm$$
$$=(I_{\pi_\pm}+2J_{c\pi_\pm}-K_{c\pi_\pm}+2J_{s\pi_\pm}-K_{s\pi_\pm}+J_{\sigma\pi_\pm}$$
$$-\frac{1}{2}K_{\sigma\pi_\pm})\pi_\pm. \quad (3)$$

Here

$$I=-\frac{1}{2}\Delta_\nu-\frac{6}{r_{c\nu}}, \quad (4)$$

$$J_{i^\nu}\phi^\nu=\left(\int\bar{\phi}_{i^\mu}\frac{1}{r_{\mu\nu}}\phi_{i^\mu}d\tau^\mu\right)\phi^\nu, \quad (5)$$

$$K_{i^\nu}\phi^\nu=\left(\int\phi_{i^\mu}\frac{1}{r_{\mu\nu}}\phi^\mu d\tau^\mu\right)\phi_{i^\nu}, \quad (6)$$

and

$$I_i=\int\phi_{i^\nu}\left(-\frac{1}{2}\Delta_\nu-\frac{6}{r_{c\nu}}\right)\phi_{i^\nu}d\tau^\nu, \quad (7)$$

$$J_{ij}=\int\phi_{i^\mu}\phi_{j^\nu}\frac{1}{r_{\mu\nu}}\phi_{i^\mu}\phi_{j^\nu}d\tau^{\mu\nu}, \quad (8)$$

$$K_{ij}=\int\phi_{i^\mu}\phi_{j^\nu}\frac{1}{r_{\mu\nu}}\phi_{j^\mu}\phi_{i^\nu}d\tau^{\mu\nu}. \quad (9)$$

Consequently, one-center integrals calculated by Ufford[7] were used. It is very difficult, however, to calculate the majority of the two-center integrals and it is assumed that the use of the Slater AO's[8] instead of the SCF AO's gives good approximations of these integrals, and they were taken from the table by Kotani et al[9]. The core-field energies were obtained from the above Fock equations (1)-(3).

From the eight available AO's, the symmetry orbitals for the C_2 radical were obtained as follows:

$$\begin{aligned}
&\sigma_1=2^{-1/2}(s+s'), && \sigma_2=2^{-1/2}(\sigma+\sigma')\\
&\sigma_3=2^{-1/2}(s-s'), && \sigma_4=2^{-1/2}(\sigma-\sigma')\\
&\sigma_5=2^{-1/2}(\pi_++\pi_+'), && \sigma_6=2^{-1/2}(\pi_-+\pi_-')\\
&\sigma_7=2^{-1/2}(\pi_+-\pi_+'), && \sigma_8=2^{-1/2}(\pi_--\pi_-').
\end{aligned} \quad (10)$$

By taking linear combinations of these, a like number of MO's of the same symmetry was formed as follows:

$$\begin{aligned}
&K=c, && K'=c'\\
&1\sigma_g=a_{11}\sigma_1+a_{12}\sigma_2, && 1\sigma_u=a_{33}\sigma_3+a_{34}\sigma_4\\
&2\sigma_g=a_{21}\sigma_1+a_{22}\sigma_2, && 2\sigma_u=a_{43}\sigma_3+a_{44}\sigma_4\\
&1\pi_g^+=a_{77}\sigma_7, && 1\pi_u^+=a_{55}\sigma_5\\
&1\pi_g^-=a_{88}\sigma_8, && 1\pi_u^-=a_{66}\sigma_6.
\end{aligned} \quad (11)$$

The prescripts 1, 2 are in the order of increasing energy within each symmetry. The coefficients of a_{ip}'s of the symmetry orbitals were chosen to satisfy the orbitals conditions:

$$\int\bar{\phi}_{i^\nu}\phi_{j^\nu}d\tau^\nu=\sum_{p,q}a_{ip}S_{pq}a_{jq}=\delta_{ij}, \quad (12)$$

where the overlap integrals S_{pq}'s are defined by

$$S_{pq}=S_{qp}=\int\sigma_p\sigma_q d\tau. \quad (13)$$

In the first place, the SCF calculation[10] was carried out for the lowest $^3\Sigma_g^-$ state $KK'(1\sigma_g)^2(1\sigma_u)^2(1\pi_u)^2(2\sigma_g)^2$, which has been considered to be close above the lowest $^3\Pi_u$ state or to be the ground state.

Next the SCF calculation was also carried out for the state $^1\Sigma_g^+$ $KK'(1\sigma_g)^2(1\sigma_u)^2(1\pi_u)^4$, which has been supposed to be the lowest singlet state. However, the energy for the lowest $^3\Pi_u$ state $KK'(1\sigma_g)^2(1\sigma_u)^2(1\pi_u)^3(2\sigma_g)^1$, was not minimized, because the properties of the state can readily be inferred from the results of the $^3\Sigma_g^-$ and $^1\Sigma_g^+$ states.

LCAO MO's

The LCAO MO's obtained by the SCF procedure are given in Table I, and the SCF solutions are given in Table II. The $^3\Sigma_g^-$

TABLE I

LCAO SCF MO's FOR $\left\{\begin{matrix}^3\Sigma_g^-\\ ^1\Sigma_g^+\end{matrix}\right\}$ STATE

	$K=c,$		$K'=c'$
$1\sigma_g=$	$\left\{\begin{matrix}0.628\\ 0.693\end{matrix}\right\}$	σ_1+	$\left\{\begin{matrix}0.395\\ 0.298\end{matrix}\right\}$ σ_2
$2\sigma_g=$	$\left\{\begin{matrix}0.609\\ 0.534\end{matrix}\right\}$	σ_1-	$\left\{\begin{matrix}0.830\\ 0.870\end{matrix}\right\}$ σ_2
$1\sigma_u=$	$\left\{\begin{matrix}1.089\\ 1.085\end{matrix}\right\}$	σ_3-	$\left\{\begin{matrix}0.303\\ 0.307\end{matrix}\right\}$ σ_4
$2\sigma_u=$	$\left\{\begin{matrix}1.658\\ 1.660\end{matrix}\right\}$	σ_3+	$\left\{\begin{matrix}1.746\\ 1.745\end{matrix}\right\}$ σ_4

$1\pi_u^\pm=0.888\,\sigma_6$, $1\pi_g^\pm=1.193\,\sigma_8$.

7) C.W. Ufford, *Phys. Rev.*, 53, 568 (1938).

8) $c=(\delta'^3/\pi)^{1/2}\exp(-\delta' r)$, $s=(\delta'^3/3\pi)^{1/2}r\exp(-\delta r)$, $\sigma=(\delta^5/\pi)^{1/2}r\exp(-\delta r)\cos\theta$, $\pi_\pm=(\delta^5/2\pi)^{1/2}r\exp(-\delta r)\sin\theta\exp(\pm i\varphi)$.
In the present calculation δ and δ' are chosen as 1.59 and 5.6875, respectively.

9) M. Kotani, A. Amemiya, T. Shimose, *Proc. Phys-Math. Soc. Japan*, 20, Extra No. 1 (1938); M. Kotani, E. Ishiguro, K. Hijikata, T. Nakamura and A. Amemiya, *J. Phys. Soc. Japan*, 8, 463 (1953).

10) In the present calculation, the following approximation was used
$$\int\bar{p}^\nu\left(-\frac{6}{r_{\gamma c}}\right)q'^\nu d\tau^\nu+2(pq':cc)-(pc:cq')$$
$$\sim\int\bar{p}^\nu\left(-\frac{4}{r_{c\nu}}\right)q'^\nu d\tau^\nu,$$
where the c, p orbitals and the q' orbital belong to different atoms. In the calculation of $\int\frac{4}{r_{c\nu}}s^\nu q'^\nu d\tau^\nu$, the orthogonalized $2s$ function was used for s, because the error due to the nonorthogonal $2s$ function is very significant near the C nucleus.

TABLE II

SELF-CONSISTENT SOLUTIONS*

			state	$^3\Sigma_g^-$	$^1\Sigma_g^+$
$S_{\sigma_1\sigma_1}$	1.45626	$G_{\sigma_1\sigma_1}$		4.2347	4.3051
$S_{\sigma_1\sigma_2}$	0.44413	$G_{\sigma_1\sigma_2}$		1.7262	1.7115
$S_{\sigma_2\sigma_2}$	1.31869	$G_{\sigma_2\sigma_2}$		4.1287	4.5383
$S_{\sigma_3\sigma_3}$	0.54374	$G_{\sigma_3\sigma_3}$		1.4686	1.5006
$S_{\sigma_3\sigma_4}$	−0.44413	$G_{\sigma_3\sigma_4}$		−1.1376	−1.1632
$S_{\sigma_4\sigma_4}$	0.68131	$G_{\sigma_4\sigma_4}$		1.7847	1.8224
$S_{\sigma_5\sigma_5}$	1.28695	$G_{\sigma_5\sigma_5}$		3.6731	3.7450
$H'_{\sigma_1\sigma_1}$	−5.7954	$\varepsilon_{1\sigma_g}$		−1.1922	−1.1196
$H'_{\sigma_1\sigma_2}$	−2.5345	$\varepsilon_{2\sigma_g}$		−0.5395	−0.2044
$H'_{\sigma_2\sigma_2}$	−5.2574	$\varepsilon_{1\sigma_u}$		−0.6375	−0.5793
$H'_{\sigma_3\sigma_3}$	−1.8011	$\varepsilon_{2\sigma_u}$		+0.2559	+0.3103
$H'_{\sigma_3\sigma_4}$	+1.4718	$\varepsilon_{1\pi_u}$		−0.5448	−0.4851
$H'_{\sigma_4\sigma_4}$	−2.0356	$\varepsilon_{1\pi_g}$		+0.0699	+0.0854
$H'_{\sigma_5\sigma_5}$	−4.3742				

* S_{pq}'s are the overlap integrals, H'_{pq}'s the core-field energy matrix elements, G_{pq}'s the electronic interaction matrix elements, ε_i's the LCAO SCF orbital energies.

state MO's also satisfy the conditions which minimize the energy of the $^1\Delta_g$ state $KK'(1\sigma_g)^2(1\sigma_u)^2(1\pi_u)^2(2\sigma_g)^2$ and the $^1\Sigma_g^+$ state $KK'(1\sigma_g)^2(1\sigma_u)^2(1\pi_u)^2(2\sigma_g)^2$, because the energy differences between these states are only proportional to the energy $K_{1\pi_u{}^+1\pi_u{}^-}$ which is independent of the LCAO-SCF procedure. These LCAO MO'S are, therefore, also the $^1\Delta_g$ state MO's and the $^1\Sigma_g^+$ MO's as well as the $^3\Sigma_g^-$ state MO's.

The coefficients of the AO's in these LCAO MO's are in good agreement with those predicted by Mulliken, and the LCAO MO's for the $^3\Sigma_g^-$ and $^1\Sigma_g^+$ states in Table I resemble each other. The special similarity for the weakly antibonding $1\sigma_u$ MO is due to the fact that the MO hardly effects the bonding property of the radical. In the strongly bonding $1\sigma_g$ MO, however, the coefficient of σ_1 for the $^1\Sigma_g^+$ state MO is rather large, but in the weakly bonding $2\sigma_g$ MO this relation is reversed, since the $2\sigma_g$ MO is vacant in the $^1\Sigma_g^+$ state while it is occupied in the $^3\Sigma_g^-$ state.

The coefficients of the AO's in the $^{1,3}\Pi_u$ MO's are generally considered to have the values between those of the $^3\Sigma_g^-$ state MO's and the $^1\Sigma_g^+$ stane MO's from the numbers of the occupied electrons in each MO's. In the total energies of the $^{1,3}\Pi_u$ states, however, the coefficients of the $K_{2\sigma_g 1\pi_u}$ are not the same and consequently the forms of the MO's will be somewhat different from each other. However, the $^3\Pi_u$ state MO's may be rather close to the $^3\Sigma_g^-$ state MO's (while the $^1\Pi_u$ state MO's may somewhat resemble to the $^1\Sigma_g^+$ state MO's), on account of the same coefficient of the $K_{2\sigma_g 1\pi_u}$. These MO's also rather resemble the N_2 ground state MO's by Scherr[11]. This is mainly due to the fact that the values of δR, R being the internuclear distance, are nearly equal and so the overlap integrals are very close in both cases.

In the $^3\Sigma_g^-$ state MO's, the orbital energy of $1\pi_u$ MO is very close to that of the $2\sigma_g$ MO. However, the result of the N_2 molecule by Scherr showed that the incomplete treatment gave the very close orbital energies for these MO's, while the $2\sigma_g$ MO energy is 0.96 eV. higher than the $1\pi_u$ MO enegy in the complete treatment. In consideration of these facts, the energy difference between these MO's will be increased by taking into account the inner-shell-outer-shell-mixing. The orbital energy of the $2\sigma_g$ MO in the $^1\Sigma_g^+$ state MO's is very high as compared with that in the $^3\Sigma_g^-$ state MO's, because the MO is vacant in the $^1\Sigma_g^+$ state and this value is the SCF orbital energy but not the orbital energy by Mulliken[12].

Electronic States

By using the LCAO MO's given in Table I, the energies of the lower electronic states were calculated without configuration interaction[13], and are shown in Fig. 1. The electronic configurations of these states are given in Table III. The energy levels calculated by both the LCAO MO's considerably resemble each other; therefore the energy levels which are to be obtained by the other state MO's than the $^3\Sigma_g^-$ and $^1\Sigma_g^+$ state MO's will be very similar to those in Fig. 1, as in the case of the CH radical.

The calculated value (2.5 eV.) of the $^3\Pi_g$ (a)—$^3\Pi_u$ (a) transition and that (5.4–5.5 eV.) of the $^3\Pi_g$ (b)—$^3\Pi_u$ (a) transition are in good

11) C.W. Scherr, *J. Chem. Phys.*, **23**, 569 (1955).
12) R.S. Mulliken, *J. chim. phys.*, **46**, 497 (1949).
13) The interactions between the wave functions arising from rotation operation were taken into consideration.

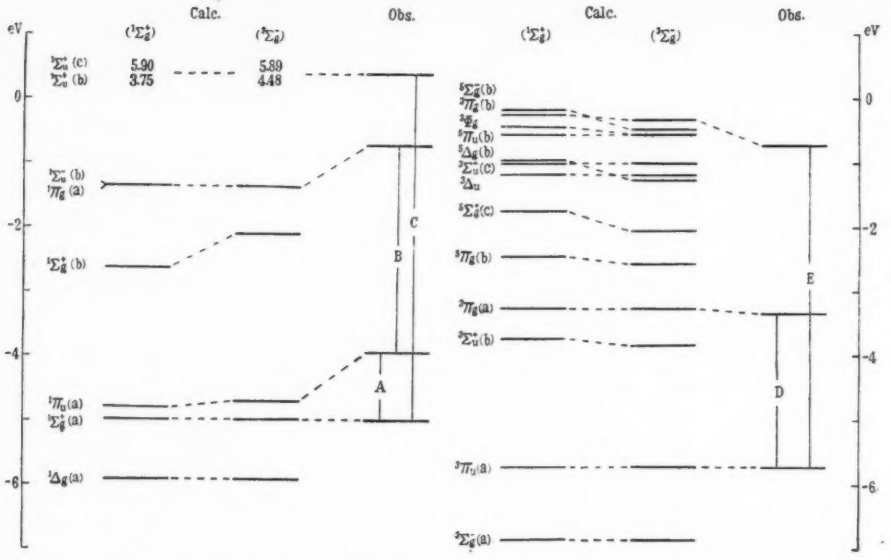

Fig. 1. Lower electronic states of the C_2 radical.
(A) The Phillips bands (B) The Deslandres-d'Azambuja bands (C) The Mulliken bands (D) The Swan bands (E) The Fox-Herzberg bands. The origin of energy is chosen to be $C(^3P)+C(^3P)$ without configuration interaction.

TABLE III

ELECTRON CONFIGURATIONS OF THE LOWER ELECTRONIC STATES

Configuration	State
$KK'(1\sigma_g)^2(1\sigma_u)^2(1\pi_u^{\pm})^2(2\sigma_g)^2$	$^1\Delta_g$(a)
〃 $(1\sigma_g)^2(1\sigma_u)^2(1\pi_u^{+})^1(1\pi_u^{-})^1(2\sigma_g)^2$	$^1\Sigma_g^+$(a), $^3\Sigma_g^-$(a)
〃 $(1\sigma_g)^2(1\sigma_u)^2(1\pi_u^{\pm})^2(1\pi_u^{\mp})^1(2\sigma_g)^1$	$^{1,3}\Pi_u$(a)
〃 $(1\sigma_g)^2(1\sigma_u)^1(1\pi_u^{\pm})^2(1\pi_u^{\mp})^1(2\sigma_g)^2$	$^{1,3}\Pi_g$(a)
〃 $(1\sigma_g)^2(1\sigma_u)^2(1\pi_u^{\pm})^2(1\pi_u^{\mp})^1(1\pi_g^{\mp})^1$	$^{1,3}\Sigma_u^+$(a), $^{1,3}\Sigma_u^-$(a)
〃 $(1\sigma_g)^2(1\sigma_u)^2(1\pi_u^{\pm})^1(2\sigma_g)^2(1\pi_g^{\pm})^1$	$^{1,3}\Delta_u$
〃 $(1\sigma_g)^2(1\sigma_u)^2(1\pi_u^{\pm})^2(2\sigma_g)^1(1\pi_g^{\mp})^1$	$^{1,3}\Phi_g$
〃 $(1\sigma_g)^2(1\sigma_u)^2(1\pi_u^{+})^2(1\pi_u^{-})^2$	$^1\Sigma_g^+$(b)
〃 $(1\sigma_g)^2(1\sigma_u)^1(1\pi_u^{+})^2(1\pi_u^{-})^2(2\sigma_g)^1$	$^{1,3}\Sigma_u^+$(b)
〃 $(1\sigma_g)^2(1\sigma_u)^2(1\pi_u^{\pm})^1(2\sigma_g)^2(1\pi_g^{\mp})^1$	$^{1,3}\Sigma_u^-$(b), $^{1,3}\Sigma_u^+$(c)
〃 $(1\sigma_g)^2(1\sigma_u)^2(1\pi_u^{+})^1(1\pi_u^{-})^1(2\sigma_g)^1(1\pi_g^{\pm})^1$	$^{1,1,3,3,3,5}\Pi_g$(b)
〃 $(1\sigma_g)^2(1\sigma_u)^1(1\pi_u^{\pm})^2(1\pi_u^{\mp})^1(2\sigma_g)^1(1\pi_g^{\pm})^1$	$^{1,1,3,3,3,5}\Delta_g$(b)
〃 $(1\sigma_g)^2(1\sigma_u)^1(1\pi_u^{+})^1(1\pi_u^{-})^1(2\sigma_g)^2(1\pi_g^{\pm})^1$	$^{1,1,3,3,3,5}\Pi_u$(b)
〃 $(1\sigma_g)^2(1\sigma_u)^1(1\pi_u^{\pm})^2(1\pi_u^{\mp})^1(2\sigma_g)^1(1\pi_g^{\mp})^1$	$^{1,1,3,3,3,5}\Sigma_g^-$(b), $^{1,1,3,3,3,5}\Sigma_g^+$(c)

agreement with the observed value (5179 Å)[14] of the Swan bands and that (2495 Å) of the Fox-Herzberg bands, respectively. The $^1\Pi_g$ (a) $-^1\Pi_u$ (a) interval (3.4-3.5 eV.) in this calculation is also in good agreement with the observed value (3865 Å) of the Deslandres-d'Azambuja bands. The experimentally known Phillips bands and Mulliken bands

14) All the observed values are taken from reference (4).

correspond to the $^1\Pi_u$ (a)—$^1\Sigma_g^+$ (a) (or $^1\Pi_u$ (a)—$^1\Sigma_g^+$ (b)) and $^1\Sigma_u^+$ (c)—$^1\Sigma_g^+$ (a) (or $^1\Sigma_u^+$ (b)—$^1\Sigma_g^+$ (b)) transitions, respectively, but the calculated transition of the latter bands is considerably larger than the experimental one. This is mainly due to the facts that the present calculation ignores configuration interaction and that the SCF procedure is carried out for the $^3\Sigma_g^-$ (a) and $^1\Sigma_g^+$ (b) states only. The calculated ground state is the $^3\Sigma_g^-$, while the lowest state observed is the $^3\Pi_u$. As pointed out by Mulliken[1], the ground state of the C_2 radical has not yet been conclusively decided from the experiment. But the $^1\Sigma_g^+$ state is most unlikely from the standpoint of spin multiplicity. On the other hand, Norrish, Porter and Thrush[15] pointed out that the separation between the $^1\Sigma_g^+$ and $^3\Pi_u$ states of 0.69 eV., as predicted by Herzberg and Sutton[16], is quite possible. In the present calculation, this separation is 0.76 eV. in good agreement with their prediction. The ground state may, therefore, be likely to be the $^3\Sigma_g^-$. In the complete treatment with the inner-shell-outer-shell-mixing, however, the $1\pi_u$ MO energy is expected to be somewhat lowered as compared with the $2\sigma_g$ MO energy, as supposed from the result of N_2 by Scherr; then the $^3\Pi_u$ (a) state may be calculated as the ground state in accord with the experiment. In a similar way, the $^1\Sigma_g^+$ (b) state will be very close to the $^1\Sigma_g^+$ (a) state, consequently the Phillips bands will be satisfactorily explained, if consideration is made of the configuration interaction between the above two $^1\Sigma_g^+$ states.

The dissociation energy of C_2 has not definitely been known. Herzberg gave the value of 3.6 eV. from spectroscopic evidence. Gaydon[17], however, pointed out that an extrapolation of the vibrational levels leads to 4–7 eV. Brewer, Gilles and Jenkins[18] have measured the variation in intensity with temperature of the Swan bands and deduced 4.95 ± 0.3 eV., which has been accepted by Gaydon. The value of about 6.2 eV.[19] has been suggested from the temperature dependence of the rate of evaporation of C_2 and graphite. Glockler[20] has given 5.9 eV. from bond energy-bond length relationships. In the present calculation, the dissociation energy obtained is 5.7 eV.[21] for the $^3\Pi_u$ state, which is rather close to the value by Gaydon, although the value will be decreased by the atomic configuration interaction.

Discussion

The results in the present calculation are qualitatively correct and also are semi-quantitatively satisfying. This is mainly due to the fact that the one-center integrals used are obtained by the SCF AO's. The two-center integrals are, however, still somewhat unsatisfying, because most of them are calculated by using the simple Slater AO's. In fact the errors due to the use of the simple $2s$ AO are not small, but the strong influence near the nucleus is modified by the approximation given in reference (10). Further, the use of the Slater AO's reduces the electronic interaction, especially between the σ-electrons, and consequently the form of the LCAO MO's will be somewhat changed by use of the two-center integrals of the SCF AO's.

The use of the fixed internuclear distance of 1.33 Å is not completely satisfactory to explain the experiment, because the equilibrium distances of the various states do not generally coincide with the value of 1.33 Å; for example, the state such as the $^1\Sigma_g^+$(b) has a rather small internuclear distance. Moreover, the interpretation of multiple bond must include the change of bond distance. Considering these facts, it is desirable to carry out the calculations for various internuclear separations. The treatment with the inner-shell-outer-shell-mixing is also desirable in a precise discussion. But the approximations in the present calculation may be fairly useful for larger molecules, if the problem is restricted to the subjects such as the order of the orbital energies, the one-electron excitation levels and so on. In the light of these facts, it is very hopeful to investigate the electronic properties of hydrocarbons with considerable accuracy by means of such a treatment.

15) R. G. W. Norrish, G. Porter and B. A. Thrush, *Nature*, **169**, 582 (1952).
16) G. Herzberg and R.B. Sutton, *Can. J. Res.*, A **18**, 74 (1940).
17) A.G. Gaydon, "Dissociation Energies and Spectra of Diatomic Molecules", Chapman and Hall Ltd., London (1953), Second Edition.
18) L. Brewer, P.W. Gilles and F.A. Jenkins, *J. Chem. Phys.*, **16**, 797 (1948).
19) T.L. Cottrell, "The Strength of Chemical Bonds", Butterworths Scientific Publications, London (1954), p. 199.
20) G. Glockler, *J. Chem. Phys.*, **19**, 124 (1951).
21) The zero-point energy is not included.

Summary

LCAO MO's and ionization energies have been calculated for the $^3\Sigma_g^-$ KK' $(1\sigma_g)^2(1\sigma_u)^2(1\pi_u)^2(2\sigma_g)^2$ and $^1\Sigma_g^+$ $KK'(1\sigma_g)^2(1\sigma_u)^2(1\pi_u)^4$ states of the C_2 radical at the internuclear distance of 1.33 Å using the LCAO-SCF method. The interactions of all the electrons have been taken into consideration, but the orthogonality relationship between the 1s and the other orbitals was assumed. The LCAO MO's obtained are in good agreement with those predicted by Mulliken. Using these LCAO MO's, the lower electronic states have been investigated without configuration interaction. The calculated levels are generally in good agreement with the experimental. The ground state obtained is the $^3\Sigma_g^-$ state, while the observed is the $^3\Pi_u$, but the result is not conclusive because of the ignorance of the inner-shell-outer-shell-mixing.

The authors wish to thank Professor S. Shida for his continued interest and kind advice.

Laboratory of Physical Chemistry, Tokyo Institute of Technology, Ookayama Meguro-ku, Tokyo

*Densities and Optical Properties of Organic Compounds in the Liquid State. VI. The Refractive Indices of Paraffin Hydrocarbons and Some of Their Derivatives**

By Maurice L. HUGGINS**

(Received November 8, 1955)

Introduction

The purpose of this paper is to relate the refractive indices, n_D, of various liquid aliphatic organic compounds at 20°C to their composition. This relationship is best shown with the aid of molal refractions (R, R' or R''), defined by the equations

$$R = V(n_D - 1), \tag{1}$$

$$R' = V(n_D^2 - 1), \tag{2}$$

and

$$R'' = V\frac{n_D^2 - 1}{n_D^2 + 2}. \tag{3}$$

V is the molal volume. These molal refractions are approximately additively calculable from contributions of the atoms, atomic groups, or bonds composing the molecule.

Although Eq. (3) has the soundest theoretical basis for simple gaseous system, for condensed systems it seems necessary to choose between these relationships on a purely empirical basis[2]. Fairly extensive calculations by the writer, both for liquid organic compounds and for glasses[3] indicate that R, R', and R'' exhibit about the same degree of additivity. For the present purpose, we choose the simplest: R.

The molal volume is the molecular weight divided by the density. If experimental density values are not available or are insufficiently accurate, the molal volume can, in many cases, be computed by simple empirical relationships.[1,4,5,6,7].

A considerable amount of accurate density and refractive-index data for organic compounds is now conveniently available[8,9].

* Communication No. 1757 from the Research Laboratories of the Eastman Kodak Company, Rochester 4, New York, U. S. A.

This paper is a revision of parts of a previously published paper[1] and of an unpublished paper, entitled "Refractive Indices of Liquid Aliphatic Organic Compounds," presented October 3, 1940 at a meeting of the Optical Society of America in Rochester, New York, U. S. A.

** Fulbright Exchange Professor, Osaka and Kyoto Universities, 1955-1956, on leave from the Research Laboratories of the Eastman Kodak Company, Rochester, 4, New York, U. S. A.

1) M. L. Huggins, *J. Am. Chem. Soc.*, **63**, 116 (1941).

2) S. S. Kurtz, Jr. and A. L. Ward, *J. Franklin Inst.*, **222**, 563 (1936); **224**, 583 (1937).

3) M. L. Huggins, *J. Opt. Soc. Am.*, **30**, 495 (1940).

4) M. L. Huggins, *J. Am. Chem. Soc.*, **63**, 916 (1941).

5) M. L. Huggins, *J. Am. Chem. Soc.*, **76**, 843 (1954).

6) M. L. Huggins, *J. Am. Chem. Soc.*, **76**, 845 (1954).

7) M. L. Huggins, *J. Am. Chem. Soc.*, **76**, 847 (1954).

8) "Selected Values of Properties of Hydrocarbons," Circular of the National Bureua of standerds C461, U. S. Government Printing Office, Washington, D.C., (1947).

9) J. Timmermans, "Physico-Chemical Constants of Pure Organic Compounds", Elsevier Publishing Co., Inc., Amsterdam (1950).

These data form the basis for the results reported here.

Hydrocarbons

The additivity relationships may be described in terms of contributions from the different types of atoms (C, H), atomic groups (CH_3, CH_2, CH, C), or bonds (C-C, C-H). For example, for normal paraffins, C_nH_{2n+2}, the best data lead to

$$R_n=7.821n+2.064, \tag{4}$$

which is equivalent to

$$R_n=5.757N_C+1.032N_H \tag{5}$$

or

$$R_n=7.821N_{CH_2}+8.853N_{CH_3}. \tag{6}$$

No similar equation, involving a uniform contribution of each C-C bond and each C-H bond, fits the data, for either normal paraffins or those of other types. By differentiating between different types of C-C and C-H bonds, however, one can deduce satisfactory additivity equations and constants.

To do this, use is made of data for several other series of saturated aliphatic hydrocarbons. These data are well satisfied by equations of the form of Eq. (4), but with different values of the constant term. Putting

$$R=R_n+k=7.821n+2.064+k, \tag{7}$$

the following values of k have been found:

2-Methyl alkanes $k_1=+0.014$ (8)

3-Methyl alkanes and 4-methyl alkanes $k_2=-0.137$ (9)

2,2-Dimethyl alkanes $k_3=+0.005$ (10)

3,3-Dimethyl alkanes and 4,4-dimethyl alkanes $k_4=-0.278$ (11)

As previously shown, these can be used to obtain relative bond refraction contributions, α_{ij}. The appropriate equations* are:

$$\alpha_{21}=(b-a)/2+2k_1-2k_2+k_3-k_4/2+5\delta$$
$$=3.325+5\delta \tag{12}$$

$$\alpha_{31}=\alpha_{22}=(b-a)/2+2k_1-2k_2+k_3-k_4/2$$
$$+4\delta=3.325+4\delta \tag{13}$$

$$\alpha_{11}=\alpha_{32}=(b-a)/2+k_1-k_2+k_3-k_4/2+3\delta$$
$$=3.174+3\delta \tag{14}$$

$$\alpha_{12}=\alpha_{33}=(b-a)/2+k_1-k_2+k_4/2+2\delta$$
$$=2.891+2\delta \tag{15}$$

$$\alpha_{13}=2.5+\delta \tag{16}$$

$$\alpha_{14}=2.0 \tag{17}$$

$$\alpha_{1H}=(b+a)/4-k_1/3+k_2/2-k_3/6$$
$$+k_4/12-\delta=2.397-\delta \tag{18}$$

$$\alpha_{2H}=(b+a)/4-k_1+k_2-k_3/2+k_4/4-2\delta$$
$$=2.248-2\delta \tag{19}$$

$$\alpha_{3H}=(b+a)/4-k_1+2k_2-3k_3/2+3k_4/4-3\delta$$
$$=1.967-3\delta. \tag{20}$$

The subscript 21 refers to a bond between a methylene carbon atom and a methyl carbon atom; the subscript 1H refers to a bond between a methyl carbon atom and a hydrogen atom; etc. The δ is an arbitrary constant, which need not be evaluated.

The molal refraction of saturated aliphatic hydrocarbons can also be represented by the equivalent relation

$$R_s=\sum_i N_i\alpha_i+\sum_{ij}N_{ij}\alpha'_{ij} \tag{21}$$

with the α_i and α'_{ij} values given in Table I.

TABLE I

REFRACTION CONTRIBUTIONS FOR SUBSTITUTION INTO EQ. (21)

i	α_i	ij	α'_{ij}
CH_3	8.853	CH-CH_3	+0.151
CH_2	7.821	C-CH_3	+ .283
CH	6.500	CH-CH	− .132
C	4.912	CH-C	− .088
		C-C	− .456

If either i or j is CH_2, the bond contribution α'_{ij} is zero. In other words, the α_i contributions given are those for i groups attached only to CH_2 groups.

Refractive indices computed with these relationships agree with the more precise experimental values to within a few units in the fourth decimal place. Since the results of extensive comparisons were summarized in Ref. 1, further comparisons need not be given here.

Derivatives

Molal refractions of a large number of ω-substituted normal paraffin have been compared with those of the parent hydrocarbons. For each homologous series, the difference is found to be quite constant. Addition of $\alpha_{CH_3}-\alpha_{CH_2}$ to these differences gives the values (α_X) of the refraction contributions of the substituents (X), for compounds in which they are attached to CH_2. The same contribution can be used for derivatives of branched-chain paraffins, provided the attachment is to a methylene carbon. Application to derivatives in which the attachment is to a carbon bonded to only one hydrogen or to none has not been adequately tested.

The contributions of 12 X substituents are listed in Table II.

The normal nitriles (X=CN) have been very carefully studied and will serve to illustrate the measure of agreement with

* The corresponding equations in Reference (1) were in error with regard to the coefficients of the k_1 and k_3 terms. Since these constants were then taken as zero, the relationships derived from these equations were not affected.

TABLE II

GROUP REFRACTION CONTRIBUTIONS FOR R-X AND R-Y-R′ COMPOUNDS

-X	α_X	-Y-	α_Y
-F	0.8	-O-	3.0
-Cl	9.6	-NH-	6.3
-Br	15.0	-S-	14.9
-I	24.6	-CO-	8.22
-OH	4.1	-CO-O-	10.6
-SH	15.1	-CO-O-CO-	19.8
-CN	8.88	-CO-NH-	14.4
$-NH_2$	7.2	$-CH(CH_3)-$	15.50
-CHO	9.7	$-C(CH_3)_2-$	23.18
$-CO_2H$	12.1		
$-NO_2$	11.2		
-ONO	11.7		

the assuption of constancy of the α contributions. (Table III)

7.897, respectively. For $m>6$, the average departure of the average R-R_m values from constancy is less than the average difference between the experimental values.

The reasons for the deviations from constancy of R-R_m, indicating deviations from additivity of the α-contributions, for the smaller values of m, will not be discussed at this time. It should be noted, however, that because of these deviation, in this and other series, refractive indices computed from the constants given here are much less accurate for the lower-molecular-weight compounds than for the higher members of the series.

The n_D (calc) values in Table III were from the experimental densities and an assumed constant value of $\alpha_{CN}=8.880$; hence R-$R_m=7.848$ and R_m is given by Eq. (4). For

TABLE III

REFRACTIONS OF n-ALKYL NITRILES, $C_mH_{2m+1}CN$

m	Ref.	d_4^{20}	R(exp)-R_m(calcd.)	n_D(expt.)	n_D(calcd.)
1	10	0.78212	8.176	1.34409	1.338
	11	.78204	8.167	1.34389	1.338
2	10	.78184	8.077	1.36600	1.363
	11	.78171	8.071	1.36585	1.363
	12	.78169	8.071	1.36585	1.363
3	10	.79090	8.031	1.38408	1.382
	11	.79085	8.027	1.38402	1.382
	12	.79085	8.010	1.38385	1.382
4	10	.79929	7.988	1.39745	1.3961
	11	.79919	7.960	1.39713	1.3960
	12	.79919	7.958	1.39711	1.3960
5	11, 12	.80531	7.925	1.40694	1.4063
6	11, 12	.80958	7.891	1.41419	1.4139
7	11	.81355	7.855	1.42018	1.42013
	12	.81362	7.850	1.42018	1.42016
	13	.81344	7.888	1.20344	1.42007
8	11	.81690	7.842	1.42522	1.42525
	12	.81684	7.847	1.42522	1.42522
9	11	.81967	7.846	1.42946	1.42947
	12	.81967	7.834	1.42940	1.42947
10	11, 12	.82180	7.838	1.43286	1.43290
11	11	.82390	7.844	1.43596	1.43597
	12	.82390	7.842	1.43595	1.43597
12	11	.82586	7.840	1.43867	1.43870
	12	.82574	7.845	1.43867	1.43864
13	12	.82792	7.848	1.44126	1.44126

The paraffin refractions R_m, were computed from Eq. (4), replacing n by m. For m greater than 5, these differ insignificantly from the best experimental values. (Cf. Ref. 1.) For m less than 5, experimental values are unobtainable. For $m=5$, the R-R_m values obtained using the *experimental* data for the paraffins from Refs. 8 and 10, are 7.912 and $m>6$, the calculated and experimental indices agree, on the average, within three units in the fifth decimal place.

Table II also lists α_Y-values, for compounds containing Y substituents bonded to two CH_2 groups. These contributions were obtained by substracting from the molal refraction of the compound R-Y-R′ that of the

hydrocarbon RR'. For comparison and for future reference, the contributions of two hydrocarbon Y groups, computed from the equations of the preceding section, are included.

Summary and Conclusion

For the saturated hydrocarbons, the more accurate data, published since the first paper of this series[1] was written, have been found to agree well with the previous additivity postulates. Revised values of the constants have been computed.

Refraction-contribution constants for various atoms and atomic groups, attached to CH_2 groups, have been deduced. Good additivity has been found, except for the compounds of lowest molecular weight in each series.

Pending further testing, caution should be observed in using the constants and additivity assumptions presented here in compounds containing C=C and C≡C bonds and in compounds in which the X and Y are attached to groups other than CH_2.

Discussion of the theoretical interpretation of the relative magnitudes of the group contributions will be postponed until a later time.

The Research Laboratory of the Eastman Kodak Company, Rochester 4, New York, U. S. A.

Studies on the Chemical Constitution of Agar-agar. XVIII[1]. *Isolation of a New Crystalline Disaccharide by Enzymatic Hydrolysis of Agar-agar*

By Choji ARAKI and Kiyoshi ARAI

(Received November 16, 1955)

The partial depolymerization of agar-agar by chemical methods, such as acid-hydrolysis[2], methanolysis[1], and mercaptolysis[3], has led to the isolation of agarobiose (4-O-β-D-galactopyranosyl-3,6-anhydro-L-galactose) (XI) or its derivatives as the chief oligosaccharide constituent so far identified. The enzymatic hydrolysis would be of great service to examine the structure of the polysaccharide, since the method might bring about oligosaccharide fragments different from those produced by chemical methods. This has been proved to be the case as reported herein.

The enzymatic hydrolysis of agar was first studied by Gran[4], who assigned the name gelase to the agar-hydrolysing enzymes of a microorganism isolated from sea water. Oshima[5] found gelase in the viscela of *Haliotus giganteus* Gm. (ear-shell), and Mori[6] also found it in the viscela, especially in hepatopancreas, of *Turbocornutus* (top-shell) and of other gastropodes. Kadota[7] prepared the enzyme solution capable of hydrolysing agar from a microorganism isolated from sea water. Fukumoto and Ishimatsu[8] gave the name agarase to the agar-hydrolysing enzymes of a microorganism isolated from putrid *tokoroten* (agar-gel). But little has been studied concerning the isolation and the structure of the hydrolysis product, until Ishimatsu and his co-workers[9] recently reported the characterization of a disaccharide, produced by the action of agarase upon agar, as its phenylosazone (m.p. 197°).

The enzyme extract used in this study has been prepared from *Pseudomonas kyotoensis*, an agar-digesting bacterium, isolated from putrid *tokoroten* by these authors[10]. An aqueous solution of agar was hydrolysed with this enzyme extract under the optimum condition until the reducing power of the solution reached a maximum value. From the resulting solution, there was obtained a mixture of reducing sugars, which were

1) Part XVII: C. Araki and S. Hirase, This Bulletin, **27**, 109 (1954).
2) C. Araki, *J. Chem. Soc. Japan*, **65**, 533, 627 (1944).
3) S. Hirase and C. Araki, This Bulletin, **27**, 105 (1954).
4) H. H. Gran, *Centralbl. Bakt. Abt.*, II, **9**, 562 (1902).
5) K. Oshima, *J. Agr. Chem. Soc. Japan*, **17**, 328 (1941).
6) T. Mori, *J. Agr. Chem. Soc. Japan*, **15**, 1070 (1939); **16**, 886 (1940).
7) H. Kadota, *Mem. Coll. Agr. Kyoto Univ.*, **59**, 54 (1954).
8) J. Fukumoto and K. Ishimatsu, *Bull. of the Osaka Municipal Technical Research Institute*, **13**, 1 (1951); K. Ishimatsu, ibid., **14**, 1 (1953).
9) K. Ishimatsu, Y. Kibesaki and S. Maitani, *Science and Industry (Japanese)*, **28**, 100 (1954).
10) C. Araki and K. Arai, *Memoirs of the Faculty of Industrial Arts, Kyoto Technical Univ.*, **3B**, 7 (1954).

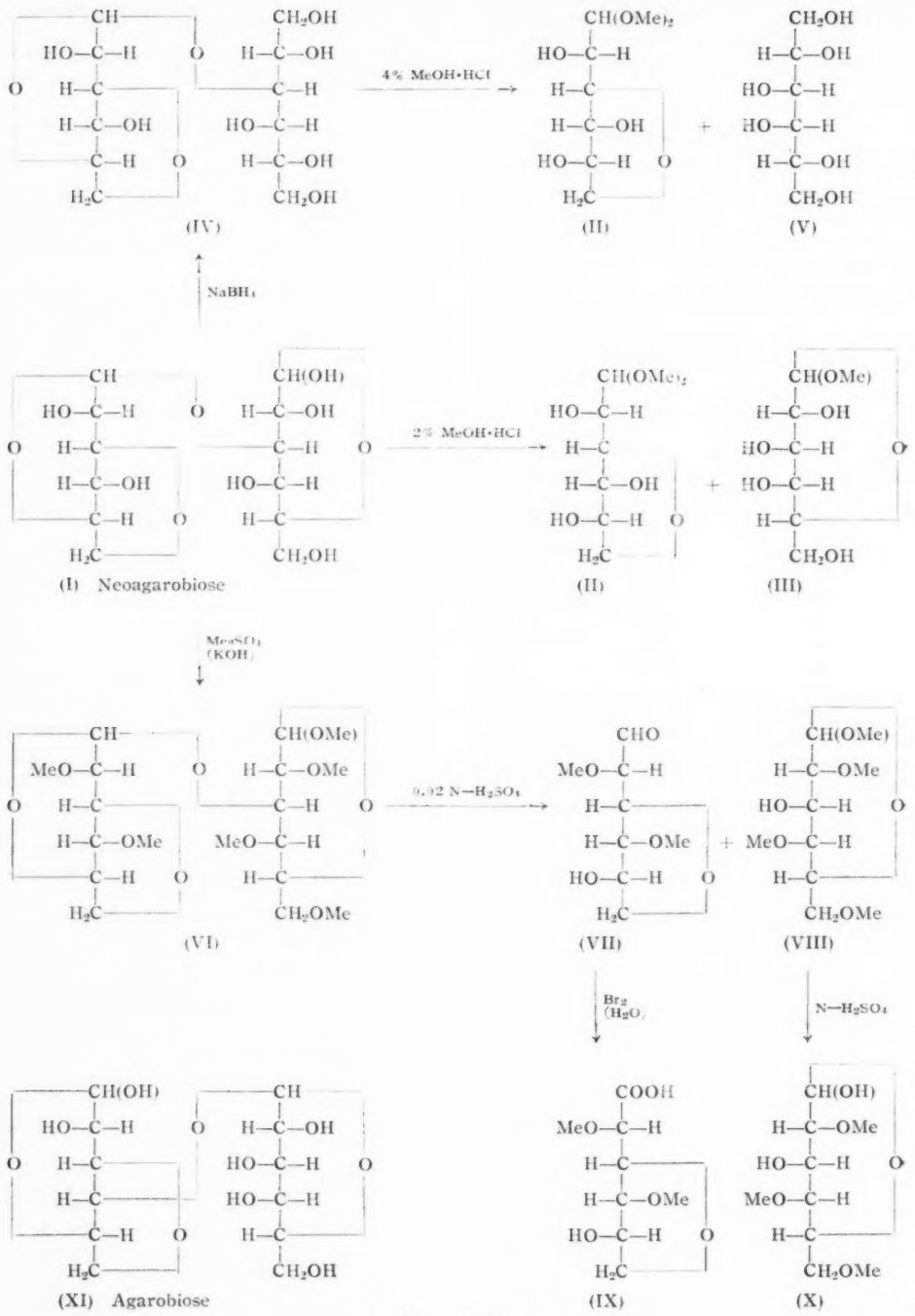
4% MeOH·HCl
NaBH4
2% MeOH·HCl
Me2SO4 (KOH)
0.02 N-H2SO4
Br2 (H2O)
N-H2SO4
(IV)
(II)
(V)
(I) Neoagarobiose
(II)
(III)
(VI)
(VII)
(VIII)
(XI) Agarobiose
(IX)
(X)

Me: $-CH_3$

shown by paper chromatography to be four oligosaccharides. The separation was possible by the charcoal chromatography of Whistler and Durso[11]. An aqueous solution of the mixture was placed on a charcoal column and developed with water and then with successive higher concentrations of ethanol in water. The four oligosaccharides were desorbed from the column on elution with 7.5, 17.5, 30 and 40% aqueous ethanol, respectively.

From the 7.5% ethanol eluate, there has been isolated a new crystalline disaccharide (I) having the composition $C_{12}H_{20}O_{10}$. Its hexaacetate and phenylosazone were also obtained in a crystalline state. The phenylosazone seems to be identical with that obtained by Ishimatsu and his co-workers[9]. The glycoside linkage of the disaccharide is so weak that it was hydrolysed to give D-galactose and 3,6-anhydro-L-galactose, when heated in a 0.02N-oxalic acid solution for two hours. Methanolysis of the disaccharide afforded 3,6-anhydro-L-galactose dimethylacetal (II) and methyl D-galactoside (III). These facts indicate that the disaccharide is composed of 3,6-anhydro-L-galactose and D-galactose residues. When the disaccharide was reduced to the corresponding glycitol (IV) with sodium borohydride and was subsequently methanolysed, 3,6-anhydro-L-galactose dimethylacetal (II) and dulcitol (V) were produced. This proves that the disaccharide is shown to be 3,6-anhydro-L-galactosyl-D-galactose, and hence that it is an isomer of agarobiose (XI) previously obtained. So the disaccharide has been named neoagarobiose.

In order to elucidate further the structure of neoagarobiose (I), it was methylated with dimethylsulfate and a potassium hydroxide solution and subsequently with Purdie's reagents. The resulting methyl penta-O-methyl-β-neoagarobioside (VI) was obtained in a crystalline state. On hydrolysis with .002 N-sulfuric acid the methylated neoagarobioside yielded a mixture of methyl 2,4,6-tri-O-methyl-β-D-galactoside (VIII) and 2,4-di-O-methyl-3,6-anhydro-L-galactose (VII). The former was separated from the latter by solvent extraction, and was obtained as crystals. On hydrolysis it gave crystalline 2,4,6-tri-O-methyl-D-galactose (X), the anilide of which was also obtained as crystals. This trimethyl-galactose and its anilide coincided in all respects with the corresponding authentic specimens. 2,4-di-O-methyl-3,6-anhydro-L-galactose (VII) was oxidised with bromine water to give crystalline 2,4-di-O-methyl-3,6-anhydro-L-galactonic acid (IX), which was further converted into the crystalline amide. These crystals were also in good agreement with the corresponding authentic specimens. The identification of VIII and VII as cleavage fragments establishes the structure of methyl penta-O-methyl-β-neoagarobioside (VI) as methyl 3-O-2′,4′-di-O-methyl-3′,6′-anhydro-L-galactopyranosyl-2,4,6-tri-O-methyl-β-D-galactopyranoside, and hence the structure of neoagarobiose (I) as 3-O-3′,6′-anhydro-L-galactopyranosyl-D-galactose.

The glycoside linkage has been suggested to be of the α'-type on the following basis. The specific rotations of α- and β-forms of methyl 3,6-anhydro-L-galactopyranoside would be in the neighborhood of $-80°$ and $+115°$, respectively, in water, the inference being drawn from the values recorded for their enantiomorphs[12]. If the 3,6-anhydro-L-galactopyranosyl group is combined through a β-type likage with D-galactose, which proper has a positive optical rotation, the resulting disaccharide would have a highly positive optical rotation. Meanwhile, if they are combined with each other through an α-type linkage, the resulting disaccharide would have a relatively low value of optical rotation, as a result of the compensation between positive and negative rotatory values of the components. The specific rotation of neoagarobiose ($[\alpha]_D$ $+34.4° \rightarrow +20.3°$) seems to fall in with the latter instance. The specific rotation of neoagarobitol (IV) ($[\alpha]_D^{aq.}$ $-20.0°$) also supports the α'-configuration on a similar consideration. In addition, the downward mutarotation observed when neoagarobiose is dissolved in water indicates that it crystallizes with the α-configuration.

Experimental

Evaporation and concentration were carried out under reduced pressure below 40°. All the melting points are uncorrected. The optical rotations are determined in aqueous solutions unless otherwise stated.

Preparation of Enzyme Extract.—A small amount of *P. kyotoensis* was inoculated to sterized media (50 cc.) having the following composition: sodium chloride 0.1%, dipotassium phosphate 0.1%, potassium nitrate 0.1%, magnesium sulfate heptahydrate 0.05%, and agar 0.5%; pH 7, adjusted with a 0.1 N-sodium hydroxide solution. The inoculated media were incubated at 30° for three days, and were diluted with the same media (400 cc.), the pH being again adjusted to 7 with a 0.1 N-sodium hydroxide solution. After incubation at 30° for a week, toluene (3 cc.) was added, and the mixture was digested at 30° for

11) R.L. Whistler and D.F. Durso, *J. Am. Chem. Soc.*, 72, 667 (1950).

12) W.N. Haworth, J. Jackson and F. Smith, *J. Chem Soc.*, **1940**, 620.

TABLE I

CHROMATOGRAPHIC SEPARATION OF ENZYMATIC HYDROLYSATES OF AGAR-AGAR

Ethanol	%	0	5	7.5	10	15	17.5	22	30	40	50
	l.	2.5	1.2	3.3	1.8	1.1	4.2	2.8	3.0	1.5	2.7
Yield	g.	0.67	0.1	3.7	0.15	0.15	5.3	0.6	1.63	0.65	0.40
$[\alpha]_D^{\circ}$ (H_2O)		—	+2.8	+17.7	+6.6	+6.8	+1.1	−9.1	−7.9	−16.9	−15.5

sixteen hours with occasional shaking. It was then filtered through an asbestos-bed, concentrated to 50 cc. below 35°, and was dialysed in a fish skin sack against running water until chlorine ions and reducing sugars were diffused (thirteen hours). The dialysed contents (110~130 cc.) were used as the enzyme extract to hydrolyse agar.

Enzymatic Hydrolysis of Agar.—Agar powder (5.5 g., or 5.27 g. as dry material), which had been defatted with acetone, was dissolved in hot water (1400 cc.) and sterized in steam, the pH of the solution being 5.2. After cooling, the enzyme extract (110–130 cc.) and three drops of toluene were added, and the mixture was kept at 40° in an incubator for about seventy two hours, when the reducing power reached a maximum value. After being heated in steam for fifteen minutes, it was filtered through double filter papers and concentrated to a sirup, to which methanol was added so that the concentration became 85 %. Insoluble precipitates were removed by filtration and washing with 85 % methanol, and the filtrate and washings were concentrated to a sirup (about 5 g.). The sirup was combined with three similar batches and extracted with hot 95 % methanol. Evaporation of the extract gave a mixture of reducing sugars as a pale brown sirup; yield 18–19 g. (moisture 10.6 %), or 71–81 % of agar in weight; $[\alpha]_D$+5.3° (*c* 1); reducing power, 26.1 % of galactose; aldose value, 43.0 % of hexose.

Paper Chromatography of Hydrolysates.—An aliquote of the above sirup was analysed on paper chromatograms (Tōyō Filter Paper No. 52) by the usual ascending method. *n*-Butanol-acetic acid-water (4:1:2 v/v) was used as an irrigating solvent and an ethanolic solution of O-aminophenol phosphate was sprayed[13]. Four yellowish brown spots were revealed: I (R_{gal} 1.30), II (R_{gal} 0.62), III (R_{gal} 0.34) and IV (R_{gal} 0.15), where R_{gal} is the rate of movement relative to that of galactose. The color of the spots presumably indicates the presence of 3,6-anhydro-galactose component.

Column Chromatography of Hydrolysates. A 10 % aqueous solution of the hydrolysates (13.4 g) obtained above was placed on a column (6.0×19.0 cm.) of active carbon Shirasagi[14] (Celite was not mixed with it), and the column was eluted with water, 5, 7.5, 10, 15, 17.5, 22, 30, 40 and 50 % aqueous ethanol in succession. Aliquotes of every 100 cc. portion of the eluates were withdrawn for examination of reducing power, and the next higher developer was added, after several continuous portions were recognized to be non-reducing. Each eluate was separately evaporated to dryness to recover the material. The result is quoted in Table I.

The water eluate left inorganic substances on evaporation. The 7.5, 17.5 and 30% ethanol eluates were chromatographically pure fractions, showing R_{gal} values 1.30, 0.62 and 0.34, respectively. Both 40 and 50% ethanol eluates were shown by paper chromatography to be mixtures of two components, whose R_{gal} values were 0.34 and 0.15. Solely the 7.5% ethanol fraction is treated in this communication.

Isolation of Neoagarobiose(I).—The 7.5% ethanol fraction was a colorless amorphous powder, which amounted to 28% of the hydrolysates. One gram of it was dissolved in a few drops of hot water, methanol was added while heating, and insoluble precipitates were removed by filtration. Crystallization of neoagarobiose was facilitated by addition of further methanol to the filtrate while heating. After standing overnight in a refrigerator, crystals were filtered, washed with methanol and ether, and dried; yield 0.85 g.; m.p. 197–198°. Recrystallization was repeated several times by dissolving it in a small amount of water and adding ethanol, until no more change of the physical constants was recognized; m.p. 207–208°; $[\alpha]_D^9$+34.4° (initial)→+20.3° (after twenty fuor hours, *c* 2.0); reducing power, 40.6% of galactose.

Anal. Found: C, 44.46; H, 6.20%; aldose equiv., 325., Calcd. for $C_{12}H_{20}O_{10}$: C, 44.44; H, 6.22%; aldose equiv., 324.

Neoagarobiose Phenylosazone.—A mixture of neoagarobiose (0.5 g.), phenylhydrazine (0.75 g.) and 50% acetic acid (0.75 cc.) in water (25 cc.) was heated at 90° for two hours. After cooling, crystals of the osazone were filtered, washed successively with water, ethanol, and ether, and dried; yield 0.35 g. The pure osazone was obtained as yellow needles on recrystallization from ethanol; m.p. 199–200°; $[\alpha]_D^{19}$+59.8° (initial)→+56.1° (after twenty four hours, *c* 0.82) in pyridine-methanol (2:3).

Anal. Found: C, 57.25; H, 6.12; N, 11.37. Calcd. for $C_{24}H_{30}O_8N_4$: C, 57.36; H, 6.02; N, 11.15%.

Hydrolysis of Neoagarobiose with 0.02N-Oxalic Acid Solution.—Neoagarobiose (0.60 g.) in a 0.02 N-oxalic acid solution (30 cc.) was heated in a boiling water bath. The progress of the reaction was followed by determination of the optical rotation of the solution; $[\alpha]_D$+17.5° (initial), +15.0° (15 min.), +14.5° (30 min.), +12.5° (1 hr.), +8.0° (2 hr.), +6.0° (2.5 and 3 hr., constant). After three hours, the solution was neutralized with calcium carbonate, filtered, and

13) S. Hirase, C. Araki and S. Nakanishi, This Bulletin, **26**, 183 (1953).

14) Product of Takeda Pharmaceutical Industries, Ltd., Osaka.

concentrated to a sirup (0.55 g.). Paper chromatographic examination revealed a distinct spot of galactose together with a diffused tailing presumably of 3,6-anhydro-galactose. This indicative evidence was made conclusive by their isolations. A 10% aqueous solution of the sirup was placed on a charcoal column and developed with water. Every 30 cc. of the eluate was determined for the optical rotation, and fractions with positive and negative rotations were separately combined and concentrated to dryness.

a) D-Galactose.—From the first eight fractions with positive rotations, there was obtained a sirup (0.35 g.), from which D-galactose was crystallized; yield 0.25 g.; m.p. and mixed m.p. with an authentic specimen 166–167°; $[\alpha]_D^{25}$ +81.5° (after twenty fourhours *c* 1.5). Nitric acid oxidation afforded mucic acid (m.p. 213°).

b) 3,6-Anhydro-L-galactose.—Next, eleven fractions with negative rotations gave on evaporation a sirupy 3,6-anhydro-L-galactose (0.18 g.). It reduced Fehling's solution at room temperature, and showed a strong Seliwanoff's reaction. Treatment with phenylhydrazine and acetic acid in the usual manner afforded 3,6-anhydro-L-galactose phenylosazone; m.p. and mixed m.p. with an authentic specimen[15] 217–218°.

Anal. Found: N, 16.23. Calcd. for $C_{18}H_{20}O_3N_4$: N, 16.46%.

Methanolysis of Neoagarobiose.—Neoagarobiose (1.0 g.) in 2% methanolic hydrogen chloride (50 cc) was boiled until the optical rotation became constant: $[\alpha]_D$ +16.0° (initial), −38.0° (15 min.), −41.0° (30 min.), −35.0° (1 hr.), −30.0° (1.5 and 2 hr.). The solution was neutralized with silver carbonate, filtered, and concentrated to a sirup (1.1 g.). Paper chromatographic examination indicated that it was a mixture of 3,6-anhydro-galactose dimethylacetal and methyl galactoside. The mixture was chromatographed on a starch column exactly in the same way as described by Araki and Hirase[1]. 3,6-Anhydro-galactose dimethylacetal was eluted with *n*-butanol saturated with water, and then methyl galactoside was eluted with 80% aqueous methanol.

a) 3,6-Anhydro-L-galactose Dimethylacetal (II).—Evaporation of butanolic eluate gave 3,6-anhydro-L-galactose dimethylacetal as a colorless sirup; yield 0.50 g.; $[\alpha]_D^{12}$ −24.6° (*c* 1.05); OCH_3, found 26.2 (calculated for $C_6H_{10}O_4(OCH_3)_2$ 29.8%). Identification was carried out by hydrolysing it to the free sugar, which was then converted into the diphenylhydrazone in the usual manner[15], m.p. and mixed m.p. with and authentic specimen 153°; $[\alpha]_D^{22}$ −34.6° (initial, methanol, *c* 1.21).

Anal. Found: N, 8.67. Calcd for a $C_{18}H_{20}O_4N_2$: N, 8.53%.

b) Methyl D-Galactoside.—Evaporation of the 80% methanal eluate gave a sirup (0.54 g.), which on crystallization from acetone-methanol (2:1) afforded crystals of methyl α-D-galactoside monohydrate; yield 0.35 g.: m.p. 109°, not depressed on admixture with an authentic specimen; $[\alpha]_D^{18}$ +174.1° (*c* 1.1).

Anal. Found: C, 39.25; H, 7.59; OCH_3, 14.60. Calcd. for $C_7H_{14}O_6 \cdot H_2O$: C, 39.60; H, 7.60; OCH_3, 14.62%.

Hydrolysis with N-sulfuric acid gave D-galactose, m.p. and mixed m.p. 168°; $[\alpha]_D^{27}$ +81.5° (after twenty four hours, *c* 1.5).

Reduction and Methanolysis of Neoagarobiose.—Neoagarobiose (1.0 g.) in water (20 cc.) was mixed with an aqueous solution (10 cc.) of sodium borohydride (0.15 g.). The mixture was kept at room temperature (10–13°) with occasional shaking for two hours, when it showed no longer the reducing power. The solution was then ice-cooled, carefully neutralized with an 1.5% aqueous acetic acid, and concentrated to dryness. Crude neoagarobitol (IV) was obtained as an amorphous solid; yield 1.2 g.; $[\alpha]_D^{16}$ −20.0° (*c* 1.25).

The glycitol (1.15 g.) was heated in boiling 4% methanolic hydrogen chloride (50 cc.) until a constant optical rotation was observed: $[\alpha]_D$ −28.3° (initial), −22.6° (15 min.), −21.7° (30 min.), −20.9° (45 min.), −20.4° (1 hr.), −21.3° (2 and 3 hr.). The solution was neutralized with silver carbonate, filtered, and concentrated to give a semi-crystalline residue.

a) Dulcitol (V).—The above residue was triturated with methanol. Crystals of dulcitol (0.35 g.), separated by filtration, were recrystallized from ethanol-water (1:1); m.p. and mixed m.p. with an authentic specimen 187–188°; $[\alpha]_D^{19}$ ±0° (*c* 1.37).

Anal. Found: C, 39.66; H, 8.06. Calcd. for $C_6H_{14}O_6$: C, 39.56; H, 7.75%.

b) 3,6-Anhydro-L-galactose Dimethylacetal (II).—The filtrate separated from crystals of dulcitol was concentrated, and chromatographed on a starch column in the same manner as described before. 3,6-Anhydro-L-galactose dimethylacetal was obtained as a colorless sirup; yield 0.48 g.; $[\alpha]_D^{7}$ −25.3° (*c* 1.2); OCH_3, found 28.4% (calcd. for $C_8H_{14}O_6$ 29.8%).

An additional specimen of dulcitol (0.12 g.) was also recovered from the column.

Hexa-O-acetyl-neoagarobiose. — Neoagarobiose (1.0 g.) was acetylated with pyridine (25 cc.) and acetic anhydride (7.0 g.) for seventy two hours in the usual manner. The reaction mixture was poured into ice-water (100 cc.) with stirring, neutralized with sodium bicarbonate, and extracted with chloroform. The extract was washed twice with water, dried with sodium sulfate, and evaporated. The hexaacetate (0.70 g.) obtained was recrystallized from ethanol; yield 0.46 g.; m.p. 112°; $[\alpha]_D^{27}$ +1.57° (chloroform, *c* 1.27); $[\alpha]_D^{29}$ +0.82° (methanol, *c* 1.22).

Anal. Found: C, 49.75; H, 5.80; CH_3CO, 45.01. Calcd. for $C_{12}H_{14}O_{10}(CH_3CO)_6$: C, 50.00; H, 5.60; CH_3CO, 44.80%.

Methyl Penta-O-methyl-β-neoagarobioside

15) C. Araki, *J. Chem. Soc. Japan*, **65**, 725 (1944).

(VI).—A 32% potassium hydroxide solution (38 cc.) and dimethylsulfate (16 cc.) were alternatively dropped during eight hours into an ice-cooled and vigorously stirred solution of neoagarobiose (2.0 g.) in water (7 cc.), care being taken to keep the medium alkaline. More potassium hydroxide solution (5 cc.) was added, and the solution was cooled and stirred for two hours. After standing overnight, the potassium hydroxide solution (106 cc.) and dimethylsulfate (47 cc.) were run in during twenty hours at room temperature (23–25°), the same care being taken. After the addition, the solution was stirred for ten additional hours, and then extracted with four 50 cc. portions of chloroform. The extracts were dried with sodium sulfate, evaporated, redissolved in ether, and again evaporated, when a crystalline mass was obtained; yield 2.16 g.; OCH_3 42.8%. This was twice methylated with methyl iodide (25 g.) and silver oxide (15 g.) in the usual manner. The final product was isolated as a crystalline mass by extraction with ether and evaporation; yield 2.20 g., OCH_3 46.0%. Recrystallization from petroleum ether (b.p. 38–43°) gave a pure sample of methyl penta-O-methyl-β-neoagarobioside; m.p. 127–128°; $[\alpha]_D^{20}$ −19.6° (methanol, *c* 1.28); $[\alpha]_D^{20}$ −22.0° (chloroform, *c* 1.28).

Anal. Found: C, 52.89; H, 8.12; OCH_3, 45.45%; M.W. (Rast's), 408. Calcd. for $C_{12}H_{14}O_4(OCH_3)_5$: C, 52.93; H, 7.90; OCH_3, 45.62%; M.W., 408.

Hydrolysis of Methyl Penta-O-methyl-β-neoagarobioside.—The sample (2.0 g.) in 0.02N-sulfuric acid (100 cc.) was heated in a boiling water bath until the optical rotation reached a constant value: $[\alpha]_D$ −18.0° (initial), −16.0° (15 min.), −15.0° (30 min.), −13.5° (45 min.), −12.5° (1 hr.), −3.5° (1.5 hr.), −1.5° (2 hr.), +1.0° (2.5 hr.), +2.0° (3 and 4 hr., constant). It was neutralized with barium carbonate, filtered, concentrated, redissolved in ether, and again evaporated, when a mixture of methyl 2,4,6-tri-O-methyl-β-D-galactoside and 2,4-di-O-methyl-3,6,-anhydro-L-galactose was obtained as a semi-crystalline residue (1.68 g.).

Methyl 2,4,6-Tri-O-methyl-β-D-galactoside (VIII).—The above mixture was extracted several times with boiling petroleum ether, an insoluble sirup (0.5 g.) being set aside. Evaporation of the extracts afforded methyl 2,4,6-tri-*O*-methyl-β-D-galactoside as a crystalline mass (1.10 g., OCH_3 47.1%). Recrystallization twice from petroleum ether gave pure silky needles (0.37 g.); m.p. 110–112°; $[\alpha]_D^{14}$ +2.90° (*c* 1.71). Araki[15] recorded m.p. 110–112° and $[\alpha]_D^{22}$ +6.38°.

Anal. Found: C, 50.61; H, 8.56; OCH_3, 51.97. Calcd. for $C_6H_8O_2(OCH_3)_4$: C, 50.85; H, 8.47; OCH_3, 52.54%.

An additional crop (0.50 g., OCH_3 50.2%) was recovered by evaporating the mother liquor of the recrystallization and extracting again with boiling petroleum ether. A petroleum ether-insoluble sirup (0.22 g.) was also obtained.

2,4,6-Tri-O-methyl-D-galactose (X).—The recovered crystals of methyl 2,4,6-tri-O-methyl-β-D-galactoside (0.50 g.) were hydrolysed with N-sulfuric acid for three hours in the usual manner. 2,4,6-Tri-O-methyl-α-D-galactose (0.45g.) was obtained as crystals, and recrystallized from ether; m.p. 113–114°, not depressed on admixture with an authentic specimen[15]; $[\alpha]_D^{24}$ +112.6° (initial)→+90.9° (after twenty four hours, *c* 1.2).

Anal. Found: C, 48.90; H, 8.04 OCH_3, 42.00. Calc for $C_6H_9O_3(OCH_3)_3$: C, 48.65; H, 8.11; OCH_3, 41.89%.

Anilide: m.p. 172–173°, not depressed on admixture with an authentic specimen[15]; $[\alpha]_D^{24}$ −84.0° (initial)→−44.8° (after twenty four hours)→+2.8° (after fourty eight hours, *c* 0.45) in acetone.

Anal. Found: N, 4.80; OCH_3, 30.20. Calcd. for $C_{15}H_{23}O_5N$: N, 4.71; OCH_3, 31.31%.

2,4-Di-O-methyl-3,6-anhydro-L-galactose (VII).—Petroleum ether-insoluble residue, separated from methyl 2,4,6-tri-O-methyl-β-D-galactoside, was proved to be 2,4-di-O-methyl-3,6-anhydro-L-galoctose[17]; a pale yellow sirup; yield 0.72 g., n_D^{25} 1.4871; $[\alpha]_D^{27}$ −6.9° (*c* 0.88); OCH_3 31.1% (Calcd. for $C_6H_8O_3(OCH_3)_2$ 32.64%). It reduced a Fehling's solution at room temperature, decolorized a neutral permanganate solution, showed a strong Seliwanoff's reaction, and restored the color to a Schiff's reagent.

2,4-Di-O-methyl-3,6-anhydro-L-galactonic Acid (IX).—Bromine (0.75 cc.) was dropped during five hours into an ice-cooled and vigorously stirred aqueous solution (30 cc.) of 2,4-di-O-methyl-3,6-anhydro-L-galactose (0.50 g.), in the presence of barium carbonate (6 g.). The stirring and cooling were continued for three more hours. After standing overnight, the non-reducing reaction mixture was aerated to remove excess bromine, filtered, and concentrated to a sirup, which was extracted with boiling chloroform. The residual barium salt was dissolved in water, and passed through a column of a cation exchange resin Amberlite IR-120, the column being then washed thoroughly with water. The acidic percolate and washings were combined, neutralized with silver carbonate, filtered before and after treatment with hydrogen sulfide, and concentrated to a sirup. Extraction with ethanol-benzene (1: 1) followed by evaporation afforded a semi-crystalline residue (0.30 g.), from which crystals of 2,4-di-O-methyl-3,6-anhydro-L-galactonic acid were separated by use of a porous plate; yield 0.22 g. The pure acid was obtained by recrystallization from ethanol-benzene (1: 1); m.p. 150°, not depressed on admixture with an authentic specimen[12,17]; $[\alpha]_D^{24}$ −60.8° (*c* 1.94).

Anal. Found: C, 46.47; H, 7.02; OCH_3, 29.8. Calcd. for $C_6H_8O_4(OCH_3)_2$: C, 46.58; H, 6.85; OCH_3, 30.12%.

Amide: The above acid was esterified with methanolic hydrogen chloride in the usual manner. The methyl ester obtained was converted into the amide in the usual manner; m.p. 150°, not

16) C. Araki, *J. Chem. Soc. Japan*, **58**, 1362 (1937).

17) C. Araki, *J. Chem. Soc. Japan*, **61**, 503 (1940).

18) I.A. Forbes and E.G.V. Percival, *J. Chem. Soc.*, **1939**, 1844.

depressed on admixture with an authentic specimen[17,18]; $[\alpha]_D^{24}$ −74.0° (*c* 0.94).

Anal. Found: N, 7.00; OCH_3, 30.12. Calcd. for $C_8H_{15}O_5N$: N, 6.83; OCH_3, 30.25%.

Summary

1. A new crystalline disaccharide has been isolated from enzymatic hydrolysates of agar. Its hexaacetate and phenylosazone have been prepared in crystalline states.

2. The name neoagarobiose has been assigned to the disaccharide isolated.

3. The structure of neoagarobiose has been shown beyond doubt to be 3-O-3′,6′-anhydro-L-galactopyranosyl-D-galactose. It has been suggested that the glycoside linkage is of α'-configuration.

The authors are indebted to Mr. N. Nakata for assistance in study, and to Mr. S. Hirase for help in description. This study has been aided by the Grant for the Fundamental Scientific Research from the Ministry of Education, for which thanks are also expressed.

Institute of Chemistry, Faculty of Industrial Arts, Kyoto Technical University, Matsugasaki, Kyoto

*Electrophoretic Studies of Tobacco Mosaic Virus**

By Itaru WATANABE and Nobuo UI

(Received November 7, 1955)

Since the early study of Eriksson-Quensel and Svedberg[1], the electrophoretic mobility of tobacco mosaic virus (TMV) has been measured by several investigators. However, the various recorded values of its mobility show some discrepancy (see Table I) and there have been few systematic studies under different conditions.

TABLE I

THE DATA OF ELECTROPHORETIC MOBILITY OF TOBACCO MOSAIC VIRUS

Buffer	Ionic Strength	pH	Temp. (°C)	Mobility $\left(\frac{-u\times10^5}{\text{cm}^2/\text{sec. volt}}\right)$	Investigator
Acetate	0.02	4.01	20	7.5	Ericksson-Quensel et al. (1936)[1]
〃	〃	4.35	〃	10.5	〃
〃	〃	4.65	〃	13.9	〃
〃	0.04	4.95	〃	18.9	〃
Phosphate	0.1	6.91	0–0.5	9.3	Pfankuch et al. (1940)[2]
Phosphate-KCl	〃	7.3	——	8.5	Miller et al (1941)[3]
Veronal-NaCl	〃	6.72	0	5.5	Cohen (1941)[4]
Phosphate	(0.05 M)	7.1	〃	8.8 (Des)	Knight et al. (1942)[5]
〃	(0.1 M)	7.5	——	39 (Des)	Frampton et al. (1946)[6]
〃	0.2	7.00	1	7.2	Fischer et al. (1949)[7]
〃	〃	7.7	0	7.5 (Des)	Watanabe et al. (1950)[8]
Acetate	〃	4.2	3.2	4.2	Kahler (1951)[9]
〃	〃	4.9	〃	8.0	〃

* Part of this paper was read before the 4th Annual Meeting of the Chemical Society of Japan held in Tokyo, April, 1951.

1) I.-B. Eriksson-Quensel and T. Svedberg, *J. Am. Chem. Soc.*, **58**, 1863 (1936).

2) E. Pfankuch, G.A. Kausche and H. Stuble, *Biochem. Z.*, **304**, 238 (1940).

3) G.L. Miller and W.M. Stanly, *J. Biol. Chem.*, **141**, 905 (1941).

4) S.S. Cohen, *Proc. Soc. Exptl. Biol. Med.*, **48**, 163 (1941).

5) C.A. Knight and M.A. Lauffer, *J. Biol. Chem.*, **144**, 411 (1942).

6) V.L. Frampton and W.N. Takahashi, *Phytopathology*, **36**, 129 (1946).

7) M.A. Fischer and M.A. Lauffer, *J. Am. Chem. Soc.*, **71**, 3800 (1949).

8) I. Watanabe, Y. Otsuka and S. Mizushima, *Repts. Radiation Chemistry Research Institute, Tokyo Univ.*, No. 5, 10(1950).

9) H. Kahler, private communication (1951).

In the present investigation the variations of the mobility of TMV with changes in concentration and ionic strength have been measured. The charge on the virus particle has been calculated from the mobility data, using Gorin's equation for long cylinders. It also seems to be interesting from the electrophoretic point of view to study such an elongated rod-shaped particle as TMV.

Experimental

Materials.—Of the several TMV preparations obtained, the most homogeneous preparation, TMV-9, was used in these studies. The virus was extracted from frozen and ground young White Burley tobacco leaves three weeks after the inoculation with common TMV and purified by differential centrifugation in a manner essentially similar to that described by Stanley[10], using a vacuum-type air-driven ultracentrifuge[11,12]. The details of the purification procedure have been reported in previous paper[12] with the results of several chemical and physical measurements of purified virus.

The homogeneity of TMV-9 was proved to be excellent by electrophoresis, sedimentation, and electron microscope measurements[12].

The final purified virus solution was stored in 0.01 M phosphate buffer at pH 7.0 in a refrigerator, and subjected to electrophoresis experiments.

Measurements.—Prior to electrophoresis, the virus solution in 0.01 M phosphate buffer was diluted to desired concentrations with a phosphate buffer of ionic strength 0.2 at pH 7.7, and dialyzed against a large quantity of the same buffer at least two days in a cold room. In the study of the variation of mobility with ionic strength, the ionic strength was varied by diluting the phosphate buffer of ionic strength 0.2 at pH 7.7 with water; no apparent change in pH was found even after ten-fold dilution.

Electrophoretic measurements were carried out at 0°C in a Tiselius-type apparatus[13] equipped with a Svensson optical system[14]. The electrolytic current was automatically controlled by a constant-current regulator[15].

The movements of the boundaries were recorded photographically at appropriate intervals and the electrophoretic mobilities were calculated by the method of Longsworth[16] from the centroidal ordinates, or the first moments, of the curves of concentration gradient versus distances. Mobility values corresponding to a temperature of 0°C were obtained by using specific conductivities of solutions measured at 0°C.

Virus concentrations were determined by micro-Kjeldahl nitrogen analysis* assuming that TMV nucleoprotein contains 16.6–16.7% nitrogen[12].

Results

This preparation of TMV, TMV-9, was found to be electrophoretically homogeneous under all conditions examined and single boundaries remained sharp during the course of electrophoresis (for example, see Fig. 1).

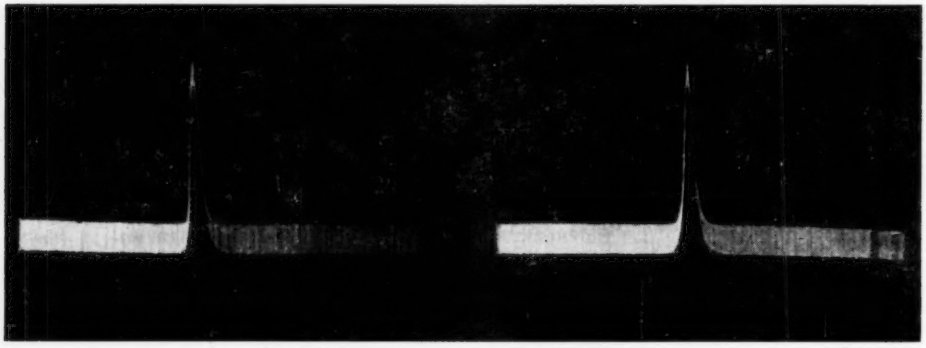

Ascending ← → Descending

Fig. 1. Electrophoretic pattern of TMV in the phospate buffer (pH 7.7, μ=0.2).

A. The Variation of Mobility with Concentration of TMV.—The variation of electrophoretic mobility with concentration of TMV was examined over the concentration range 0.17–1.08% in the same phosphate buffer, pH 7.7, at a constant ionic strength of 0.2. These results are given in Table II together with the relative viscosity of solutions[17]. It can be easily seen, from Table II, that the mobility is essentially independent of the concentration although the relative viscosity of the

10) W.M. Stanley, *J. Am. Chem. Soc.*, **64**, 1804 (1942).
11) S. Sasaki and O Taniguchi, *J. Japan Soc. Mech. Eng.*, **54**, 255 (1951).
12) I. Watanabe and Y. Kawade, This Bulletin, **26**, 294 (1953).
13) A. Tiselius, *Trans. Faraday Soc.*, **33**, 524 (1937).
14) H. Svensson, *Kolloid-Z.*, **87**, 181 (1939).
15) H. Noda and N. Ui, *Kagaku*, **20**, 179 (1950).
16) L.G. Longsworth, *J. Am. Chem. Soc.*, **65**, 1755 (1943).
* The nitrogen determinations were made by Miss T. Kitamura in our laboratory.
17) Y. Kawade, *Repts. Institute of Science and Technology, Univ. of Tokyo*, **8**, 115 (1954).

TABLE II
THE VARIATION OF MOBILITY WITH CONCENTRATION OF TMV AT 0°C
(In Phosphate Buffer of Ionic Strength 0.2 and pH 7.7)

Conc. (%)	Field strength* (volt/cm.)	Mobility ($-u\times10^5$cm²/sec. volt)		Relative viscosity of solution (η_r)
		Descending	Ascending	
0.17	3.60	7.1_5	7.2_5	1.11
0.24	3.57	7.1_5	7.3_0	1.17
0.44	3.62	6.9_5	7.1_0	1.36
0.65	3.65	7.0_0	7.1_0	1.59
1.08	3.72	7.0_0	7.1_0	2.24
Average.....		7.0_5	7.1_5	

* In our preliminary test, it was confirmed that the mobility is essentially independent of the field strength.

solutions increases by more than twofold. Similar phenomena were also observed in the electrophoretic studies of deoxypentose nucleic acid[18–20]. In this connection, it is very interesting to recall the fact that the sedimentation rates of both TMV[21–23] and deoxypentose nucleic acid[24–25] strongly depend upon their concentration and that, especially in the case of TMV, this concentration dependency of sedimentation coefficient is directly related to the viscosity of the solution[21]. This difference in dependence of sedimentation coefficient and electrophoretic mobility upon concentration is of considerable interest and, as yet, no reasonable explanations have been proposed.

The average value of descending mobilities in the phosphate buffer of ionic strength 0.2 and pH 7.7 was calculated to be $-7.0_5\times10^{-5}$cm²/sec. volt and is in close agreement with that reported by Fischer and Lauffer[7].

B. The Dependence of Mobility on Ionic Strength.—The ionic strength was varied over the range 0.02–0.2 at constant pH. The results obtained are given in Table III and Fig. 2, in which mobilities are plotted against the square roots of ionic strengths. It is evident from Fig. 2 that the mobility increases greatly with the reduction of ionic strength.

TABLE III
THE VARIATION OF MOBILITY OF TMV WITH IONIC STRENGTH AT 0°C
(In Phosphate Buffer at pH 7.7)

Ionic Strength	Conc. (%)	Field Strength (volt/cm.)	Mobility ($-u\times10^5$cm²/sec. volt)	
			Descending	Ascending
0.02	0.49	3.24	15.7	17.5
0.05	0.37	3.79	11.6	11.9
0.1	0.52	3.47	9.0_5	9.2_5
0.2	.....	.....	7.0_5*	7.1_5*

* Average value given in Table II.

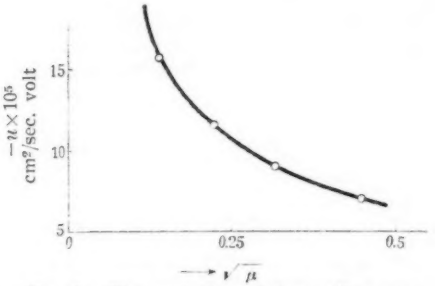

Fig. 2. The variation of descending mobility of TMV with ionic strength at 0°C (in phosphate buffer at pH 7.7).

Discussion

A. The Net Charge on TMV Molecule.—The single particles of TMV were found to be rod-shaped, of about 280 mμ to 300 mμ in length and 15 mμ in diameter, and have molecular weight of about 4×10^7 to 5×10^7 [22,27,28]. Similar molecular size and shape have also been observed for the virus preparation (TMV-9) used in these studies[12], by sedimentation, diffusion, viscosity, and electron microscopic measurements. In the following calculations TMV particles were regarded as long cylinders, 300 mμ in length and 15.2 mμ in diameter: these values correspond to a molecular weight of 4.5×10^7 [12].

The net charge, Q, on such a long cylinder as TMV can be related to the experimentally measured mobility, u, by the following equation developed by Gorin[29]:

$$Z|e|=Q=\pi\eta\cdot F'(\kappa a)\cdot(l+2a)\cdot u\Big/2\left[\frac{K_0(\kappa a+\kappa r_i)}{(\kappa a+\kappa r_i)\cdot K_1(\kappa a+\kappa r_i)}+\ln\left(\frac{a+r_i}{a}\right)\right] \qquad (1)$$

18) E. Stenhagen and T. Teorell, *Trans. Faraday Soc.*, **35**, 743 (1939).
19) J.M. Creeth, D.O. Jordan and J.M. Gulland, *J. Chem. Soc.*, **1949**, 1406.
20) N. Ui and I. Watanabe, *Repts. Radiation Chem. Research Institute, Tokyo Univ.*, No. 5, 17 (1950).
21) M.A. Lauffer, *J. Am. Chem. Soc.*, **66**, 1195 (1944).
22) G. Schramm and G. Bergold, *Z. Naturforsch.*, **2b**, 108 (1947).
23) H.K. Schachman and W.J. Kauzmann, *J. Phys. & Colloid. Chem.*, **53**, 150 (1949).
24) H. Kahler, *J. Phys. & Colloid Chem.*, **52**, 676 (1948).
25) R. Cecil and A.G. Ogston, *J. Chem. Soc.*, **1948**, 1382.
26) Y. Kawade and I. Watanabe, *Biochem. et Biophys. Acta*, in press.
27) M.A. Lauffer, *J. Am. Chem. Soc.*, **66**, 1188 (1944).
28) R.C. Williams, R.C. Backus and R.L. Steere, *J. Am. Chem. Soc.*, **73**, 2062 (1951).
29) H.A. Abramson, L.S. Moyer and M.H. Gorin, "Electrophoresis of Proteins," Reinhold, New York (1942).

Here, Z is the valency of ion, $|e|$ is the electronic charge, l and a are the length and the radius of the cylinder, respectively, r_i is the average radius of the ions in the ionic atmosphere, κ is the Debye-Hückel function, i. e., the inverse of the thickness of the double layer, and η is the viscosity coefficient of the solvent. $F'(\kappa a)$ is the function developed by Gorin to account for the random orientation of cylinders, and K_0 and K_1 are Bessel functions, values of which have been given by Abramson, Moyer, and Groin[29] together with the values of $F'(\kappa a)$.

The valency at ionic strength 0.02 can be calculated directly from the equation (1) and is given in Table IV A. In this calculation the valeus of l and a were taken as 3000 Å and 76 Å respectively, and the value of r_i was assumed to be 2.5 Å. The value of κ at 0° C is $3.24\times10^8\sqrt{\mu}$, where μ is the ionic strength. In the calculations of the valencies at higher ionic strengths, however, an alternative indirect method was adopted by using Gorin's calculation of the ratio (R) of the mobility of the cylinder to that of the sphere of the same molecular volume and charge[29]. After obtaining the mobility as the sphere, the charge can be calculated from the following equation:

$$u(\text{sphere})=\frac{Z|e|(1+\kappa r_i)\cdot f(\kappa r)}{4\pi\eta a(1+\kappa r+\kappa r_i)} \qquad (2)$$

Here, r is the radius of the equivalent sphere above-mentioned, which was calculated to be 240 Å, and $f(\kappa r)$ is a function of κr given by Henry[30] (often called the Henry factor). These results were shown in Table IV B. From Table IV it is clearly shown that the valency of TMV is independent of the change in ionic strength within the error of calculation and is about $-1,800$.

In the above calculation, it was assumed that no change in the molecular state occurred with the variation of ionic strength, although the concentration of buffer was reported to have some effect on the degree of aggregation of TMV[23]. There are, moreover, many assumptions and limitations in Gorin's equation* and the meaning of the value obtained is not yet so self-evident.

This electrophoretic valency of TMV, $-1,800$, seems to be too small, compared with its very high molecular weight. Our calculations based upon the amino acid analyses of Knight[32] and the amide nitrogen analyses of Ross[33] indicate a valency of about $-800\sim-900$ at pH 7.7. In this calculation, the molecular weight of TMV was taken to be 4.5×10^7 and any contribution of nucleic acid was neglected. Although this figure appears to be in the same order of magnitude as that obtained from the mobility, the presence of the nucleic acid should be taken into consideration to obtain a correct theoretical value.

Considering the contribution made by pentose nucleic acid as free acid, the theoretical valency of TMV was calculated to be about $-9,000$. This value is very large, when compared with the surface charge calculated from the electrophoretic mobility, but is in fairly good agreement with that obtained from the titration experiments by Fischer

TABLE IV

THE NET CHARGE ON TMV PARTICLE*

A. THE VALUE CALCULATED FROM EQ. (1)

μ	$u\times10^5$ (cm²/sec. volt)	κ	$\kappa a+\kappa r_i$	$\frac{K_0(\kappa a+\kappa r_i)}{(\kappa a+\kappa r_i)K_1(\kappa a+\kappa r_i)}$	$F'(\kappa a)$	η (poise)	Z
0.02	−15.7	0.46×10^7	3.6	0.24	5.3	1.80×10^{-2}	−1.720

B. THE VALUE CALCULATED FROM EQ. (2)

μ	$u\times10^5$	R**	u(sphere) $\times10^5$	κ $\times10^{-7}$	κr	κr_i	$f(\kappa r)$	η (poise)	Z
0.02	−15.7	0.39	−40.3	0.46	11.0	0.1	0.84	1.80×10^{-2}	−1.800
0.05	−11.6	0.38	−30.5	0.72	17.3	0.2	0.88	1.81×10^{-2}	−1,800
0.1	− 9.0$_5$	0.38	−23.8	1.02	24.5	0.3	0.91	1.83×10^{-2}	−1,800
0.2	− 7.0$_2$	0.38	−18.5	1.45	34.8	0.4	0.93	1.87×10^{-2}	−1,800

* $r_i=2.5$Å; $R=2.4\times10^2$Å.

** $R=u$(cylinder)/u(sphere). To calculate these values, asymmetry$=S_r=l/2a$ was taken as 19.7.

* The limitations of Gorin's equation were discussed in detail by Abramson, Moyer, and Gorin[29] and Overbeek[31].

30) D.C. Henry, *Proc. Roy. Soc. London*, **133A**, 106 (1931).

31) J.Th.G. Overbeek, *Advances in Colloid Sci.*, **3**, 97 (1950).

32) C.A. Knight, *J. Biol. Chem.*, **171**, 297 (1947).

33) A.F. Ross, *J. Biol. Chem.*, **143**, 685 (1942).

and Lauffer[7]*.

It is very interesting to investigate the reason why the surface charge obtained from the electrophoretic experiments is much smaller than the calculated or the titration value. In this respect, it seems not inadequate to point out that the charge of horse serum albumin derived from the mobility agrees very well with the titration value[35].

B. The Dilution Factor in a Three-Ion System Containing TMV.—Strong "boundary anomalies"[36] are usually observed in electrophoretic experiments of proteins such as albumin, globulin, etc. It was found in our studies, however, that these "boundary anomalies" were greatly diminished in TMV solutions. First, the ascending mobility is not so different from descending mobility (see Table II); second, both the δ- and ε-boundaries are very small and hardly recognized (see Fig. 1); and third, the descending boundary is also as sharp as the acending one**.

All these characteristic phenomena of TMV in electrophoresis may be interpreted by the fact that the charge density of TMV is very small. Now we are trying to calculate a dilution factor[37], ξ, which is a measure of the divergence of real systems from the ideal behaviour and becomes unity at sufficiently low protein concentrations. In a three-ion system, ξ is given by the following equation[37]:

$$\xi=1+\left(\frac{r_S-r_R}{r_S}\cdot\frac{r_A}{r_A-r_R}-\frac{1}{2}\right)\frac{C_S^\alpha}{C_A^\gamma} \qquad (3)$$

Notations are the same as in the paper of Longsworth[37]. The subscript A, R, and S refer to Na^+, HPO_4^{--}***, and the negatively charged protein ion; and the superscripts γ and α mean buffer and protein solutions respectively. r is the mobility of ion relative to that of Na^+ ion (22.7×10^{-5} cm²/sec. volt) taken as unity and C is the equivalent concentration of ion.

In Table V are shown the results of the

TABLE V

THE DILUTION FACTOR AND BUFFER-CONCENTRATION BOUNDARY IN A THREE-ION SYSTEM

1% Protein Solutions in Sodium Phosphate Buffer (pH 7.7, Ionic Strength 0.2)
A: Na^+; R: HPO_4^{--}; S: Protein Ion;
$r_A=1,000$ (unity); $r_R=-1.101$; $C_A^\gamma=0.14$;
$K_{AR}=0.0148$

Protein	TMV	Horse serum albumin B
M (molecular weight)	4.5×10^7	67,100
Z (valency)	−1,800	−15.7
u (mobility)	$-7.0_0\times10^{-5}$	$-5.8_4\times10^{-5}$
r_S (relative mobility)*	−0.308	−0.257
C_S^α (euivalent per liter)	−0.00040	−0.00234
ξ (dilution factor)	1.005	1.035
Δn (ε-boundary)	0.000010	0.000072

* Taken the mobility of sodium ion as unity.

calculations on one per cent solutions of TMV and horse serum albumin B (according to Kekwick[38]) in sodium phosphate buffer of ionic strength 0.2 and pH 7.7. It is clear from Table V that ξ is very close to unity in the case of TMV. This low value of $\xi-1$ in TMV solution is in good accord with the fact that no marked divergence from an ideal electrophoretic behaviour can be observed. Since ξ is equal to the ratio of ascending mobility to decending one as a first approximation[37], the small differences between ascending and descending mobilities of TMV can qualitatively be explained.

The change in refractive index across the buffer-concentration boundary, so-called "ε-boundary", in the descending side can be expressed as follows[37]:

$$\Delta n=K_{AR}(\xi-1)C_A^\gamma$$

$$=K_{AR}\left(\frac{r_S-r_R}{r_S}\cdot\frac{r_A}{r_A-r_R}-\frac{1}{2}\right)C_S^\alpha \qquad (4)$$

Here, Δn is the difference in refractive index and K_{AR} is the increment of refrective index per equivalent of AR or Na_2HPO_4. Δn is also found to be very small in the case of TMV (see Table V) and small areas of both δ- and ε-boundaries may be expected from this fact.

When ξ becomes close to unity, the change in the conductivities across the boundary is also largely reduced and the boundary pattern, therefore, becomes independent of the

* Fischer and Lauffer[7] obtained a value of—3,900 for the valency at pH 7 by titration studies. They reported, in their original paper, a value of—8,300 for the theoretical valency, but they re-examined their calculation and have found that the correct theoretical value should be about—1,000 instead of—8,300[34]. In their calculations, they neglected the presence of nucleic acid and assumed a molecular weight of 3.4×10^7.

34) M.A. Lauffer, private communication.

35) I. Watanabe, N. Ui and M. Nakamura, *J. Phys. & Colloid Chem.*, **54**, 1366 (1950).

36) L.G. Longsworth and D.A. MacInnes, *J. Am. Chem. Soc.*, **62**, 705 (1940); *Chem. Revs.*, **24**, 271 (1939).

** In Fig. 1 the descending boundary seems to be slightly sharper, but it is due to the difference in the sharpness of the initial boundaries.

37) L.G. Longsworth, *J. Phys. & Colloid Chem.*, **51**, 171 (1947).

*** To simplify the problem, buffer solution was assumed to consist of only Na^+ and HPO_4^{--} ions.

38) R.A. Kekwick, *Biochem. J.*, **32**, 552 (1938).

direction of the current. In this limiting case, the ascending pattern should be the mirror image of the descending one. Thus the reason why the descending boundary of TMV solution moves as sharply as the ascending one may be easily understood.

In the solution of serum albumin, on the contrary, the ascending boundary moves more rapidly than the descending one and, moreover, the later becomes more diffuse. In addition, the areas of the δ- and ε-boundaries become very significant. The values of ξ and Δn in Table V also explain these considerable "boundary anomalies" in the case of horse serum albumin.

At any rate, it may be conculded that a condition which is closer to the ideal case for electrophoresis can be easily attained in TMV solution even though its concentration is relatively high.

Summary

The variations of the mobility of tobacco mosaic virus (TMV) in phosphate buffer at pH 7.7 with changes in concentration and ionic strength have been investigated. The mobility is essentially independent of the concentration and has an average value of $-7.0_5 \times 10^{-5}$ cm²/sec. volt in the phosphate buffer of ionic strength 0.2. On the other hand, the mobility increases greatly with the decrease of ionic strength. The net charge on the TMV particle, calculated from the mobility data by the aid of Gorin's equation, was found to be constant (about $-1,800$) all over the range of ionic strength examined. Although it is considerablly lower than the theoretical valency calculated from the analytical data, this low value of the valency from the mobility is quite reasonable to explain the observation that there is no serious divergence from the ideal behaviour in the electrophoresis of TMV solution.

The authors are indebted to Dr. J. Hitaka, Tobacco Experimental Station at Hatano, Kanagawa Prefecture, for tobacco leaves. Part of the expense of this investigation was defrayed by the Grant in Aid of the Ministry of Edcation for the Scientific Research.

Institute of Science and Technology,
The University of Tokyo,
Tokyo

Kinetics of the Oxydation of Red Phosphorus by Potassium Bromate

By M. VENUGOPALAN and K. J. GEORGE

(Received September 20, 1955)

Potassium bromate is a powerful oxidising agent in acid solution. Reducing agents convert it smoothly into the bromide:

$$BrO_3^- + 6H^+ + 6\epsilon = Br^- + 3H_2O.$$

At the end of the reaction free bromine appears:

$$BrO_3^- + 5Br^- + 6H^+ = 3Br_2 + 3H_2O.$$

Numerous quantitative oxidation processes involving the use of potassium bromate show that its oxidising property is almost equivalent to that of potassium iodate[1-5].

Many quantitative oxidation reactions with potassium bromate[6], iodate[7], periodate[8], ceric sulphate[9], and iodine[10] as powerful oxidising agents for the oxidation of red phosphorus have been studied by earlier workers.

The use of potassium bromate in the volumetric determination of elementary red phosphorus has been investigated by Deshmukh and Sant[3]. They have observed that the addition of acidified potassium bromate solution to phosphorus leads to its gradual disappearance accompanied with a rapid evolution of bromine. The method is based on the oxidation and subsequent conversion of phosphorus into phosphoric acid. Bromine liberated during the process or the unreacted bromate after the completion of the reaction is estimated iodometrically and the amount of phosphorus is calculated from the following reaction mechanism:

$$2P + 2KBrO_3 + H_2SO_4 + 2H_2O \longrightarrow 2H_3PO_4 + Br_2 + K_2SO_4.$$

1) S. György, *Z. anal. Chem.*, **32**, 415 (1893).
2) A. Kurtenacker and J. Wagner, *Z. anorg. allgem. Chem.*, **120**, 261 (1922).
3) R. Lang, *Z. anal. Chem.*, **106**, 12 (1935).
4) R. Lang, *Z. anorg. allgem. Chem.*, **142**, 229 (1925).
5) E. Rimini, *Gazz. chim. ital.*, **29**, 265 (1899).
6) G.S. Deshmukh and B.R. Sant, *Anal. chem.*, **24**, 901 (1952).
7) T.F. Büehrer and O.E. Schupp, *J. Am. Chem. Soc.*, **49**, 9-15 (1927).
8) G.S. Deshmukh and M. Venugopalan, *J. Ind. Chem. Soc.*, **32**, 309-312, (1955).
9) G.S. Deshmukh, *Analyst*, **76**, 604, (1951).
10) G.S. Deshmukh and M. Venugopalan, *J. Ind. Chem. Soc.*, **30**, 747-750 (1953); **32**, 305-308 (1955).

Experience, however, has shown that the rate of the above oxidation process is measurably slow at ordinary temperatures. Hence, it was of interest to study the kinetics of this oxidation process in some detail.

Experimental

Red phosphorus of British Drug House laboratory reagent grade quality was purified by Buehrer and Schupp's method[7] and subsequently by the copper phosphide process[8]. Its purity was checked by the magnesium pyrophosphate and bromate procedures.

An accurately weighed quantity of the sample was introduced in a ground-glass stoppered Erlenmeyer flask to which a known excess of standard potassium bromate solution was added, followed by 5 to 10 ml. of carbontetrachloride. Acidified with about 5 to 10 ml. of 4N sulphuric acid so that the overall acidity of the system was maintained at or about 0.5N sulphuric acid. The flask was maintained at a desired constant temperature for thirty minutes prior to the addition of potassium bromate and also during the course of subsequent observations in an electrically heated thermostat fitted with an accurately calibrated automatic thermoregulator. The contents of the flask were swirled from time to time and an aliquot portion (5 ml.) of the clear supernatent aqueous layer was pipetted out carefully at different time intervals and titrated iodometrically by standard thiosulphate[11]. Series of experiments were carried out at different temperatures, viz., 30°, 35°, 40°, 45°, 50° atd 55°C using the same conditions for concentrations and also by varying the concentrations of potassium bromate and the weight of red phosphorus over a fairly wide range.

Results and Discussion

From the initial titre value of bromate and that obtained at various time intervals during the course of the oxidation, the order of the reaction was calculated by the integration method. Under the given operative conditions the value of K was found to be constant and within limits of experimental error according to the following equation:

$$K=\frac{2.303}{tC_\infty}\log_{10}\frac{C_t(C_0-C_\infty)}{C_0(C_t-C_\infty)}$$

where C_0—initial concentration of potassium bromate;
C_t—concentration of potassium bromate at time t;
C_∞—concentration of potassium bromate at time ∞;
and t—time in minutes.

A representive group of results is shown in Table I.

11) A.I. Vogel, "Text Book of Quantitative Inorganic Analysis," London, Longmans, Green and Co., 1945, p. 451.

TABLE I

Temperature: 45°C Weight of phosphorus: 0.02 g.
Reaction mixture: 5 ml. Concentration of $KBrO_3$: 40 ml. N/5 solution.

Time	N/10 Thiosulphate	$\log_{10}\frac{C_t(C_0-C_\infty)}{C_0(C_t-C_\infty)}$	$K\times10^{-3}$
0 min.	8.5 ml.	—	—
5	8.2	0.0174	1.8
15	7.85	0.0405	1.4
30	7.3	0.0774	1.4
50	6.7	0.1438	1.5
85	6.05	0.2477	1.5
∞	4.4	—	—

Mean $K=1.5\times10^{-3}$

The results in Table I therefore show that the oxidation of red phosphorus by potassium bromate is an overall second order reaction.

A reaction of the second order depends principally on the initial concentration of the reactants, the half value period and the temperature at which the reaction is carried out. The variation of the velocity constant K with temperature for the same initial concentrations of the reactants is represented in Table II.

TABLE II

Weight of Phosphorus taken: 0.02 g.
Concentration of bromate: 40 ml. N/5 solution.
Normality of thiosulphate: 0.1 N.

Temperature (t)	Mean $K\times10^{-3}$
30°C	0.35
35	1.00
40	1.40
45	1.50
50	1.90
55	4.85

From the results, it can be inferred that the velocity constant K increases as the temperature increases; the values of $\log_{10}\frac{C_t(C_0-C_\infty)}{C_0(C_t-C_\infty)}$ plotted against time t for different temperatures, at which the reaction has been studied, are represented graphically in Fig. 1.

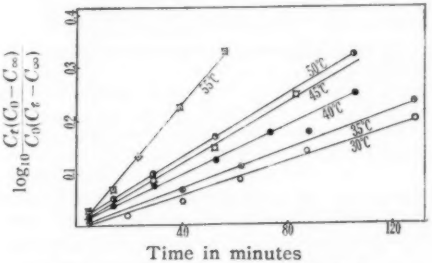

Fig. 1. Variation of $\log_{10}\frac{C_t(C_0-C_\infty)}{C_0(C_t-C_\infty)}$ with temperaure.
Wt. of P=0.02 g.
Conc. of $KBrO_3$=40 cc. N/5 soln.

The variation of the velocity constant K for different initial concentrations of the reactants has been studied by varying the concentration of bromate solution and keeping the weight of phosphorus constant in all the experiments. A typical set of results is returned in Table III.

TABLE III

Temperature: 30°C.
Weight of phosphorus taken: 0.02 g.
Normality of thiosulphate: 0.1 N.

Expt. No.	Concentration of $KBrO_3$ added	Mean $K\times10^{-3}$
1.	40 ml. N/5 solution	0.35
2.	〃 N/6 〃	0.52
3.	〃 N/9 〃	0.94

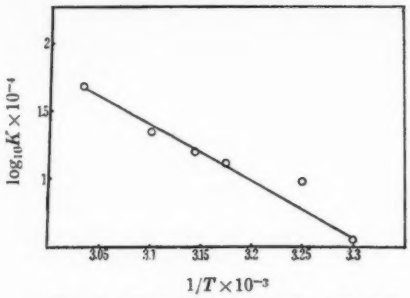

Fig. 3. Variation of $\log_{10}K$ with $1/T$.

Fig. 2 represents graphically the variation of $\log_{10}\frac{C_t(C_0-C_\infty)}{C_0(C_t-C_\infty)}$ with time for different initial concentrations of bromate at the same temperature.

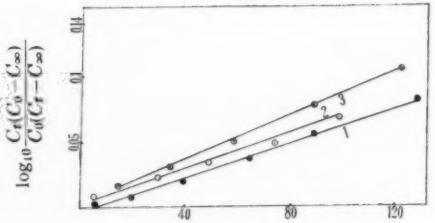

Time in minutes

Fig. 2. Variation of $\log_{10}\frac{C_t(C_0-C_\infty)}{C_0(C_t-C_\infty)}$ with time for different concentration of potassium bromate.
Wt. of P=0.02 g. Conc. of $KBrO_3$
1. 40 ml. N/5 soln.
2. 〃 N/6 〃
3. 〃 N/9 〃

The energy of activation and the temperature coefficient were calculated from the values obtained for K at different temperatures T_1 and T_2 as indicated in Table IV.

The variation of log K with $1/T$ is shown in Table V; the results are plotted in Fig. 3. The linear relationship between log K and $1/T$ (Fig. 3) is in accord with the Arrhenius equation[12] which expresses the influence of temperature on reaction velocity.

TABLE IV

Temp. absolute T_1-T_2	$K_1\times10^{-3}$	$K_2\times10^{-3}$	Temp. coeff. K_2/K_1	Energy of activation $E=\frac{2.303\log_{10}K_2/K_1\times R\times T_1\times T_2}{T_2-T_1}$
303–313°	0.35	1.40	4.00	26290 g. cals.
308–318	1.00	1.50	1.50	7942
313–323	1.40	1.90	1.36	6215
318–328	1.50	4.85	3.23	24450

TABLE V

Temp. absolute	$1/T\times10^{-3}$	$K\times10^{-4}$	$\log_{10}K\times10^{-4}$
303	3.30	3.5	0.5441
308	3.25	10.0	1.0000
313	3.17	14.0	1.1461
318	3.14	15.0	1.1761
323	3.10	19.0	1.2788
328	3.05	48.5	1.6857

The essential bimolecularity of the overall oxidation process shows that the molecular ratio of P to $KBrO_3$ is 1:1 which is in agreement with the earlier observation of Deshmukh and Sant[6].

Nature of the Reactions involved

The reactions involved in the oxidation of phosphorus by $KBrO_3$ have been found to take place as follows:

$$5P+3BrO_3^-+3H^++6H_2O = 3/2Br_2+5H_3PO_3 \quad \text{(i)}$$

This reaction is slow and goes partially to phosphoric acid.

$$2P+3Br_2+6H_2O=6H^++6Br^-+2H_3PO_3 \quad \text{(ii)}$$

This reaction is quite rapid.

$$5H_3PO_3+2BrO_3 = Br_2+3H^++5H_2PO_4^-+H_2O \quad \text{(iii)}$$

This reaction is very slow as is strikingly shown by adding $KBrO_3$ to a phosphorus

12) Arrhenius, *Z. phys. Chem.*, 4, 226 (1889); *Trans. Farad. Soc.*, 33, 72 (1937).

acid solution. Very little bromine is liberated even on refluxing the solution for some time.

$$H_3PO_3+Br_2+H_2O=3H^++2Br^-+H_2PO_4^- \quad \text{(iv)}$$

This reaction has been shown by a number of authors to be slow, and to depend in large measure upon the acid concentration. It appears that the oxidation of phosphorus acid by bromine determines the rate of reaction as a whole.

$$5Br^-+BrO_3^-+6H^+=3Br_2+3H_2O \quad \text{(v)}$$

This latter reaction is instantaneous and complete. The possibility of adopting this reaction for a quantitative oxidation of red phosphorus to phosphoric acid bromometrically is being investigated.

Summary

Kinetics of the oxidation of Red Phosphorus by Potassium Bromate in acid solution has been studied. Using varying concentrations of potassium bromate and the quantity of red phosphorus between 0.01 g. and 0.02 g., the reaction has been found to be bimolecular with respect to potassium bromate over a temperature range of 30–55°C. The energy of activation and temperature coefficient of the reaction have been calculated. Further work on the oxidation of red phosphorus by bromide-bromate mixture in acid solution is suggested.

Grateful thanks of the authors are due to Professor S. S. Joshi for facilities and kind interest in the work.

Chemistry Department, Banaras Hindu University, Banaras, India

---

Studies on the Cold-drawing of Polymers (Part III).[1] *The Quasi-static Drawing of Polycapramide. III.** *The Effects of Heat-treatments and the Temperature Dependencies of the Heterogeneous Structure in Polymers*

By Hirosuke YUMOTO

(Received October 3, 1955)

Introduction

In the development of the investigation on the cold-drawing of polymers (for example, polycapramide), the influences of temperature and humidity (the moisture adsorption) on the quasi-static drawing have been reported in Part I[2] and Part II[1]. In succession the effects of heat-treatment were investigated.

In addition to drawing behaviors, densities were chosen for the measure of the structure change through heat-treatment. Each of various singular temperatures obtained is considered as the transition temperature of each micro-region in the heterogeneous structure. Then the temperature dependencies of polycapramide are brought to light and some experimental foundations for conjecturing the drawing mechanism are established. Such experimental results and the discussion on them are the subject of this paper.

Experiments

(1) The Specimens.—60 denier (ϕ 0.086 mm.) polycapramide semidull unstretched monofilament was used which was spun from the melt through chilling by air and contained about 2% of caprolactam monomer and oilgomers.

(2) The Methods of Heat-Treatments.—For the heat-treatment in the dry state, the above specimen had been inserted in a glass tube, which was sealed after substituting air with carbon dioxide, and was heated at a constant temperature (±1°C) from 50° to 200°C in a bath of an appropriate boiling organic liquid or in an electric thermostat. For the heat-treatment in water or in the saturated water vapor, water was let into a tube together with the specimen before sealing; in case of the former the specimen was entirely steeped in water and in case of the latter the specimen was placed apart above the water in the tube. The heating procedure of the sealed tube was the same as in the case of the treatment in the dry state. The specimens in the tube were always tensionless.

After the heating, the tubes were always cooled in room temperature without particular means for rapid or slow cooling.

1) H. Yumoto, This Bulletin, 29, 141 (1956).

* H. Yumoto, presented at the 8th annual meeting of the Chemical Society of Japan in Tokyo, April 2, 1955.

2) H. Yumoto, This Bulletin, 29, 45 (1956).

(3) The measurements of Isothermal Quasi-static Elongation-Stress Curves.—The methods were the same as those described in Part I. Measuring was performed on the drawing at 80°C in completely dried state or at 20°C in water.

(4) The Measurements of Densities.—The densities in dried state were measured at 25± 0.005°C by the floatation method using ethylene chloride: xylene mixtures[a] as media. Specimens were previously cut into about 0.5 mm. of length and dried completely with phosphorous pentoxide in a desiccator. The mixture was poured on to pieces so finely cut and dried under the vacuum as to avoid bubbles remaining on the pieces and the equilibrium between floatation and precipitation was brought about by controlling the mixture ratio of medium at 25°C. The densities of media at the equilibrium were measured with an Ostwald picnometer. The error of measurement was about ±0.0005 g./cc.

Results of Measurement

(1) Density

The densities (25°) of specimens subjected to various heat-treatments are shown in Table I. The specimens treated in air give slightly larger densities than those treated in carbon dioxide; this fact may be attributed to the increase of molecular weight owing to the combination of oxygen, because polycapramide kept in air at high temperature suffers oxidation. When the temperature and the medium for treatment are the same, the density seems to converge to a certain level; i.e. even if the time of treatment is prolonged, the density does not increase apparently beyond a certain value. Such limiting values are shown in Fig. 1.

TABLE I

DENSITIES OF POLYCAPRAMIDE SUBJECTED TO VARIOUS HEAT-TREATMENTS AT 25°C

Heat-Treatment			Density at 25°C (g./cc.)
Temp. (°C)	Time (hr.)	Medium	
	Untreated		1.1340
115	10	air	1.1375
〃	5.0	CO_2	1.1355
138	2.0	air	1.1410
139	1.0	CO_2	1.1410
〃	3.0	〃	1.1420
150	2.0	air	1.1450
158	2.0	air	1.1465
〃	3.0	CO_2	1.1425
〃	5.0	〃	1.1420
168	1.0	CO_2	1.1430
171	3.0	〃	1.1465
183	1.0	〃	1.1505
〃	3.0	〃	1.1505
190	1.0	〃	1.1590
〃	3.0	〃	1.1580
203	1.0	〃	1.1705
205	3.0	〃	1.1720
ca. 20	240	benzene	1.134
〃	240	H_2O liquid	1.135
40	30	〃	1.137
60	2.0	〃	1.140
80	20	〃	1.143
100	2.0	〃	1.148
120	2.0	〃	1.157
140	2.0	〃	1.168
60	2.0	H_2O vapor	1.137
80	2.0	〃	1.141
100	2.0	〃	1.142
120	2.0	〃	1.156
140	2.0	〃	1.170

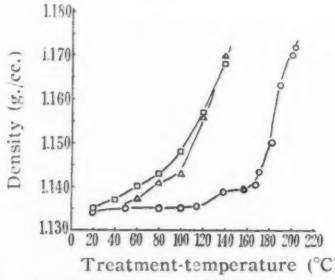

Fig. 1. Densities at 25°C limitted with varicus treatment-temperatures.
○ Treatment in dried state
□ Treatment in liquid water
△ Treatment in saturated vapor of water

The heat-treatment is the process where some of the distortions in substances diminish through the thermal Brownian motion of structural elements; therefore the time of treatment is an important factor. In polymers some microscopic movements cannot come into effect before exceedingly long elapse of time. Nevertheless the

a) Using carbon tetrachloride: xylene mixture, the same values were obtained. Using benzene: nitrobenzene mixture slightly lower values were obtained.

transfiguration due to the movements, which will be caused after times of treatment have elapsed, can be considered to be negligibly small because of the limit of density increment as above described.

Fig. 1 indicates the following facts. In case of the treatment in dried state, the increase of density is not apparent at the temperature below ca. 100°C, but becomes apparent beyond ca. 120°C, and is remarkable at 180–200°C. In case of the treatment in water (liquid), the specimen treated even at room temperature gives somewhat greater density than the untreated one. The increase of density with rise of the treatment temperature, is just noticed from 40°C and is remarkable beyond ca. 100°C. In case of the treatment in water vapor the increase of density is similar to that in case of the treatment in liquid water; the densities in both cases at the same treatment-temperature are the same above 120°C, but the former is somewhat less than the latter below 100°C.

Under the apprehension that the increase of density through steeping in water for 240 hrs. might be attributed to the removal of caprolactam monomer through extraction, the density of specimen which had been freed from monomer by steeping in benzene for 240 hrs. was measured on trial; but the increase of density was not noticeable. Therefore, the increase of density through steeping in water is caused in conclusion not by the removal of monomer but by the transfiguration of fine structure.

(2) Drawing Behaviors

Only the specimens, which had attained to the limit of density increment by heat-treatment at each of the temperatures, were subjected to the drawing experiment. The elongation-stress curves at 80°C in dried state and at 20°C in water are given in Figs. 2, 3 and Figs. 4, 5. Polycapramide, even if heat-treated, can be easily stretched in these conditions; but below 80°C in dried state it is quite difficult to stretch it and breaking happens mostly before 20–30% elongation. The obtained curve takes the similar shape with that of the untreated specimen, which gives the steep rise of stress from the environs of 100% elongation at any case. When the temperature of treatment is higher, the stress at the same elongation and the Young's modulus are higher. It is noteworthy that, in spite of exhibiting maximum and minimum of stress in case of drawing at 80°C in

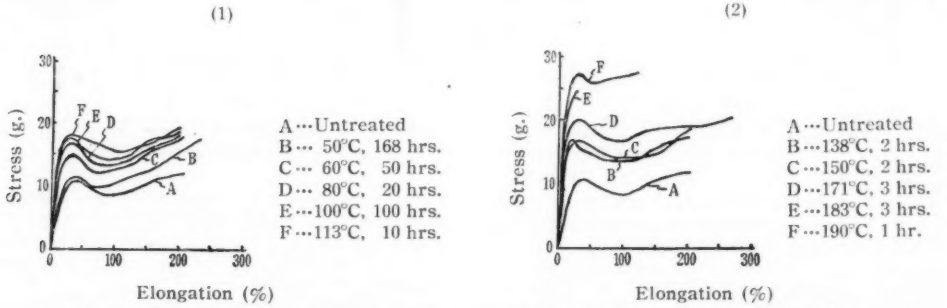

Fig. 2. The quasi-static elongation-stress curves of polycapramide subjected to heat-treatments in dried state at various temperatures on drawing at 80°C in completely dried state.

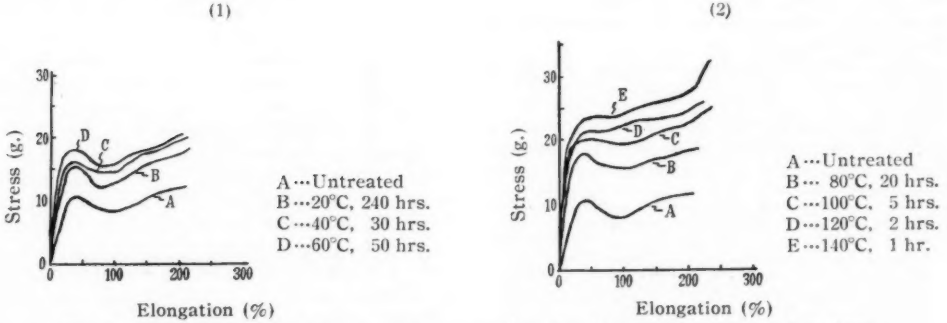

Fig. 3. The quasi-static elongation-stress curves of polycapramide subjected to heat-treatments in liquid water at various temperatures on drawing at 80°C in completely dried state.

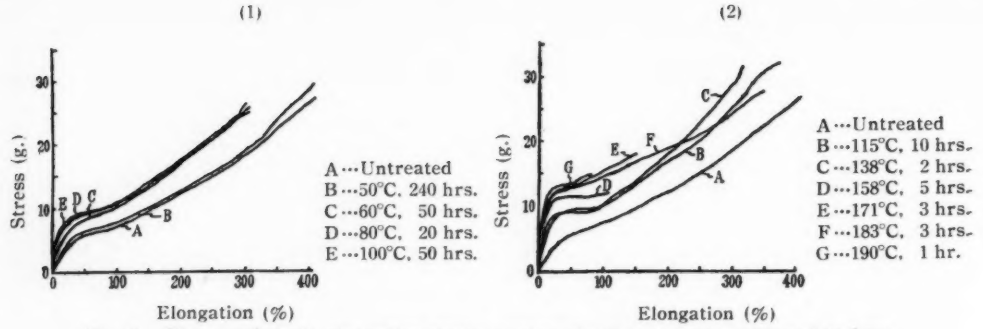

Fig. 4. The quasi-static elongation-stress curves of polycapramide subjected to heat-treatments in dried state at various temperatures on drawing at 20°C in water.

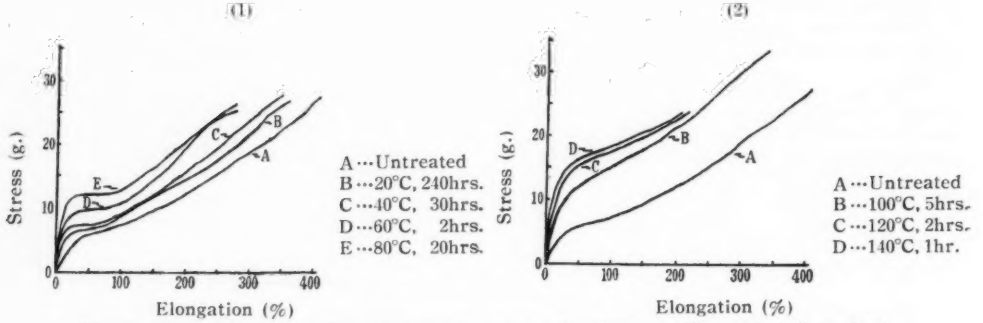

Fig. 5. The quasi-static elongation-stress curves of polycapramide subjected to heat-treatments in liquid water at various temperatures on drawing at 20°C in water.

dried state, most[b] of the heat-treated specimens are stretched homogeneously, without necking, towards rupture. In case of the drawing at 20°C in water, all are stretched homogeneously, and neither maximum nor minimum of stress are found in the curves. But an inflection part is found as shown in Fig. 4; the part following after the inflection lies on the identical line in every case of dry treatment below 140°.

(i) Drawing at 80°C in Dried State.—The tentative yield stresses (*We*), which are the minimum stresses in curves as explained in Part I or II, are plotted against the temperatures of heat-treatment in Fig. 6.

Fig. 6 indicates the following facts. In case of the treatment in dried state, *We* increases with temperature below ca. 120°C, especially at ca. 60°C, and is almost invariable from ca. 120°C to ca. 170°C; but the great increase of *We* is noticed between 170–180°C. In case of the treatment in liquid water, even if merely being steeped for a long time in water at room temperature, *We* is somewhat higher. *We* increases peculiarly at ca. 40°C and 80–100°C, but scarcely alters in the other temperature ranges.

Consequently it is found that the increase of yield stress is not parallel with the increase of density (cf. Fig. 8).

(ii) Drawing at 20°C in Water.—The stress at the inflection part, which is well assumed as the tentative yield stress (*We*), increases with rise of the treatment-temperature as shown in Fig. 7.

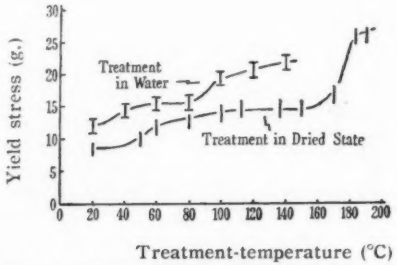

Fig. 6. The relations between yield stresses at 80°C in completely dried state and treatment-temperatures.

b) No specimens treated in water above 40°C or in dried state at higher temperature gave necking in this drawing condition. If treatment was executed in dried state at lower temperatures (the limit of temperature could not be determined), the necking appeared. On the other hand the untreated specimen showed the necking distinctly, even if drawing was carried out at 160°C. Although appearance of necking depends on the rate of drawing, it is evident that the appearance of max. and min. in the curves is not always attended with the appearance of the necking.

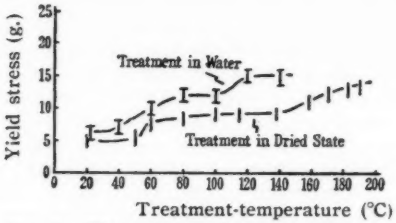

Fig. 7. The relations between yield stresses at 20°C in water and treatment-temperatures.

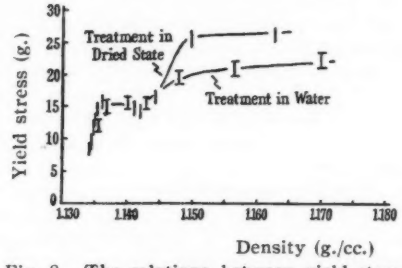

Fig. 8. The relations between yield stresses at 80°C in completely dried state and densities at 25°C.

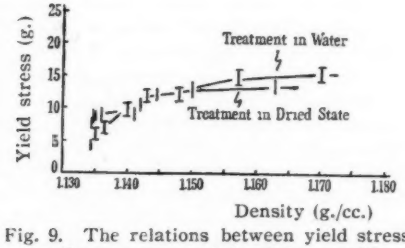

Fig. 9. The relations between yield stresses at 20°C in water and densities at 25°C.

Discussion

(1) The Dry Heat-Treatment

The singular temperatures in respect to the treatment in dried state exist at near 60°, 120°, and 180°C; those at 120° and 180°C are noticed on both of density and yield stress but at 60°C on the yield stress alone. (Fig. 10, where maxima of stress in Fig. 2 are plotted against treatment-temperature, gives singularities more clearly than Fig. 6.) Any of them is thought to be a sort of transition temperature. The temperature near 180°C is assumed as the softening temperature explained in Part I[2], at which the macro-Brownian motion in any micro-region begins to be effectual. Hence there will be tow transition temperatures, 60°C and 120°C, in which the micro-Brownian motion participates. This indicates the coexistence of two micro-regions; the one where the micro-Brownian motion comes into effect easily, and the other where it is relatively difficult for it to do so. Presumably the former can be assumed as the amorphous region [Am.], but the latter cannot be simply assumed as the crystalline region. The sharp increase of density by heat-treatment above 120°C suggests the latter to be assumed as the intermediate state between amorphous and crystalline, i. e. the mesomorphous state [Qcr.]. Therefore the complete crystalline region [Cry.] (containing a little disorder) must exist as the another region. The thermal behaviors of these three hypothetical regions may be taken into account under the experimental facts, setting aside the question how such regions are distributed.

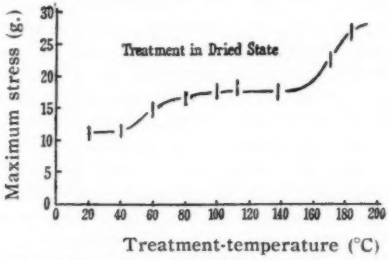

Fig. 10. The relation between maximum stresses at 80°C in completely dried state and treatment-temperatures.

The peculiar temperature at which the micro-Brownian motion becomes effectual[c] is denoted by Tf. The heat-treatment relaxes the frozen distortion and brings about the thermal equilibrium. The treatment at above Tf of [Am.] makes part of [Am.] transformed into [Qcr.] or [Cry.] (1st.-transformation), and still that at above Tf of [Qcr.] makes [Qcr.] transformed into [Cry.] (2nd.-transformation). Hence it can be said from Figs. 1, 4, 6, and 10, that through the 1st.-transformation the stress at deformation is increased but the density is scarcely altered, and on the other hand through the 2nd.-transformation the increase of stress is little but the increase of density is large. The relation is recognized more explicitly in Fig. 8 where *Wc* are plotted against densities. Therefore it is proved that, by drawing, the large flow between the chain molecules is caused only in the amorphous regions [Am.] and is not done in more or less orderly regions [Cry.], [Qcr.]. If this prove to be the case, the crystallization[3] brought about

c) The meaning of "effectual," is that the effects of elementary transfiguration, owing to the movement within ordinary time of observation or heat-treatment, become observable.

3) K. Fuchino and A. Okada, *Scientific Reports of Toyo Rayon Co.*, No. 13, 1 (1949) (in Japanese). J. Fankuchen and H. Mark, *J. Appl. Phys.*, 15, 364 (1944).

by drawing must be attributed to the transformation of [Qcr.] into [Cry.] resulting from the slip of small extent in [Qcr.] caused by the stress; the elongation due to this slip is negligibly small in comparision to the entire elongation. Tf is lowered under the large stress[4] (about the motion only parallel to the stress) and the transformation becomes possible at the temperature where it is impossible in the ordinary state.

The reason, why the increase of density is not apparent through the 1st.-transformation, is probably due to the little difference between densities of [Am.] and [Qcr.][d].

By treatment at the temperature above the softening temperature (ca. 180°C), both the yield stress and the density are markedly increased. In polymer there are distortions which cannot be removed by the micro-Brownian motion of each individual element (segment) but can removed by the simultaneous co-operative movement of some individual elements. The simultaneous co-operative movement of many elements means the macro-Brownian motion, and the temperature at which such a movement becomes effectual is denoted by Tm. The experimental facts show that the distortions are markedly removed through heating at the temperature above the softening temperature, which is considered to be Tm of the amorphous region. (Tm of the orderly region can be assumed as the melting point 220°C).

(2) The Heat-Treatment in Water

The singular temperatures in respect of the treatment in water exist at about 100°C and 40–50°C. The latter is obscure; but taking into account the fact that, when lactam monomer and oligomers are removed from the chip of polycapramide by scouring with water, the rate of extraction is very much smaller below 40°C than from 60°C to 100°C, it is also supposed to be a certain singular temperature. It is found in Figs. 1, 6, and 8 that singularities at 100°C and 40°C in water resemble those at 180°C and 120°C in dried state, respectively; this indicates Tf of [Qcr.] in water to be ca. 40°C and Tm of [Am.] in water to be ca. 100°C. Tm and Tf are much largely lowered in water than in dried state.

The specimens of the same density give generally the same yield stress, but the density being beyond 1.15 g./cc. the dry treatment gives larger yield stress than the wet treatment as shown in Fig. 8. Such distinction of properties among specimens of the same density also appears on the elongation to rupture; namely the dry treatment gives apparently small value as shown in Figs. 2 and 3. Besides it has been observed qualitatively that the wet treatment gives the lower water adsorption and higher dyeability than the dry treatment. Even if the mean value of density is the same, the variation of density distribution in the structure of polymers will probably cause such distinction of properties.

(3) The Effects of Water

The effects of water on the heat-treatment is very remarkable. If water molecules coexist with polyamide molecules, it is expected that the resistance against flow between chain molecules decreases, Tf is lowered, and the internal pressure is generated by swelling. Some of these effects are revealed on experiment as described already. That Tf of [Qcr.] is lowered by steeping the samples in water, indicates the penetratability of water molecules into [Qcr.] regions.

It is noteworthy that the effects of heat-treatment are much smaller in the case of the drawing in water at 20°C than in the case of the drawing in dried state at 80°C; especially such tendency is large in the case of the dry treatment. For example, the specimens subjected to the dry treatment between 60–138° give the same elongation-stress curve beyond 100% elongation (Fig. 4). This fact suggests that the drawing in water can bring about the similar effect with some of the effects caused by heat-treatment.

(4) Further Considerations of Each Micro-Region

The above description has been deduced on assuming the coexistence of [Am.], [Qcr.], and [Cry.] micro-regions and the transformation among them, but the aspect, how these regions are mixed, has not yet been mentioned. Such aspect cannot be ascertained only by this experiment, nevertheless it can be discussed under consideration of the facts formerly known.

The spherulites are observed in various polymers under the microscope[7,10]. The spherulite is an aggregate of crystallites which is thought to be the inevitable form

4) R.F. Boyer and R.S. Spencer, *J. Appl. Phys.*, **16**, 594 (1945).

d) The density of [Am.] at 25°C is presumed to be about 1.1 by extrapolating densities of the melt at the various temperatures[5]. The density of [Qcr.], which is well assumed as the defective crystallite of frozen α-form as described later, is presumed to be about 1.13 from X-ray data[3,6]. The density of [Cry.] is presumed to be 1.21 from X-ray data[3,6]. Then the difference of density between [Am.] and [Qcr.] is very smaller than that between [Qcr.] and [Cry.].

5) H. Yumoto, *Scientific Reports of Toyo Rayon Co.*, No. 25, 6 (1953) (in Japanese). Y. Kinoshita, ibid. No. 27, 1 (1954) (in Japanese).

6) R.Z. Brill, *Z. Phys. Chem.*, B 53, 61 (1943); *C.A.*, 37, 4576 (1943); *J. Prakt. Chem.*, **161**, 49 (1942); *C.A.*, 37, 4608 (1943).

7) C.W. Bryant, *J. Polymer Sci.*, 2, 547 (1947).

in the crystallization of linear polymers. Concerning polycapramide, although spherulites have been observed practically in the case of the specimens crystallized by slow cooling of the melt or by evaporation of the solution, spherulites which are too small to be observable are generally be expected to be formed. It has been known that spherulites are deformed in proportion with the deformation of specimen[8] and the rupture occurs only along the boundaries between spherulites or along the radii of them[10]. Then [Am.] regions, where flow can occur, must exist in both the boundary and the interior of spherulites. Consequently a spherulite is constituted from [Am.], [Qcr.], and [Cry.] micro-regions, and [Qcr.] or [Cry.] is assumed as a sort of crystallite.

It was already reported in 1925[11] that the crystal structure of paraffine (C_{20}—C_{30}) transforms at much lower temperature than the melting point, and also on polyethylene[12], polyamide[12,3,5] such phenomena were observed. The structure stable at lower or higher temperature has been called by β- or α-form. The transition temperature of polycapramide, although uncertainly, a has been found to be about 150°C[3,5] by means of X-ray. α-Form does not take the stable configuration as the ordinary crystal and is rather assumed as the state where chain molecules arrange in parallel lines into a bundle, having lower entropy-than the amorphous state; i. e. all of the elements of chain molecule do not take the *trans*-configuration of rotational isomers. (All of the structural elements take the *trans*-configurations in β-form.) The micro-Brownian motion in α-form always alters the configuration but it does so only partially so as not to lose the whole arrangement. It is most reasonable to suppose that [Cry.] is the crystallite of β-form and [Qcr.] is that of α-form frozen at lower temperature by rapid cooling. If the transition temperature as regard the α, β-transformation is said to be about 150°C[e], it should be Tf of [Cry.]. In the course of the treatment at a higher temperature than Tf of [Cry.], [Cry.] (β-form) can transform into α-form while it is heated, but it can retransform, if not rapid, into β-form on cooling. Then, as far as the effect of heat-treatment is concerned, the singularity can not be observable at about 150°C.

Now let us consider the relations to the micro-regions, U, Vab, and Vc described in Part II[1]. U region, i. e. the micell, where chain molecules are fairly arranged, corresponds to [Cry.] or [Qcr.], and Vab region, i. e. the boundary region between micells, where molecules are partially arranged, and Vc region, i. e. the intermiceller region, where each of the molecules is completely entangled, both correspond to [Am.]. Therefore [Am.] is divided into two sorts which are different in the order. Taking all things together, Tf of [Am.] in this paper will correspond to Tf (70–80°C) of Vab in the previous paper. Then another Tf of [Am.] corresponding to Tf of Vc must be found; the singularity found at about −40°C on polycapramide[13] will be probably due to Tf of Vc.

Summary

The obtained results are summarized in Tables II and III.

The values in these tables are not precise because of the methods of evaluation, and the shift of ca. ±10°C will be admitted.

All of these temperatures is not always observed in any experiment. The revelation of this singularity is dependent on the character measured and the state of the specimen.

TABLE III

THE EFFECTS OF HEAT-TREATMENT

	Temp. °C	Increase of Density	Increase of Yield Stress	Change in Structure
Treatment in	below ca. 60	none	none	none
Dry State	ca. (60–120)	small	large	Am.→Cry. or Qcr.
	ca. (120–180)	large	small	Qcr.→Cry.
	above ca. 180	very large	very large	Am.→Cry.
Treatment in	below ca. 50	small	large	Am.→Cry. or Qcr.
Water	ca. (50–100)	large	small	Qcr.→Cry.
	above ca. 100	very large	very large	Am.→Cry.

8) C.M. Langkammer and W.E. Catlin, *J. Polymer Sci.*, **3**, 305 (1948).
9) C.W. Bunn, "Fibres from Synthetic Polymers", R. Hill, Elsevier Publ. Co. (1953), pp. 251-6.
10) F.P. Reding and A. Brown, *Ind. Eng. Chem.*, **46**, 1962 (1954).
11) Müller and Saville, *J. Chem. Soc.*, **127**, 599 (1925).
12) W.O. Baker, "Advancing Fronts in Chemistry", S.B. Twiss, Reinhold Publ. Corp. (1945), p. 145.
13) T. Kawaguchi, Unpublished.

TABLE II

THE MICRO-REGIONS IN POLYCAPRAMIDE AND THEIR TRANSITION TEMPERATURES

(1) At Lower Temperature

Micro-Region		Temp. at which the micro-Brownian motion becomes effectual in relaxed state (Tf), °C	
		Dry State	In Water
Am.	Completely amorphous region (Vc)	ca. −40[13]	*
	Partially arranged region (Vab)	ca. 60, 70~80	below 20
Qcr.	Defective crystallite (U) of frozen α-form	ca. 120	ca. 40–50
Cry.	Crystallite (U) of β-form	ca. (150)[e]	*

(2) At Higher Temperature

Micro-Region		Temp. at which the macro-Brownian motion becomes effectual (Tm), °C	
		Dry State	In Water
Am.	Vc	—	—
	Vab	ca. 180 (softening pt.)	ca. 100
Qcr. (Cry.)	Mesomorphous state of α-form (U)	215–220 (melting pt.)	*

Conclusions

The densities and drawing behaviors of polycapramide subjected to various heat-treatments give the useful facts in fiber manufacturing applications. And the reasonable considerations on them suggest the coexistence of some micro-regions, i. e. the heterogeneity of polymer structure. In connection with the results described in Part II, where influences of humidity are considered, the following are concluded. Polymers are constituted from micells (U), boundaries between micells (Vab), and intermiceller regions (Vc). The crystallites of β-form [Cry.] and the defective crystallites of frozen α-form [Qcr.] are U regions. Both of Vab and Vc are amorphous regions [Am.]; Vab indicates a partial arrangement and Vc is completely amorphous. Various singular temperatures can be assigned as the following. At dried state Tf (the temperature at which the micro-Brownian motion becomes effectual) of Vc, Vab, [Qcr.] and [Cry.] are about −40°C[13], 70°C, 120°C and (150°C)[e] respectively. In case when the sample is steeped in water Tf of Vab is lower than 20°C and that of [Qcr.] is about 40°C. (Water molecules can penetrate into [Qcr.]). At dried state Tm (the temperature at which the macro-Brownian motion becomes effectual) of Vab and [Qcr.] are about 180°C (softening point) and 220°C (melting point). (Above Tf of [Cry.] discrimination of [Cry.] and [Qcr.] is lost.) At the state of the sample steeped in water Tm of Vab is about 100°C. The effects of various heat-treatments are compatible with the characters above described.

The other important conclusion is that, by drawing, flow between chain molecules can occur in [Am.] alone; but only a slip of some extent, negligibly small in comparision with the entire elongation, can be caused in [Qcr.].

The density is largely increased by the transformation of [Qcr.] into [Cry.], and the yield stress is largely increased by that of [Am.] into [Cry.] or [Qcr.].

Such precise definitions of micro-regions may be unaccountable, but considerable definite divisions among them can be suggested from the experimental facts. Later, it is hoped that the theoretical interpretation on it can be given.

The author wishes to thank Dr. K. Hoshino and Dr. H. Kobayashi, who instructed him and approved this publication, and M. Nakata who assisted him on experiments.

Nylon Laboratory, Research Department
Toyo Rayon Co. Ltd., Ohe-cho
Minato-ku, Nagoya

e) The value of 150°C is quoted from the X-ray diffraction data of Dr. Fuchino[8], but the thermal analysis[14] gives no singularity at this temperature and gives development of a slight latent heat at 168-173°C. Whether this latent heat is due to the beginning of macro-Brownian motion in [Am.] or to transformation of β to α owing to the beginning of micro-Brownian motion in [Cry.], and then 150°C is still uncertain.

14) Y. Kinoshita, Unpublished.

Heats of Dilution of Polyvinylalcohol Solution. I

By Kazuo AMAYA and Ryoichi FUJISHIRO

(Received October 10, 1955)

Introduction

The measurement of heats of dilution of polymer solutions is important for investigating the thermodynamical behavior of polymer solutions as well as for industrial purposes. Previously we reported the heats of dilution of several polystyrene solutions. In this paper we shall report the heats of dilution of polyvinylalcohol solutions using water as a solvent.

Experimental

Apparatus and Procedures.—The apparatus used was an older type though an improved one had been already described in the previous paper[1]. The former is different from the latter in two points, (1) using A.C. bridge instead of D.C. bridge combined with the converter, and (2) introducing the solution directly into the Dewar vessel as shown in Fig. 1. The thermister has resistance of about 33 KΩ at 30°C, and its temperature

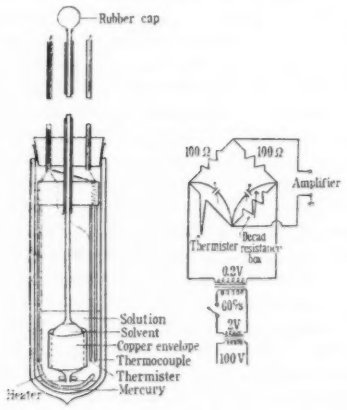

Fig. 1.

coefficient is about 5%. The resistance change of 0.1 Ω can be detected and this corresponds to about 0.005 cal. Fifteen or 20 cc. of solution was introduced with a pipet in the Dewar vessel and 5 or 10 cc. of water was taken into the solvent container. By raising the solvent container and pushing the rubber cap, mixing was performed. Stirring of the mixed solution was operated manually after mixing. Other procedures were the same as those described in the previous paper[1].

1) K. Amaya and R. Fujishiro, This Bulletin **29**, 270 (1956).

Samples*.—The degree of polymerization of polyvinylalcohol used in this experiment was 450 and 600. The content of acetyl radical of the latter sample was less than 0.3 mol. %, but that of the former one was 1.7 mol. %.

Results and Discussion

The heats evolved $-\Delta H$ when the polyvinylalcohol solutions are diluted successively with water at 30°C, are shown in Table I.

TABLE I

HEATS OF DILUTION OF P.V.A. SOLUTIONS

Exp. series	V* cc.	v_r*	v* cc.	v_r'*	$-\Delta H$* cal.	α	T_p* °C.
	System I. Solution of P.V.A. of D.P. 450.						
	15	0.155	5	0.115	0.312	−4.3	30
	20	0.115	5	0.092	0.252		
	25	0.092	5	0.077	0.172		
	System II. Solution of P.V.A. of D.P. 600.						
1	15	0.100	5	0.075	0.112	−3.2	70
	20	0.075	5	0.059	0.074		
	25	0.059	5	0.049	0.046		
	30	0.049	5	0.042	0.010		
2	20	0.143	5	0.114	0.192	−2.3	100
	25	0.114	5	0.094	(0.119)**		
	20	0.094	5	0.075	0.069		
	25	0.075	5	0.062	0.050		
	30	0.062	10	0.046	0.063		
	40	0.046	10	0.037	0.044		
3	25	0.114	5	0.094	0.120	−2.3	100
	30	0.094	5	0.081	0.090		
	35	0.081	5	0.071	0.078		
	40	0.071	5	0.063	0.046		
	45	0.063	5	0.056	0.037		

* These notations are as follows: V: Volume of solution before dilution. v_r: Volume fraction of polymer before dilution. v: Volume of water added. v_r': Volume fraction of polymer after dilution. $-\Delta H$: Heat evolved. T_p: Pre-heating temperature.

** This value in the brace is the expected one owing to the failure of the experiment.

Both systems, solutions of P.V.A. of D.P. 450 and 600, proved to be exothermic.

Assuming that the heat of mixing is represented by the van Laar form, we find

* We are indebted to Dr. S. Matsumoto of the Kurashiki Rayon Company and Mr. H. Inagaki of Kyoto University for these samples.

easily that the integral heat of dilution ΔH_0 from the volume fraction of polymer v_r to v_r' is given by

$$\Delta H_0 = aV_r(v_r - v_r')$$

where a is a constant describing the interaction between polymer and solvent and V_r is the volume of polymer in the solution.

Plotting ΔH_0 or $\Delta H_0/V_r$ as ordinate and V_r as abscissa for each series, we obtain straight lines as shown in Fig. 2 and this

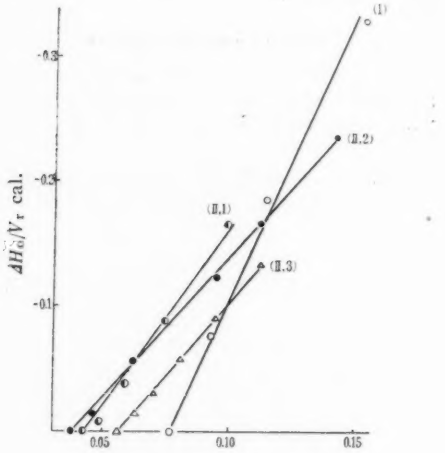

Fig. 2.

result suggests that the assumption mentioned above is satisfied. In the figure we adopt the integral heat of dilution per unit volume of polymer $\Delta H_0/V_r$, as ordinate for the sake of convenience. The values of a can be derived from the tangent of the straight lines in the figure and these values from each series are given in Table I.

As ethanol may be regarded as a monomer-unit of P. V. A., the value of a obtained from the heat of mixing of ethanol solution may be compared with that of P. V. A. solution. Using the data in the literature[2], we find that the value of a for the ethanol-water system is about $-40\sim-20$ cal./cc. in the equal concentration range. This value is the same in sign as that of our experiment, but its magnitude is remarkably larger. According to G. Gee[3] and P. Meares[4], the value of a for the polymer solution is said to be 70–80% of that of the corresponding monomer-unit solution, owing to the increase of polymer-polymer contacts in the polymer solution. But the value of a for the P. V. A.-water system is only 10% of that of the ethanol-water system. This suggests that the strong intersegmental hydrogen bonds in P. V. A. exist and the apparent interaction between P. V. A. and water decreases considerably.

In the system I the solution was introduced into the Dewar vessel after warming to about 30°C. But in the system II before being introduced into the calorimeter, solutions were warmed to about 70°C or 100°C respectively, corresponding to series 1 or 2 and 3. From the values of a of both systems the effects of pre-heating was observed. In other words the absolute magnitude of a is in the inverse relation to the temperature of pre-heating.

It may be considered that the P. V. A.-water system being exothermic the polymer-water contact is energetically more stable than the polymer-polymer contact and therefore, by raising the temperature, the number of polymer-polymer contacts having higher energy increases owing to intersegmental associations of P. V. A.. This state produced by heating is expected to be maintained to some extent even after cooling the solution to 30°C. The higher the temperature of heating, the more the number of polymer-polymer contacts increases and the more that of polymer-water contacts decreases. Thus the number of polymer-water contacts is the most in the system I, next in the series 1 of the system II and the least in the series 2 and 3 of the same system. Consequently on dilution the change in these numbers may be in the same order.

The fact that high degree of intersegmental association by hydrogen bonding is present is more confirmed by other experimental facts. The one is the heats of solvation for lower polyalcohol homologues which were measured by S. Seki and K. Suzuki[5]. They showed that the more the number of hydroxyl radicals in a molecule, the stronger the intramolecular hydrogen bonds are and the apparent interaction between solute and solvent per unit hydroxyl radical decreases considerably even for lower alcohols. Their results seem to be consistent with our ones that the values of a for the polymer solutions are remarkably lower than that for the ethanol solution. Secondly, according to our unpublished data[6], the value of a increases by substituting a fraction of hydroxyl radicals with acetyl. This may be due to the hindrance of intersegmental hydrogen bonds

2) E. Bose, *Z. physik. Chem.*, **58**, 585 (1907).
3) G. Gee and W. J. C. Orr, *Trans. Faraday Soc.*, **42**, 507 (1946).
4) P. Meares, *Trans. Faraday Soc.*, **47**, 699 (1951).
5) S. Seki and K. Suzuki, This Bulletin, **26**, 63 (1953).
6) To be published in the forthcoming paper.

by acetyl radicals and seems to support our interpretation.

Summary

The heats of dilution of P. V. A. solutions were measured and the interaction parameter α between P. V. A. and water was found to be in the range of $-2\sim-4$ cal./cc. That these values are remarkably lower than that of ethanol solution suggests the presence of strong intersegmental hydrogen bonds of P. V. A.. The effect of pre-heating was also observed. It may be attributed to the increase of intersegmental associations by heating.

We would like to express our gratitude to Professor Y. Morino of Tokyo University and Professor A. Kotera of Tokyo University of Education for their encouragements and discussions.

Department of Chemistry, Faculty of Science, Kobe University, Mikage Kobe

The Relationship between Longifolic and Isolongifolic Acids

By Isao OGURA

(Received March 4, 1955)

Naffa and Ourisson[1] and later Zeiss and Arakawa[2] observed that the longifolic acids are monobasic with formula $C_{15}H_{24}O_2$ and not $C_{14}H_{22}O_2$. The present author obtained the same results, and furthermore confirmed the fact that the logifolic and isolongifolic acids are isomers in endo- and exo-forms.

Simonsen[3] and others[4] reported that the oxidation of longifolene with chromic acid in acetic acid or with potassium dichromate in sulfuric-acetic acid furnishes isolongifolic and α-longifolic acids besides longifolic acid, that longifolic and isolongifolic acids are isomers having formula $C_{14}H_{22}O_2$, that longifolic acid isomerizes to isolongifolic acid on treatment with mineral acid, and that longifolic acid is considered to be one of the C_{14}-acid varieties.

Zeiss and Arakawa obtained these acids by the oxidation of longifolene with potassium dichromate and reduced them as well as their esters with lithium-aluminum hydride. Namely, when isolongifolic acid and methyl isolongifolate were reduced with the reagent, they were converted into isolongifolol ($C_{15}H_{25}O$), m. p. 112°C. Longifolic acid was converted mainly into isolongifolol and partly into longifolol, m. p. 78.5–80.5°C. α-Longifolic acid gave isolongifolol and impure alcohols rich in isolongifolol. From these results it is obvious that longifolic and α-longifolic acids are mixtures consisting chiefly of isolongifolic acid.

Further, oxidation of isolongifolol with potassium dichromate in sulfuric-acetic acid regenerated isolongifolic acid. On treatment with phosphorus pentachloride in ether at room temperature, it gave an olefin which proved to be longifolene on the basis of optical rotation and infrared spectrum. From these results Zeiss and Arakawa presumed that longifolic and α-longifolic acids are probably epimeric mixtures, and determined that they are monobasic acids of formula $C_{15}H_{24}O_2$.

Longifolene used in the present experiments was regenerated from longifolene hydrochloride (m. p. 59–60°C). The former was oxidized with chromic acid in acetic acid under the same conditions as used by Simonsen[5] and others. Longifolic acid obtained by this treatment was esterified with dimethyl sulfate in the usual manner, and the ester was separated by distillation to give methyl longifolate and methyl isolongifolate, m. p. 54–55°C, which on saponification with alcoholic potash gave longifolic acid, m. p. 152–153°C, and isolongifolic acid, m. p. 136–137°C, respectively. These melting points agreed with other workers' results. Analyses and experiments described below gave values for C_{15}-acid. When dihydrolongifolene, obtained by the catalytic hydrogenation of longifolene, was oxidized similarly, isolongifolic acid was produced. When methyl longifolate and methyl isolongifolate were treated with phenyl magnesium bromide, a crystalline carbinol,

1) P. Naffa and G. Ourisson, *Chem. and Ind.*, **1953**, 917.
2) H.H. Zeiss and M. Arakawa, *J. Am. Chem. Soc.*, **76**, 1653 (1954).
3) J. L. Simonsen, *J. Chem. Soc.*, **1920**, 117, 578; ibid., **1923**, 125, 2624.
4) A.E. Bradfield, E.M. Francis and J.L. Simonsen, *J. Chem. Soc.*, **1934**, 118.
5) J.L. Simonsen, loc. cit.

m. p. 120.5–121.5°C, was obtained from the former, and another carbinol, m. p. 117–118°C, from the latter. On trating it with formic acid, or with potassium bisulfate, or on distilling under diminished pressure, the two carbinols gave the same dehydration product, m. p. 109–110°C, the carbinol of m. p. 117–118°C being dehydrated more easily. These results assumptively show that the two carbinols differ in the steric arrangments of the diphenyl carbinol group and the hydrogen atom ttached to the ring carbon atom which originally possessed the carboxyl group in the longifolic acids. Thus, longifolic and isolongifolic acids are stereo-isomers as regards the carboxyl group and the hydrogen atom. This relationship is imaginable from the results of Zeiss and Arakawa. Just as the endo form (I) and the theoretically possible exo form (II) in dihydrocamphene[6], longifolic and isolongifolic acids may be considered to be in a similar relation.

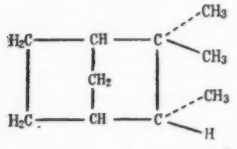

(I)

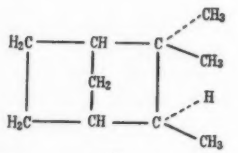

(II)

According to the structural formula presented by Naffa and Ourisson, the relationship is represented as forms (III) and (IV).

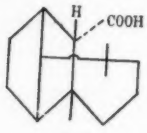

(III)

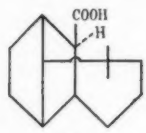

(IV)

The infrared spectra of longifolic and isolongifolic acids showed absorptions at 5.93 μ and 5.90 μ respectively in the solid state, and both at 5.87 μ in carbon tetrachloride solution. All these data proved that longifolic and isolongifolic acids are endo and exo isomers, and it was concluded from the infrared spectra that isolongifolic acid is the endo form.

Experimental

1. Longifolene.—Terpentine oil obtained from oleo-resin was distilled under diminished pressure, and the fraction boiling at 149–152°/36 mmHg or 122–125°/10 mmHg was collected. The longifolene fraction was refluxed with metallic sodium for one hour, and then hydrogen chloride was passed for five to eight hours with cooling in ice-water. Longifolene hydrochloride thus obtained in needles melting at 59–60°C was treated with acetic anhydride and sodium acetate under reflux for three hours to give longifolene. 180.5 g. of this longfolene was dried with calcium chloride, and fractionated under a pressure of 10 mmHg as follows:

Fraction	b.p., °C	Yield, g.	d_4^{25}	n_D^{25}
1	–123	0.9	—	—
2	123–124	157.0	0.9300	1.5025
3	124–125	19.3	0.9303	1.5026
4	125–126	2.1	0.9303	1.5028
5	126–	1.2	0.9351	1.5051

Mol. Refract. (Fraction 2): 64.53. Calcd. for $C_{15}H_{24}(F_1)$: 64.40.

Fraction 2 was used in the following experiments.

2. Methylation.—Longifolene was oxidized according to the procedures of Simonsen and others. The acids obtained were dried and esterified with dimethyl sulfate in the usual way. 51.7 g. of the ester were subjected to fractional distillation:

Fraction	b.p. °C (8.5 mmHg)	Yield, g.	d_4^{25}	n_D^{25}
1	139.5–140.5	16	1.0378	1.5012
2	140.5–142	13	1.0278	1.5012
3	142 –143.5	7	1.0382	1.5016
4	143.5–145	2.5	crystals	
5	145 –147	7	〃	
6	147 –150	3	〃	
7	150 –	2	〃	

Recrystallization of the crystalline fractions from alcohol gave a substance melting at 54–55°C, which agreed with methyl isolongifolate obtained by Simonsen and others.

Anal. Found: C, 76.42; H, 10.16. Calcd. for $C_{16}H_{24}O_2$: C, 76.75; H, 10.4%.

Hydrolysis of the crystalline fractions with alcoholic potash gave an acid which melted at 136–137°C which agreed with isolongifolic acid.

Anal. Found: C, 76.16: H, 10.25. Calcd. for $C_{15}H_{24}O_2$: C, 76.22; H, 10.23%.

On the other hand, the acid obtained from fractions 1–3 by similar treatment was identified with longifolic acid, m.p. 152–153°C.

Anal. Found: C, 76.41; H, 9.75. Calcd. for $C_{15}H_{24}O_2$: C, 76.22; H, 10.23%.

Thus, fractions 1–3 were methyl longifolate (yellowish oil) and other fractions were rich in methyl isolongifolate.

3. Grignard Reaction.—Methyl longifolate (30 g.) was treated with a Grignard reagent prepared from brombenzene (47.1 g.) and magnesium (7.2 g.) in ether solution. The ethereal solution was dried, and evaporated left to stand for two or three days, the residue gave the crystalline carbinol melting at 120.5–121.5°C.

Anal. Found: C, 86.29; H, 9.41. Calcd. for $C_{27}H_{34}O_2$:C, 86.58; H, 9.15%. A similar treatment of methyl isolongifolate gave the carbinol melting at 117–118°C, (Found C, 86.49; H, 9.14). The presence of hydroxyl group in these molecules was

6) H. Alder and G. Stein, *Ann.*, 525, 236 (1936).

indicated by the Deniges reagent and by the analysis described above.

4. Dehydration of Carbinols.—The product from methyl longifolate and the Grignard reagent were immediately distilled before the crystals separated out, to give the following results:

Fraction	b.p., °C (10 mmHg)	Yield (g.)	d_4^{25}	n_D^{25}
1	–120	1.5	1.0775	1.5140
2	120–142	2.5	1.0475	1.5240
3	142–146	2.0	1.0413	1.4998
4	146–148	3.0	1.0264	1.5030
5	148–	5.0	crystals	

The residual crystalline substance obtained in the above fractional distillation had a melting point of 109–110°C after recrystallized from alcohol. The presence of a double bond and a phenyl group was inferred from the infrared absorptions at 6.27 μ and 6.70 μ, respectively. Analysis showed it was a hydrocarbon, $C_{27}H_{32}$.

Anal. Found: C, 90.55; H, 9.17. Calcd. for $C_{27}H_{32}$: C, 90.95; H, 9.05%. Another crystalline hydrocarbon, m.p. 67–68°C was obtained from fraction 2. Found: (C, 93.60; H, 6.71). It was not investigated further.

When the carbinols from methyl longifolate and methyl isolongifolate were treated with formic acid or potassium bisulfate under reflux for 1.5 hours, they gave the same hydrocarbon $C_{27}H_{32}$ melting at 109–110°C.

The author is indebted to Prof. T. Kubota, Osaka City University, for his advice and direction, and to Mr. M. Yamaguchi, Osaka City University, for the measurement of the infrared absorption.

Kinki University, Fuse City, Osaka

---

*The Kinetic Study of Surface-chemical Reactions at Extremely Low Pressures. I. The Thermal Reaction between Water Vapor and a Tungsten Filament. Part I**

By Nobuji SASAKI** and Takuya HAMAMURA

(Received February 28, 1955)

Introduction

For the kinetic study of a series of chemical reactions on the solid surface, the reaction between water vapor and a tungsten filament at high temperatures was first chosen, because the filament can readily provide an extremely clean surface by merely flashing it at a high temperature. The equilibrium study of the system of W, O_2, and H_2 has been reported by some investigaters. Chaudron[1] studied the equilibrium by starting from tungsten trioxide and hydrogen at temperatures ranging from 600 to 1100°C. Wöhler[2] and Gulbransen[3] started from water vapor and tungsten at temperatures below 1000°C. Alterthum[4] extrapolated Wöhler's results to obtain the equilibrium constant at 3000°C where vapors of tungsten oxides also must be taken into consideration and concluded that water vapor in equilibrium must almost completely be decomposed.

From these reports, however, nothing can be guessed about the reaction-kinetic behaviour of water molecules impinging upon the heated surface of tungsten.

The Principle of the Experiment

A tungsten filament is heated inside a cold glass vessel through which a reacting gas is rapidly flowing at a sufficiently low pressure. In this way some unnecessary complications can be avoided, namely, the rate of diffusion of the reacting gas has no influence on the rate of reaction, and the reaction products diffuse away to the cold wall of the reaction vessel to escape any secondary reaction in the gas phase. The collision frequency of gas molecules with the reacting surface can be calculated easily, so that the reaction probability per collision of the reacting gas molecule can be evaluated provided that the over-all rate of the reaction can be determined separately. The surface area of the filament can be determined from

* Read before the Sixth Annual Meeting of the Chemical Society of Japan, held on April 1953.

** Department of Chemistry, Faculty of Science, Kyoto University.

1) M.G. Chaudron, *Compt. Rend.*, **170**, 1056 (1920).
2) L. Wöhler and R. Gunther, *Z. Elektrochem.*, **29**, 276 (1923).
3) E.A. Gulbransen, *J. Phys. Colloid. Chem.*, **53**, 690 (1949).
4) H. Alterthum and F. Koref, *Z. Elektrochem.*, **31**, 508 (1925).

the apparent area by multiplying a certain factor correcting for the roughness[5]. The method of obtaining a high temperature for a chemical reaction by heating a filament electrically has the advantage of dispensing with a special refractory material and heating devices.

The flow method is preferred to the static one to avoid the effect of the adsorption of water vapor on the wall, which is inevitable in the static method at very low pressures.

Apparatus.—The apparatus of all soda-glass is shown schematically in Fig. 1. Reservoir 1 containing about 3 cc. of purified water can be connected directly to the reaction vessel by breaking a thin glass bulb 2 by means of a glass rod containing an iron core and disconnected from it by chipping constriction 3 when the experiment is finished.

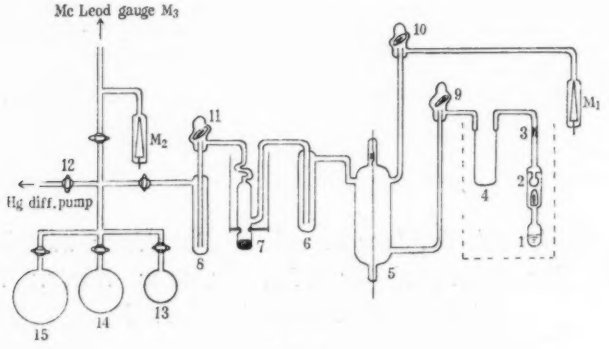

Fig. 1.

Water was purified by repeating sublimation in a high vacuum, dry ice being used for condensation. Capillary tube 4 controls the flow of water vapor. The reservoir and the capillary are immersed in a thermostat. Reaction vessel 5 is 3.5 cm. in diameter and 12 cm. long, so that the pressure gradient along the vessel may be negligibly small. Manometer M_1 used to measure the pressure of condensible water vapor is a 70 mm. long hair pin of 0.3 mm. diameter quartz fibre. It was calibrated against a McLeod gauge using oxygen and hydrogen. The vapor pressure within the reaction vessel can be changed by the change of temperature of the thermostat. A tungsten filament 0.114 mm. in diameter and 120 mm. long was cleaned by dipping in the boiling 40 percent caustic soda solution for five minutes followed by wiping off aqua dag with filter paper, and then it was stretched along the axis of the vessel by means of a tungsten spring. Trap 6 cooled in liquid nitrogen freezes out undecomposed water vapor coming from the reaction vessel. Permanent gasses untrapped are compressed by mercury diffusion pump 7 into glass balloons 13, 14, 15 of different volume from 634 to 6543 cc. connected in a desired combination by means of stop cocks. To determine the composition of the permanent gasses consisting of hydrogen and possibly a small amount of oxygen, the pressure is measured with McLeod gauge M_3 and quartz fibre manometer M_2 at the same time. From the measurement the apparent molecular weight and therefore the composition of the gas can be determined. One percent oxygen added to pure hydrogen reduces by about 7 seconds the interval of time (195 seconds at 50×10^{-4} mmHg.) required for the amplitude to decrease to half value. Trap 8 cooled with dry ice is to prevent grease vapor from entering into the reaction vessel. Particular precautions have been taken to keep the filament from grease vapor contamination by using greaseless stop cock 9, 10, 11, which can be operated with a magnet.

The Procedure.—Prior to the proper experiment, all the apparatus is evacuated for several days by a mercury diffusion pump with a liquid nitrogen trap before it. The reaction vessel is heated at 300°C for ten hours in an electric furnace, and the other tubes are baked out by a hand burner. After thorough evacuation of the cooled vessel the filament is heated at 2400°K for twelve hours.

After the degassing schedule is over, trap 6 is dipped into liquid nitrogen, and glass bulb 2 is broken, the thermostat being kept at a desired temperature. Water vapor flows into the reaction vessel through the capillary tube to be frozen out in trap 6. Pressure measurements with quartz fibre manometer M_1 will show the moment when the flow has become stationary. The filament is now heated, and the temperature is measured with an optical pyrometer. As the reaction proceeds the pressure in the glass balloons increases gradually and this increase is measured with McLeod gauge M_3 at suitable intervals for about eight minutes. The filament is then cooled and the balloons are evacuated through cock 12.

Experimental Result

The pressure of the balloons increases linearly with the time of heating. Some

5) L. Tonks, *Phys. Rev.*, **38**, 1030 (1931).

typical examples are shown in Fig. 2. The

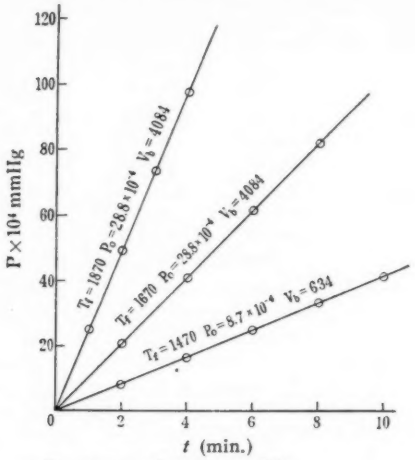

T_b=temp. of filament (°K)
P_0=press of H_2O (mmHg)
V_b=vol of balloons (cc.)

Fig. 2. The pressure change of the glass balloons with the time of heating.

linearity can be observed for more than thirty minutes. This shows the stability both of the flow of water vapor and the surface condition of the filament. The rate of increase of the pressure gives the rate of reaction which is shown in Fig. 3 as a

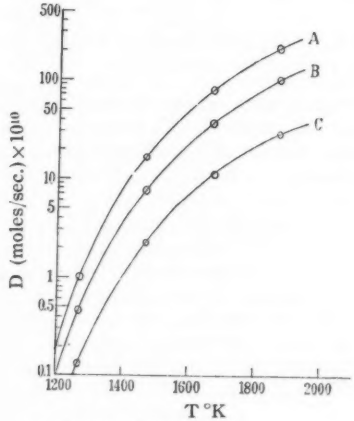

A ; $P_0=64\times10^{-4}$ mmHg
B ; $P_0=28.8\times10^{-4}$ mmHg
C ; $P_0=8.7\times10^{-4}$ mmHg

Fig. 3. Rate of reaction at various filament temperature.

function of the filament temperature. The gas analysis carried out as mentioned above shows the gas produced to be pure hydrogen for varied conditions of the reaction. The temperature increase of the reaction vessel is negligibly small when the filament is heated.

Discussion

From the reaction rates thus obtained, it is possible to evaluate the probability of reaction of a water molecule with the surface of tungsten when a molecule impinges upon it. If the pressure of water vapor is low and the mean free path is comparable with the diameter of the vessel and the length of the vessel is not too long, the following conditions are satisfied.

1. The composition and the pressure of the gas are uniform throughout the vessel.
2. The temperature of water molecules inside the vessel is equal to that of the wall.
3. The flow of gas molecules through the outlet tube obeys Knudsen's law of molecular flow.

Now, if the filament is heated, and water vapor is introduced into the vessel, a part of the water molecules reacts with the filament and leaves the vessel together with the unchanged molecules which are caught in the trap. The quantity in moles of water vapor thus trapped per second is

$$\frac{8\pi r^3}{3l}\times\frac{P}{\sqrt{2\pi MRT}} \qquad (1)$$

where r and l are respectively the radius and the length of the outlet tube in cm, P the partial pressure of water vapor inside the vessel in dyne/cm², M the molecular weight of water, and R the molar gas constant.

Putting $\frac{8\pi r^3}{3l}=A$ and $\frac{1}{\sqrt{2\pi MRT}}=B$ in (1) it becomes

$$ABP. \qquad (1')$$

The quantity in moles of water vapor which reacts per second with the filament is

$$kSBP \qquad (2)$$

where k is the probability of reaction of the water molecule with the filament for a single collision, and S the surface area in cm² of the filament. The quantity of water vapor G which enters into the vessel through the inlet tube per second is equal to the sum of (1′) and (2),

thus $$G=ABP+kSBP. \qquad (3)$$

On the other hand

$$G=ABP_0 \qquad (4)$$

if P_0 is the pressure of water vapor inside the reaction vessel when the filament is cold.

The stationary state being assumed, the quantity in moles of the permanent gas produced in the vessel per second is equal to that of the gas D carried into the balloons per second by mercury pump 7 so that

$$D=kSBP \tag{5}$$

provided that one mole of hydrogen alone is produced from one mole of water. From Eqs. (3) and (5), P which is difficult to measure directly is given by

$$P=\frac{G-D}{AB}. \tag{6}$$

Eliminating P and G from Eq. (3), we get

$$k=\frac{AD}{S(ABP_0-D)}. \tag{7}$$

Thus k, the probability of reaction of the water molecule with the filament for a single collision, may be evaluated from all measurable quantities for various filament temperatures and water vapor pressures.

For the conductance A of the outlet tube the value of 0.047 cm² is used which has been obtained by actually passing carbon dioxide, (the calculated value is 0.055 cm²) and for the roughness factor of the filament the value of 1.225 is used according to the result of Tonks[5].

Results

The probabilities of reaction for a single collision of the water molecule with the heated tungsten surface thus evaluated are shown in Table I.

The conclusion therefrom is that the major part of water molecules which hit the hot surface rebound without reacting with it even at the high temperatures employed, and the reaction is of the first order with regard to the pressure of water vapor. The relation between the reaction probability and the temperature of the filament is given in Fig. 4. The mechanism of the reaction will be discussed in the succeeding paper.

6) Roughness factor of the tungsten filament.

TABLE I

Temp. of filament (°K)	Probability of reaction ($k\times1.225$[5])	Press. of water P_0 (mmHg)	Press. of water P (mmHg)
1270	4.5×10^{-5}	8.7×10^{-4}	8.7×10^{-4}
	4.8×10^{-5}	29×10^{-4}	29×10^{-4}
	4.6×10^{-5}	64×10^{-4}	64×10^{-4}
1470	7.9×10^{-4}	8.7×10^{-4}	8.7×10^{-4}
	8.2×10^{-4}	29×10^{-4}	29×10^{-4}
	8.0×10^{-4}	64×10^{-4}	64×10^{-4}
1670	4.2×10^{-3}	8.7×10^{-4}	8.4×10^{-4}
	3.9×10^{-3}	29×10^{-4}	28×10^{-4}
	3.8×10^{-3}	64×10^{-4}	62×10^{-4}
1870	1.1×10^{-2}	8.7×10^{-4}	7.9×10^{-4}
	1.2×10^{-2}	29×10^{-4}	26×10^{-4}
	1.1×10^{-2}	64×10^{-4}	58×10^{-4}

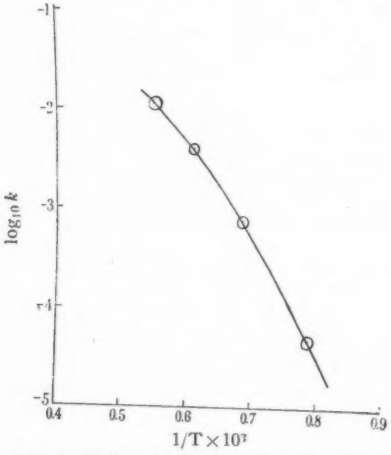

Fig. 4. Effect of the filament temperature on the reaction probability.

We wish to express our sincere thanks to Professor K. Kodera of Kyoto Technical University for his kind discussion and encouragement.

Department of Chemistry, Faculty of Industrial Art, Kyoto Technical University, Kyoto

Interaction between Surface Active Agents and Proteins. II. Electrophoretic Investigation of the System Sodium Dodecyl Sulfate and Egg Albumin

By Koichiro AOKI*

(Received August 12, 1955)

Introduction

Precipitation occurs when the anionic detergent and the protein are mixed at a lower pH than that of the isoelectric point of the protein, and no precipitation occurs when they are mixed at a higher pH than that of the isoelectric point of the protein. In the latter case a transparent solution is obtained, so we cannot confirm whether or not they react, merely from the appearance of the solution when mixed. It is known by the electrophoretic investigation, however, that the complex is formed in the solution. Lundgren et al.[1] proved the existence of the complex in the system alkylbenzenesulfonate-egg albumin, and Putnam and Neurath[2] proved the existence of the complex in the system sodium dodecyl sulfate-horse serum albumin. Further, Yang and Foster[3] studied the interaction between sodium dodecylbenzenesulfonate and egg albumin, and also between this detergent and bovine serum albumin by both the electrophoretic method and the dialysis equilibrium method, holding a different opinion on the behavoir of serum albumin toward detergent from that of Putnam and Neurath.

We discussed in Part I[4] the precipitation reaction which occurred when sodium dodecyl sulfate and egg albumin were mixed at a lower pH than that of the isoelectric point of the protein. No electrophoretic investigation has yet been made on the interaction between sodium dodecyl sulfate (SDS) and egg albumin on the alkaline side of the isoelectric point of the protein. For this reason we investigated this interaction electrophoretically at various pH's and the results obtained are discussed.

* Present temporary address: Department of chemistry, Purdue University, Lafayette, Indiana, U.S.A.

1) H.P. Lundgren, D.W. Elam and R. A. O'Connell, *J. Biol. Chem.*, **149**, 183 (1943); H.P. Lundgren and R.A. O'Connell, *Ind. Eng. Chem. Ind. Ed.*, **36**, 370 (1944).

2) F.W. Putnam and H. Neurath, *J. Biol. Chem.*, **159**, 195 (1945).

3) J.T. Yang and J.F. Foster, *J. Am. Chem. Soc.*, **75**, 5560 (1953).

4) K. Aoki and J. Hori, This bulletin, **29**, 104 (1956).

Experimental

SDS and egg albumin used were prepared by the same method as described in Part I.

We used Hitachi's electrophoretic apparatus equipped with the Schlieren diagonal system. The size of the cell for electrophoresis is $2\times15\times40$ mm. All experiments were carried out in a thermostat at 25 ± 0.01°C.

We prepared and electrophoretically analyzed a series of samples, the weight mixing ratio of which varied, while the sum of the concentration of SDS and that of egg albumin was kept constant at 1.0%. In the same way an electrophoretic study was made on samples the total concentration of which was 0.5%. The ionic strength (μ) of all the buffer solutions used was 0.1. The value of pH and composition of buffer solutions are as follows. No dialysis of the sample was

pH	Composition
5.4	sodium acetate and hydrochloric acid
6.8	sodium monohydrogenphosphate and sodium dihydrogenphosphate
7.6	〃 〃
9.6	〃 〃
9.9	sodium carbonate and sodium bicarbonate
10.8	〃 〃 〃 〃

carried out before electrophoresis, because we found that a small quantity of SDS was dialysed through the membrane into the outer solution and that the composition of egg albumin to SDS was slightly changed during the dialysis.

Results

Fig. 1 shows typical electrophoretic patterns. Fig. 2 shows the mobilities of components calculated from the distance of migration on the descending side. We can decide from this figure that the two components existing in the region of albumin excess are egg albumin and complex, and that the two components in the region of SDS excess are complex and SDS.

We can calculate the number of positive and negative charges on one egg albumin molecule. Curve A in Fig. 4 shows the numbers of positive charges on one egg albumin molecule at each pH.

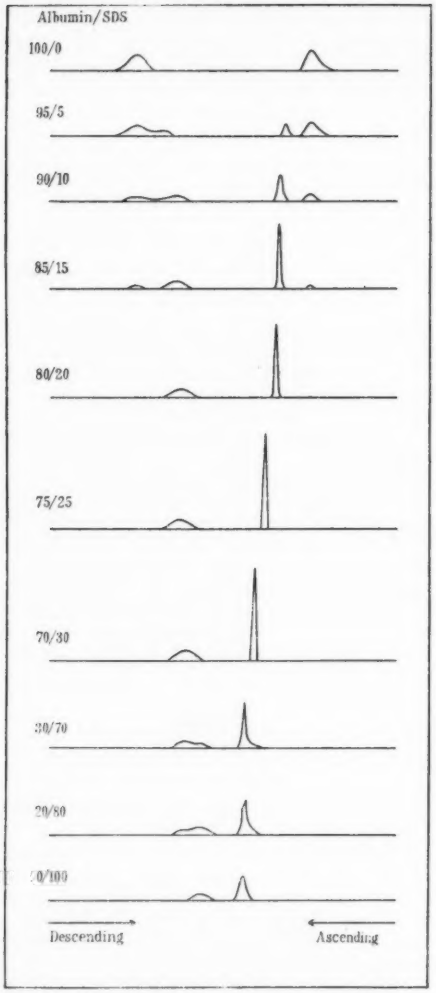

Fig. 1. Electrophoretic patterns of the system sodium dodecyl sulfate–egg albumin at pH 6.8 and ionic strength 0.1. Total concentration is 1.0%.

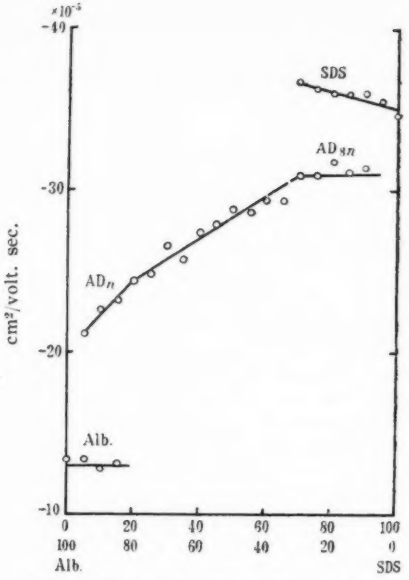

Fig. 2. Electrophoretic mobilities of components in the sodium dodecyl sulfate–egg albumin system.

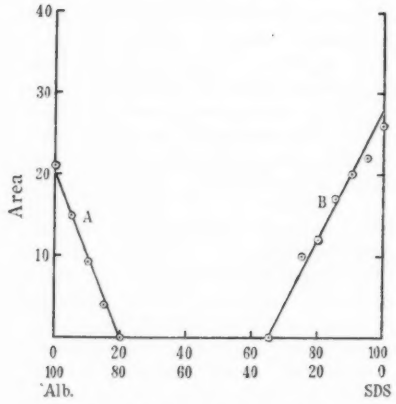

Fig. 3. A: Relation between the area of egg albumin boundary (in arbitrary unit) and the mixing ratio. B: Relation between the area of SDS boundary (in arbitrary unit) and the mixing ratio.

Discussion

Electrophoretic Patterns at pH 6.8.—Electrophoretic patterns obtained can be divided into the following three groups.

The first group comprises the patterns obtained when the mixing ratio albumin/SDS is between 100/0 and 80/20, each pattern having two components, i.e., albumin and complex. With the change of the mixing ratio albumin/SDS, the area of the complex boundary in the pattern increases and that of egg albumin boundary decreases. The electrophoretic pattern on the mixture of albumin/SDS ratio of 80/20 shows merely a trace of the albumin boundary. In Fig. 3, the relation between the composition and the area of albumin boundary is shown. From the slope of the straight line A and the value of 46000 and 288 for the molecular weight of egg albumin and SDS respectively, we can calculate and confirm the fact that about 40 molecules of SDS are bound to one

molecule of egg albumin. In other words, when the mixing ratio albumin/SDS is between 100/0 and 80/20, the composition of the complex is constant and has the formula AD_{40} (A: albumin, D: detergent). We can find that 46 detergent molecules are bound to one egg albumin molecule at pH 6.5, if we use the data given by Lundgren et al. for the electrophoretic experiment on the system alkylbenzenesulfonate-egg albumin[1]. Yang and Foster[3] studied the interaction between sodium dodecylbenzenesulfonate and egg albumin, and found that 43 detergent molecules were bound to one egg albumin molecule at pH 7.6. Further, as described before, we found that about 40 molecules of SDS were bound to one egg albumin molecule at pH 4.2, a lower pH than that of the isoelectric point of egg albumin. Thus, the number of detergent molecules which are bound to one egg albumin molecule seems to be nearly the same for all cases.

As seen in curve A in Fig. 4, the number of positive charges of one egg albumin molecule at pH 6.8 is 38. We found that the composition of the complex first formed was AD_{40}, and this number 40 is almost equal to the number of positive charges on one egg albumin molecule at pH 6.8. Therefore we can assume that the complex is formed through the electrostatic attraction between one negative charge of dodecyl sulfate ion and one of the positive charges on egg albumin molecule.

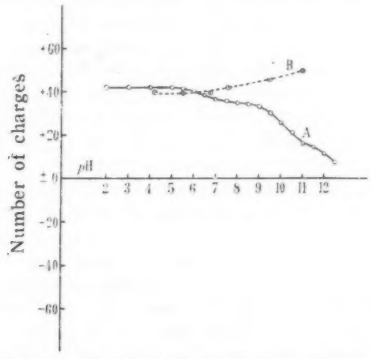

Fig. 4. A: Number of positive charges on one egg albumin molecule at each pH. B: Number of SDS bound to one molecule of egg albumin.

The second group of patterns are obtained when the mixing ratio albumin/SDS is between 80/20 and 35/65. All patterns of this group have only one complex. The mobility of the complex changes continuously with the mixing ratio, so we can assume that the composition of this complex changes continuously with the mixing ratio. As pointed out before, the composition of the complex at the point albumin/SDS=80/20 is AD_n (n=40). The composition of the complex formed at the point albumin/SDS=35/65 is AD_{8n}. It is our opinion that the composition of the complex changes continuously after the formation of AD_n to the completion of AD_{8n}.

The thired group of patterns are obtained when the mixing ratio albumin/SDS is between 35/65 and 0/100. In this region, the patterns have two components, i. e., complex and SDS, and the mobilities of both components are constant, independent of the mixing ratio. Thus, in the region of SDS excess, the mobility of the complex is constant and an unreacted SDS boundary appears. This means that the range of composition of the complex is limited. The line B in Fig. 3 shows the relation between the area of SDS boundary and the mixing ratio. The composition of the complex coexisting with unreacted SDS is found to be AD_{8n} in the same manner as described in the preceding section.

It may be added that our division of the electrophoretic patterns of the syetem SDS-egg albumin is not the same as that presented by Putnam and Neurath for the system SDS-horse serum albumin.

In the case of solutions in which the total concentration was 0.5%, the electrophoretic results were almost the same as those obtained with solutions of total concentration 1.0%.

Curve A in Fig. 5 shows the relation between the relative viscosity (value compared

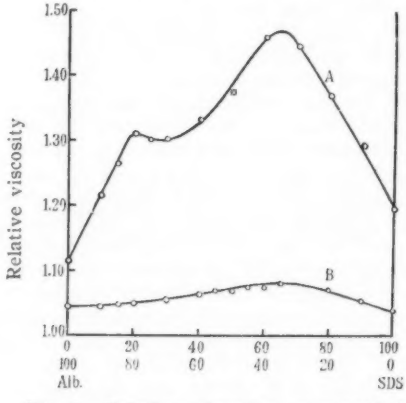

Fig. 5. Relative viscosity, compared to the buffer solution, of the system egg albumin-SDS at pH 6.8 and ionic strength 0.1. A: Total concentration 4.0%. B: Total concentration 1.0%. 25±0.01°C.

with that of the buffer solution) and the mixing ratio, the total concentration being kept at 4.0%. We can see that there are two maxima at points where albumin/SDS=80/20 and 35/65.

The compositions at these maxima are equal to those which divide the electrophoretic results into three groups.

Electrophoretic Patterns at Various pH's.—Similar experiments as above were carried out at a total concentration 1.0%, and at pH 5.4, 7.6, 9.6, 9.9 and 10.8.

At each pH the electrophoretic patterns change with the mixing ratio in a similar manner as when pH is 6.8, but in the region of albumin excess, there is a slight change in values of the mixing ratio at which the albumin boundary disappears. The number of SDS molecule bound to one molecule of egg albumin at this mixing ratio increases from 40 to about 50 with the increase of pH. Curve B in Fig. 4 shows the relation between pH and the number of bound SDS to one egg albumin molecule.

Comparing curves A and B in Fig. 4, we can see that below pH 7 the number of positive charges of one egg albumin is almost equal to the number of SDS molecules which are bound to one egg albumin molecule. In this region it is possible to assume that one positive charge on egg albumin and one negative detergent ion combine electrostatically as described above, but when pH is above 7 this relation cannot hold. The cause of this is not made clear in this study alone. In the experiment at different pH from 6.8, in the region of SDS excess, SDS boundary disappears when the mixing ratio albumin/SDS is between 35/65 and 30/70.

Mechanism of the Combination of Egg Albumin and SDS.—Now we compare the next two electrophoretic patterns with each other: the one obtained on the sample pH 6.8, μ 0.1, albumin/SDS=95/5 and the total concentration 1.0%, and the other pH 6.8, μ 0.1, albumin/SDS=95/5 and the total concentration 0.5%. We can find that the shapes of the patterns are identical, although the areas covered by the corresponding boundaries are unequal. In addition, as seen in Fig. 5a in Part I[1], the CMC of SDS is 0.04% (0.0013 mol./l.) when the ionic strength is 0.1, so that in the first sample the micellar SDS exists, but in the second sample SDS exists as a single ion not forming a micelle. Considering these facts we can find in the reaction between egg albumin and SDS that it is not reasonable to assume that SDS reacts only in a micellar form, and that it is reasonable to assume that a single ion, not forming a micelle, can react.

Summary

We studied electrophoretically the interaction of SDS and egg albumin in the pH range between 5.4 and 10.8, higher pH's than that of the isoelectric point of egg albumin. Results obtained are as follows.

(1) The electrophoretic patterns of the system egg albumin-SDS can be divided into three groups. This method of division is different from that in the system SDS-horse serum albumin by Putnam and Neurath. The first group of the division contains the patterns obtained when the mixing ratio albumin/SDS is between 100/0 and 80/20, and here the complex AD_n (n=40, A: albumin, D: detergent) and egg albumin coexist. The second group contains the patterns obtained when the mixing ratio albumin/SDS is between 80/20 and 35/65 and in this region the composition of the complex changes continuously from AD_n to AD_{8n}. The third region appears when the mixing ratio albumin/SDS is between 35/65 and 0/100 and here the complex AD_{8n} and SDS coexist. The above mixing ratio values are obtained at pH 6.8, and they change somewhat as a function of pH.

(2) Below pH 7, a number n of the first complex AD_n equals the number of positive charges on one egg albumin, but above pH 7, this relation cannot hold.

(3) In the reaction between egg albumin and SDS, it is not assumed that SDS reacts only in a micellar form but that SDS existing as a single ion can react.

The author is sincerely greateful to Professor Rempei Goto of the Institute for Chemical Research, Kyoto University for his kind guidance during this study.

Chemical Laboratory, Nagoya City University, Nagoya

On the Base Strength of Some Nitrogen Heterocycles in the Excited State

By Noboru MATAGA, Yozo KAIFU and Masao KOIZUMI

(Received October 27, 1955)

Introduction

Some properties of a molecule such as basicity and acidity or its ability of dydrogen bonding etc., depend in general upon its electronic structure. Therefore, it may be expected that the above-mentioned properties in the excited electronic state are different as compared with the ground electronic state, and we really have such examples.

Th. Förster and A. Weller[1,2] have investigated the ionization tendency of naphthols, aminopyrene derivatives, etc. in their excited electronic states by measuring the fluorescene spectra and fluorescene intensities and confirmed that the degree of dissociation in the excited state is far greater than that in the ground state. Hence these compounds can be said to have a greater acidity in the excited state than in the ground state. As for hydrogen bonding, the present authors[3] have measured the absorption and fluorescence spectra and fluorescene intensities of *n*-hexane solutions of naphthols with addition of various proton acceptors, and found that the excited naphthols have a greater tendency to form hydrogen bond and that a new equilibrium is reached during the lifetime of the excited state.

Now in order to compare the basicity of a molecule in the ground and excited state, same nitrogen heterocycles such as quinoline, acridine and 2,8-diaminoacridine were chosen and their fluorescene and absorption spectra were measured over a wide pH range. In addition their spectra and fluorescene intensities in various organic solvents were compared. The present paper reports the results obtained with some discussions about the electronic structures of these molecules.

Experimental

Apparatus.—Fluorescene spectra were taken with Hilger E_2 type quartz spectrograph and small type glass prism spectrograph. For the excitation of fluorescene spectra, a high-pressure mercury lamp was used with appropriate filters for each samples.

Filters: for quinoline, K_2CrO_3 aq. solution (0.2 g./l.) which takes out 310 mμ line.

for acridine, Matsuda color filter UV-DI which takes out 360 mμ line.

for 2,8-diaminoacridine, Matsuda color filter UV-DI, which takes out 360 mμ or VC-I and IR-OI which together take out 405 and 435 mμ lines.

For the measurement of absorption spectra in solution, Beckman spectrophotometer model DU was used.

The apparatus used for the measurement of fluorescence intensity was the same as described elsewhere.* In the case of quinoline, the filters used were the same as before*, and in the case of acridine, Matsuda color filter UV-DI was used for exciting light and the solution of acridine in *n*-hexane, ca. 10^{-3} mol./l., was used as a filter for the fluorescent light.

Reagent.—Extra pure grade quinoline was dried over K_2CO_3 and distilled under the atmosphere of dry nitrogen before use.

Chemical pure grade acridine was recrystallized from alcohol.

A synthesized and purified sample of 2,8-diaminoacridine was kindly supplied by Mr. T. Tokuyama of this institute.

For the pH control of aqueous solution, citrate-phosphate-borate buffer was used. The reagents were of extra pure grade, and were used without further purification.

n-Hexane, CH_3CO_2Bu and CCl_4 were the same samples as described elswhere*. Extra pure grade benzene was recrystallized and distilled. Ethanol used was 99% in purity.

Extra pure grade *n*-butanol and pyridine were used without further purification.

Experimental Results

a) Dependence of the Absorption and Fluorescence on the Hydrogen Ion Concentration in Aqueous Solution

The absorption spectra of quinoline in aqueous solution of various pH values are shown in Fig. 2.

Quinoline being isoelectronic with naphthalene, its absorption spectrum is similar to that of the latter, with three absorption regions in the near ultraviolet; 295–320 mμ (band I), 250–295 mμ (band II) and the region

1) Th. Förster, *Z. Elektrochem.*, **54**, 42, 531 (1950).
2) A. Weller, *Z. Elektrochem.*, **56**, 662 (1952); *Z. physikal. Chem. N.F.*, 3, 238 (1955).
3) N. Mataga, Y. Kaifu and M. Koizumi; *Nature*, **175**, 731 (1955).

* N. Mataga, Y. Kaifu and M. Koizumi; to be published in this Bulletin.

near 220 mμ (band III). The absorption spectra in the pH range <1.4 and >8 coincide with the curve (1) and (6) respectively, and between ca. pH=7 and 2, they gradually change with isosbestic point at ca. 290 mμ. Therefore this spectral change can be attributed to the change of the concentration of free quinoline (A) and quinolinium ion (AH^+), according to the equilibrium relation $A+H^+ \rightleftharpoons AH^+$. pK value is easily obtained from the inspection of these changes, and is depicted in Fig. 1 as a pH value at which [A]=[AH^+].

It is seen from Fig. 2 that in A the intensity of band I is rather smaller than that of band II, while in AH^+, the former becomes far greater, and the latter is diminished. It is noteworthy that λ_{max} of band I remains constant throughout the whole change, though in AH^+ there appears a slight hump in the neighbourhood of 330 mμ. The fluorescene spectrum shifts from 305–350 mμ band of A to 340–440 mμ band of AH^+ as indicated in Table I, but the change occurs at larger pH value compared with that of absorption spectrum. The line depicted in Fig. 1 is the pH value at about the middle point of the region in which the spectral change occurs.

TABLE I

RANGE OF FLUORESCENCE SPECTRA OF A, AH^+, AH_2^{++} AND AH_3^{+++} (in mμ)

	A	AH^+	AH_2^{++}	AH^{3+++}
Quinoline	305–350	340–440	——	——
Acridine	390–500	390–600	——	——
2,8-Diaminoacridine	——	450–610	505–610	420–610

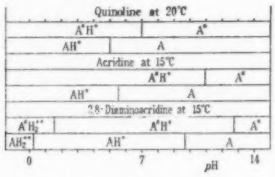

Fig. 1. Shift of the equilibrium in the excited state as revealed by the change of fluorescence and absorption spectra.

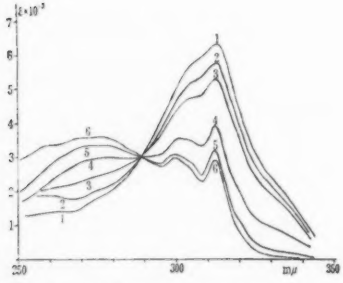

Fig. 2. pH Dependence of the absorption spectrum of quinoline in aqueous solution. at ca. 20°C
concentration of quinoline, 1.08 ×10⁻⁴ mol./l.
pH: 1. 1.42
2. 4.45
3. 4.89
4. 5.59
5. 6.47
6. 8.04

ii) Acridine.—The absorption spectrum of acridine is similar to that of isoelectronic anthracene, and there are 300–400 mμ band (Band I) and the band near 250 mμ (band II)*.

pK value or pH value at which [A]=[AH^+] is ca. 5 as shown in Fig. 3. The intensity of band I is stronger in AH^+ than in A and the position of maximum remains constant throughout the whole pH range. In the acidic solution, a new broad band appears in the region 380–440 mμ, and two isosbestic points are seen at 360 mμ and 377 mμ. λ_{max} of band II (249 mμ) in A shifts to 254 mμ in AH^+ with the intensity somewhat decreased.

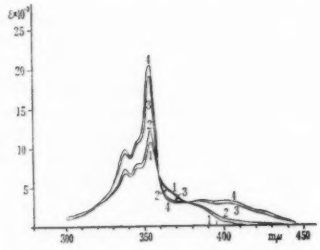

Fig. 3. pH Dependence of the absorption spectrum of acridine in aqueous solution. at ca. 15°C
concentration of acridine, 5.78 ×10⁻⁵ mol./l.
pH: 1. <8.04
2. 6.47
3. 4.88
4. >3.69

The fluorescence spectrum are shown in Fig. 4. At first sight, it appears as if there are two steps of change, i.e. at pH=ca. 10

* The nomenclature in this case is rather conventional.

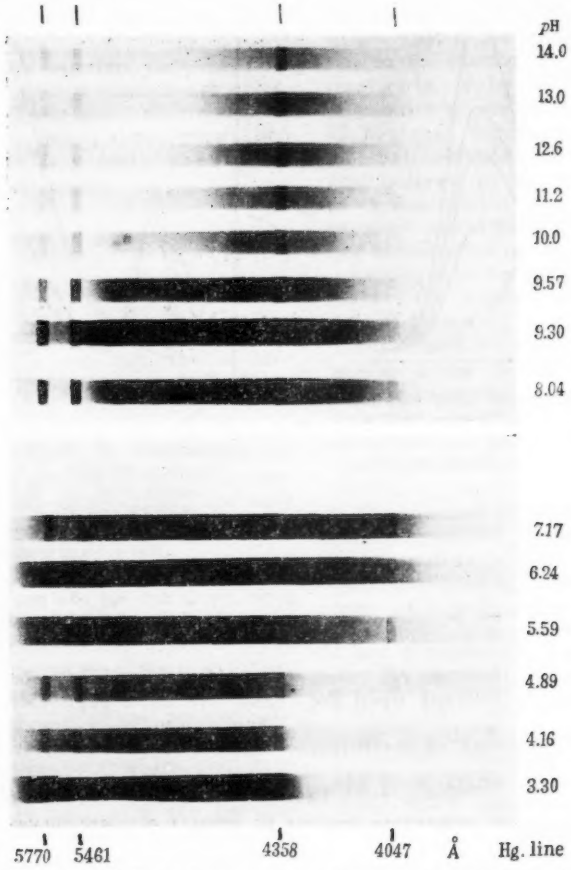

Fig. 4. pH Dependence of the fluorescence spectrum of acridine in aqueous solution, at ca. 15°C.

and pH=ca. 5. But the latter change is most probably attributed to the reabsorption of fluorescence by 380–440 mμ band, which is prominent when pH<5. It seems that the change of colour in the fluorescence of acridine cited in Pringsheims' book[4] corresponds to this apparent change. There scarcely remains any doubt that the real change of fluorescence spectrum occurs at far greater pH value compared with that of absorption spectrum.

iii) 2, 8-Diaminoacridine.—This molecule has three nitrogen atoms each of which may act as a proton acceptor. Accordingly, the spectral changes seem to occur in three stages. As indicated by Craig et al.[5], the first proton may attach to the ring nitrogen. In this first stage, the spectrum shows a marked change as shown in Fig. 5a. The spectrum shifts to longer wave length from $\lambda_{max}=395$ mμ to $\lambda_{max}=443$ mμ with the isosbestic point at 410 mμ, and the absorption intensity increase remarkably.

The change of fluorescence spectrum in the first stage occurs at far greater pH value than that of absorption spectrum as shown in Fig. 1. The two succeeding stages are not so clear-cut as the first one, but the following features may be observed from Fig. 5b. In the second stage, there appear two peaks at 455 mμ and 360 mμ with two isosbestic points at 470 mμ and 370 mμ, and the change of fluorescence spectrum occurs at larger pH value. In the third stage the band at 360 mμ and 455 mμ decline and a new band appears at 350 mμ. In this case,

4) P. Pringsheim, "Fluorescence and Phosphorescence" Interscience Publishers Inc., 1949, p. 416.

5) D.P. Craig and L.N. Short, *J. Chem. Soc.*, 1945, 419.

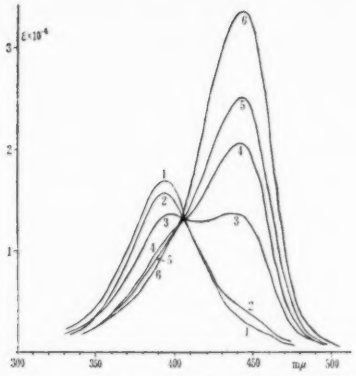

Fig 5a. pH Dependence of the absorption spectrum of 2,8-diaminoacridine in aqueous solution, at 15°C
concentration of 2,8-diaminoacridine, 1.28×10^{-5} mol./l.
pH: 1. 13~12
2. 11.24
3. 10.06
4. 9.57
5. 9.30
6. 4.89~1.92

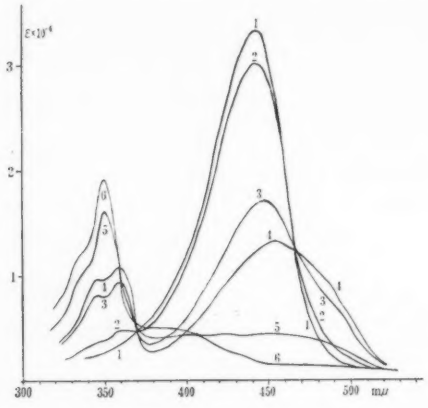

Fig. 5b. pH Dependence of the absorption spectrum of 2,8-diaminoacridine in aqueous solution, at ca. 15°C
concentration of 2,8 diaminoacridine, 1.28×10^{-5} mol./l.
1. pH 1.925
2. pH 1.038
3. pH O.
4. 3.6 N H_2SO_4
5. 12.6 N H_2SO_4
6. 18 N H_2SO_4

the spectral change of fluorescence and absorption occur almost at the same pH value.

b) Effect of Organic Solvent upon the Spectrum

In Table II the variations of absorption spectra in several solvents are indicated. When the solvent molecule increases in its proton-donating power from *n*-hexane to ethanol, band I grows and band II declines regularly in the case of quinoline, and in the case of acridine 373 mμ band becomes broader and the band edge shifts to longer wave length also in a regular manner. These changes conform completely to the already mentioned changes induced by the proton addition. Thus the parallelism exists between the spectral change induced by proton addition and that induced by the hydrogen bonding.

TABLE II

CHANGE OF ABSORPTION SPECTRA IN SEVERAL ORGANIC SOLVENTS

Quinoline

Solvent		*n*-Hexane	CCl_4	CH_3CO_2Bu	BuOH	EtOH
Extinction coeff. of abs. max. ($\times10^3$)	band I	2.1	2.3	2.1	2.8	3.0
	band II	3.6	4.1	3.6	3.4	3.3

Acridine

Solvent	*n*-Hexane	Benzene	Pyridine	BuOH	EtOH
Edge of the longest wave length band	392	393	395	397	402
			(in mμ)		

TABLE III

EFFECT OF SOLVENT ON THE FLUORESCENCE INTENSITY

Solvent	*n*-Hexane	Benzene	BuOH	EtOH	H_2O
Quinoline	$\lesssim10^{-3}$	$\sim10^{-3}$	$\sim3\times10^{-2}$	$\sim3\times10^{-2}$	~1.0 (pH 4.79)*
Acridine	——§	$\sim10^{-3}$	$\sim2\times10^{-2}$	$\sim3\times10^{-2}$	~1.0 (pH 6.30)*

* pH was not controlled by buffer, and measured by glass electrode pH meter.

§ Fluorescence was not detectable with our apparatus.

c) Effect of Solvent upon the Fluorescence Intensity

In Table III the relative yield of fluorescence in quinoline and acridine are given. The data in this Table were determined in the following way. When the concentration of a fluorescer is very small, the relation $I_f = \varepsilon c \Phi I_o$ must hold, where,

I_f ; Fluorescence intensity
Φ ; Quantum yield of fluorescence
ε ; Extinction coefficient at the exciting wave length
c ; Concentration of fluorescer
I_o ; Intensity of exciting light

Hence when I_o is constant, the relative yield is easily calculated from $\Phi'/\Phi = I'_f \varepsilon c / I_f \varepsilon' c'$.

As seen from Table III, the fluorescence yields in the solvents such as *n*-hexane and benzene which are not able to make hydrogen bond with nitrogen heterocycles, are only 10% or smaller compared with those in the solvents such as BuOH or EtOH.

The fluorescence intensity of AH^+ in aqueous solution can not be compared with those data, because the spectral range of fluorescence is considerably different (For quinoline, in *n*-hexane; 305–350 mμ, in EtOH; 305–370 mμ against 340–440 mμ of AH^+. For acridine in EtOH; 360–480 mμ against 450–610 mμ of AH^+) and the exact calibration of the wave length sensitivity of the phototube was not undertaken. It is certain, however that the sensitivity falls with the increase of wave length*, and if one takes this into account, the fluorescence yield of AH^+ is expected to be far greater than the fluorescence yield of A in organic solvents. In the case of 2,8-diaminoacridine, however, fairly strong fluorescence is observed even in the non-polar solvent such as benzene, and the hydrogen bond formation or proton addition is not necessarily indispensable for the fluorescent transition.

Discussion

I. The Increase of the Basicity in the Excited State

It can be concluded from the experimental results, that in these nitrogen heterocycles the excited electronic structure is more liable to proton addition than the ground state electronic structure. Thus the stabilization energy by proton addition is larger in the excited state than in the ground state. As Förster and his collaborators have confirmed, naphthols and some other compounds have greater acidity in the excited state, while in the present investigation, it has been confirmed that N-heterocycles have larger basicity in the excited state. Both effects will most certainly be attributed to the increase of polarity in the excited state. In the case of naphthol, for example, the migration of lone pair electrons of oxygen atom to the ring is larger in the excited state, the result of which makes the oxygen atom more repulsive toward proton. Nitrogen atom in the heterocycles on the contrary, will become more negative in the excited state and this makes the excited state more attractive toward proton.

The increase of electronegativity of N atom in the latter case will be interpreted in various ways but here the problem will be discussed on the basis of the electronic structures of cata-condensed hydrocarbons which are isoelectronic to their aza derivatives.

The so-called cata-condensed hydrocarbons generally exhibit three main band systems in the near ultraviolet or visible region of the spectrum. The prototypes of all these systems are to be found in benzene, which shows a weak band system in the 2500 Å region, exhibits absorption of moderate intensity around 2000 Å, and absorbs strongly near 1750 Å. Band systems of a similar type also occur for the higher homologs. According to Moffitt's notation[6], these are N→V, N→U and N→Y transitions, respectively. Among these, N→Y transition corresponds to the so-called "intramolecular charge transfer spectrum" of Mulliken[7]. From the standpoint of VB method, Y state is mainly contributed by ionic structures.

Now in the case of inductive substitution such as the replacement of —CH= by —N=, the effect of this perturbation is to mix the unperturbed V state to which transition from the ground state is virtually forbidden, with some contribution from Y state to which transition is strongly allowed. The result is that the partial transfer of intensity from N→Y transition to N→V transition occurs as is actually confirmed by the comparison of the absorption spectra of N-heterocycles and of their isoelectronic cata-condensed hydrocarbons. V state thus acquires considerable ionic character with negative charge at nitrogen atom, and this is the reason why the interaction energy with proton is larger in the excited state than in the ground state.

The intensification of the spectrum in the acidic region as observed in acridine, may

* The phototube used is ultraviolet sensitive one.

6) W. Moffitt, *J. Chem. Phys.*, **22**, 320 (1954).
7) R.S. Mulliken, *J. Chem. Phys.*, **7**, 20, 353 (1939).

be attributed to the further increase of such a polar structure since the electronegativity of N becomes larger by the attachment of a proton. But the conspicuous change of spectra in the case of quinoline and 2,8-diaminoacridine can not yet be interpreted.*

II. Solvent Effect on Fluorescence Intensity

It is almost certain that in the case of acridine and quinoline, the settlement of non-bonding electrons by proton addition or hydrogen bonding increases the fluorescence efficiency. The mechanism may presumably be interpreted in the following way.

In these compounds, $^1\Gamma_{\pi\to\pi^*}$ which is produced directly by the illumination has probably a large tendency of transfer to $^1\Gamma_{n\to\pi^*}$, because the authors have newly found the spectra of quinoline due to $n\to\pi^*$ transition and moreover, their positions are in the neighbourhood of $\pi\to\pi^*$ band (see Appendix).

If $^1\Gamma_{n\to\pi^*}\to{}^1\Gamma_{n\to\pi^*}$ transfer occurs, then it is followed by $^1\Gamma_{n\to\pi^*}\to{}^3\Gamma_{n\to\pi^*}$ with considerable ease[8]. Then owing to the long life of $^3\Gamma_{n\to\pi^*}$ state, emission is scarcely to be expected. This may be the reason why the fluorescence is not observed in non polar solvents. By proton addition or hydrogen bonding, however, the non-bonding character is lost almost completely or to some extent and the level of $^1\Gamma_{n\to\pi^*}$ state is raised remarkably. Accordingly, it becomes quite difficult for $^1\Gamma_{n\to\pi^*}\to{}^1\Gamma_{n\to\pi^*}$ transition to occur and the result is that the molecule emits more easily.

In the case of 2,8-diaminoacridine, the reasonance interaction between π-electron system and substituent-NH_2, makes $n\to\pi^*$ transition shift to blue, while $\pi\to\pi^*$ transition to red[9]. As the result of this perturbation, $^1\Gamma_{\pi\to\pi^*}\to{}^1\Gamma_{n\to\pi^*}$ transition becomes energetically difficult. This will be the reason why the fluorescence of 2,8-diaminoacridine can be observed even in the non-polar solvent.

Appendix

$n\to\pi^*$ Spectrum of Quinoline Vapor

The absorption spectrum of quinoline vapor was photographed by Hilger E_2 type quartz spectrograph. The quartz absorption cell was 50 cm. in length with a side tube for reserving sample. As a light source an A. C. high voltage hydrogen discharge tube with water cooling was used. The temperature of bath was 90°C and that of absorption cell was 95°C. The slit width was 0.05 mm. and the time of exposure was about 2 min.

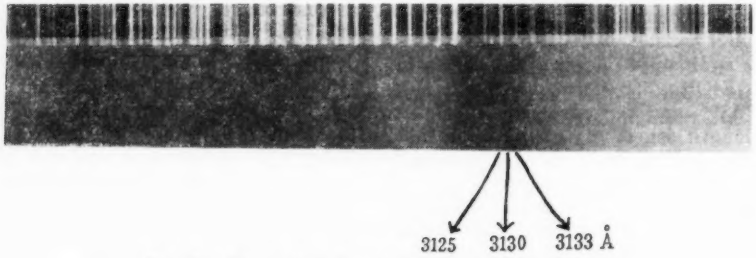

Fig. 6. Absorption spectrum of quinoline vapor.

As seen from Fig. 6, the line spectra at 3125, 3130 and 3133 Å are clearly observed, and these line spectra may most certainly be interpreted as due to the $n\to\pi^*$ transition.

In general, when molecule becomes larger, $\pi\to\pi^*$ transition becomes superposed by strong $\pi\to\pi^*$ transition[10], and moreover the oscillator strength of $n\to\pi$ transition becomes smaller[9]. Hence the observation of $n\to\pi^*$ transition is difficult in larger molecules. In fact the $n\to\pi^*$ transition of pyridine has been reported in literature, while that of quinoline has not been observed as yet, and we really had much difficulty in taking the line spectra in question.

In solution, the $n\to\pi^*$ spectra can never be observed even in *n*-hexane. It is certain from these line spectra, that $n\to\pi^*$ state of quinoline is nearly at the same energy level with $\pi\to\pi^*$ state.

* Note added in prof:
An alternative interpretations of these spectral changes are as follows. We divide the 300-400 mμ band of acridine into two parts, i.e., 300-370 mμ band (band I) and 370-400 mμ band (band II), and regard these bands as corresponding ones to N→V and N→U band, resqectively. In quinoline, the assignment is; band I←→N→V, band II←→N→U. By proton addition, band II of acridine shifts to red and somewhat strengthened, whereas band I does not shift although it is enhanced. The spectral changes of quinoline are similar to those of acridine, but in the case of quinoline, the shift of band II is very great, and the slight hump near 330 mμ may be attributable to this shifted band II. Moreover, the longest wave length band of 2,8-diaminoacridine may plausibly correspond to N→U transition, shifted to red by resonance interaction with substituent amino groups.

8) M. Kasha, *Discuss. Farad. Soc.*, No. 9, 14 (1950).

9) L. Goodman and H. Shull, *J. Chem. Phys.*, 22, 1138 (1954).

10) J.R. Platt, *J. Chem. Phys.*, **19**, 101 (1951).

Summary

1. The fluorescence and absorption spectra of aqueous solutions of quinoline, acridine and 2,8-diaminoacridine were observed at various pH values, and it became clear that the stabilization energy by proton addition is larger in the excited state than in the ground state.

2. The effects of hydrogen bonding and proton addition upon the spectra were confirmed to be the same in tendency.

3. On the basis of the fluorescence intensities in various organic solvents, some discussions were made about the contribution of non-bonding electron to the inner quenching of fluorescence.

4. The vapor spectrum of quinoline was taken and line spectra were observed, which are most certainly attributable to $n \rightarrow \pi^*$ transition.

The Institute of Polytechnics
Osaka City University
Osaka

Geochemical Investigations of Volcanoes in Japan. XXXII. Residual Magmatic Waters in Cavities of Trachyandesitic Basalt in Imari District, Saga Prefecture, Japan*

By Iwaji IWASAKI, Nobuhide KOKUBU and Takashi KATSURA

(Received September 16, 1955)

Introduction

It is of high importance to understand the nature of water and other volatile components in magmas for the study of many important phenomena such as the nature of the primary hot springs, the primary atmosphere, the primary hydrosphere, magmatic differentiation, ore deposits, etc. But our knowledge of the nature of the magmatic substances is very scanty. Although many reports[1] related to the magmatic water have been published, the most part of these works is only the survey of the nature of the magmatic waters and gases. There have been only a few reports[2] on the relation between the real magmatic waters and these geochemical phenomena from the geochemical point of view.

In the previous paper[3] one of the present authors (Iwasaki) has given the definition of the real magmatic state that we can see on the surface of the Earth's crust, and in the present paper this definition described in the following paragraph was also adopted.

The real magmatic state near the surface of the Earth's crust can be defined as natural molten state of the rock-forming material such as molten lavas at lava lake of Volcano Kilauea in Hawaii and Volcano Mihara, Oo-sima, Idu in Japan[3]. Substances derived directly from these rock-forming materials in the real magmatic state can be called the magmetic substances, and the waters derived directly from these magmatic substances can be also called the magmatic waters. By this definition, the waters contained in these natural rock-forming minerals of igneous rocks are no doubt magmatic, but all of them are not always juvenile, because the molten rock-forming material may come from the resulting substances, some of which can be already solidified on the surface of the Earth before the introduction of them into the magmatic chemical system by remelting, assimilation or migmatization.

According to the theory of the magmatic

* XXXI; *J. Chem. Soc. Japan*, **76**, 1116 (1955).

1) H. Davy, *Phil. Trans.*, II, 367 (1822); *Ann, Chim. et Phys.*, **21**, 132 (1822); D. Brewster, *Trans. Roy. Soc. Edinburgh*, **10**, 1 (1826); R.T. Simmler, *Pogg. Ann.*, **105**, 460 (1858); H.C. Sorby, *Geol. Soc. London Quart. Journ.*, **14**, 453 (1858); A.W. Wright, *Am. J. Sci.*, **21**, 209 (1881); W. Ramsay, *Proc. Roy. Soc.*, **58**, 65 (1895); A. Gautier, *Compt. rend.*, **132**, 58, 189 (1901); *Econ. Geol.*, **1**, 688 (1906); R.T. Chemberlin, "The Gases in Rocks", (1908); A. Brun, "Recherches sur L'Exhalaison Volcanique", (1911); A. L. Day and E. S. Shepherd, *Bull. Geol. Soc. Am.*, **24**, 573 (1913); E.S. Shepherd, *Am. J. Sci.*, **35** A, 311 (1938); J. Jaggar, ibid., **238**, 313 (1940); E.F. Holden, *Am. Mineralogist*, **10**, 203 (1925); W.H. Newhous, *Econ. Geol.*, **27**, 419 (1932); **28**, 744 (1933); S.T. Yuster, *Am. J. Sci.*, 5 ser. **31**, 363 (1936); E. Ingerson, *Am. Mineralogist*, **32**, 375 (1947); P.A. Peach, ibid., **34**, 413 (1949); H.S. Scott, *Econ. Geol.*, **43**, 637 (1948).

2) S. Tsuboi, K. Sugawara and S. Oana, *Science* (*Kagaku*), **14**, 102 (1944); K. Sugawara, S. Oana and T. Koyama, *Proc. Imp. Acad. Tokyo*, **20**, No. 10, 721 (1944); *Proc. Japan Acad.*, **25**, No. 3, 103 (1949).

3) I. Iwasaki, *Journ. of Grography* (Japan), **60**, 140 (1951).

differentiation by N. L. Bowen[4] and V. M. Goldschmidt[5], along with lowering of temperature fractional crystallizations of magmas take place with a separation of solids and mother liquors or residual magmas, and the aqueous magmatic solutions derived from the volatile components of magmas will remain when most of the parts of rock-forming silicate minerals have crystallized out from the magmas and the temperature of the residual magmas is lowered below the critical point of water (374.3°C, 217.7 atm.). These aqueous magmatic solutions which remained in the cavities of igneous rocks and rock-forming minerals as liquid inclusions, etc. can be called the residual magmatic water.

From these points of view the present authors have distinguished the magmatic waters obtained directly from the molten magmatic substances such as molten lavas from the residual magmatic waters which remained in the cavities of their mother igneous rocks and minerals. In the present paper some of the results obtained on the residual magmatic waters from trachyandesitic basalt in Imari district which has been found by K. Muta, Geological Institute, Faculty of Engineering, Kyushu University, in 1948, and the related problems are reported.

line, Kuhara, Saga Prefecture as shown in Fig. 1. These rocks have higher alkali contents than the volcanic rocks in the Fuji Volcanic Zone as will be seen in Table I, and lots of amygdaloidal cavities, some of which are filled with mineral substances mainly carbonate and silicate minerals; some are empty and some have mineral substances and aqueous solutions.

Fig. 1. Locality map.

TABLE I

CHEMICAL COMPOSITION OF VOLCANIC ROCKS FROM IMARI DISTRICT, NAGAHAMA, HAMADA-SI, SIMANE PREFECTURE AND THE FUJI VOLCANIC ZONE

	Imari District				Hamada Nephline-basalt	Fuji Volcanic Zone	
	No. 1	No. 2	No. 3	No. 4			
SiO_2	48.87	50.46	54.90	56.17	34.98	49.60	54.66
TiO_2	1.24	2.12	1.94	1.00	2.39	1.40	1.10
Al_2O_3	16.00	18.41	17.38	16.83	11.18	16.96	17.91
Fe_2O_3	5.52	2.10	1.35	1.62	5.99	5.40	1.92
FeO	5.16	7.08	5.66	5.43	8.83	6.65	6.26
MnO	0.21	0.29	0.15	0.14	0.26	0.21	0.18
MgO	8.66	4.03	4.46	2.83	8.36	5.92	5.45
CaO	8.97	7.11	7.25	6.98	13.52	10.03	8.42
Na_2O	2.75	3.35	3.04	4.18	4.22	2.48	2.89
K_2O	0.86	1.28	0.84	1.17	3.99	0.58	0.42
H_2O	2.04	3.70	2.63	4.55	3.63	0.62	1.04
P_2O_5	n.d.	n.d.	n.d.	n.d.	2.53	0.20	0.10
S	n.d.	n.d.	n.d.	n.d.	0.10	n.d.	n.d.
Cl	0.015	n.d.	0.012	0.029	0.013	n.d.	0.010
Total	100.29	99.93	99.71	100.93	100.01	100.05	100.49

Occurrence and the Nature of Mother Rocks and their Cavities

The trachyandesitic basalts in question are distributed in hill country running close to the south of a railway-station of the Matuura-

According to Dr. H. Kuno, Geological Institute, Faculty of Science, Tokyo University, these trachyandesitic basalts have intergranular texture and holocrystalline structure, and a relatively small amount of phenocrysts (olivine, titaniferous augite, etc.) in the groundmass, in which labradorite, potash-andesine, olivine and augite are seen. And also in the druses of these rocks, calcite, aragonite, siderite and ankerite are seen.

These rocks show a remarkably heterogeneous appearance; for instance in some

4) N.L. Bowen., "The Evolution of the Igneous Rocks", (1928).
5) V.M. Goldschmidt, *Z. Elektrochem.*, 28, 411 (1922).

parts of the mother rocks many cavities are clustered, but few cavities in the other parts. The size of these cavities varies from extremely small to about 10 cm. long, and these cavities are irregularly distributed in their mother rocks. There seems to be no remarkable regularity among their distribution of their sizes, number and inclusions (minerals, solutions and gases). The nature of these cavities in their mother rocks from Imari district closely resembles that of nepheline-basalts from Nagahama, Hamada-si Simane Prefecture, but there are some distinct differences between the properties of these two volcanic rocks. The cavities of nepheline-basalt are lined by zeolite (often bearing a smaller amount of calcite crystals), and the great part of larger cavities have irregularly angular form. On the other hand the forms of the cavities in trachyandesitic basalts are smoothly amygdaloidal, and in them the carbonate minerals such as calcite, aragonite and siderite are remarkably abundant. From the facts mentioned above, it seems that the rocks in Imari district have not been subjected to so large a pressure that their amygdaloidal cavities had changed their forms during their solidification as in the case of nepheline-basalt from Nagahama district, and are, therefore, more suitable to be used in the study of the nature of the magmatic substances.

The locations from which the samples for the chemical analysis were collected, are also shown in Fig. 1. The chemical compositions of the minerals co-existing with magmatic waters in the cavities are also shown in Table II. For example, one of the modes of occurence of these minerals is shown in Fig. 2. The number in Fig. 2. is the same as Table II.

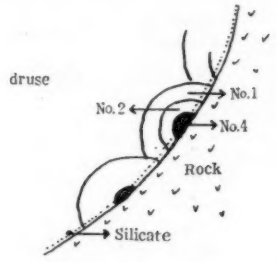

Fig. 2. The mode of occurrence of these minerals in the cavities of rocks.

Chemical Composition of the Residual Magmatic Solutions

Although it has already been found by Sugawara et al.[2] that each chemical composition of the inclusion waters from various cavities in nepheline-basalt in Hamada district varies remarkably each others, we are obliged to study the mixed sample from several cavities, because we cannot collect a sufficient amount of waters from only a single cavity for the complete chemical analysis on account of the nature of their occurrence. But some of the ingredients of these solutions, such as pH, Cl^-, NO_3^-, NO_2^-, NH_4^+, are determined for each cavity as shown in Table III.

As pH values in Table III were measured by pH test paper (B. T. B.), these values are not exact as already mentioned in the previous papers[1], but we can guess the outline of the properties of the waters and their variation from these so-called pH values.

TABLE II

CHEMICAL COMPOSITIONS OF THE MINERALS IN THESE CAVITIES

	Calcite ⟷ Siderite					Silicate	
CO_2	42.57	41.82	26.43	38.88	35.63	—	—
CaO	50.47	49.58	33.84	14.58	1.28	1.82	1.33
MgO	1.17	1.71	2.57	5.84	1.43	11.18	14.15
FeO	2.56	3.83	22.28	36.23	58.19	1.88	2.39
Fe_2O_3	0.31	1.44	2.33	3.06	1.41	14.93	13.26
MnO	1.68	1.47	7.05	0.73	0.76	0.32	0.62
SiO_2	—	—	2.52	—	—	41.02	44.13
Al_2O_3	—	—	1.76	0.38	0.51	2.89	0.60
H_2O (−)	—	—	—	—	—	20.53	18.04
H_2O (+)	—	—	—	—	—	6.19	5.63
P_2O_5	—	—	—	—	—	0.12	0.06
Cl	—	—	—	—	—	0.002	0.002
Total	98.76	99.85	98.78	99.70	99.21	100.88	100.21

6) I. Iwasaki, "Geochemistry", in "Chemical Experiments", (1941) II, Vol. 12, 1; I. Iwasaki, M. Ieyosi, *J. Chem. Soc. Japan*, **64**, 1456 (1943); I. Iwasaki, *Japan Analyst*, **1**, 175 (1952).

TABLE III

CHEMICAL COMPOSITION OF THE RESIDUAL MAGMATIC WATER IN THE CAVITIES OF TRACHYANDESITIC BASALT FROM IMARI DISTRICT

Sample	Date of sampling	Location	Amount collected (g.)	pH	Cl (mg./l.)	NH_4 (mg./l.)	NO_2 (mg./l.)	NO_3 (mg./l.)
M	Aug. 1948	Kusuku	0.4594	—	76	71.2	—	—
A1	Mar. 1949	〃	—	7.0	—	—	—	—
A2	〃 〃	〃	—	6.6	—	—	—	—
A3	〃 〃	〃	0.4789	6.9	7.2	40.5	0.8	0.2
A4	〃 〃	〃	0.4135	6.7	5.8	61.6	0.4	0.4
A6	〃 〃	〃	—	6.4	—	—	—	—
A8	〃 〃	〃	—	6.6	—	—	—	—
1	Oct. 1949	Kuhara	—	6.6	—	—	—	—
2	〃 〃	〃	—	6.8	—	—	—	—
3	〃 〃	〃	0.3934	6.8	9.0	66.7	0.3	0.3
4	〃 〃	〃		6.8				
B1a	〃 〃	Kusuku	0.8209	6.0	29.2	11.4	0.4	0.2
B1b	〃 〃	〃	1.1465	〃	12.5	15.9	0.2	0.6
B1c	〃 〃	〃	0.1896	〃	4.0	72.2	0.3	1.7
B2	〃 〃	〃	0.5834	〃	6.2	10.0	0.2	0.7
B3a	〃 〃	〃	0.9982	〃	7.2	10.1	0.7	0.2
B3b	〃 〃	〃	0.9455	〃	6.6	17.1	0.3	0.3
B3c	〃 〃	〃	1.4472	〃	9.8	4.7	0.04	0.2
River water	〃 〃	〃	—	6.8	3.7	0.8	0.8	—
K	Nov. 1950	〃	100 cc.	7.0	10.1	0.63	0.005	0.033
River water	〃 〃	〃	—	6.7	9.1	0.096	0.000	0.030

TABLE IV

CHEMICAL COMPOSITION OF NATURAL WATERS FROM VARIOUS ORIGINS

	Residual magmatic waters			River water	Sea water+
	Imari (mg./l.) (K)	Hamada (mg./l.) (1)	(2)	Imari (mg./l.)	(mg./kg.)
pH	7.0	5.6	3.6	6.7	7.5–8.8
Evaporation residue	280	—	—	—	35,500
Na	30.2	139	491	48.4	10,600
K	29.0	—	120	9.0	380
Ca	126	76	112	10.2	400
Mg	0.0	22	11	0.0	1,300
Fe	0.67	4.1	2.3	0.64	0.002
Al	<0.6	11.	16	<0.6	0.1
NH_4	0.8	0.08	14	0.096	—
Cl	10.1	170	732	9.1	19,000
SO_4	4.2	173	326	3.0	2,600++
NO_3	0.033	4.4	97	0.030	—
NO_2	0.005	21	0.54	0.000	—
SiO_3	—	35	28	—	—

\+ V.M. Goldschmidt, "Geochemistry", (1954) p. 49.

++ Calculated from S=880 mg./kg.

pH values vary from about 6.0 to about 7.2, and the tendency of going to the alkaline side of these values after collection of samples from the mother rocks for location B is perhaps due to the fact that dissolved carbon dioxide escapes from the sample waters when they are exposed to the atmosphere, in which carbon dioxide content is very small as 0.03% (vol.), by crushing the mother rocks. This fact indicates that the waters in the cavities are almost neutral or slightly acidic and absence of the extremely acidic and basic substances, so far as the data tell. And also this fact will easily be understood if they have already reacted completely with the substance around the cavities and have

already attained nearly completely to the equilibrium between them. This nature is quite different from that of the residual magmatic waters in rocks from Hamada district where acidic (pH 3.6; 5.6) and alkaline (pH 8.1) waters were found.

Chlorine content of these waters (4.0–29.2 mg./l.) is very small compared with that (25–1220 mg./l.) of the waters from Hamada district and comparable with that of the river waters near the mother rocks in this district as will be seen in Table IV.

On the contrary, NH_4^+ content of the waters in this district ranging from 0.63 to 66.7 mg./l. seems as a whole to be remarkably higher than that of the waters in Hamada district and the river waters described above.

NO_3^- and NO_2^- content of these waters ranging from 0.005 to 0.8 mg./l. and 0.033 to 1.7 mg./l. respectively are very small compared with that (4.4–97; 0.54–21 mg./l.) of the waters in Hamada district as the case of chlorine content.

As will be seen in Table IV, the concentrations of the other components such as Na, K, Mg, Fe, Al, SO_4, in these waters are remarkably lower than that of the waters from Hamada district. But only the calcium content of these waters is very high compared with that of the other components, and comparable with that of the waters from Hamada district. This nature is also quite different from that of the waters from Hamada district and sea water. It seems to be the corresponding nature that calcium carbonate minerals are very abundant in the cavities of the mother rocks in Imari district.

As will be seen in Tables III and IV, the variation in the chemical compositions of the inclusion waters from each cavity is quite remarkable like that recognized in Hamada district. Consequently we can conclude that these volatile components of magmas are not always collected uniformly in each cavity during the fractional crystallization of magmas depending on their geological environments and the nature of magmas and volatile components. This fact is also recognized from the irregular distribution of the cavities; their inclusions and minerals in their cavities as described above.

Discussion

a) Real Magmatic Waters.—The real magmatic waters defined above have already been obtained from lava lake at Volcano Kilauea in Hawaii by A. L. Day and E. S. Shepherd[1], and at Volcano Mihara, Oo-sima, Idu in Japan by the present authors[3]. In the magmatic waters from lava lake at Volcano Kilauea, a large amounts of many volatile components, such as Na, K, Ca, Fe, Al, Cl, F, Ti, S, are determined together with many volcanic gases such as CO_2, CO, H_2, SO_2. Afterward these results have been confirmed by Shepherd[1] and J. Jaggar[1] in lava lake at Volcano Kilauea and Mauna Loa in Hawaii. From these results we can conclude that all these magmatic waters obtained from lava lakes in Hawaii are of acidic nature. The magmatic waters obtained from lava lake at Volcano Mihara are also strongly acidic as will be seen in Table V.

TABLE V

CHEMICAL COMPOSITION OF THE MAGMATIC WATER OBTAINED FROM LAVA LAKE AT VOLCANO MIHARA, OO-SIMA, IDU, JAPAN

Sample: April 1, 1950.

Acidity	1.4 N
Cl	67.6 g./l.
Total S	0.16 〃
Si	0. 〃
Fe	69.8* 〃
Ca	0. 〃
Mg	0. 〃
Ti	0. 〃
Al	(trace) ?

* Mixed with iron chloride derived from iron tube.

As the temperature of molten lavas in these active lava lakes mentioned above is as high as about 1100°C, a remarkable distillation of the volatile matters in lavas is thought to take place. As a result, many volatile components of magmas (volcanic sublimates) issued in the volcanic gases are dissolved in distillates, magmatic waters, and some of them are hydrolyzed, and these magmatic waters acquire an acidic nature. These facts are already demonstrated by laboratory experiments. For example, when the mixture of sodium chloride and quartz powder is heated with water at about 1000°C, a large amount of hydrogen chloride is distillated with water[7]. Thus, we can understand easily that these magmatic waters have acidic nature, but the chemical composition of these real magmatic waters from different volcanoes, and the same volcano at different times and also different parts of the same lava lake of one volcano at the same time are evidently very dissimilar in appearance depending on the nature of the magmas, especially the surface of the magmas as that volcanic gases in lava lake at Volcano

7) For example, R. Kiyoura and Y. Ito, *J. Ceram. Assoc. Japan*, **60**, 325 (1952).

Kilauea[1] and Volcano Mihara[3,8].

When these magmatic waters spring out directly on the surface of the Earth's crust, they form the primary hot springs, which are consequently of acidic nature, and are thought to be distributed usually in the vicinity of volcanic active centers. On the other hand, when these magmatic gases and waters remain in the cavities of the mother rocks, the acidity of these solutions is decreased gradually by the reactions, with their country rocks either before or after the condensation of these volatile magmatic components into aqueous solutions. Consequently it will easily be understood that all these residual magmatic solutions in the cavities of their mother rocks as found in Hamada and Imari districts are almost all neutral or slightly acidic or slightly alkaline in nature as described above. And when these reactions with their country rocks proceed still more, these waters must gradually become alkaline in nature depending on their nature. And also it will easily be understood that there are many kinds of chemical compositions of magmatic waters depending on time elapsed after separation from their magmas, and the nature of their mother magmas and volatile components and chemical reactions with their country rocks after separation from their magmas.

b) Primary Hot Springs.—The primary hot springs distributed in the vicinity of active volcanic craters as described above are usually of acidic nature. But, needless to say, there are many acidic hot and cold (mineral) springs in the world which are distributed in various places where no relations with volcanic activity can be seen, or in the special places where oxidation process by oxygen in the atmosphere easily takes place owing to the special geological conditions. These acidic mineral springs have usually a characteristically large amount of sulphate ion compared with the other hot springs as already shown in the hot springs of Japan by the present authors[9], and their acidity is thought to be due to the existence of a large quantity of sulphuric acid formed by the oxidation of sulphur compounds in these springs by the atmospheric oxygen near the surface of the Earth's crust (Table VII). Considering these facts, these acidic mineral springs are thought to be of secondary origin[10]. Thus, the primary hot springs of acidic nature are distinguished from these cold acidic mineral springs of secondary origin. Some of these primary hot springs formed by condensation of the volatile components of magmas after the separation from their magmas are easily distinguished from the other hot springs by means of determination of distribution of radioactive components such as radon and thoron between a gas phase and an aqueous phase as already reported in the previous papers[11]. In these primary hot springs Rn and Tn are distributed in a gas phase in excess of the equilibrium content which is calculated on the basis of partition law between a gas phase and an aqueous phase. On the contrary, in the ordinary hot springs Rn or Tn are distributed usually in an aqueous phase in excess.

When these primary acidic hot springs react for a long time with their country rocks and the other substances around their ways to the surface of the Earth's crust the properties of these hot springs will gradually change, and in the end become of alkaline nature as the residual magmatic solutions in the cavities of volcanic rocks in Hamada and Imari district. If all alkaline hot springs are thus formed from these primary acidic hot springs, the alkaline hot springs are of course of secondary nature. But on the other hand, it is well known that alkaline aqueous solutions can be derived directly from the residual magmatic solutions as in the cavities of volcanic rocks in Hamada and Imari district. When these alkaline aqueous solutions spring out directly on the surface of the Earth's crust, they also form the primary alkaline hot springs. Consequently, it will easily be understood that there are two kinds of alkaline hot springs (primary and secondary in this sense), but they cannot yet be distinguished from each other by observations. When the springs which contain the magmatic substances are genetically called hot springs as is done by Allen and Day[12,10] the hot springs must have various kinds of chemical compositions and temperature depending on the nature of their geological environments, and the chemical compositions of the magmatic and meteoric substance introduced into the chemical system of hot springs. On the other hand it has been found by T. Terada[13] that hot springs which have no relations to volcanic activities are

8) I. Iwasaki, H. Shimojima and M. Tsuda, *Mass Spectroscopy*, No. 1, 52 (1953); No. 4, 39 (1955).

9) I. Iwasaki, *J. Chem. Soc. Japan*, **56**, 1427 (1935); *J. Balneol., Soc. Japan*, Vol. I, No. 3 and 4, 106 (1942).

10) E.T. Allen and A.L. Day, "Hot Springs of the Yellowstone National Park", (1935) p. 39.

11) I. Iwasaki, T. Katsura, H. Shimojima and M. Kamada, "Radioactivity of volcanic gases in Japan", Bull. Volcanologique, in press.

12) E.T. Allen, *Econ. Geol.*, **30**, 1 (1935); A.L. Day, *Bull. Geol. Soc. Am.*, **50**, 317 (1939).

13) T. Terada, *Bull. Earthq. Res. Ins.*, 8, 377 (1936).

formed by the heat produced by crustal movements. Considering these facts, we cannot distinguish the hot springs of magmatic origin from the other mineral springs only by their chemical compositions and temperature of their waters, because we have no method to distinguish the magmatic substances from the others. These facts give the basis to the genetical definition of hot springs reported in the previous papers[14] that hot springs can be defined genetically as the springs which contain more or less magmatic substances regardless of their chemical compositions and temperatures.

c) Primary Hydrosphere and Primary Atmosphere.—The nature of the primary hydrosphere and the primary atmosphere are largely conditioned by the mode of origin of the Earth. There have been many reports on the origin and formation of the Earth, but up to the present, we cannot understand completely yet the chemical processes of the formation of the Earth without any serious objection. The formation of the hydrosphere starts with the condensation of water vapour. On the geochemical processes of the formation of the primary atmosphere and the primary hydrosphere, there are distinct differences between Goldschmidt's theory[15] and the accretion theory[16] developed recently. According to Goldschmidt, the primary atmosphere and the primary hydrosphere are mainly formed by the condensation of the original atmosphere, which was formed at the first stage of the geochemical distribution of the chemical elements in the Earth, and they have increased unceasingly by addition of volcanic gases during the long geologic time. On the other hand, according to the accretion theory the primary atmosphere and the primary hydrosphere are thought to be mainly formed gradually from the volcanic gases expelled by heating from the cold original Earth material.

But in all cases, it has been shown that the volcanic gases occupy the important part of the formation of both the atmosphere and the hydrosphere. From these points of view, it seems to be able to estimate the nature of the primary hydrosphere and the primary hydrosphere from the properties of the volatile magmatic substances, especially the magmatic waters and volcanic gases. As already reported in the previous paper[17], water, nitrogen and carbon dioxide expelled from volcanic rocks by heating have larger contents in the gases expelled at relatively lower temperature (up to about 500°C) than in that expelled at high temperature (800–1200°C). And also we can detect many halogen and sulphur compounds in the volcanic gases from lava lakes and fumaroles of high temperature, but cannot detect any halogen compounds in the volcanic gases from fumaroles of low temperature. Although sulphur compounds such as hydrogen sulphide are detected in many fumarolic gases of low temperature, the main components of these fumaroles are usually nitrogen, carbon dioxide and water vapour. From these model experiments descibed above[17] and the nature of the volcanic gases, by accretion theory we can guess that during the period of relatively low temperature up to about 500°C the contents of sulphur and halogen compounds in atomsophere and hydrosphere should be very small, but when the temperature reached above about 800°C, sulphur and halogen compounds are abundantly expelled from the original Earth material, and consequently the hydrosphere condensed from these volcanic gases will have more sulphur and halogen compounds. In the initial stage of the formation of the hydrosphere, its acidity would increase by the addition of hot acidic rain waters[18] condensed from the volcanic gases of high temperature until active chemical reactions with country rocks which occurred in hydrosphere used up these acids supplied by these volcanic gases. Then the acidity of the hydrosphere would decrease gradually to that of the present hydrosphere (Table IV). The chemical nature of the hot acidic rain waters will be able to be estimated from magmatic waters as will be seen in Table V, and the waters condensed from fumaloric gases. And the chemical properties

TABLE VI

CHEMICAL COMPOSITION OF THE RESIDUAL MAGMATIC GASES IN THE NEPHELINE-BASALT IN HAMADA DISTRICT

Dissolved gases in the inclusion.

	No. 13	No. 19
O_2	0.00 cc./l.	0.00 cc./l.
N_2	6.32 〃	13.54 〃
CO_2	2.25 〃	1.23 〃
H_2	0.00 〃	0.00 〃
CH_4	0.00 〃	0.00 〃
Tension of nitrogen gas	0.366 atm.	0.795 atm.

14) I. Iwasaki, *J. Chem. Soc. Japan*, **56**, 252 (1935).
15) V. M. Goldschmidt, *Z. Elektrochem.*, **28**, 411 (1922); "Geochemistry", (1954) p. 11.
16) H.O. Urey, *Geochim. et Cosmochim. Acta*, **1**, 209 (1951); 263 (1952).
17) I. Iwasaki, T. Katsura and N. Sakato, *J. Chem. Soc. Japan*, **76**, 778 (1955).
18) I. Iwasaki, "Introduction to Geochemistry", (1953) p. 206; I. Iwasaki, T. Nitta and T. Tarutani, *J. Chem. Soc. Japan*, **74**, 1003 (1953).

of the primary atmosphere will also be able to be estimated from the chemical compositions of the residual magmatic gases and volcanic gases from various volcanoes[1,3,8] and various kinds of volcanic rocks[1,17,19]. Chemical compositions of the residual magmatic gases in the nepheline-basalt in Hamada district reported by Sugawara et al[2] are shown in Table VI.

From these volcanic gases we can completely understand that there is no free oxygen in the primary atmosphere. This fact is in good aggreement with the nature of the original atmosphere by Goldschmidt[15].

The primary hydrosphere formed by condensation of the original atmosphere by Goldschmidt must also be acidic nature owing to the dissolution of volcanic exhalation by the violent volcanic action as in the case of the accretion theory. In all cases, the acidic nature of the primary hydrosphere is derived from volcanic exhalations and by unceasing reactions with the country rocks, its acidity would decrease until it became equal that of the present hydrosphere. The chemical nature of the primary hydrosphere at the initial stage, especially primary ocean, seems to be able to be estimated from the chemical composition of hot river waters which are formed by the condensation of the volcanic gases and by running on the hot volcanic rocks erupted recently[18]. After violent chemical reactions with country rocks the nature of the hydrosphere seems to resemble that of the residual magmatic waters and the hot springs. The average contents of main components, such as Cl, SO_4, HCO_3, Na, Ca, Mg, of the hot springs in Japan calculated by the present author[9] are shown in Table VII.

From these points of view, it seems that the content of carbon dioxide in the primary atmosphere is larger than that of the present atmosphere, and the salt content of the primary ocean is about one-tenth that of the present hydrosphere.

d) Magmatic Substances in the Cavities.— As already shown in the description of the nature of the mother rocks and their cavities in this paper, these rocks and the distribution of cavities show remarkably heterogeneous appearance from one part to another. There seem to be no remarkable regularities among their distribution and the nature of their cavities (sizes, inclusions, such as minerals, solutions and gases). Some of the cavities are empty (only filled with gases); on the other hand, some of them are completely filled with mineral substances, mainly carbonates and silica and silicate minerals, and some of them hold mineral substances and aqueous solution in addition to the residual gases. From the nature of these cavities it might be safely concluded that these mineral materials, waters and gases, are easily mobile in the mother rocks at the stage of the formation of these cavities. If these characteristics are excluded, it seems to be impossible to understand the fact that some of these cavities are completely filled with the mineral substances or are empty. From this point of view, the computation of the concentration of the inclusion water before the minerals, lining the cavity-wall, separated was carried out by K. Sugawara et al.[2], and they showed that the concentration is very high (280.88 g./l.); that is, 3.65 times higher than the Japanese record of hot spring salinity, 77.1 g./l. of Arima-shin-onsen.

TABLE VII

AVERAGE CONTENTS OF MAIN COMPONENTS OF THE HOT SPRINGS IN JAPAN

	Number of sample	Salt content (g./kg.)	Na (g./kg.)	Ca (g./kg.)	Mg (g./kg.)	Cl (g./kg.)	SO_4 (g./kg.)	HCO_3 (g./kg.)
Acidic "hot spring" (>25°C)	63	2.21	0.305	0.195	0.0537	0.787	1.51	0.257
Acidic mineral spring (<25°C)	162	6.09	0.692	0.210	0.0833	1.07	4.51	0.547
Neutral "hot spring" (>25°C)	25	2.76	0.631	0.247	0.0199	1.01	0.472	0.321
Neutral mineral spring (<25°C)	23	4.08	0.873	0.438	0.0829	1.98	0.471	0.532
Alkaline "hot spring" (>25°C)	331	2.19	0.534	0.192	0.0198	0.847	0.349	0.246
Alkaline mineral spring (<25°C)	108	6.78	2.06	0.300	0.107	3.20	0.337	1.34
Total hot spring	712	3.86	0.768	0.221	0.0557	1.25	1.70	0.491

19) E.S. Shepherd, *J. Geol.*, **33**, 289 (1925); E.S. Shepherd and H.E. Merwin, *J. Geol.*, **35**, 97 (1927).

Conclusion

From the definition of the real magmatic state, many kinds of the magmatic waters should be formed even from the same magma depending on their geological environments. The residual magmatic water described above can be distinguished from the magmatic waters derived directly from the molten lavas. The magmatic waters are acidic on account of dissolution of volatile magmatic components, but the residual magmatic waters must be usually neutral, slightly alkaline or acidic owing to the chemical reactions with their country rocks. These magmatic waters are not always juvenile, and their temperature, salt contents and chemical composition must cover a wide range. Consequently these magmatic waters cannot be distinguished distinctly from the ordinary natural waters by means of their temperature and chemical compositions.

When the hot springs are defined as the springs which contain the magmatic waters, many kinds of springs should be formed owing to the mechanism of the formation of hot springs. Even the primary hot springs derived directly from the magmatic waters have also a wide variety. For example, the acidic primary hot springs formed directly from the magmatic waters can be changed gradually into the alkaline hot springs by the reactions with their country rocks and the introduction of the other substances. On the other hand, the primary alkaline hot springs can also be formed directly from the residual magmatic waters.

From the nature of the magmatic waters and volcanic gases, the chemical nature of the primary hydrosphere and the primary atmosphere in their initial stage can be estimated. The primary hydrosphere must be acidic on account of the hot acidic rain waters at first, and change gradually into alkaline nature by the reactions with their country rocks and the other substances introduced by river waters. The primary atmosphere has no free oxygen, but has larger carbon dioxide content than the present atmosphere.

From these facts that all the cavities of the mother rocks in question have a quite distinct boundary and the distribution of the magmatic substances in these cavities are quite dissimilar, it also might be safely concluded that these mineral substances must be easily mobile in the initial stage of the formation of these cavities. The problems on the mechanism of this surprising concentration of these mineral materials into the small cavities will be answered by the geochemical investigations in future.

Summary

1) The nature of the residual magmatic waters in the cavities of the trachyandesitic basalt in Imari district is described with the nature of their mother rocks and druse minerals.

2) From the definition of the real magmatic state, temperature, and chemical properties of many kinds of magmatic waters are discussed, and the residual magmatic waters are distinguished from the magmatic waters derived directly from lava lakes. It is concluded that the magmatic waters are not always juvenile.

3) The formation of the various kinds of the primary hot springs are discussed from the definition of hot springs and the various kinds of the magmatic waters.

4) Chemical nature of the primary hydrosphere and the primary atmosphere in the initial stage of their formation are discussed from the chemical properties of the magmatic waters and volcanic gases.

5) The important properties of the magmatic substances in the cavities of the volcanic rocks are discussed from the standpoint of the distribution of the magmatic substances in the cavities.

The authors wish to express their hearty thanks to Professor H. Kuno of Tokyo University, Assistant Professor N. Saito, T. Ishimori and S. Taneda, Mr. H. Yamamoto of Kyushu University for their kind advice and help. The cost of this research was defrayed from the Scientific Research Grant from Ministry of Education, to which the writers' thanks are due.

Laboratory of Analytical Chemistry and Geochemistry, Tokyo Institute of Technology, Tokyo
and
Chemical Institute, Faculty of Science, Kyushu University, Fukuoka

On the Attribution of the Super Oxidation-resistance of Cemented Chromium Carbide

By Kazuhiko OGAWA and Tamotsu FUKATSU

(Received October 25, 1955)

Introduction

At present, the various kinds of the titanium carbide, TiC, or chromium carbide, Cr_3C_2, base sintered products have been successfully investigated as a superior heat-resistant material. Among them, the cemented chromium carbide, "CR", gives promise of many useful practices of chemical engineering because of its supper oxidation- and corrosion-resistance.

On the method of manufacture of the "CR" product and its properties, some valuable studies have been published[1]. Recently, the effect of the added chromium carbide on the oxidation-resistance of the other cemented carbide products was studied by J. Hinnüber and co-workers[2], yet much remains to be investigated on the cause of this remarkable oxidation-resistance.

Therefore the experimental work of this report has been to investigate the relationship between the structure of the surface oxidized film and the oxidation-resistance. Namely, the crystal structural change of the surface oxidized film at various temperatures was examined mainly by the electron diffraction method, and, at the same time, its microstructural change was also observed by electron microscope.

Experimental Method

The "CR" alloy was produced by sintering a compacted body of Cr_3C_2 powder mixed with 15 weight per cent of pure Ni powder with the same process reported by Y. Matsuyama, S. Kasahara and H. Hase[3]. The specimens of "CR" used here were given by Tungaloy Co.. Their characters were as shown in Table I.

Specimens for electron diffraction were prepared by the following procedures: making a bar with 4 mm. of diameter and about 10 mm. of length from this "CR" alloy, polishing the one end of the bar and then cleaning it with 10% HCl solution, distilled water, methyl alcohol and benzen in this order.

TABLE I

THE PROPERTIES OF THE "CR" ALLOY

Properties \ Alloy	CR
Density	~6.9 g./cm³
Hardness	at Room Temp. 84–88 Hr A at 500°C 83–36 at 900°C 73–31
Trans. Rupt. St.	70 kg./mm²
Ther. Expans.	at 30–750°C 11.5×10^{-6}
Elect. Resist.	$\sim4.3\times10^{-4}$ Ω cm.
Magnetic Prop.	(non-magnetic)

CR: Cemented chrome-carbide, Cr_3C_2, contained 15% Ni.

This was oxidized in air up to 1000°C at every 100°C in a ceramic crucible to prevent contamination. These oxidized specimens were at once mounted on the specimen holder of electron diffraction camera and surface film of them was examined by the reflection method. The diffraction unit used was attached to on the Simazu SM-C2 electron microscope, the camera length 15.9 cm. and acceleration voltage 50 kV.

At the same time, a micro structural change of the surface oxidized film at various temperatures was observed by electron microscope with the polysthylene-Al replica method. On the other hand, the process of oxidizing of the carbide powder itself was also observed by means of X-ray analysis and electron microscopy.

Moreover, the structure of the sintered product as determined with a special X-ray diffraction method and at the same time the Curie point of this specimen was also measured with magnetic balance.

Experimental Results

I. On the Oxidation Resistance of "CR" at High Temperature

According to J. Hinnüber's results, the "CR" alloy increased in weight by being heated in air at each temperature of 500, 600, 700, 800, 900 and 1000°C for one hour. As shown in Table II, the weight-gain was so small that the advancing of oxidation was not confirmed below 800°C. Though the weight-increase was small, it came to be measurable at 1000°C. In our results, the lustre of the polished surface changed little at 300°C, then faded gradually with the rise of temperature and vanished completely at

1) J.D. Kennedy, *Steel*, **131**, 92 (1952); P. Schwarzkopf and R. Kieffer, "Refractory Hard Metals", (1953) p. 122.

2) J. Hinnüber and O. Rüdiger, *Archv. für Eisenhüttenwesen*, **24**, 267 (1953).

3) Y. Matsuyama, S. Kasahara and M. Hase, Reported in the annual meeting of Japan-Kinzoku-Gakkai (1954).

TABLE II

WEIGHT INCREASES OF "CR" BY OXIDATION AT VARIOUS TEMPERATURS FOR TWO HRS. IN AIR, FROM J. HINNÜBER AND CO-WORKER'S RESULTS

Temperature °C	Weight increase g./m², hr.
500	<0,1
600	<0,1
700	0,2
800	0,2
900	0,75
1000	1,2

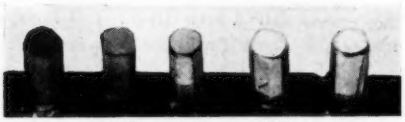

1000°C 800°C 500°C 300°C Polished surface

Photo. I. The lustre change of the polished surface by oxidation at various temperatures for 1 hr. in air.

From these results, it shoult be concluded that the "CR" alloy is useful for practical purposes of long time operation at such high temperature as 800°C in air. It must be studied whether such an excellent oxidation-resistance is based on these starting materials themselves or any characteristic structure of these oxidized films. Firstly, oxidizing the chrome carbide powder, Cr_3C_2, itself at various temperatures, the weight-increase was measured as shown in Table IV, and also, the crystal structural change of its powder was observed by the X-ray method such as illustrated in Photo II. This indicated that Cr_3C_2 had begun to change into Cr_2O_3 at 500°C already, and then the weight-gain step by step increased with rising temperature. On the other hand, the oxidation-resistance of nickel, which was the binder of "CR", was checked: Ni plate was heated in air and the structure of surface was examined by the electron diffraction. The patterns obtained were shown in Photo. III. It also indicated that the formation of NiO are faintly observed at 300°C and clearly at 500°C. It is worth being discussed that, as understood from these above results, though each component of "CR" alloy, Cr_3C_2 and Ni becomes unstable at even lower temperature than 500°C, the sintered products were stable for oxidizing for a long time at such a high temperature as about 800°C. This result suggests that the oxidation-resistance of "CR" alloys is attributed to the formation of some desirable protective film.

TABLE III

THE CHANGES OF THE COLOR, THE STRUCTURE AND THE COMPOSITION OF THE OXIDE FILM DURING OXIDATION

Temperature °C	Color	The composition of the oxide-film	Remarks
100	Metallic lustre	Imperfect Cr_2O_3	
200	Metallic lustre	Imperfect Cr_2O_3	
300	Metallic lustre, Very faint bronze-like color	Cr_2O_3	Little oriented crystals
350	Metallic lustre, Faint bronze-like color	Cr_2O_3	Little oriented crystals
500	Lustre, Bronze-like color	Cr_2O_3	At random orientation
800	Faded lustre, Green black color	Cr_2O_3	〃
1000	Non-lustre Green and gray	Cr_2O_3 and $NiO-Cr_2O_3$	〃

TABLE IV

WEIGHT INCREASES OF Cr_3C_2 POWDER BY HEATING AT VARIOUS TFMPERATURES FOR ONE HOUR IN AIR

Temperature °C	Weight increase	By X-ray※ diffraction
300	−5 mg./g. hr.	—
500	5 〃	3%
800	150 〃	60%
1000	——	90%

※ The estimation was measured by comparing the observed intensities of oxide lines with the standards.

1000°C or up (Photo. I), while a faint color appeared first at 300°C for two hours, then changed with the rise of temperature. These results were described in Table III. These changes of lustre and color corresponded with the above weight-increase.

II. The Structure of Oxide Film

Therefore, to confirm the formation of such protecting surface film, the variations of the surface structure with oxidizing at various conditions were examined by the electron diffraction.

The abstract of the main results from these observations were enumerated in Table III.

Phot. II. The shape and structural change of chrome-carbide powder during oxidation process.

(a)

at 300°C for 1 hr.

Cr_3C_2

(b)

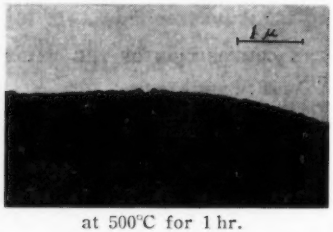

at 500°C for 1 hr.

Cr_3C_2

(c)

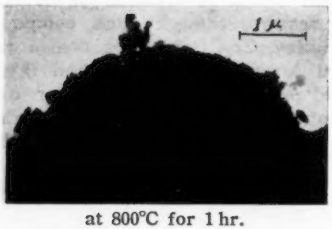

at 800°C for 1 hr.

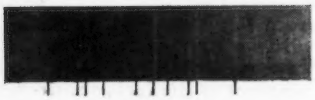

Cr_2O_3

(d)

at 1000°C for 1 hr.

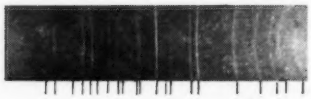

Cr_2O_3

Photo. III. The electron diffraction pattern of the oxidized Ni plate at 500°C for 1 hr. in air.

Among them, the interesting results would be reviewed as follows.

i) The surface film consisted of one kind of chromic oxide, Cr_2O_3, only and not of other chromium oxide or nickel oxide below 800°C. When at such higher temperature as about 1000°C, remarkable oxidation was observed by weight-increasing, then both Cr_2O_3 and the chromium-nickel spinel, $NiO \cdot Cr_2O_3$, were first observed in the oxide film.

ii) Concerning the chromic oxide filme below 800°C, the variation of its structure corresponding to the rise of temperature was so remarkable as not to be expected previously. Namely, the surface films heated from the room temperature to 250°C for one hour consisted of very fine and imperfect crystallites of Cr_2O_3 and, moreover, were very flat. Heating it at 300°C in air continuously, the imperfect crystallites of Cr_2O_3 in the oxide film altered into perfect ones and tended to be oriented, their basal planes being parallel to the surface. This tendency was observed up to 500°C. However, in the oxidized film at higher temperature than 500°C, such orientation became at random and, the surface, also, became rough step by step. On these problems, the further sufficient explanations must be supplied as follows.

a) The confirmation that the oxide film at lower temperature was composed of imperfect and minute crystallites was based on the experimental evidences of the diffraction patterns. The diffraction patterns as Photo. IV (1) and Fig 1, are interpreted to be two-dimensional-like patterns diffracted by imperfect crystallites of Cr_2O_3 with the crystal basal planes slipped at random as observed in the polished graphite pattern[4]. At the same time, the diffuse ring patterns indicated that the crystallites were very minute. In the sample, oxidized at higher temperature,

Photo. IV. The electron diffraction patterns of oxide film formed on the surface of "CR" by oxidation at various temperatures for 1 hr. in air.

(1)

at 300°C for 1 hr.

(2)

at 300°C for 2 hr.

(3)

at 350°C for 1 hr.

(4)

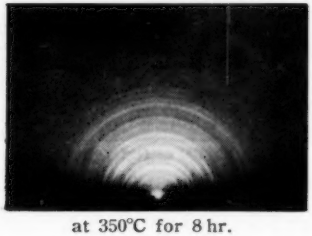

at 350°C for 8 hr.

(5)

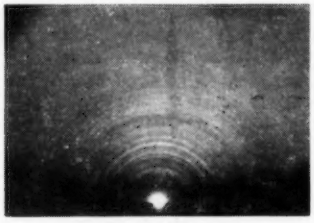

at 500°C for 1 hr.

(6)

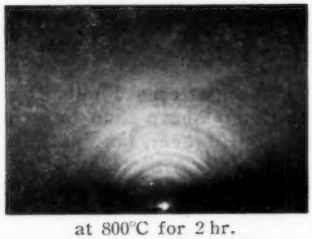

at 800°C for 2 hr.

(7)

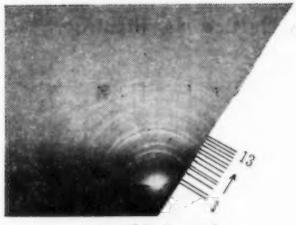

at 1000°C for 1 hr.

Comparison between observed spacing and the spacing of spinel oxide, Cr_2O_3NiO

	Observed	Spinel
1	4.75 A	4.79 A
2	4.26	4.15
3	2.96	2.94
4	2.52	2.50
5	2.40	2.40
6	2.12	2.10
7	1.92	1.91
8	1.73	1.77
9	1.64	1.63
10	1.50	1.50
11	1.44	1.445
12	1.347	1.345
13	1.299	1.297

(8)

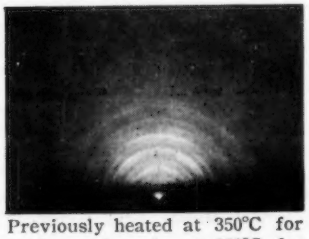

Previously heated at 350°C for 1 hr. and again at 800°C for 1 hr.

Fig. 1. The sketch of the electron diffraction pattern of the polished surface.

the diffraction patterns Photo. IV, (6) were more remarkably sharp than those at lower temperature. However, both patterns always coincided with Cr_2O_3 patterns.

b) The appearance of arcing in Photo. IV (2) must suggest that these chromic oxide crystallites were oriented. Orientation was determined by the ordinary method, using the reciprocal lattice as illustrated in Fig. 2.

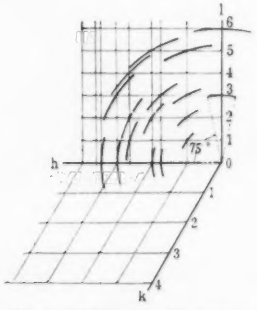

Fig. 2. The schematic diagram of the diffraction pattern of oriented chromic oxide crystals with their C-axis inclined 75°C to the matrix surface, in reciprocal lattice.

This figure shows the diffraction pattern of oriented Cr_2O_3 crystals with their C-axis inclined at the angle of 75° to the matrix surface.

c) Film-thickness or flatness can be estimated from the electron-microscopic photographs substantially, also by the ring width or diffusing behavior of the electron diffraction pattern. The arcs of the diffraction patterns obtained from the specimens below 500°C, diffused toward the centre of the ring. This diffused ring was different from the usual halo pattern and interpreted to be originated from a refraction of electrons because of the very flat surface.

d) In the oxidized film at 1000°C, the existence of the spinel type oxide, $NiO \cdot Cr_2O_3$ was confirmed with the result of Photo. IV (7). This pattern and spacing showed a good agreement with the spinel type oxide observed previously on the surface oxide film of Ni–Cr alloy. It has been reported by several workers[5,6] that the oxidation-resistance of this alloy at high temperature took place because of the formation of the densed and flexible oxide film of $NiO \cdot Cr_2O_3$.

However, in this experimental result, the oxide film composed of this spinel oxide did no longer act the most effective part in preventing the oxidation. Though it is interesting to consider why this spinel oxide was formed on the surface of this product, this will be discussed in the later.

From the above-mentioned results, it will be suggested that the tendency of the oxidation-resistance declines with the increasing roughness of the surface film, because of the crystal-growth of Cr_2O_3 crystallites. To study this problem, the micro-structural change of surface must be observed sufficiently.

III. Observation of the Microstructure of the Surface

The microstructure of each surface film treated at various conditions were illustrated in Photo. V. It was proved from these figures

Photo. V. The electron-microscopic structure of each surfaces of "CR" in various stages in oxidation.

(1)

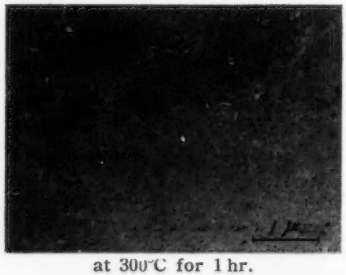

at 300°C for 1 hr.

(2)

at 500°C for 1 hr.

4) G.P. Thomson and W. Cochrane, "Theory and Practice of electron diffraction", (1939) p. 185.

5) J. Iidaka and S. Miyake, *Nature* **137**, 457 (1935).

6) A. Gulbransen and W. R. McMillan, *Ind. Eng. Chem.*, 45. 1734 (1953).

(3)

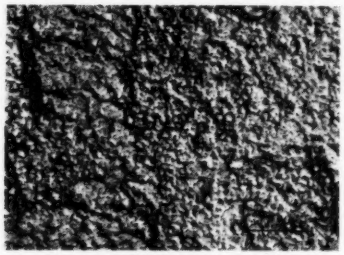

at 800°C for 1 hr.

(4)

at 1000°C for 1 hr.

(5)

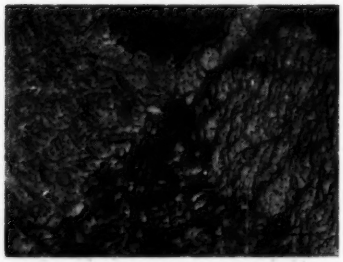

Previously heated at 250°C for 1 hr. and again at 1000°C for 1 hr.

that the appearance of the surface up to 500°C was very flat, and the grain size was too small to be measurable as already suggested. However, the oxidized surface above 800°C, became more rouge consequently, and, in this film, the coarse chromic oxide crystals were observed as showed in Photo. V (4).

Moreover, in the oxidized film at 1000°C, the grains became so coarse that their diffraction pattern rings were spotty as shown in Photo IV, (7). Sometimes, as appeared in Photo. V (4), piramid-like large grains of one micron order were observed and the surface began to break out into small cracks.

From such a result, it will be confirmed that the increasing roughness of the surface may be caused by the coarsening of the minute chromic oxide crystals.

It is a valuable new result to discover that the stability of protective film may be more responsible for the structure of film, than the kinds of oxide.

IV. The Inner Structure of "CR" Tip

Lastly, it must be studied why the oxidized film below 800°C consisted of one kind of the chromic oxide, Cr_2O_3, though the nickel binder metal was oxidized already into NiO at 500°C.

Concerning this problem, though it was recently suggested by J. Hinnüber that the binder phase would exist in the alloying state, yet it has not been confirmed experimentally.

Therefore, the inner structure was examined by X-ray and magnetic balance. The method of the X-ray diffraction of "CR" tip was outlined in Fig. 3 and its photographs were illustrated in Photo. VI in which were observed the ortho rhombic structure, Cr_3C_2 and a face centered cubic structure.

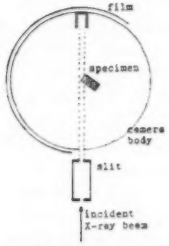

Fig. 3. The method of mounting specimen in this X-ray diffraction.

Photo. VI. The X-ray diffraction pattern of "CR" showing some f.c.c. structure.

Though the difference between the lattice constants of this f. c. c. and Ni was almost never observed, it seemed that this f. c. c. was perhaps not the pure Ni. This f. c. c. did not appear in the specimen sintered at such a lower temperature as 500°C, but appeared first clearly at the higher temperature at which the reaction between Cr_3C_2 and Ni occurred. However, the reason was not yet clear that the pure Ni was not observed by X-ray diffraction patterns in the specimen sintered at the lower temperature.

Therefore, when the magnetic properties of these specimens were measured, the intensity of saturation magnetization of the specimen sintered at the temperature which the f. c. c. appeared, was more remarkably small than that of the sintered one at the lower tem-

perature. On the other hand, the Curie temperature of the specimen was measured by magnetic balance. One of these results was shown in Fig. 4.

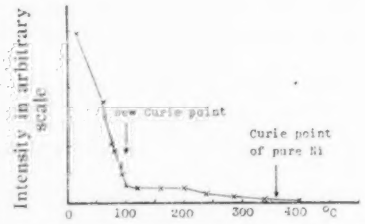

Fig. 4. Magnetization curve of "CR".

This indicated a Curie temperature of 100°C differing from the usual one, 358°C of the pure Ni. Curie points lay below 150°C, and the amount of these materials which have these Curie points are more numerous than pure Ni, as they can be estimated from Fig. 4.

If this alloy is assumed to be Ni-Cr solid solution, it will be expected that the quantity of Cr dissolved in Nickel binder phase is 5 per cent or more by weight. Therefore, it can be confirmed that the binder phase no longer exists as pure Ni, but as some Ni-Cr alloy or some intermetallic compound of double carbide of Cr_3C_2-NiC. If this assumption is true, then the appearing of nickel chrome spinel at 1000°C coincides with the previous works.

General Discussion

From these experimental results, two subjects to be discussed more sufficiently were as follows.

a) The oxidation of "CR" was nothing but the complicated process combined with the following to processes: the decarburization and oxidation of the Cr_3C_2 grain, and the oxidation of some Ni-Cr alloy in the part of binder.

b) The dense and flat oxidized film composed of the chromic oxide crystallites very suitable for oxidation-resistance. In such film, these minute crystallites tend to have a orientation.

With the coarsening of these crystallities, the surface became rough gradually, and broke out into small cracks. Such film was not sutiable to prevent oxidation. Generally speaking, it was confirmed that the tendency of oxidation-resistance depended not only on the kind of oxide but on the chracteristic structure of the surface film.

Firstly, from the above mentioned experimental confirmation that "CR" consisted of both Cr_3C_2 and some Ni-Cr alloy, the consideration in the item a) was concluded.

From the previous experimental results, the reason was easily understood why the formation of the spinel oxide, $NiO \cdot Cr_2O_3$, was observed in the oxidized film at 1000°C or up. However, to our regret, the reason of the nickel oxide not being found in the oxidized film below 800°C has not yet been revealed.

According to the information of the oxidation process of Ni-Cr alloy by J. Gulbransen, the nickel mono-oxide was observed at such a low temperature at 500°C, and its tendency depended considerably on the composition of such alloy.

Though this difference between our result and Gulbransen's might have been due to small amounts of Ni-Cr alloy in "CR", further studies were necessary.

Secondly, as described in the item b), the oxidation-resistance depended also on the structural change of the surface film. Therefore, it was necessary to understand a mechanism of the decarburization and oxidation of Cr_3C_2, during which process the structure of the oxide film changed with rise of temperature. To understand it easily, some models of oxidation process were sketched schematically in Fig. 5. This film consisted of small

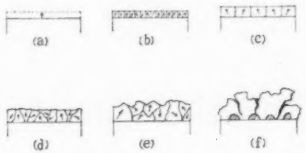

Fig. 5. The models of the oxide film at various stages of oxidation.

bricks, which were the chromic oxide crystallites, and the noted arrow in the bricks was the direction of C-axis. The brick pictured with the broken line was the imperfect crystal. The shaded one was the spinel-type oxide. As shown in these figures (a) (b) (c), the surface film was the aggregation of the chromic oxide crystallites. With the rise of temperature, these changed in size as well as in the crystal structure. In the figure (c), the oxide film composed of these oriented crystals carried out the effective role in preventing the oxidation. These models were devised from the above-mentioned experimental results by the electron diffraction. In the figures (d, e), the surface became more rough corresponding to the crystal growth of these crystallites. In this stage, these crystals grew remarkably at random and the rate of oxidation increased rapidly. This model was devised from the

experimental results concerning the surface micro-structural change of "CR" and the shape-change of Cr_3C_2 powder in oxidation. During the oxidation of the chrome carbide (Cr_3C_2) powder at various temperatures the irregularities were formed on the surface of powder, and increased with the rise of temperature. This result was shown in Photo. II (2).

Lastly, a little more description of the oriented film was added.

When the specimen already heated to have the oriented film was heated again at higher temperature with the virgin one, the latter tended to be more remarkable in the crystal growth and the increasing roughness of surface than the former. Such tendency was observed from the comparison in Photo. V (4, 5).

From this experimental result, it was confirmed that the oriented film was more suitable for oxidation-resistance than the non-oriented one, yet much remained to be investigated.

The authors wish to express their great indebtedness to Professor Keizo Iwase for helpfull advice, and Professor Ryoji Uyeda for useful discussions in the part of the electron diffraction pattern. Thanks are due to Mr. Kazuichi Sugiura for aid in the electron microscope work, and also Tungaloy Products Co. which kindly offered them the specimens.

Chemical Department, Faculty of Science
Kyoto University, Kyoto
and
Tungaloy Products Co.

Detection of ^{103m}Rh in the "Bikini Ashes"

By Kenjiro KIMURA, Nagao IKEDA* and Kenji YOSHIHARA**

(Received December, 1, 1955)

Introduction

The radiochemical analysis of the so-called "Bikini Ashes" which fell on a Japanese fishing boat, the No. 5 Fukuryu Maru on March 1, 1954, was carried out in our laboratory[1] and in several other university laboratories[2]. In the course of their studies, scientists detected ^{103}Ru (half-life: 39.8 d.) in the ashes together with ^{106}Ru (half-life: 1.0 y.) and its daughter ^{106}Rh (half-life: 30 s.). As is well known, ^{103}Ru decays into ^{103m}Rh (half-life: 57 m.) which successively disintegrates into stable ^{103}Rh by isomeric transition. The half-life of ^{103m}Rh is rather short and the energy of the converison electron of ^{103m} Rh is so low (0.034 Mev) that it has been still remained undetected in the ashes. The present authors tried to separate ^{103m}Rh from its parent ^{103}Ru in the carrier-free form by the ion exchange resin method in a short time and to detect the weak radioactivity by the use of the windowless gas flow counter.

* Department of Chemistry, Faculty of Science, Tokyo University of Education, Koishikawa, Tokyo, Japan.

** Electrotechnical Laboratory, Agency of Industrial Science and Technology, Ministry of International Trade and Commerce, Tanashi, Tokyo, Japan.

1) K. Kimura, E. Minami et al. *Japan Analyst*, 3, 335 (1954). (in Japanese).

2) T. Shiokawa, et al, ibid., 349; H. Yamatera, et al., ibid., 356.

Experimental

1. Materials and Apparatus

Materials.—The sample ashes are so-called "Bikini Ashes" which fell on board No. 5 Fukuryu Maru sailing near the Bikini Atoll on March 1, 1954. The chemical and radiochemical compositions of the ashes were already reported in the previous paper[1]. The ashes used in this experiment were collected on board the boat and contained fairly large amounts of dust.

Apparatus for Activity Measurements.—The Geiger-Müller counter model TGC-2 made by Tracerlab Inc. was used for the general activity counting. The thickness of the mica window of the counter tube is 1.4 mg./cm^2 and counting efficiency is about 10%. For the measurement of the weak activity of rhodium fraction, 2π Q-gas flow counter model D42A made by Nuclar Instrument and Chemical Corporation was used.

2. Separation of Ruthenium from "Bikini Ashes"

At first, ruthenium fraction was separated from the ashes by the procedure written below. The sample of some ten million cpm. was taken and ignited to burn away all combustible substances. Then, it was dissolved with 6 N hydrochloric acid, and the insolubles were filtered off. The activity of a small aliquot of the filtrate was measured on the second shelf of the Geiger-Müller counter. Total activity was estimated about 10^5 cpm., 10 mg. of ruthenium was added to the filtrate as a carrier, the acidity of the solution was adjusted

to 2 N, and then hydrogen sulfide was passed through to precipitate ruthenium as sulfide. The precipitate was dissolved with nitric acid. The solution thus obtained was then treated according to the D. N. Hume's procedure[3]; to the ruthenium solution were added an appropriate amount of water, potassium permanganate and concentrated sulfric acid, then ruthenium was distilled off as ruthenium tetroxide. The distillate was caught in a small volume of water containing a small amount of hydrogen proxide.

The appropriate aliquot portion of the distillate was taken in a counting dish, evaporated up to dryness and the activity was measured under the same measuring condition as in the case of the starting sample solution. The total activity of the distillate was considered to be 1.5×10^5cpm.

The absorption curve of the distillate for aluminum foil was also investigated. The result is shown in Fig. 1. The activity is considered to

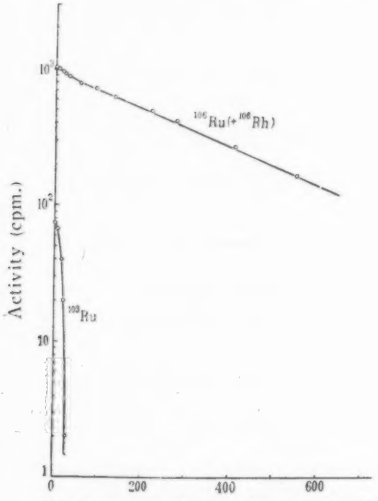

Fig. 1. Absorption curve of Ru*+Rh* fraction (Apr. 5, 1955).

be composed of two parts; rather high energy β-ray of some 3.9 MeV and low energy β-ray of less than 0.3 MeV. The former is considered to correspond to that of ^{103}Rh (3.55 MeV), the daughter of ^{103}Ru, and the latter to that of ^{103}Ru (0.22 MeV).

3. Separation of Rhodium from Ruthenium and Detection of ^{103m}Rh

The separation of rhodium from ruthenium for the purpose of detecting ^{103m}Rh includes two essential problems; (1) the half-life of ^{103m}Rh is very short (57 m.), so that the separation must be finished in a short time, (2) the energy of internal conversion electron of ^{103m}Rh is very low (0.034 MeV). Therefore, it is desirable for it to be separated in as high a specific activity as possible to minimize the effect of self-absorption.

P. C. Stevenson, et al.[4] reported that rhodium adhers to the cation exchange resin, Dowex-50, and it is easily eluted out by passing 2 N hydrochloric acid. The workers thus succeeded in the separation of rhodium from such platinum group elements as platinum, palladium and iridium. On the other hand, it is known that ruthenium in 0.2 N hydrochloric acid solution passes through Dowex-50 resin without adhering. The procedure for the separation of rhodium and ruthenium which the present authors used in this experiment is based in principle on this difference of the properties of these elements against resin.

The resin used in this experiment was a cation exchange resin, Dowex-50 in HR-type, 50–100 mesh, ane 1.0 cm. $\phi\times$6.0 cm. in dimension. The flow rate of the solution was 1 ml./min.

The appropriate aliquot of the above mentioned ruthenium distillate was evaporated up to dryness and the residue was dissolved in a small amount of hydrochloric acid. The evaporation and dissolution processes were repeated several times; then, the acidity and total volume of the hydrochloric acid solution were adjusted to 0.2 N and 10 ml., respectively. The solution thus obtained was allowed to flow through the resin bed. After the resin bed was washed with a small quantity of 0.2 N hydrochloric acid, 2 N hydrochloric acid was passed through as the elutriant for rhodium. The effluent was collected and evaporated up to dryness in a counting dish. The activity of the residue was then measured with the 2π Q-gas flow counter, and its decay curve was observed.

The result is shown graphically in Fig. 2-I

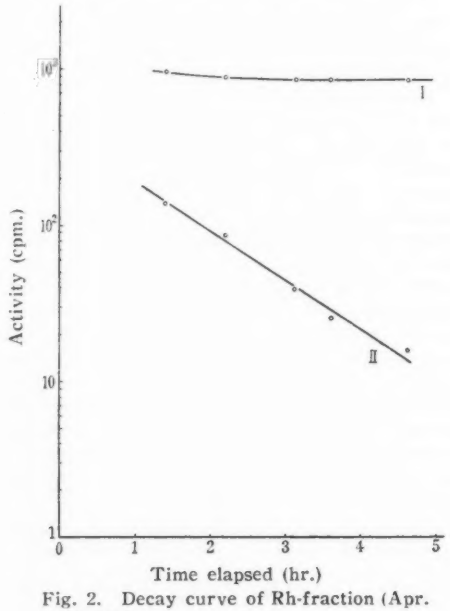

Fig. 2. Decay curve of Rh-fraction (Apr. 14, 1955).

3) D. N. Hume, *NNES-PPR*, 9, 1557 (1951).

4) P. C. Stevenson, et al., *J. Am. Chem. Soc.*, 75, 4876 (1953).

representing the logarithm of the radioactivity against the time which has elapsed. The activity decreases rather considerably for the first several hours[5], and then it becomes approximately constant. In order to analyse this decay curve, the above-mentioned approximately constant value of the later period was subtracted from the activity values for the earlier period, and the differences were again plotted against time. Then, a virtually straight line is obtained as shown in Fig. 2-II. As its inclination coincides with that corresponding to the half-life fifty-seven minutes, the activity can be attributed to that of ^{103m}Rh. Judging from its absorption curve for aluminum foil, the radioactivity which still remains after the decay of ^{103m}Rh is attributed to the radioactivites of ^{103}Ru and ^{101}Ru + ^{101}Rh. It is shown that rhodium separated by the above-mentioned method is still accompanied with considerable amounts of radioactive ruthenium.

The ruthenium fraction which passed through the resin bed was set aside and let stand over several hours to allow the growth of its daughter ^{103m}Rh and used for the next separation of ^{103m}Rh. Thus, the separation experiment of ^{103m}Rh was repeated three times in the above-mentioned way, and always observed the radioactivity which should be assigned to ^{103m}Rh.

As to the energy of the internal conversion electron of ^{103m}Rh, it was rather difficult to measure directly in the 2π Q-gas flow counter for its short half-life and low activity. Therefore, the authors applied the following conventional method; after the rhodium fraction was separated and collected in the counting dish in the way mentioned above, the dish was wrapped with the aluminum foil of 4.75 mg./cm^2 thickness[6] and its activity decay was measured. The result is shown in Fig. 3, indicating no decrease in activity. It

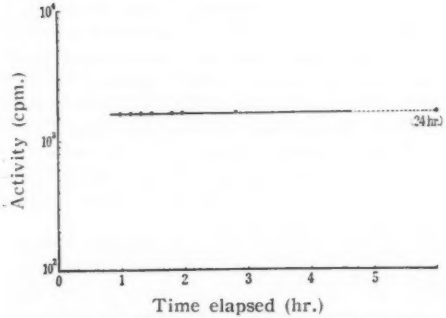

Fig. 3. Masking of ^{103m}Rh decay by 4.75 mg./cm^2 Al-foil (Apr. 21, 1955).

seems to be concluded deservedly that the radioactivity of the shorter half-life observed in this fraction in the former experiments is perfectly absorbed by the alumium foil of 4.75 mg./cm^2 thickness, and this low energy activity shoud be attributed to the internal conversion electron of ^{103m}Rh whose energy is described 0.034 MeV.

5) The initial time ($t=0$) corresponds to the middle time when the sample solution starts and finishes passing through the resin bed.

6) The aluminum foil of 4.75 mg/cm^2 thickness corresponds to the maximum range of β-ray of 0.05 MeV energy.

Conclusion

It can be now concluded that ^{103m}Rh is directly detected in the "Bikini Ashes" in the above mentioned way.

As the separation of rhodium must be done in as short a time as possible because of the short half-life of ^{103m}Rh, the efficiency of separation of rhodium from ruthenium in this experiment is by no means satisfactory from the analytical point of view. The rapid and clean-cut separation of ruthenium and rhodium from each other is the problem still remaining to be solved.

The radionuclides detected in the ashes are summarized in Table I including newly

TABLE I

RADIONUCLIDES DETECTED IN THE "BIKINI ASHES"

Nuclides detected	Half-life	Activity percentage of each nuclide (on March 26, 1954) (%)
^{32}P	14.30 d	—
^{35}S	87.1 d	0.1±0.05
^{45}Ca	152 d	0.2±0.1
^{89}Sr	53 d	1±0.5
^{90}Sr	19.9 y	0.02±0.01
^{90}Y	61 h	0.02±0.01
^{91}Y	61 d	8±3
^{95}Zr	65 d	5±2
^{95m}Nb	90 h	—
^{95}Nb	35 d	3±1
^{103}Ru	39.8 d	8±5
^{103m}Rh	57 m	
^{106}Ru	1.0 y	0.9±0.2
^{106}Rh	30 s	
^{125}Sb	2.7 y	—
^{129m}Te	33.5 d	—
^{129}Te	72 m	—
^{132}Te	77.7 h	—
^{131}I	8.141 d	—
^{132}I	2.4 h	—
^{137}Cs	33 y	—
^{140}Ba	12.80 d	5±1
^{140}La	40.0 h	6±1
^{141}Ce	33.1 d	7±5
^{144}Ce	282 d	2±1
^{143}Pr	13.7 d	16±5
^{144}Pr	17.5 m	2±1
^{147}Nd	11.3 d	9±4
^{147}Pm	2.6 y	—
^{237}U	6.75 d	20±10
^{239}Pu	24360 y	α: (4±2)×10^{-4}

detected ^{103m}Rh as well as ^{35}S[7], ^{125}Sb[8] and ^{137}Cs[8] which are also detected after the issue of the previous paper. In addition, the contribution of each nuclide to the total activity is tabulated in Table I. These numerical values are all expressed by the percentage contribution of activity on March 26, 1954 —twenty-five days after detonation of the Bikini bomb—when the quantitative measurements of activity of the ashes were started.

7) K. Kimura, N. Ikeda and M. Inarida, Read before the Annual Meeting of the Japan Society for Analytical Chemistry, Oct. 1954 Osaka.

8) M. Honda, Y. Sasaki, Read before the Annual Meeting of the Chemical Society of Japan, Apr. 1955, Tokyo.

Summary

^{103m}Rh having very short half-life (57 m) and very low energy in electron conversion (0.034 MeV) was searched for and detected in the "Bikini Ashes". It was separated from the ashes by the method using the cation exchange resin, Dowex-50, and its activity was measured by the 2π Q-gas flow counter.

The radionuclides detected in the ashes are briefly summarized in a table.

Department of Chemistry, Faculty of Science, The University of Tokyo, Tokyo

Studies on the Infrared Spectra of Ephedrine and Related Compounds. I. On the Discrimination between Diastereoisomeric Ephedrines

By Tokunosuke KANZAWA

(Received November 29, 1955)

The discrimination whether a compound like ephedrine, which has two asymmetric carbons, belongs to the erythro or threo series has been tried by various physical or chemical methods. For example, it was reported that a large difference in the rate of N→O acyl migration in N-acyl ephedrine and in N-acyl *Ψ*-ephedrine was available for the discrimination between diastereoisomeric ephedrines, N-methylephedrines and 1,2-diphenyl-2-methylaminoethanols-(1)[1]. On the other hand, the fact that pKa of *Ψ*-ephedrine is larger than that of ephedrine was applied to the determination of the relative configuration of 8- and 9-carbon atoms in quinine and quinidine[2]. It was also reported that from the observations of the infrared absorption spectra no general relationship was obtained for the discrimination between diastereoisomers of *β*-oxyamino-acids[3] and chloramphenicols[4], although it had been postulated that in their spectra finger print region should show marked differences.

Many chemical evidences revealed that spatial configuration of erythro compound like ephedrine differed from that of *Ψ*-ephedrine[5] and that hydroxyl and methylamino groups were placed near each other in *Ψ*-ephedrine and far apart in ephedrine. However, recent investigations of crystal structure of ephedrine hydrochloride[6] and of reaction mechanism of ephedrine[7] confirmed spatial approach of the two polar groups also in ephedrine. Accordingly there seems to be a contradiction between these results and the old conclusions. If the earlier view of spatial configurations of diastereoisomeric ephedrines be correct, there should be hydrogen bond between the hydroxyl and methylamino groups only in *Ψ*-ephedrine. Then it will be expected reasonably that the existence of this hydrogen bonding should cause some characteristic difference in the infrared spectra of diastereoisomers.

One of the purposes of the present investigation is to find some correlation, if any, useful for the discrimination between diastereoisomers in the infrared spectra of ephedrines and related compounds.

Experimental

Materials.—All compounds used in the present experiments were prepared by Dr. K. Tanaka

1) G. Fodor, V. Bruckner, J. Kiss and G. Ohegi, *J. Org. Chem.*, **14**, 337 (1949).

2) V. Prelog and O. Haefliger, *Helv. Chim. Acta*, **33**, 2021 (1950).

3) H.E. Carter, J.B. Harrison and D. Shapiro, *J. Am. Chem. Soc.*, **75**, 4705 (1953); E.D. Bergmann, H. Bendas and E. Resnick, *J. Chem. Soc.*, **1953**, 2564; W.A. Bolhofer, *J. Am. Chem. Soc.*, **71**, 1322 (1954).

4) R.A. Cutler, C.M. Martini and F.C. Nachod, *J. Am. Pharm. Assoc. Sci. Ed.*, **43**, 697 (1954).

5) L.H. Welsh, *J. Am. Chem. Soc.*, **71**, 3500 (1949); W.J. Close, *J. Org. Chem.*, **15**, 1131 (1950); K. Tanaka, *J. Pharm. Soc. Japan*, **70**, 212, 216, 220 (1950).

6) G.D. Phillips, *Acta Cryst.*, **7**, 159 (1954).

7) M. Murakami and T. Fukumoto, *J. Chem. Soc. Japan (Pure Chem. Sect.)*, **76**, 270 (1955).

and Mr. S. Sugawa and their m.p.'s and $[\alpha]_D$'s were consistent with the already reported values.

Solvents.—*Chloroform.*—Washed with dilute NaOH solution, and water, distilled after drying with anhydrous sodium sulfate and before use, dried with phosphorous pentoxide for two hours.

Carbon tetrachloride.—Washed with conc. sulfuric acid, dilute NaOH solution and water. After drying with anhydrous sodium sulfate, distilled over phosphorous pentoxide through a 40 cm., glass helix-packed column. Used after confirmation of the elimination of water by the absence of OH absorption at 2.70 μ in a 2 cm. cell.

Infrared Measurement.—A Perkin-Elmer double beam infrared spectrophotometer Model 21 was used. Spectra of solid materials were taken in Nujol mull with NaCl optics. The thickness of cell spacer was 0.01 mm. Concentration of chloroform solution was about 20 mg./cc. and a sealed cell of 0.056 cm. thickness with NaCl windows was used. The absorption of the solvent was compensated by placing a variable thickness cell filled with the solvent in the reference beam. The spectra in the case of NaCl optics were taken under the following conditions; gain 5, response 1, suppression 4, resolution 3. The spectra of carbon tetrachloride solution were taken with LiF prism in a 2 cm. glass cell having calcium fluoride windows. Ammonia-treated casein paste was used to attach the windows to the glass cell. The absorption curves were obtained by subtraction of optical densities of solvent from that of solution. The following operating conditions were used (LiF); gain 7, response 2, slit 30 μ, suppression 0, scanning speed 10–15 min./μ. Under these conditions the absorption spectra of ethylene glycol and N-methyl acetamide in the dilute carbon tetrachloride solutions were in good agreement with those reported by other authors[8].

Experimental Results and Discussion

A. Absorption Spectra of Solid Materials 3600–1800 cm^{-1} Region.—In this region the appearance of absorption bands due to OH and NH stretching vibrations are expected. As shown in Table I, most of the compounds examined show only one band near 3300 cm^{-1}, but exceptions are diastereoisomers of 1-chloro substituted ephedrine hydrochlorides and of O-benzoyl ephedrine hydrochloride, which have no OH group and no absorption band near 3300 cm^{-1}. These two compounds, however, show a well-defined band near 2400 cm^{-1}, which is observed also in the

Table I

Absorption bands of solid materials in 3 μ region

Substance	Absorption bands (cm^{-1})		
dl-ephedrine hydrochloride	3333 (3333)*	2740	2460
l- 〃	3328 (3330)	2740	2460
dl-Ψ-ephedrine hydrochloride	3260 (3247)	2710	2455, 2425
d-Ψ- 〃	3250 (3230)	2710	2465, 2425
dl-ephedrine	3300 (3300)		2340 (?)
l-ephedrine (liquid)	3290	2786	
〃 (solid)**			2330 (?)
dl-Ψ-ephedrine	3300 (3290)		2350
d-Ψ- 〃	3200 (3216)		
dl- and *l*-1-chloro-1-phenyl-1-2-methyl-aminopropan hydrochloride		2670	2460
dl- and *d*-Ψ-1-chloro-1-phenyl-2-methyl-aminopropan hydrochloride		2670	2470, 2430
dl-N-benzoyl ephedrine	3310	2660	
dl-N-benzoyl Ψ-ephedrine	3240	2660	
dl-O-benzoyl ephedrine hydrochloride		2700	2450
dl-O-benzoyl Ψ-ephedrine hydrochloride		2700	2415
l-N-methylephedrine	***		2350 (?)
d-Ψ-N-methylephedrine (liquid)	3330	2780	
dl-N-methylephedrine hydrochloride	3215	2674	2494, 2421
dl-erythro-1, 2-diphenyl-2-methylamino-ethanol-(1) hydrochloride	3280		2421, 2300
dl-threo-1, 2-diphenyl-2-methylamino-ethanol-(1) hydrochloride	3290	2667	2494, 2353

* Values in parentheses were taken with LiF prism in perfluorocarbon mull.
** Monohydrate.
*** A broad band superposed on CH absorption.

8) a) L. P. Kuhn, *J. Am. Chem. Soc.*, **74**, 2492 (1952);
b) M. Tsuboi, *Bull. Chem. Soc. Japan*, **22**, 215 (1948).

spectra of ephedrine hydrochlorides, not so marked in those of ephedrines and absent in those of N-benzoyl compound having no NH group. Since a band near 3300 cm^{-1} of N-methyl ephedrine and N-benzoyl ephedrines is undoubtedly due to OH group, it seems to be reasonable to assign ν (OH) to the band near 3300 cm^{-1}.

Following the above-mentioned assignment of ν (OH), it may be said that absorption due to free NH vibration, for which Randall et al.[9] quote an overall range of 3480–3050 cm^{-1}, is absent near 3300 cm^{-1}. Therefore, either a band near 2700 cm^{-1} or one near 2400 cm^{-1} may be due to perturbed NH vibration. The latter band seems to be due to the ionic form like $>NH_2^+$, at least in the case of hydrochlorides, because the evidences for the existence of such a band were found in the cases of bydrochlorides of triethylamine (2540 cm^{-1})[10], pyridine (2425 cm^{-1})[10], myosmine and nicotine (2560–2360 cm^{-1})[11], and in the fact that N-benzoyl ephedrine without NH group shows no absorption near 2400 cm^{-1}. As to the absorption band near 2700 cm^{-1} it seems to be related not to NH group, but to $N\text{-}CH_3$ group as will be seen in chloroform solution, since this band is observed forN-methylephedrine and N-benzoyl ephedrine, having no NH group.

Three absorption bands in the 1950–1800 cm^{-1} region can be ascribed to a monosubstituted benzene ring from their position and intensity relationship[12].

It will be noticed that there are systematic differences in ν (OH) of hydrochlorides of diastereoisomeric ephedrines near 3300 cm^{-1}. That is, Ψ-ephedrine hydrochloried shows an absorption of frequency about 100 cm^{-1} lower than that of ephedrine hydrochloride and the corresponding racemic modifications. The same is the case for N-benzoyl compounds, but not so marked in the cases of ephedrines and 1, 2-diphenyl-2-methylamino-ethanols-(1). From these observations and the generally accepted explanation that formation of hydrogen bond in a crystal causes a lowering of the OH absorption frequency from its normal position and that the magnitude of the shift is related to the strength of the hydrogen bond, it will be said that the hydrogen bond is formed in crystals of both of the corresponding diastereoisomers, it being only stronger in Ψ-ephedrine than in the normal one. Although such a tendency cannot be said to be general for all of the test compounds in crystalline state, it is worth noticing that a difference in the OH absorption frequency is found between diastereoisomers and between optically active, *d*- or *l*-compound and the corresponding recemic modification.

1800–1600 cm^{-1} Region.—From Figs. 1 and 2 it is seen that a band common to all compounds appears at 1600 cm^{-1}. Absorption bands which are expected to appear in this region are those due to a benzene ring and NH deformation vibration. Since the latter band is generally very weak, the 1600 cm^{-1} band may be assigned to C-C vibration of benzene ring in conjunction with 1500 cm^{-1} band observed[12].

N-benzoyl compounds show a strong band near 1600 cm^{-1}, which may be due to C=O vibration of the benzoyl group (Fig. 2). For

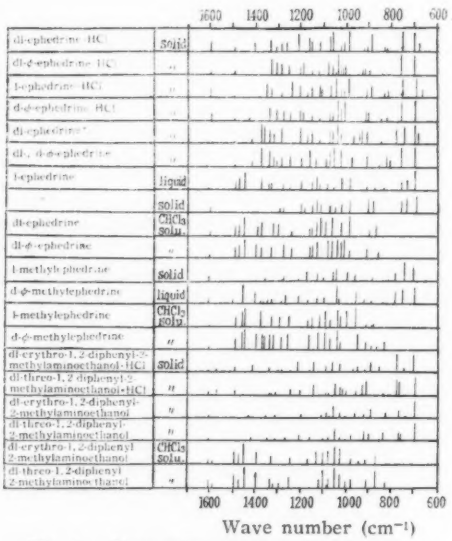

Fig. 1. Absorption spectra of ephedrine and related compounds in Nujol mull and in chloroform solution: 1600–600 cm^{-1}.

it can be considered that hydrogen bonding may lower the C=O frequency from 1670–1630 cm^{-1}, which is normal absorption frequency range for C=O group in disubstituted amide[12], to 1590–1613 cm^{-1}. Here again, pseudo compounds give a lower C=O frequency than that of the normal ones. On the other hand, O-benzoyl compounds also show a C=O band of slightly lower frequency (1715 cm^{-1}) than that for the C=O group in

9) H.M. Randall, R.G. Fowler, N. Fuson and J.R. Dangle, "Infrared Determination of organic structures", Van Nostrand (1949).
10) R.C. Lord and R.E. Merrifield, *J. Chem. Phys.*, **21**, 166 (1953).
11) B. Witkop, *J. Am. Chem. Soc.*, **76**, 5597 (1954).
12) L.J. Bellamy, "The infrared spectra of complex molecules", Methuen & Co. London (1954).

methyl benzoate (1754 cm^{-1})[13].

Finger Print Region.—From a survey of the spectra of all the compounds examined in the finger print region, it is noticed that there is a marked difference between the spectra of diastereoisomer for both optically active and corresponding racemic pairs. If there is any systematic difference in band position, this will be available for the discrimination between diastereoisomers. Bolhofer[3] attributed the erythro structure to the substituted β-phenyl-serines showing a band at 11.90–11.95 μ (840 cm^{-1}). However, his assignment stands in contradiction with observation by Cutler et al.[4] on the substituted chloramphenicols and that on the present series of compounds.

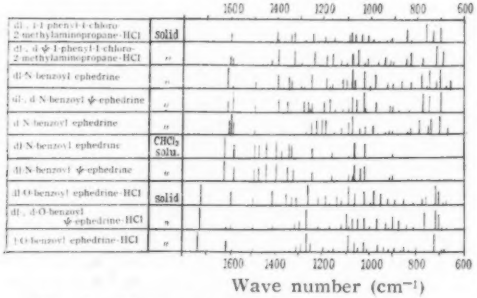

Fig. 2. Absorption spectra of ephedrine derivatives: 1800–600 cm^{-1}.

pending on compounds. It will be noticed that the pseudo-compounds give a lower frequency absorption than that of the normal ones, except ephedrine and Ψ-ephedrine. This fact may be used to discriminate diastereoisomers in conjunction with the absorption in other region such as 3 μ region.

Besides these, the following observation may be added that Ψ-ephedrine, N-benzoyl Ψ-ephedrine, O-benzoyl Ψ-ephedrine hydrochloride and both diastereoisomers of 1-chloro-substituted ephedrine give the same spectra for both the optically active compound and its racemic modification. These facts may suggest that some factors like steric configuration of molecule and the existence of a polar group capable of forming hydrogen bond affect the formation of crystal of racemic compounds as Sensi and Fagioli[14] observed on chloramphenicols.

B. Absorption Spectra in Chloroform Solution

In Fig. 3 absorption spectra in 3 μ region of chloroform solutions of ephedrines, N-methylephedrines, 1,2-diphenyl-2-methylaminoethanols-(1) and N-benzoyl ephedrines are shown. There is a remarkable similarty among these spectra; that is, all of the compounds examined show two bands in a region 2.7–3.2 μ, one of which is sharp (the higher frequency) and the other is broad (the lower frequency). The higher frequency band near 2.7 μ may

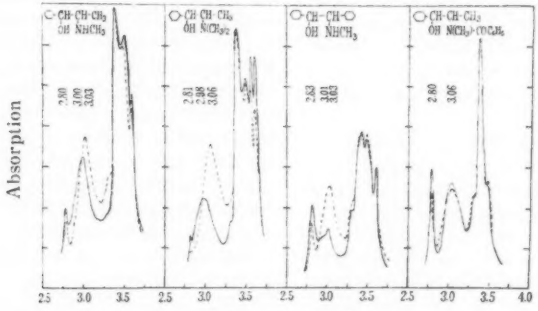

Fig. 3. Absorption of ephedrine and related compounds in chloroform solution (~0.1 mol./l.) near 3 micron.
——— erythro (normal), ----- threo (pseudo). NaCl prism.

It is usually accepted that the absorption due to secondary alcohol occurs near 1100 cm^{-1} and 1300 cm^{-1} [12], the former being fairly strong. As seen in Figs. 1 and 2, there appears a strong band within a range of 1030–1060 cm^{-1}, the position of which varies de-

be due to free OH vibration, but the lower one near 3.1 μ will be due to hydrogen-bonded OH vibration, free NH vibration or superposition of these. Since in N-methylephedrine the lower frequency absorption can be ascribed undoubtedly to the bonded OH vibration, the

13) E. J. Hartell, R. E. Richards and H. W. Thompson, *J. Chem. Soc.*, **1948**, 1436.

14) P. Sensi and O. Fagioli, *Gaz. Chim. Italiana*, **83**, 73 (1953).

same assignment seems to be reasonable for the other compounds. Moreover, the frequency difference between the sharp band and the broad one seems to be larger for pseudo-compounds than for normal ones, except in the case of N-benzoyl ephedrines.

The absorption bands near 3.4 μ are assigned to CH stretching vibration of methyl and $-CH_2-$ groups. 3.59 μ band of ephedrine, 3.56 μ band of 1,2-diphenyl-2-methylaminoethanol-(1) and 3.56 μ and 3.62 μ bands of N-methyl ephedrine, which are lower than any of CH vibration frequency of saturated hydrocarbon, could be regarded as due to CH_3-N group.

The absorption due to monosubstituted benzene derivatives in 2000–1800 cm^{-1} region appear very clearly in the spectra of chloroform solution. Absorption spectra with frequency lower than 1600 cm^{-1} are shown in Figs. 1 and 2. The spectra of the diastereoisomers show closer similarity than those in solid state. A strong band near 1000–1100 cm^{-1} has the same position for both isomers, except for ephedrines.

C. Absorption Spectra of Dilute Carbon Tetrachloride Solution[15]

As mentioned above a molecule like ephedrine may have an intramolecular hydrogen bond and this should be proved by spectra taken in a dilute carbon tetrachloride solution within the concentration range causing no intermolecular association. To ascertain more precisely the results of chloroform solution, spectra of diastereoisomers in 3 μ region were taken in carbon tetrachloride solution under a concentration of about 0.005 mol./l., by using LiF prism. The results are shown in Fig. 4.

In this case also, all compounds give very similar spectra, consisting of a higher frequency sharp band (3615–3621 cm^{-1}) and a lower frequency broad band (3329–3466 cm^{-1}). However, it is worthy of notice that only exceptionally erythro 1,2-diphenyl-2-methylaminoethanol-(1) shows two sharp bands near 3600 cm^{-1}. The difference in the frequency of the sharp and the broad band is always greater in a pseudo compound ($\Delta\nu$=ca. 200 cm^{-1}) than in the corresponding normal one ($\Delta\nu$=ca. 150 cm^{-1}). Thus, the results obtained in chloroform solutions were fully confirmed. According to the generally accepted explanation the sharp bands (3615–3621 cm^{-1}) may be attributed to free OH vibration and the broad ones (3329–3466 cm^{-1}) to the hydrogen-bonded OH vibration. Since the concentration dependence of the ratio of the optical densities of the two bands was not appreciable and also since it was reported from the result of molecular weight determination in benzene solution that the association of the alkamines did not occure over the concentration range such as in the present experiments[16], it might be said that in a sense the hydrogen bond is that of an intramolecular type. Then, it will be concluded that a hydrogen bond exists in molecules of both of corresponding diastereoisomers, only strong in *l*-ephedrine than in a normal one. This conclusion confirms the above-mentioned suggestion based on results of the experiments in the solid state and chloroform solution, and the discrimination between diastereoisomers of ephedrine and its derivatives can be carried out simply and clearly by comparing the magnitude of the frequency difference between the free and the hydrogen-bonded OH vibrations.

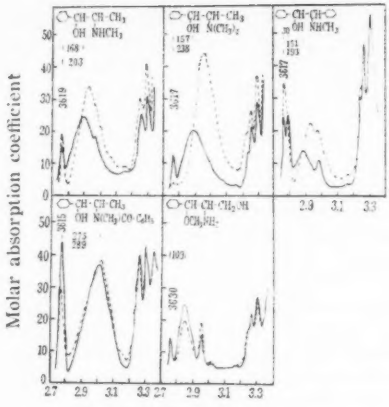

Fig. 4. Absorption of ephedrine and related compounds in carbon tetrachloride solution (~0.005 mol./l.) near 3 micron.
——— erythro (normal).
----- threo (pseudo). LiF prism.

On applying this method of discrimination between diastereoisomers to other compounds, it should be noted that the method is only applicable to compounds having two polar groups directly attached to the two adjacent asymmetric carbon atoms like ephedrines and forming a five-membered hydrogen bond ring. For example, N-benzoyl ephedrine isomers show almost the same frequency difference, because of the formation of a six-membered hydrogen bond ring, probably formed between OH and C=O group in the benzoyl radical (Fig. 4). Another example is shown in Fig. 4. 1-Phenyl-1-methoxy-2-aminopropanol-(3)

15) Partly reported as communication. T. Kanzawa, *Pharm. Bull.*, **3**, 71 (1955).

16) E.D. Bergmann, E. Gil-Av and S. Pinchas, *J. Am. Chem. Soc.*, **75**, 68 (1953).

which may form hydrogen bond between the amino group attached to asymmetric carbon and the OH group in the terminal CH_2OH, shows almost identical band position for diastereoisomers.

The author wishes to express his sincere thanks to Professor I. Nitta of Osaka University for his kind guidance and to Dr. K. Tanaka and Mr. T. Sugawa in this Laboratory for the kind supply of many materials. The author's thanks are also due to Dr. S. Kuwada, head of this Laboratory, and to Dr. A. Watanabe, head of the department, for their continued encouragement.

Research Laboratory, Takeda Pharmaceutical Industries Ltd., Osaka

*Ultraviolet Spectrophotometric Determination of Nickel with α-Benzildioxime**

By Yasumitsu UZUMASA and Shigenari WASHIZUKA**

(Received November 4, 1955)

α-Benzildioxime was first used by Tschugaeff[1] for the detection of nickel. The reagent was further studied by Atack and others for its estimation[2,3]. Though this reagent is superior to dimethylglyoxime as a precipitant of nickel, very few methods have been hitherto proposed for the colorimetric as well as spectrophotometric determination of microgram quantities of the element, the dimethylglyoxime method being thus still widely utilized[4].

In the present paper a sensitive spectrophotometric method for determining nickel with α-benzildioxime is proposed. This method comprises extraction of the nickel (II) chelate compound with chloroform and subsequent photometric measurement in the ultraviolet region. Recently, Ni (II)-α-furildioxime in 1,2-dichlorobenzene[5] and also Ni (II)-dimethylglyoxime in chloroform[6] have been recommended as colored complexes suitable for the direct determination of nickel. However, because of the higher sensitivity of its colored system, the present procedure seems to have some advantage over these two methods.

The absorbance readings for the determination have been carried out at the wave lengths of 275, 358, and 406 mμ. The characteristic absorption maximum at 275 mμ is more sensitively measured than those at 358 and 406 mμ. On account of intense spectral absorption of α-benzildioxime itself in the ultraviolet region, the absorbance reading at 275 mμ can not be performed unless the excessive reagent is completely eliminated from the solvent. The present method is available for the determination of nickel in the presence of copper.

Reagent and Apparatus

The stock solution of nickel was prepared by dissolving 4.805 g. of nickel sulfate heptahydrate in 0.1 N sulfuric acid and diluted with the same to 1 liter. An aliquot of this solution was again diluted with 0.1 N sulfuric acid and the resultant solution containing 2 μg. of nickel per ml. served as standard.

The α-benzildioxime 0.02% solution was prepared by dissolving 0.02 g. of the reagent in 100 ml. of a mixture of ethyl alcohol and concentrated ammonia (95 to 5 by volume).

Redistilled chloroform was used for extraction and sodium tartrate or citrate 10% solution for preventing the precipitation of ferric hydroxide.

Glass stoppered test tubes (20 mm. × 150 mm.) and a shaking apparatus (200 cycles per minute) were most conveniently utilized for extraction and washing.

All absorbance readings were made with a Beckman Model DU spectrophotometer equipped with 1 cm. quartz cells.

* On October 31, 1954, part of this paper was read before the 3rd Annual Meeting of the Japan Society for Analytical Chemistry.

** Present address, Laboratory of Chemistry, Hokkaido Gakugei University, Asahigawa.

1) L. Tschugaeff, *Z. anorg. Chem.*, **46**, 144 (1905).
2) F.W. Atack, *Analyst*, 38, 316 (1913); *C.A.*, 7, (1913); *J. Chem. Soc.*, **1913**, 103 1317.
3, 7) Frank J. Welcher, "Organic Analytical Reagents", Vol. III., D. Van Nostland Company, Inc. New York, 1947, pp. 224-7; W.F. Hillebrand, G.E.F. Lundell, H.A. Bright, J.I. Hoffman, "Applied Inorganic Analysis", 2nd Ed., John Wiley & Sons, Inc., New York, 1953, pp. 411-2.
4, 9) E.B. Sandell, "Colorimetric Determination of Traces of Metals", 2nd, Ed., Interscience Publishers, Inc., New York, (1950) pp. 469-74.
5) A.R. Gahler, and A.M. Mitchell with M.G. Mellon, *Anal. Chem.*, **23**, 500 1951.
6) W. Nielsch, *Z. anal. Chem.*, **140**, 267 (1953).

Absorption Spectra of α-Benzildioxime and its Nickel Chelate in Chloroform

Nickel compound was precipitated according to the procedure described to the ordinary analytical method[7] and recrystallized from chloroform. It was dissolved in chloroform and subjected to the spectral measurements at the wave lengths between 250 and 500 mμ. Three distinct absorption bands of the chelate appeared at λ=275, 358, and 406 mμ, among which the band at 275 mμ was most pronounced in intensity[8].

In Fig. 1, curve 1 shows the absorption spectrum of nickel chelate obtained by the extraction process. In the region shorter than 300 mμ there appears a continuous absorption. This is obviously due to the intense absorption of the excessive reagent transferred to the chloroform layer during the extraction. However, the absorption curve showed a maximum at 275 mμ when the chloroform solution was washed with a dilute sodium hydroxide solution (curve 2). Curves 3 and 4 represent the absorption spectra of α- benzildioxime before and after being washed with sodium hydrodroxide. From these observations it was made clear that the excessive reagent transferred frkm the aqueous solution into the chloroform layer can be almost entirely removed by washing.

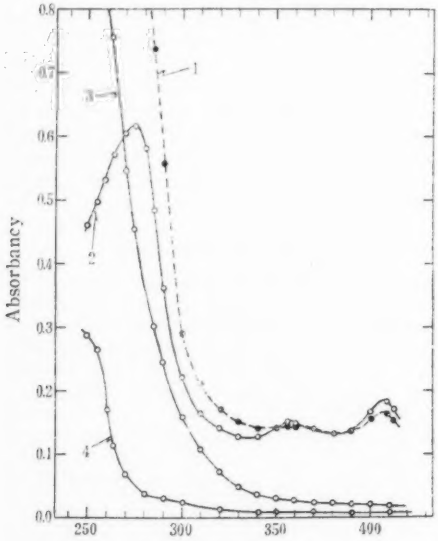

Fig. 1. Absorption spectra of α-benzildioxime and its nickel (II) chelate in chloroform.
1: Ni chelate, 0.8 p.p.m. as nickel, 2: Ni chelate washed with dil. NaOH, 0.8 p.p.m. as nickel, 3: α-benzildioxime, 4: α-benzildioxime washed with dil. NaOH.

Absorption Spectra of Copper (II) and Cobalt (II) combined with α-Benzildioxime

Copper was found to be also transferred to the chloroform phase to a great extent in the said extraction process which certainly caused an interference in the estimation of nickel. This interference was nearly obviated, however, since a striking color change from brown to yellow took place when the liquid was shaken with a dilute sodium hydroxide solution. Further elimination of the copper from the chloroform phase could be made if the chloroform phase was shaken with dilute ammonia. In case of the dimethylglyoxime method[9] copper may be entirely removed from the chloroform extract when shaken with dilute ammonia. However, the removal of copper α-benzildioxime from the chloroform phase is not satisfactory if the extract is washed only with ammonia.

Cobalt is also transferred to the chloroform phase in the extraction process, and the interference of this metal could not be simply eliminated by washing with sodium hydroxide

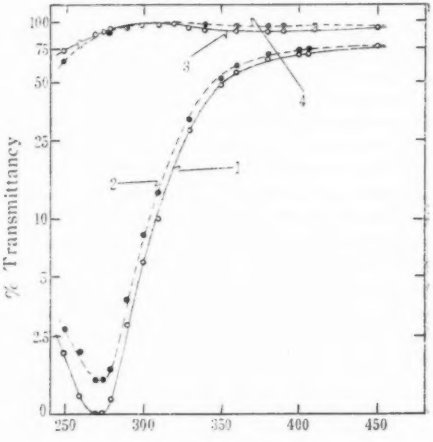

Fig. 2. Absorption spectra of copper with α-benzildioxime in chloroform.
1: copper in original extract, 2: washed with dil. ammonia, 3: washed with dil. NaOH, 4: washed with dil. NaOH, then with dil. ammonia.

solution and ammonia. These effects are shown in Fig. 2 and are summarized as follows:

8) K. Sone, *J. Am. Chem. Soc.*, 75, 5207 (1953).

Metal,	Color in chloroform,	Color after washing with NH_4OH,	with NaOH,	with NaOH then NH_4OH
Ni-complex	yellow	yellow	yellow	yellow
Cu-complex	brown	brown	yellow	colorless
Co-complex	yellow	yellow	yellow	yellow

From these experimental results it was confirmed that the positive error due to the presence of copper is most effectively minimized by washing the chloroform extract first with a dilute sodium hydroxide solution and then with dilute ammonia.

Fig. 3 indicates that by this treatment the absorption of the copper compound becomes almost negligible in the region longer than 300 mμ whereas the band due to cobalt whose maximum is 260 mμ still predominates. This fact suggests to us that the present procedure allows us to estimate nickel in the solution which contains a certain amount of copper but no cobalt.

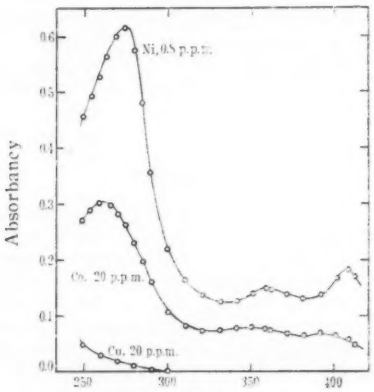

Fig. 3. Absorption curves of nickel, cobalt, and copper.

Conditions for Color Development and Extractions

Effect of pH.—Completeness of precipitation and extractability with chloroform using buffer solutions with pH ranging from 6.0 to 11.4. The optimum pH for the extractions was found to be 8.8 or above. When pH of the solution exceeds 8.8 the nickel complex precipitates immediately, allowing the extraction to be carried out rapidly. This fact shows that the strict adjustment of pH is not necessary, thus eliminating the use of a buffer.

Duration and Number of Extractions.—In order to determine the duration of extraction a series of solutions containing a definite amount of nickel were extracted by shaking the containers mechanically with a shaking apparatus (200 cycles per min.) for some time. Data in Table I show that the duration of two minutes is sufficient for removing the complex from the aqueous solution provided that 5 ml. of chloroform is used. Complete removal was confirmed by the absence of the spectral absorption due to the nickel chelate in the second chloroform extract. When the volume of the aqueous solution was 5 to 50 ml., complete extraction was established by shaking with 5 ml. of chloroform for two minutes.

TABLE I

EFFECT OF DURATION ON EXTRACTION

Duration, min.	Absorbancy 358 mμ	406 mμ
2	0.666	0.740
5	0.668	0.744
10	0.666	0.744
15	0.666	0.744

Aqueous volume, 15 ml. Nickel taken, 20 μg.
Organic solvent, 5 ml. of chloroform at a time.

Amount of Reagent. — The solubility of α-benzildioxime in ethyl alcohol is about 0.2 g. per liter, which increases to some extent in ammoniacal medium. In the present method the reagent solution of 0.02% was prepared, 2 ml. of which was required to extract 20 μg. of nickel (theor. mole ratio of the reagent for nickel was 1 : 2.5) this was the maximum concentration (4 p.p.m. in chloroform) available in this determination. Although up to 4 ml. the reagent was found to give no effect on the absorbancy of the nickel chelate in the measurements at 358 and 406 mμ, 2 ml. was used lest the reagent should make any disturbance. Since the absorption, especially at 275 mμ, due to α-benzildioxime itself, was intense the use of more of the reagent must be avoided.

General Procedure

Isolation of Nickel.—To about 15 ml. of slightly acidic sample solution in a glass stoppered test tube, containing up to 20 μg. of nickel, add 2 ml. or more of 10% sodium tartrate or citrate solution to prevent the precipitation of hydroxide of ferric iron. Make the solution ammoniacal by adding 2 ml. of 10% ammonia or a few drops of concentrated ammonia in excess, add 2 ml. of 0.02% α-benzildioxime solution, and shake the tube for ten seconds by hand. As red precipitate appears immediately, add exactly 5 ml. of chloroform with a pipet. Shake the tube for two minutes horizontally with a shaking apparatus (200 cycles per min.), and extract the precipitate.

Washing. — Draw off the aqueous layer by suction, introduce 10 ml. of 1% sodium hydroxide solution into the tube, and shake the tube for one minute as before. Draw off the alkaline layer by suction, and wash the chloroform layer once with 10 ml. of 0.5% ammonia, then with two 10 ml. portions of 1% sodium hydroxide solution for one minute successively.

Photometric Determination of Nickel.—After the last washing liquid is nearly completely removed, the chloroform solution is taken up with

a dry pipet and filtered into a 1 cm. quartz cell using dry filter paper of small size. Prepare a blank reagent solution by introducing about 15 ml. of distilled water into the tube and treating the water by the same procedure. The standard nickel solutions prepared for setting up the calibration curves should be also treated by the same procedure as the sample solution. Make the absorbance measurements for the chloroform solutions of the sample, standard, and reagent blank at 275, 358, or 406 mμ respectively, pure chloroform being put in the reference cell. Subtract the absorbancy of the reagent blank from that of the sample as well as the standard, and determine the amount of nickel in the given sample. Fig. 4 gives the calibration curves for nickel at 275, 358, and 406 mμ. As shown in Fig. 4 and Table II, the maximum sensitivity on the present spectrophotometric method is attained when the absorbance readings at 275 mμ are used. The sensitivity is superior to that of he classical dioxime method.

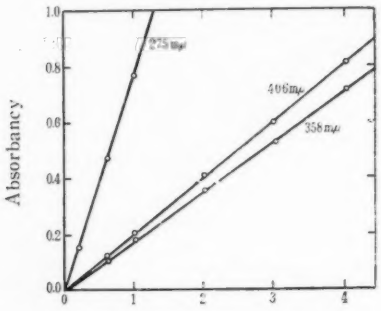

Fig. 4. Calibration curves for nickel. Beckman Model DU spectrophotometer, with 1 cm. quartz cells.

TABLE II

SENSITIVITY FOR α-BENZILDIOXIME METHOD (Solvent, chloroform)

Ni taken, p. p. m.[a]	Ni, p. p. m./($A_s \times 10^3$)[b] 275 mμ	358 mμ	406 mμ
0.2	1.31×10^{-3}	5.56×10^{-3}	4.76×10^{-3}
0.4	1.33 〃	5.55 〃	4.88 〃
0.6	1.29 〃	5.56 〃	4.92 〃
1.0	1.31 〃	5.59 〃	4.74 〃
2.0		5.62 〃	4.95 〃
4.0		5.59 〃	4.95 〃
Average	1.31 〃	5.59 〃	4.94 〃

(a) Microgram of nickel per ml. of chloroform.

(b) Sensitivity, by Sandell's definition[10]. A_s, absorbancy.

10) E. B. Sandell, "Colorimetric Determination of Traces of Metals", 2nd Ed., Intersince Publishes, Inc. New York, 1953, p. 49.

Influence of Foreign Ions

By observing the conditions prescribed above better extractability and stability of the complex are attained thusall owing much more satisfactory separation of nickel from ferric iron, aluminum, zinc, chromate, vanadate, and molybdate ions. In Table III the results for the determination of nickel in the presence of ferric iron and other interfering elements such as copper and cobalt are shown. This table shows that when as much as 5 μg. of nickel is to be determined the allowable concentration for copper is as high as 0.1 mg. and for cobalt 0.01 mg.

As already discussed copper is readily extracted into the chloroform phase from which it is eliminated by washing with sodium hydroxide solution and ammonia. In case where its concentration is higher than 0.1 mg., however, copper may hinder nickel from reacting with the reagent (expt. Nos. 4 and 5 in Table III). Therefore, if the concentration of copper should be much higher than that of nickel, the amounts of the reagent as well as chloroform must be increased.

TABLE III

EFFECT OF COPPER, COBALT, AND IRON ON THE DETERMINATION OF NICKEL

No.	Foreign ion added, mg.	Ni found, μg. 275 mμ	358 mμ	406 mμ
1	0.01 Cu	5.0	5.0	5.0
2	0.05 〃	5.1	5.1	5.0
3	0.1 〃	5.4	5.1	5.2
4	0.5 〃	1.0	1.0	0.7
5	1.0 〃	1.2	1.2	0.8
6	0.005 Co	4.9	5.0	5.0
7	0.01 〃	5.1	4.9	5.0
8	0.05 〃	5.5	5.5	5.6
9	5.5 Fe (III)	5.1	5.0	5.0
10	11.0 〃	5.1	5.0	5.0

Ni taken in 10 ml. of aqueous solution, 5.0 μg. 10 % sodium citrate solution added, 4 ml. Reagent solution added, 2 ml. Chloroform, 5 ml.

TABLE IV

REPRODUCIBILITY OF DETERMINATION OF NICKEL IN SYNTHETIC SOLUTION

	Ni found, absorbancy, 275 mμ	358 mμ	406 mμ	Deviation from Av. absorbancy 275 mμ	358 mμ	406 mμ
	0.755	0.181	0.212	0.019	0.003	0.004
	0.783	0.184	0.216	0.009	0.000	0.000
	0.780	0.178	0.217	0.006	0.006	0.001
	0.775	0.180	0.216	0.001	0.004	0.000
	0.785	0.189	0.217	0.011	0.005	0.001
	0.770	0.188	0.214	0.004	0.004	0.002
	0.768	0.187	0.218	0.006	0.003	0.002
Av.	0.774	0.184	0.216			
	Av. deviation			0.0080	0.0036	0.0014
	Max. deviation			0.019	0.006	0.004
	Av. relative deviation			1.03%	1.96%	0.65%
	Max. relative deviation			2.45%	3.26%	1.85%

Composition of the synthetic solution, Fe (III) 54.5%, Cu (II) 1.0%, Cr (VI) 1.1%, Al 32.7%, Mo (VI) 4.4%, V (V) 0.7%, Zn 5.5%, Ni 0.1%. Total amount of elements, 5.0 mg. in 10 ml.

In order to test the precision of the method, the determination was made with the synthetic solution which contained ferric iron, aluminum, zinc, chromate, vanadate, molybdate, copper, and nickel ions whose total amount was 5.0 mg. The absorbance readings of seven determinations showed average and maximum relative errors to be 1.03 and 2.45% at 275 mμ, 1.96 and 3.26% at 358 mμ, and 0.65 and 1.85% at 406 mμ respectively. These are shown in Table IV.

Summary

A new method described here involves the extraction of nickel (II)-benzildioxime with chloroform and the spectrophotometric measurements of the colored system in the same solvent. The wide pH range for the extraction eliminates the use of a buffer, and nickel is readily separated from ferric iron, aluminum, zinc, chromate, vanadate, and molybdate ions. By obviating the excessive benzildioxime with dilute alkali, the most sensitive absorbance readings are achieved, and the sensitivity at 275 mμ is 0.0013. Beer's law holds up to 1 p. p. m. of nickel at 275 mμ, and up to 4 p. p. m. at 358 and 406 mμ. The nature and degree of interference of copper and cobalt on the color development are also discussed, and their allowable amounts are determined.

Department of Chemistry, Faculty of Science, Hokkaido University
Sapporo

On the Dielectric Constant of Polar Liquid

By Masasi YASUMI and Hitoshi KOMOOKA

(Received November 15, 1955)

Introduction

The Debye's theory for the dielectric constant of polar fluids seems to be inadequate to explain quantitatively most of the experimental results for the polar liquids.

The origin of the failure of the theory has been discussed by many authors[1]. It is concluded that the inadequacy of the assumption concerning the local field adopted by Debye[2] plays the most important role.

Assuming an simplified model for the polar liquid, Onsager has obtained a quite different expreession for the local field and succeeded in deriving a formula for the dielectric constant of polar liquid[1]. In spite of the rather over-simplified model, the Onsager's formula seemed to be able to eliminate the difficulties appearing in Debye's theory[1]. Although the Onsager's theory succeeded in explaining the experimental results (at least semiquantitatively), the problem of the local field in polar liquid seems not to have been solved completely.

In the present work, we have obtained an expreession for the local field, from the point of view of the classical electrodynamics in the continuous medium. Using this expersion for the local field we have obtained also an expression for the dielectric constant. [section 2-A]

The result is as follows: a Wyman type relation between dielectric constant ε and absolute temperature T exists, i.e. $\varepsilon \sim 1/T$.

If we take into account the fluctuation of the internal field, a slightly different expression is obtained. [section 2-B]

The Internal Field and the Dielectric Constant

We assume that polar fluid is continuous and that its dipolar density $\vec{p}$ is expressed as follows:

$$\vec{p} = \vec{\mu}/v \qquad (1)$$

where v is the volume element in the polar liquid and $\vec{\mu}$ is the dipole moment of this volume element. If we assume that the shape of the molecule of which the dipolar substance consists is the sphere of the radius a, we may choose $\frac{4}{3}\pi a^3$ as volume element v, and μ may be considered as the dipole mo-

1) L. Onsager, *J. Am. Chem. Soc.*, 58, 1486 (1936). J.H. Van Vleck, *Ann. N.Y. Acad. Sci.*, 40, 289 (1940). S. Oka, "Theory of Dielectrics", Iwanami-shoten, (in Japanese) (1954).

2) The local field adopted by Debye is sometimes called Lorentz field. However, Lorentz applied this field only to the case of induced polarization. As shown below, the Lorentz field is correct when applied within this limitation.

ment of the molecule i. e.

$$v=\frac{4}{3}\pi a^3 . \tag{2}$$

[A] The case when we do not take into account the fluctuation of the internal field.

The electric field, the external field, the internal field and the self-field of the volume element v are denoted by $\vec{E}$, $\vec{E_0}$, $\vec{F}$, $\vec{E_S}$, respectively. The expression of the $\vec{E_S}$ is determined when we know the type of the self-field (i. e. dipolar, quadrupolar, etc.).

On the other hand the expression of the internal field, which is the vector sum of the external force and the forces of all other volume elements in the dielectric medium, may have a complicated form.

However, in the continuous medium, the expression of the internal field may be obtained as follows.

In the continuous medium the electric field $\vec{E}$ is resolved into the internal field and the self-field, i. e.[3,4]

$$\vec{E}=\vec{F}+\vec{E_S} . \tag{3}$$

If the self-field $\vec{E_S}$ is assumed to be dipolar and if the Eq. (2) is valid, $\vec{E_S}$ is represented as[4]:

$$\vec{E_S}=-\frac{4\pi}{3}\vec{p}=-\frac{\vec{\mu}}{a^3} . \tag{4}$$

The dipole moment of a molecule consists of two parts i. e. the permanent dipole moment $\vec{\mu_0}$ and the induced dipole moment $\alpha\vec{F}$,

$$\vec{\mu}=\vec{\mu_0}+\alpha\vec{F} \tag{5}$$

where α is the polarizability of the molecule.

The case when the molecule has not a permanent moment (non-polar molecule), the following equation holds

$$(n^2-1)\vec{E}=4\pi\vec{p} \tag{6}$$

where n is the refractive index.

In this case

$$\vec{E_S}=-\frac{(n^2-1)}{3}\vec{E} . \tag{7}$$

From the Eqs. (3), (4) (6) and (7) $\vec{F}$ is represented as:

$$\vec{F}=\vec{E}+\frac{n^2-1}{3}\vec{E}=\frac{n^2+2}{3}\vec{E} . \tag{8}$$

This is the Lorentz-Lorenz internal field.

On the other hand from the Eqs. (7), (1) and (2) (taking $\mu_0=0$)

$$\vec{p}=\frac{\alpha\vec{F}}{(4/3)\pi a^3} . \tag{9}$$

From the Eqs. (5) and (9)

$$\frac{\alpha}{a^3}=\frac{n^2-1}{n^2+2} . \tag{10}$$

Eq. (10) is the well-known Lorentz-Lorenz formula.

For the case of the polar liquid, the internal field $\vec{F}$ is expressed as: (Eqs. (3), (4) and (5) being used)

$$\vec{F}=\frac{1}{(1-\alpha/a^3)}\left[\frac{\vec{\mu_0}}{a^3}+\vec{E}\right]. \tag{11}$$

Putting (10) into (11), we obtain

$$\vec{F}=\frac{n^2+2}{3}\left[\frac{\vec{\mu_0}}{a^3}+\vec{E}\right]. \tag{12}$$

Using this equation and the Eq. (5) we have,

$$\vec{\mu}=\frac{n^2+2}{3}(\vec{\mu_0}+\alpha\vec{E}) . \tag{13}$$

The component of $\vec{\mu}$ along the direction of $\vec{E}$ is denoted by μ_E, and the mean value of μ_E is denoted by $<\mu_E>$.

Assuming Boltzman statistics, we have the following equation,

$$<\mu_E>=\int\mu_E\cdot e^{-\frac{U}{kT}}d\Omega\Big/\int e^{-\frac{U}{kT}}d\Omega \tag{14}$$

where U is the potential energy of the dipole $\vec{\mu}$ in the electric field and $d\Omega$ is an elementary solid angle. U has the following expression

$$U=-\left\{\frac{1}{2}\alpha F^2+(\vec{\mu_0}\cdot\vec{F})\right\} . \tag{15}$$

Let the angle between $\vec{E}$ and $\vec{\mu_0}$ be θ,

$$\mu_E=\frac{n^2+2}{3}(\mu_0\cos\theta+\alpha E) . \tag{16}$$

Inserting (15) and (16) in (14) and making a simple calculation we have the following expression for $<\mu_E>$,

$$<\mu_E>=\frac{n^2+2}{3}\alpha E+\left(\frac{n^2+2}{3}\right)^3\frac{\mu_0^2}{3kT} . \tag{17}$$

In this calculation $e^{-\frac{U}{kT}}$ is expanded in the power series of E, and only the terms proportional to E are retained.

The dielectric constant is related to $<\mu_E>$ by the following equation.

$$(\varepsilon-1)E=\frac{4\pi N}{V}<\mu_E> , \tag{18}$$

where N is Avogadro's number and V is

3) J.H. Van. Vleck, "Theory of Electric and Magnetic Susceptibilities".

4) H. Fröhlich, "Theory of Dielectrics". Oxford (1949).

molecular volume. In our model of the dipolar molecule,

$$\frac{N}{V}=\frac{1}{(4\pi/3)a^3} \quad . \tag{19}$$

Using the Eqs. (18), (17), (19) and (10), we have

$$\varepsilon-n^2=\frac{4\pi N}{V}\left(\frac{n^2+2}{3}\right)^2\frac{\mu_0^2}{3kT} \quad . \tag{20}$$

J. Wyman proposed the following simple experimental formula for the dielectric constant of polar liquids[5],

$$\varepsilon+1=K_w p \quad , \tag{21}$$

where

$$p=\frac{4\pi}{3}\cdot\frac{N}{V}\cdot\frac{\mu_0^2}{3kT} \quad . \tag{22}$$

K_w represents a constant and amounts to about 8.5 for most of normal polar liquids.

In the case when ε is much greater than n^2, the form of the Eq. (20) is similar to that of the Eq. (21), i. e.

$$\varepsilon\simeq 3\left(\frac{n^2+2}{3}\right)^2 p \quad . \tag{23}$$

Moreover if $n=1.5$ the factor of p $\left(\text{i. e } 3\left(\frac{n^2+2}{3}\right)^2\right)$ amounts to about 8.5. Since the refractive index of most of the liquid is about 1.5 the validity of the Wyman's relation is explained by our theory.

[B] The case when the fluctuation is taken into account.

In the above-mentioned treatment, we have assumed that the local field is expressed by means of the self-field and the electric field. However, actually the form of the local field may be very complicated, since it is the sum of the external field and the fields of all other molecules. It is beyond our ability to treat this problem rigorously.

We attempt to solve this problem making an assumption for the form of the fluctuating local field $\vec{F}_f$, when it is slightly different from its mean value $\vec{F}_m$.

Consider at first the static equilibrium. In this case, $\vec{F}_m=\vec{F}$. Next we imagine that the molecule considered changes its orientation by some action. In this case we assume that the arrangement of the sorrounding molecules does not change. That is to say, the magnitude of F_f is equal to that of F_m, but its orientation is not the same as in the static equilibrium.

5) J. Wyman, *J. Am. Chem. Soc.*, 58, 1482 (1936).

In other words, the direction of $\vec{F}_f$ can take any direction independent of the direction of $\vec{\mu}_0$. Moreover we assume that the probability of orientation is regulated by Boltzmann's factor.

The expression for $\vec{F}_f$ and $\vec{\mu}$ may have the following forms:

$$\vec{F}_f=\left(\frac{n^2+2}{3}\right)\left(\vec{E}+\frac{\mu_0}{a^3}\vec{u}_1\right) \tag{24}$$

$$\vec{\mu}=\alpha\vec{F}_f+\mu_0\vec{u}_2 \quad , \tag{25}$$

where $\vec{u}_2$ is the unit vector along the direction of $\vec{\mu}_0$, and $\vec{u}_1$ represents the unit vector along the direction of the fluctuating local field. In this case, the electric field (denoted by $\vec{E}_f$) also fluctuates about the direction of $\vec{E}$.

$$\vec{E}_f=\vec{F}_f+\vec{E}_S=\vec{E}+\frac{\mu_0}{a^3}(\vec{u}_1-\vec{u}_2) \quad . \tag{26}$$

In the case of absence of the fluctuation $u_1=u_2$, then $\vec{E}_f$ coincides with $\vec{E}$.

The potential energy of a molecule assumes the following form:

$$U=-\left\{\frac{1}{2}\alpha F_f^2+\mu_0(\vec{u}_2,\vec{F}_f)\right\} \quad . \tag{27}$$

In this case $<\mu_E>$ is expresses as:

$$<\mu_E>=\iint(\vec{\mu},\vec{\mu}_0)e^{-\frac{U}{kT}}d\Omega_1 d\Omega_2\Big/\iint e^{-\frac{U}{kT}}d\Omega_1 d\Omega_2 \tag{28}$$

where $\vec{u}_0$ denotes the unit vector along $\vec{E}$. $d\Omega_1$ and $d\Omega_2$ represent the elementary solid angles the around directions of $\vec{u}_1$ and $\vec{u}_2$ respectively.

A calculation transforms the Eq. (28) to the following expression:

$$<\mu_E>=E\left[\frac{n^2+2}{3}\alpha+\frac{\mu_0^2}{3kT}\left(\frac{n^2+2}{3}\right)\times\left\{1+\left(\frac{n^2-1}{3}\right)^2\right\}+\frac{2\mu_0^2}{3kT}\left(\frac{n^2-1}{3}\right)\left(\frac{n^2+2}{3}\right)L(y)\right] \tag{29}$$

$$y=\frac{n^2+2}{3}\frac{\mu_0^2}{a^3kT} \quad , \tag{30}$$

where $L(y)$ denotes Langevin function. As in the previous case, $e^{-\frac{U}{kT}}$ is expanded in the power series of E and only the terms proportional to E are retained.

Inserting this expression for $<\mu_E>$ to the Eq. (18) we have this expression for ε,

$$\varepsilon - n^2 = \frac{4\pi N}{V}\frac{\mu_0^2}{3kT}\left(\frac{n^2+2}{3}\right)\left\{1+\left(\frac{n^2-1}{3}\right)^2\right\} + \frac{4\pi N}{V}\frac{2\mu_0^2}{3kT}\left(\frac{n^2+2}{3}\right)\left(\frac{n^2-1}{3}\right)\mathrm{L}(y). \quad (31)$$

For the large value of y, $\mathrm{L}(y)$ is approximately equal to 1. Then the Eq. (31) coincides with the Eq. (20).

For the value of y greater than 3, $\mathrm{L}(y)\fallingdotseq 1-1/y$. In this case the Eq. (31) is approximated as follows:

$$\varepsilon - \frac{n^2+2}{3} = \frac{4\pi N}{V}\frac{\mu_0^2}{3kT}\left(\frac{n^2+2}{3}\right)^3. \quad (32)$$

For most of polar liquids, the approximate Eq. (32) is sufficient, because the values of y are greater than 3 for them.

Comparison of Our Formula with Experiments

The coefficient K_w in the Wyman's formula, takes the value 8.5 for most of the normal polar liquids but fluctuates from 6.2 to 11. K_w corresponds to $3\left(\frac{n^2+2}{3}\right)^3$ in our formula (32). $3\left(\frac{n^2+2}{3}\right)^3$ takes the value 6.2 when $n=1.34$, and 11 when $n=1.62$.

For example, we calculate the dielectric constant of some of the polar liquids referred to in Wyman's paper[5], by means of our formula (32).

In Table I, the dielectric constants of esters, chlorides and nitro-compounds calculated with the Eq. (32) are given, and compared with those calculated with the Wyman's formula (21). The observed values are also given. The values of $\bar{p}$ are taken from the Wyman's paper[5].

The values of refractive indices for sodium D line n are taken from "International Critical Tables" and are also given in Table I.

TABLE I

THE DIELECTRIC CONSTANTS OF ESTERS, CHLORIDES AND NITROCOMPOUNDS

Name	n	$3\left(\frac{n^2+2}{3}\right)^3$	$\bar{p}$	$\varepsilon(Y-K)$	$\varepsilon(W)$	ε(obs.)*
Ethyl formate	1.358	6.35	1.21	9.2	9.3	8.6
Isobutyl formate	1.386	6.67	0.93	7.5	6.9	8.0
Methyl acetate	1.359	6.35	1.03	7.8	7.8	7.3
Isobutyl acetate	1.391	6.76	0.81	6.7	5.8	5.6
Ethyl salysilate	1.525	8.85	1.55	15.2	12.2	8.6
Ethyl cinnamate	1.544	9.20	0.95	10.2	7.1	6.6
Methyl benzoate	1.518	8.73	0.87	9.0	6.7	6.9
Ethyl nitrate	1.385	6.68	2.4	17.3	19.4	19.7
Acethyl chloride	1.390	6.75	2.38	17.5	19.2	15.9
Ethylidene chloride	1.417	7.15	1.15	9.5	8.8	10.9
Allyl chloride	1.415	7.10	1.27	10.3	9.8	8.2
p-Chlorotoluene	1.519	8.75	0.89	9.2	6.6	6.2
tert-Amyl chloride	1.408	6.98	1.04	8.5	7.9	9.5
Nitromethane	1.381	6.60	{3.82 5.81	{26.5 39.7	{31.5 43.4	39.4
Nitroethane	1.390	6.75	{3.26 4.76	{23.3 33.3	{26.7 39.5	30.0?
Nitrobenzene	1.553	9.40	{3.05 3.74	{30.1 36.6	{24.9 30.8	36.1
o-Nitrotoluene	1.547	9.32	2.78	27.4	22.6	27.4

* $\varepsilon(Y-K)$ is the value calculated with our formula.
$\varepsilon(W)$ is the value calculated with the formula of Wyman.
ε(obs.) is the observed value.

As Wyman has stated[5], the values of $\bar{p}$ are not satisfactorily reliable. Accordingly, we cannot bring up detailed discussion with the above-described comparison. We can only say that from the experimental point ot view, our formula (32) has applicability comparable to that of Wyman.

Next we calculate the dielectric constants of benzonitrile, nitrobenzene, ethyl bromide, ethyl iodide and chlorobenzene.

For these substances the dielectric constants in the liquid state have been measured over a considerably wide range of temperature[6]. The values are given in Table II. The densities are calculated with the equa-

6) R.J.W. Le Fevre, *Trans. Faraday Soc.*, 34, 1127 (1938).

tion referred to in "International Critical Tables".

The refractive indices are calculated from the value of molecular refraction[7] according to the Lorentz-Lorenz formula.

a) Benzonitrile.—The values of ε are calculated with the Eq. (32).

TABLE II-1

THE DIELECTRIC CONSTANTS OF BENSONITRILE

$\mu_0 = 4.39$ D[8]

t(°C)	d	n	$3\left(\frac{n^2+2}{3}\right)^2$	$\overline{p}$	ε(calcd.)	ε(obs.)
0	1.0228	1.539	9.26	4.23	40.7	27.6
18	1.0070	1.529	9.07	3.94	37.3	25.85
25	1.0018	1.526	9.02	3.83	36.0	25.2
40	0.9874	1.517	8.85	3.60	33.2	24.0
50.3	0.9782	1.511	8.74	3.45	31.5	23.28
60	0.9697	1.506	8.64	3.32	30.2	22.7
70	0.9607	1.501	8.55	3.19	28.7	22.1

b) Nitrobenzene.—The values of ε are calulated with the Eq. (32).

TABLE II-2[9]

THE DIELECTRIC CONSTANTS OF NITROBENZENE

$\mu_0 = 4.19$ D[10]

t	d	n	$3\left(\frac{n^2+2}{3}\right)^2$	$\overline{p}$	ε(calcd.)	ε(obs.)
10	1.222	1.563	9.75	3.98	40.3	37.9
25	1.168	1.550	9.48	3.76	37.1	34.9
30	1.193	1.547	6.42	3.68	36.2	34.0
40	1.183	1.542	9.32	3.53	34.3	32.3
60	1.163	1.531	9.12	3.26	31.2	29.1

c) Ethyl Bromide.—The values of ε are calculated with the Eq. (32).

TABLE II-3

Ethyl bromide

$\mu_0 = 2.01$ D[11]

t	d	n	$3\left(\frac{n^2+2}{3}\right)^2$	$\overline{p}$	ε(calcd.)	ε(obs.)
−30	1.564	1.461	5.70	1.463	9.57	11.69
−20	1.543	1.454	5.64	1.359	8.97	11.20
−10	1.5215	1.446	5.58	1.290	8.56	10.68
0	1.5014	1.439	5.52	1.226	8.09	10.19
10	1.4813	1.433	5.47	1.166	7.73	9.71
25	1.4500	1.422	5.40	1.087	7.21	9.01

d) Ethyl Iodide.—The values of ε are calculated with the Eq. (32).

TABLE II-4

Ethyl iodide

$\mu_0 = 1.87$ D[11]

t	d	n	$3\left(\frac{n^2+2}{3}\right)^2$	$\overline{p}$	ε(calcd.)	ε(obs.)
0	1.980	1.528	9.03	0.995	10.42	8.33
10	1.958	1.521	8.88	0.950	9.86	8.00
25	1.924	1.510	8.70	0.887	9.15	7.64
35	1.902	1.503	8.55	0.848	8.68	7.37
45	1.880	1.496	8.44	0.812	8.29	7.11
55	1.859	1.490	8.32	0.779	7.88	6.90
65	1.839	1.483	8.23	0.746	7.54	6.66

7) "International Critical Tables", Vol. VII, p. 32.

8) L.G. Groves and S. Sugden, *J. Chem. Soc.*, 1934, 1094.

9) The values of n and d are calculated as in the previous cases.

10) K.B. McAlpine and C.P. Smyth, *J. Chem. Phys.*, 3, 55 (1934).

11) L.G. Groves and S. Sugden, *J. Chem. Soc.*, 158 (1937).

e) Chlorobenzene.—The values of ε are calculated with the Eq. (29).

TABLE II-5

Chlorobenzene
μ_0=1.70 D[10]

t	d	n	ε(calcd.)	ε(obs.)
21	1.1053	1.524	6.05	5.67
25	1.1014	1.522	5.98	5.61
40	1.0847	1.512	5.69	5.37
48	1.0761	1.508	5.46	5.23
70	1.0520	1.495	5.10	4.89

Conclusions and Remarks

It is suprising that our theory can fairly explain the experimental data. For our theory is based upon the above-described over-simplified assumption.

As in the case of the Wyman's equation, our theory cannot be applied to the so-called abnormal liquids.

It seems that our Eqs. (31) and (32) become in better agreement with the experimental data near the boiling point than near the melting point.

The degree of coincidence of our theory with the experimental data seems to depend on the chemical structure of the molecule forming the liquid considered.

As stated by Wyman[9], if a linear relation between ε and $\bar{p}$ exists, the critical frequency ν_c will be represented as

$$2\pi\nu_c\tau=1\,, \tag{33}$$

where τ denotes the relaxation time, because the value of $<\mu_E>$ in the case of an alternating field may be represented as:

$$<\mu_E>=\left\{\frac{1}{1+i\omega\tau}\frac{\mu_0^2}{3kT}\left(\frac{n^2+2}{3}\right)+\left(\frac{n^2+2}{3}\right)\alpha\right\}E, \tag{34}$$

where ω denotes the angular frequency.

Inserting Eq. (34) into Eq. (18), ε (complex quantity) is obtained, and Eq. (33) is readily obtained.

We are grateful to Prof. San-ichiro Mizushima for his kind advice and encouragement throughout this work. Our thanks are also due to the Ministry of Education for a grant in aid of this research.

Summary

An equation for the dielectric constant of polar fluids is obtained from the point of view of the classical theory of electricity in the continuous medium.

The obtained equation has a close relationship to the empirical equation of Wyman.

The comparison with the experimental data are represented.

Institute of Science and Technology, The University of Tokyo, Tokyo

Polar Structures in the VB-Theory of Conjugated Molecules

By Hiroshi KOKADO and Yuji MORI

(Received Nobember 29, 1955)

Introduction

The parameters appearing in the semi-empirical valence bond (VB) calculation of the electronic structure of molecules, have been estimated on the basis of thermochemical data of molecules. For instance, the value of the exchange integral for π-electrons between adjacent atoms r and s,

$$\alpha=\int\cdots r(i)s(j)\cdots H\cdots s(i)r(j)\cdots d\tau$$
$$=-1.92\,\text{eV.}, \tag{1}$$

was determined from the heat of hydrogenation of unsaturated hydrocarbons by Sklar[1]. However, two improprieties are inevitable in his procedure; one is the underestimation of the ionic contribution and the other is the disregard of the compression energy resulting from bond compression in molecules. Recently Craig[2], adopting this value for α, evaluated three more quantities which enter in a rather detailed theory including polar structures,

$$\eta=\int\cdots r(i)r(j)\cdots H\cdots r(i)s(j)\cdots d\tau \tag{2}$$

$$\xi=\int\cdots r(i)r(j)\cdots H\cdots r(i)r(j)\cdots d\tau$$
$$-\int\cdots r(i)s(j)\cdots H\cdots r(i)s(j)\cdots d\tau \tag{3}^*$$

$$\zeta=\int\cdots r(i)r(j)\cdots H\cdots s(i)s(j)\cdots d\tau \tag{1'}$$

1) A.L. Sklar, *J. Chem. Phys.*, 5, 669 (1937).

2) D.P. Craig, *Proc. Roy. Soc.*, A 200, 390 (1950).

* This is recognized to be the difference between Coulomb integral of polar structure Q′ and that of non-polar one Q.

as —0.54, 4.28 and —0.48 eV. respectively, from the consideration of the spectrum of ethylene. On the other hand inconsistent with Craig's evaluation, Mulliken's approximation formula[3] claims that

$$\alpha=\int r(i)s(j)Hs(i)r(j)\mathrm{d}\tau_{ij}$$

$$=S_{rs}\int r(i)r(j)Hr(i)s(j)\mathrm{d}\tau_{ij}=S_{rs}\eta\,, \qquad (4)$$

where S_{rs} is the overlap integral between atomic orbitals of atoms r and s. This great discrepancy occurs clearly from the adoption of the above large value of α without any criticism. Keeping this fact in mind, we shall attain a new set of the semi-empirical values of integrals, making use only of spectroscopically observed results of ethylene, and examine the applicability of them to the calculation of *trans*-butadiene. In the last part of this paper, the role of η and α will be discussed in connection with the importance of the ionic character of conjugated molecules.

Evaluation of Integrals

First, the wave functions of ethylene as following are used;

$$^1\mathrm{A_g}\,(\text{ground})\quad \Psi_0=a\psi_a+\frac{b}{\sqrt{2}}(\psi_b+\psi_{b'}), \qquad (5)$$

with a relation between the coefficients $a^2+b^2=1$, and

$$^1\mathrm{B_{1u}}\,(\text{excited})\quad \Psi_1=\frac{1}{\sqrt{2}}(\psi_b-\psi_{b'}), \qquad (6)$$

in which ψ_a is written for the non-polar structure and ψ_b, $\psi_{b'}$ for the two polar ones (see Fig. 1). Then ignoring overlap, these

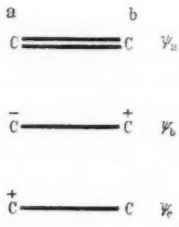

Fig. 1.

lead to a formula for the $^1\mathrm{A_g}-^1\mathrm{B_{1u}}$ excitation energy ΔE,

$$\Delta E=-2\alpha+\frac{\xi}{2}+\sqrt{\xi^2/4+4\eta^2}\,. \qquad (7)$$

Another representation of this is

$$\Delta E=\xi-2b^2\xi-2\alpha-4\sqrt{2}\,ab\eta-2b^2\alpha. \qquad (7')$$

3) R.S. Mulliken, *J. Chem. Phys.*, **46**, 497 (1949).

In order to determine the numerical values for a and b, the oscillator strength,

$$f=1.085\times10^{11}\omega(\int\Psi_0\vec{r}\,\Psi_1\,\mathrm{d}\tau)^2 \qquad (8)$$

$$=1.085\times10^{11}\omega(R^2\times10^{-16}b^2)$$

may be turned to use, where ω is the frequency of the transition in $\mathrm{cm^{-1}}$, $\vec{r}$ is the sum of the position vectors of π-electrons and R is the C=C bond distance in ethylene of ground state. Information on experimental results (ΔE=7.6 eV., f=0.25, bond length =1.35Å) makes it possible to calculate a, b, and with a further assumption of the relation (4), α, ξ and η numerically. If 0.28 is employed for S in equation (4), then we have

$$\left.\begin{aligned}a&=0.889\\b&=0.498\end{aligned}\right\} \qquad (9)$$

$$\left.\begin{aligned}\eta&=-2.15\ \text{eV.}\\\xi&=3.51\ \text{eV.}\\\alpha&=-0.60\ \text{eV.}\end{aligned}\right\} \qquad (10)$$

Much attention must be paid to the comparison of the present set of η, ξ and α with that given by Craig[2,*]. Moreover, a striking fact is that the values attained here allow the VB calculation to come very near the semi-empirical molecular orbital (MO) method which was developed quite successfully by Pariser and Parr[5] in recent years. η has a comparable numerical value as the resonance integral β (=2.75 eV.) in the semi-empirical MO calculation. This is owing to the fact that these are quite similar quantities by nature. That is, if overlap is put equal to zero,

$$\eta=\int r(i)r(j)Hr(i)s(j)\mathrm{d}\tau_{ij}\fallingdotseq\int r(j)H's(j)\mathrm{d}\tau_j=\beta.$$

On the other hand, ξ can be approximated as

$$\xi=(\mathrm{aa:aa})-(\mathrm{aa:bb}) \qquad (11)$$

where,

$$(\mathrm{rr:ss})=\int r(i)s(j)\frac{e^2}{r_{ij}}r(i)s(j)\mathrm{d}\tau_{ij}. \qquad (12)$$

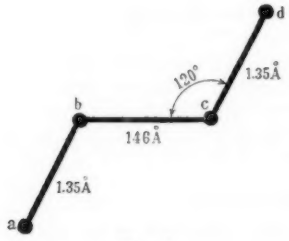

Fig. 2.

* ζ is set equal to α, like the treatment by Sklar (reference 1).

5) R. Pariser and R.G. Parr, *J. Chem. Phys.*, **21**, 466, 766 (1953)

According to the reference 5, this difference is predicted to be 10.53−7.38=3.15 eV. being close to the present value.

Another set of parameters which can be determined from the consideration of the singlet-triplet separation of ethylene, is not useful, because of the small value of ξ*.

Application to *trans*-Butadiene

In order to examine the applicability of the new set of η, ξ and α to other molecules, *trans*-butadiene is chosen. All the polar and non-polar structures are taken into account, but a simplification of considering only single exchange integrals between adjacent atoms is allowed. Corrections for η, ξ, α should be made, corresponding to the change of the internuclear distances (Fig. 3). These are done according to the following procedures**.

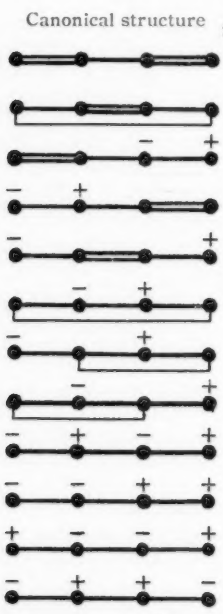

Fig. 3.

(a) $\phi_{c'}$'s are given by inversion respect to the center of molecule from ϕ_c's.

$$\left.\begin{aligned}\eta_{rs}&=\int\cdots r(i)r(j)\cdots H\cdots r(i)s(j)\cdots d\tau=S=_{rs}\eta_0\\ \alpha_{rs}&=S_{rs}\eta_{rs}=S_{rs}^2\eta_0.\end{aligned}\right\}\quad(13)$$

where η_0 is a constant to be determined by insertions of η_{rs} and S_{rs} for ethylene into (13). So, if $S_{ab}=0.27$ and $S_{bc}=0.23$ are used*,

$$\eta_{ab}=-2.07,\ \eta_{bc}=-1.77\text{ eV.};\ \alpha_{ab}=-0.56,\ \alpha_{bc}=-0.41\text{ eV.}\quad(14)$$

Moreover as to ξ next relation holds;

$$\xi=Q'-Q=(\Sigma I+\Sigma K)_{Q'}-(\Sigma I+\Sigma K)_{Qi}\quad(15)$$

where I and K are respectively core and Coulomb type repulsion integrals,

$$I=\int r(i)\sum_{p\neq r}U_p(i)r(i)d\tau_i$$

$$K=\int r(i)r(i)\frac{e^2}{r_{ij}}s(j)s(j)d\tau_{ij}=(rr:ss).$$

$U_p(i)$ signifies the potential of electron i in the field of the p-th carbon atom less its $2p\pi$-electron. Being used the Sklar type potential,

$$U_p(i)=U_p^0(i)-\int s(j)^2\frac{e^2}{r_{ij}}d\tau_{ij}$$

and zero $U_\mu^0(i)$(i. e., the potential of electron i in the field of the neutral p-th carbon atom) asumed, the problem is reduced to an estimation of Coulomb type repulsion integrals (rr : ss) only. In the case of $r=s$, i. e., (rr : rr), by a simple approximation it can be set equal to the difference between the ionization potential and the electron affinity of carbon atom (=10.53 eV.)[5]. When this is accepted, (rr : ss) corresponding to 1.34Å ($r-s$ separation for ethylene) is obtainable to be 10.53−3.51=7.02 eV., from the value of ξ. Repulsion integrals at arbitrary separations, may then be easily found supposing a linear relation to Pariser and Parr's result. Seven ξ's required are estimated by this procedure as follows (see Fig. 3).

$$\left.\begin{aligned}\xi_1&=(aa:aa)-(aa:bb)=3.53\text{ eV.}\\ \xi_2&=(aa:aa)-(aa:dd)=6.97\text{ eV.}\\ \xi_3&=(aa:aa)-(bb:cc)=3.74\text{ eV.}\\ \xi_4&=(aa:aa)-(aa:cc)=5.45\text{ eV.}\\ \xi_5&=2\xi_1+2(aa:cc)-(aa:dd)\\ &\quad-(bb:cc)=6.87\text{ eV.}\\ \xi_6&=2\xi_4+2(aa:bb)-(aa:dd)\\ &\quad-(bb:cc)=14.63\text{ eV.}\\ \xi_7&=2\xi_1-2(aa:cc)+(aa:dd)\\ &\quad+(bb:cc)=7.25\text{ eV.}\end{aligned}\right\}\quad(17)$$

The calculated energy diagram is shown in Fig. 4 together with results by several other methods.

* See reference 2.

** These formulae which contain S explicitly, never mean the inclusion of S in the actual calculation. Here, S should be recognized as a parameter defining the integrals in a function of internuclear distances.

* These values are obtained conveniently using the calculated bond orders p by the simple LCAO method, according to

$$S=0.080p+0.115$$

(N. Müller et al., *J. Am. Chem. Soc.*, **76**, 4770 (1954)).

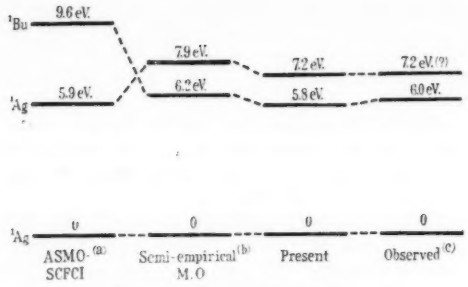

Fig. 4. Energy diagrams

(a) Y. Mori, This Bulletin, **28**, 291 (1955).
(b) Reference 5.
(c) R. S. Mulliken, Rev. Mod. Phys., **14**, 265 (1942).

The wave functions of the ground state and the first excited singlet state are

$$\left.\begin{aligned}
(^1A_g)\quad \Phi_0 &= 0.671\phi_a + 0.062\phi_b + 0.305(\phi_c+\phi_{c'}) \\
&\quad +0.337(\phi_d+\phi_{d'}) + 0.044(\phi_e+\phi_{e'}) \\
&\quad +0.103(\phi_f+\phi_{f'}) + 0.074(\phi_g+\phi_{g'}) \\
&\quad +0.070(\phi_h+\phi_{h'}) + 0.153(\phi_i+\phi_{i'}) \\
&\quad +0.009(\phi_j+\phi_{j'}) + 0.131\,\phi_k \\
&\quad +0.153\,\phi_l, \\
(^1B_u)\quad \Phi_1 &= 0.366(\phi_c-\phi_{c'}) + 0.376(\phi_d-\phi_{d'}) \\
&\quad +0.204(\phi_e-\phi_{e'}) + 0.131(\phi_f-\phi_{f'}) \\
&\quad +0.176(\phi_g-\phi_{g'}) + 0.173(\phi_h-\phi_{h'}) \\
&\quad +0.323(\phi_i-\phi_{i'}) + 0.034(\phi_j-\phi_{j'}).
\end{aligned}\right\} \quad (17)$$

Finally the oscillator strength of the transition $^1A_g - ^1B_u$ is calculated to be 0.62 (observed 0.53).

These agreements with experimental observations are sufficient to confirm the conclusion that our first evaluation of quantities η, ξ, α is not at all an irresponsible one. The resemblance to the semi-empirical MO is a natural consequence of our arrangement of the integral values.

Discussion

The most marked point in our method exists, of course, in an estimation of a great deal of ionic contribution to electronic structures. On the contrary, the semi-empirical VB-method heretofore in use, estimates little about this but a great amount of the interaction between non-polar configurations. Now, it will be worth while to study the signification of our evaluation of the quantities η and α. If the Mulliken's approximation is allowable, the extent of contribution of interaction between polar and non-polar structures may be measured by the degree of overlapping. A large overlap suggests much contribution of polar structures and vice versa. So, we shall try a VB calculation of ethylene, studying the influence of the overlap integral. The wave function are

$$\left.\begin{aligned}
&^1A_g(\text{ground}) \\
&\Psi_0 = \alpha\Psi_a + \frac{b}{\sqrt{2(1+S^2)}}(\psi_b+\psi_{b'}) \\
&^1B_{1u}(\text{excited}) \quad \Psi_1 = \frac{1}{\sqrt{2(1-S^2)}}(\psi_b-\psi_{b'}).
\end{aligned}\right\} \quad (18)$$

where ψ_a, ψ_b and $\psi_{c'}$ are normalized.

The secular equation for ^1A_g state is

$$\begin{vmatrix}
\frac{1}{1+S^2}(Q+\alpha)-E_1 & \frac{2}{1+S^2}(\eta-SE^1) \\
\frac{2}{1+S^2}(\eta-SE_1) & \frac{1}{1+S^2}Q+\xi+\alpha)-E_1
\end{vmatrix} = 0 \quad (19)$$

$$\frac{1}{1-S^2}(Q+\xi-\alpha)-E_2=0. \quad (20)$$

Here, we shall try to express η and α in functions of S. Coulomb integral Q is given by direct integration.

$$\begin{aligned}
Q &= 2W_{2p\pi}+2(U_a:\text{bb})+(\text{aa}:\text{bb}) \\
&= 2W_{2p\pi}+(U_a:\text{bb})+(U_a^0:\text{bb})
\end{aligned}$$

where, $W_{2p\pi}$ is the energy of $2_{p\pi}$ electron of carbon atom. Consequently

$$QS = 2W_{2p\pi}S+(U_a:\text{bb})S+(U_a^0:\text{bb})S \quad (22)$$

while η is

$$\begin{aligned}
\eta &= 2W_{2p\pi}S+(U_a:\text{bb})S+(U_a:\text{ab})+(\text{aa}:\text{ab}) \\
&= 2W_{2p\pi}S+(U_a:\text{bb})S+(U_a^0:\text{ab}). \quad (22)
\end{aligned}$$

Then from equations (21) and (22) it is seen that

$$QS = \eta-(U_a^0:\text{ab})+(U_a^0:\text{bb})S. \quad (23)$$

Furthermore, $(U_a^0:\text{ab})$ is approximated by the method of Sklar, thus*

$$(U_a^0:\text{ab}) = S(U_a^0:\text{b'b'}). \quad (24)$$

Numerical values of the penetration integrals $(U_a^0:\text{b'b'})$ and $(U_a^0:\text{bb})$, i.e., -8.739 and -1.091 eV.** respectively, give

$$\left.\begin{aligned}
&\eta = SQ-7.648S \\
&\text{and} \\
&\alpha = S^2Q-7.648S^2.
\end{aligned}\right\} \quad (25)$$

Inserting Eqs. (25) and an adequate numerical value of ξ into Eqs. (19) and (20), one can calculate the excitation energy ΔE in function of S. Fig. 5 shows the results of calculations in the cases of $\xi=3.51$ and 7.69 eV. The latter is true in the non-empirical calculation. The amount of ionic contribution is accounted for by the ratio b/a, and also by the ratio of the calculated stabilization

* b' is a $2p\pi$ function located midway between a and b atoms.

** Calculated from the paper of R.G. Parr and B.L. Crawford, *J. Chem. Phys.*, 18, 1049 (1948).

energy of the ground state including polar structures to that excluding them. These ratios are seen in Fig. 5. The experimental

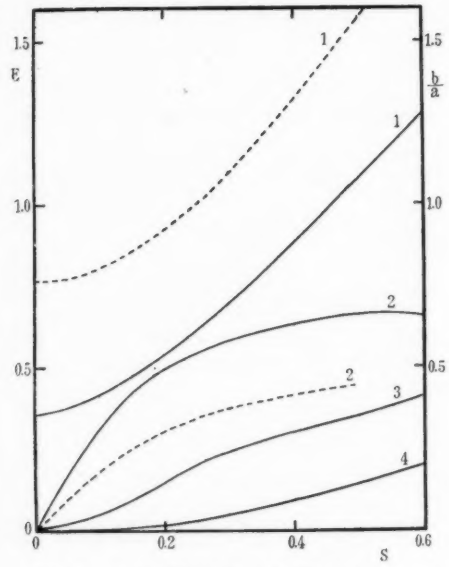

Fig. 5. Ionic Character of Ethylene.
1. Excitation energy ΔE
2. Ratio of b to a
3. Binding energy calculated from (18)
4. Binding energy calculated using ϕ_a only
Broken lines show results of using $\xi=7.69$ eV.

excitation energy is attainable at the value of the overlap integral by 0.3, consistent with our first assumption ($S=0.28$). When the overlap integral is small like this, η causes the most part of the stabilization energy and as S becomes large, the importance of polar structures of the molecule, consequently the contribution of η, decreases to the ground state.

Conjugated molecules, so far as we are dealing only with the π-electron system, have small S in general. Concerning this fact, one may understand that the simple MO method, which ignores the exchange and overlap integrals and includes a large amount of polar structures, is reliable in the calculation of π-electron systems and the good agreement with experiments of the results obtained by Pariser and Parr[5] may not be accidental. In the present calculation of *trans*-butadiene, the small value of α does not cause the contravention to the experiments and furthermore the disregard of the exchange integrals will cause the results of the calculation to come near those by the method of Pariser and Parr.

However, in the treatment of σ-bond, say like a hydrogen molecule, in which the overlap of atomic orbitals is large that it can never be excluded from the calculation, the approximation we have used here will not fit. In such cases, non-polar configurations will play an important role.

Conclusion

The usual VB-method, in spite of its theoretical infirmity that all or at least the large part of ionic influence is entirely ignored, has been served for predications and interpretations of electronic phenomena. But from a different point of view, we have described another direction of the VB-theory, and applying that to butadiene, we have shown that excellent agreements with experiments can be realized. A further study on the polar character of conjugated molecules could give an assurance to the propriety of our procedure. Our method was found to be very near the semi-empirical MO-method, but a large complication accompanies the practical calculation*. In this point, VB-method must fall below the MO-method.

Finally, from the present study, it was pointed out that the old VB-method in the semi-empirical theory of conjugated molecules, although it sometimes could lead to a good result, never represents the essential figure of a molecule and also that its agreement with experimental facts was accidental.

Laboratory of Physical Chemistry
Tokyo Institute of Technology
Tokyo

* Benzene is a rather simple and important object in the discussion of the propriety of a theory of electronic structures. But it is almost impossible to represent the wave function of benzene by VB-theory, since in order to expect a statisfactory result it requires inclusion of all kind polar structures, even triply-polar ones.

Synthetic Studies on Oxirane Compounds. I. Ammonolysis of 2,3-Epoxyl-3-pheny-1-propanol

By Tetsuo SUAMI, Ichiro UCHIDA and Sumio UMEZAWA

(Received December 20, 1955)

The study described in the present communication was a part of a program involving synthetic studies on chloramphenicol which is an important antibiotic found by the scientists of Parke, Davis and Co.. An attractive synthetic path to chloramphenicol involves the opening of the oxide ring of 1-phenylglycidol with ammonia. Although it has been shown recently by Fusco and Trave[1] that 1-*p*-nitrophenyl-1-amino-2, 3-propanediol is obtained by the action of ammonia on 1-*p*-nitrophenylglycidol, the substituent exerts often a profound effect on the direction of opening of the oxide ring, an example apparently being found in the reaction of nitrostyrene oxide[2] with hydrogen chloride. The direction of opening is opposite to that observed with styrene oxide[3]. This possibility made it desirable to attempt the ammonolysis of 1-phenylglycidol. The experiments described here established, however, the fact that 1-phenyl-1-amino-2, 3-propanediol (II) is obtained by the action of methanolic ammonia on 1-phenylglycidol, the direction of opening being much the same as that observed with 1-*p*-nitrophenylglycidol.

mation of 1-phenyl-1-amino-2, 3-propanediol (II), m. p. 90–91°, which depressed the melting point of the authentic sample of DL-threo-1-phenyl-2-amino-1, 3-propanediol, m. p. 87–88°. Treatment of II with *p*-nitrobenzaldehyde gave a Schiff base (IV), m. p. 149–150°, which

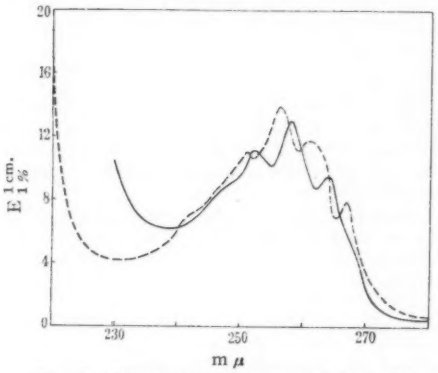

Fig. 1. Ultraviolet spectra of 1-phenyl-1-amino-2, 3-propanediol.
(----- : in 1 N hydrochloric acid;
——— : in ethanol)

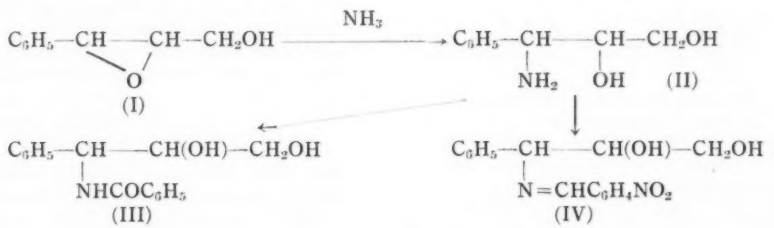

1-Phenylglycidol was prepared from cinnamyl alcohol and perbenzoic acid and had essentially the same boiling point with that reported by Platt and Hibbert[4]. By treatment with an excess of ammonia in absolute methanol in an autoclave, the epoxide ring of 1-phenylglycidol was split with the formation of 1-phenyl-1-amino-2, 3-propanediol (II), m. p. 90–91°, which depressed the melting point of the authentic sample of DL-threo-1-phenyl-2-amino-1, 3-propanediol, m. p. 87–88°. Treatment of II with *p*-nitrobenzaldehyde gave a Schiff base (IV), m. p. 149–150°, which also depressed the melting point of the corresponding Schiff base (V), m. p. 143–145°, prepared similarly from DL-threo-1-phenyl-2-amino-1, 3-propanediol.

To establish the identity of 1-phenyl-1-amino-2, 3-propanediol (II) the known 1-phenyl-1-benzamido-2, 3-propanediol was synthesized by the method of Lott[5] from cinnamyl benzoate bromohydrin and ammonia and did not depress the melting point of the benzoyl

1) R. Fusco and R. Trave, *Gazz. chim. ital.*, **80**, 366 (1950).
2) F. Arndt, B. Eistert and W. Partale, *Ber.*, **61 B**, 1107 (1928).
3) C. Golumbic and D.L. Cottle, *J. Am. Chem. Soc.*, **61**, 996 (1939).
4) M.E. Platt and H. Hibbert, *Can. J. Research*, **7**, 629 (1932); *C.A.*, **27**, 1334.
5) Lott, U.S. patent 2,103,266. The structure was elucidated by Controulis et al., who found that the migration of benzoyl group from O to N takes place during ammonolysis. *J. Am. Chem. Soc.*, **71**, 2463 (1949).

derivative (III) of the product (II) from the cleavage of 1-phenyl-glycidol (I). Ultraviolet absorption (Fig. 1) agreed in every respect with that obtained by Controulis et al..

On treatment of II with hot acetone an *iso*-propylidene derivative was produced which regenerated II readily by hydrolysis with hydrochloric acid at room temperature.

Experimental

1-Phenylglycidol (I) (2, 3-Epoxy-3-phenyl-1-propanol).—To a solution of 8.8 g. of perbenzoic acid in 100 cc. of chloroform was added 8.0 g. of cinnamyl alcohol. The solution was kept at 0° for about twenty-four hours and was shaken frequently during the first hour. The benzoic acid was removed from the chloroform solution by shaking with an excess of 10% sodium hydroxide solution, the alkali was removed by washing with water, and the chloroform solution was dried with sodium sulfate. It was then fractionated. Removal of the chloroform left a practically colorless liquid which distilled at 117–118°/1.5 mm. The yield was 4.5 g. (45% of the theoretical amount). Platt and Hibbert[1] described already the b. p. 136–137°/5 mm.

1-Phenyl-1-amino-2, 3-propanediol (II) (Cleavage of I with Ammonia).—The phenylglycidol (I) (13.6 g.) was heated with 350 cc. of a saturated solution (at 0°) of ammonia in absolute methanol at 80–90° for five hours in a stainless-steel autoclave. The solution was concentrated to a dark brown gum under reduced pressure which crystallized on trituration with ether. The ether-mixture was kept in a stoppered flask for about twenty hours. The crystals formed 9 g. and were collected on a filter. Three times of recrystallization from chloroform-ethylacetate (1 : 1) gave colorless needless melting at 90–91°. (Found: N, 8.22. Calcd. for $C_9H_{13}O_2N$: N, 8.38%.)

This depressed the melting point of an authentic sample of DL-threo-1-phenyl-2-amino-1, 3-propanediol, m. p. 87–88°.

1-Phenyl-1-benzamido-2, 3-propanediol (III).—0.5 g. Sample of the above described product (II) was treated with a small excess of benzoyl chloride in 1 N sodium hydroxide. The precipitate was recrystallized from water, colorless needles, m. p. 163–164°. This did not depress the melting point of 1-phenyl-1-benzamido-2, 3-propanediol, m. p. 163–164°, prepared by the method of Lott[5] from cinnamyl benzoate bromohydrin and ammonia.

1-Phenyl-1-(*p*-nitrobenzylidene)-amino-2, 3-propanediol (IV).—1.0 g. Sample of (II), m. p. 89–90° was mixed with 0.9 g. of *p*-nitrobenzaldehyde in 5.0 cc. of ethylacetate and warmed. Soon the resulting clear solution began to precipitate pale-yellow crystals. After standing overnight at room temperature the crystals were collected on a filter, washed with ethylacetate and ether, m. p. 140–143°. The yield was 1.0 g. Further recrystallization from methanol gavé pale-yellow needles, m. p. 149–150°. (Found: N, 9.23. Calcd. for $C_{13}H_{13}O_4N_2$: N, 9.33%.)

1-Phenyl-2-(*p*-nitrobenzylidene)-amino-1, 3-propanediol.—The condensation of *p*-nitrobenzaldehyde with DL-threo-1-phenyl-2-amino-1, 3-propanediol was carried out exactly as described above and led to 1-phenyl-2-(*p*-nitrobenzylidene)-amino-1, 3-propanediol, pale-yellow needles, m. p. 137–140°, 1.0 g. Recrystallization from acetone gave pale-yellow needles, m. p. 143–145°. (Found: N, 9.44. Calcd. for $C_{16}H_{17}O_4N_2$: N, 9.33%.)

This depressed the melting point of a sample of IV.

***iso*-Propylidene Derivative of II.**—A portion of 0.5 g. of the dark brown gum from which 1-phenyl-1-amino-2, 3-propanediol (II) described above was isolated, was dissolved in acetone by warming on a steam-bath. After standing at room temperature a colorless crystalline precipitate 0.3 g. was obtained, m. p. 93–96°. After recrystallization from acetone, the *iso*-propylidene derivative melted at 102.5–103°. (Found: N, 6.47. Calcd. for $C_{12}H_{17}O_2N$: N, 6.76%).

A sample of 0.2 g. of the *iso*-propylidene derivative was hydrolyzed with 1 cc. of 2 N hydrochloric acid at room temperature in a few minutes. The hydrolysate was neutralized with potassium carbonate and evaporated to dryness under reduced pressure. The colorless residue was dissolved in 1 cc. of water, made alkaline to pH 10 and extracted with ethylacetate. The ethylacetate solution was dried over sodium sulfate and evaporated to a syrupy residue, 0.1 g., which crystallized from ether. Recrystallization from ethylacetate-chloroform (1 : 1) gave colorless needles, 0.05 g., m. p. 89.5–90°. The mixed melting point with an authentic sample of II showed no depression.

An attempt was made to prepare *iso*-propylidene derivative from DL-threo-1-phenyl-2-amino-1, 3-propanediol by the same procedure described above. However, only a syrup was obtained.

Summary

1-Phenyl-1-amino-2, 3-propanediol, m. p. 90–91°, was obtained by ammonolysis of 2, 3-epoxy-3-phenyl-1-propanol. Several derivatives of this compound were described.

A part of the cost of the present research has been defrayed from the Scientific Research Encouragement Grant from the Ministry of Education, to which the authors' thanks are due.

Department of Applied Chemistry, Engineering Faculty of Keio University, Tokyo

The Synthesis and the Estrogenic Activity of Bis-2, 4-dihydroxyphenyl Disulfide and the Related Thiophenol

By Yoshiyuki URUSHIBARA and Gen KOGA

(Received December 28, 1955)

One of the authors (Y. U.) and T. Takahashi[1] reported the synthesis and the estrogenic activity of 2, 4, 2′, 4′-tetrahydroxyazobenzene. It produced full estrus in 100% animals (mice) at a dosage of 20 γ injected subcutaneously in two portions. The estrogenic activity of 4, 4′-dihydroxyazobenzene being very small (active in 80% at 1 mg.), the 2, 2′-hydroxyl groups of 2, 4, 2′, 4′-tetrahydroxyazobenzene were considered to form a double chelation, thus effecting a rigid, chrysene-shaped structure favorable for the development of a strong estrogenic activity. The infrared absorption spectrum of the crystals in Nujol showed the presence of hydrogen bonding between the azo nitrogen atom and the phenolic hydroxyl group. The insolubility of the tetrahydroxyazobenzene defied the measurement of its infrared absorption in solution, but 2-hydroxyazobenzene, a reference compound, in carbon tetrachloride solution showed a broad absorption at 3.4–3.5 μ due to an intramolecular hydrogen bonding[2], and thus gave an indirect evidence for the presence of chelation in the tetrahydroxyazobenzene at least in dilute state as when administered to the animal. If the supposed double chelation exists in the tetrahydroxyazobenzene, it is necessarily connected with a coplanar structure of the molecule, which was supposed to be one of the reasons why the substance is less active than the most potent synthetic estrogens[3].

The present authors expected bis-2, 4-dihydroxyphenyl disulfide (IV) might be a compound with a structure similar to that of 2, 4, 2′, 4′-tetrahydroxyazobenzene but not coplanar and thus a stronger estrogen, because of the presence of two unshared pairs of electrons in the valence shell of the covalent-bonded sulfur atom.

C. Lefevre and Ch. Desgrez[4] reported in 1934 that they prepared phenol disulfides by heating several phenols with sulfur and sodium carbonate in glycerol solution at 120°, and that from the ordinary phenol they obtained a disulfide melting at 116°, and from resorcinol a disulfide decomposing without fusion. They assigned the constitutions of bis-4-hydroxyphenyl disulfide and bis-2, 4-dihydroxyphenyl disulfide, respectively, without stating any detailed investigation of their structures. In 1890 R. Leuckart[5] already described bis-4-hydroxyphenyl disulfide melting at 150–151°, and in 1947 S. Magnusson, J. E. Christian, and G. L. Jenkins[6] prepared the same disulfide melting at 151–152°. Hence, the structures of the disulfides of Lefevre and Desgrez were probably different from the supposed. The present authors synthesized bis-2, 4-dihydroxyphenyl disulfide in the following way:

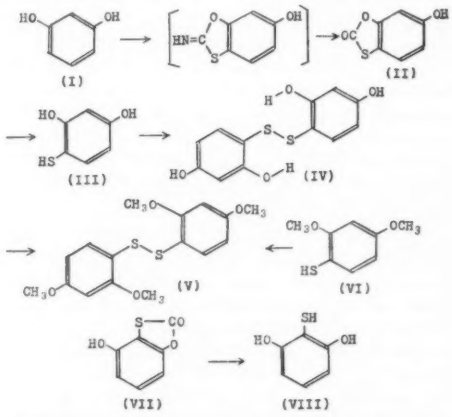

6-Hydroxy-1, 3-benzoxathiolone-(2) (II), m. p. 154.5–155°, was prepared from resorcinol (I), copper sulfate, and ammonium thiocyanate, by a method similar to that described by M. Pantlitschko and H. Benger[7] but without using sodium carbonate. It was hydrolyzed to 2, 4-dihydroxythiophenol (III), m. p. 110–111° by treatment with caustic soda. Oxidation of the thiophenol with hydrogen peroxide gave bis-2, 4-dihydroxyphenyl disulfide (IV), m. p. 170–171°, in white crystalline powder.

Pantlitschko and Benger observed that the product (m. p. 160°) from the reaction of

1) This Bulletin, **26**, 162 (1953).
2) T. Takahashi, *J. Chem. Soc. Japan*, **74**, 673 (1953).
3) Cf. M. Ōki and Y. Urushibara, This Bulletin, **25**, 109 (1952).
4) *Compt. rend.*, **198**, 1791 (1934).
5) *J. prakt. Chem.*, **41**, 179 (1890).
6) *J. Am. Pharm. Assoc. Sci. Ed.*, **36**, 257 (1947).
7) *Monatsh.*, **81**, 293 (1950); *Chem. Abstr.*, **45**, 2471 (1951).

resorcinol, copper sulfate, and ammonium thiocyanate, was 4-hydroxy-1, 3-benzoxathiolone-(2) (VII), from which they obtained 2, 6-dihydroxythiophenol (VIII), m. p. 83–84°. G. Werner[8] claimed a preparation of the same or isomeric compound melting at 158°, and, although the Chemical Abstracts, Vol. 38, gives the name 6-hydroxy-1, 3-benzoxathiolone-(2) for the substance in the Index, it is not shown in either the Chemical Abstracts or the original patent comment how its constitution was determined. It is also unknown whether the substance of G. Werner is identical with the substance melting at 154.5–155° obtained by the present authors or not. The following facts, however, support the structures assigned to the substances described in this paper.

Namely, the methylation of the disulfide, m. p. 170–171°, gave a product identical with the bis-2, 4-dimethoxyphenyl disulfide (V) prepared from the known 2, 4-dimethoxythiophenol (VI). The latter compound (VI) was prepared, and the constitution was determined, by C. M. Suter and H. L. Hansen[9]. The estrogenic activity of the disulfide (IV) and the thiophenol (III) is also a strong evidence for their structures.

Bis-2, 4-dihydroxyphenyl disulfide (IV) produced full estrus in 100% animals (mice) at a dosage of 10 γ by a single subcutaneous injection in oil solution, while 2, 4-dihydroxythiophenol (III) was fully active in 60–70% animals at the same dosage and in 100% at 20 γ. 2, 4-Dihydroxythiophenol appears to be an estrogen of the least molecular weight ever known, but it must be considered that it is oxidized in vivo to bis-2, 4-dihydroxyphenyl disulfide and acts as such.

Bis-4-hydroxyphenyl disulfide, 4-$HOC_3H_4 \cdot SSC_3H_4OH$-4, prepared by the method described by Magnusson et al., showed much less activity. Namely, it was totally inactive at 50 γ, but produced estrus in 20–40% animals at 100 γ and in 80% at 500–1000 γ. The structure of this compound may be non-coplanar contrary to those of 4, 4'-dihydroxyazobenzene and 4, 4'-dihydroxystilbene, considering the possible repulsion of the unshared pairs of electrons of the two sulfur atoms, and considering certain results from the investigations on the molecular structure of sulfur monochloride S_2Cl_2 by means of electron diffraction[10] and on the dipole moments of diphenyl disulfides[11]. Bis-4-hydroxyphenyl disulfide and bis-2, 4-dihydroxyphenyl disulfide may possibly possess the same or very similar twisted conformation of the hydrogen peroxide type, and then it may facilitate a chelation in the latter compound because one of the two unshared pairs of electrons of each sulfur atom is oriented towards the ortho hydroxyl group of the farther ring, but the distance between the two para hydroxyl groups may be shorter than the optimum for estrogenic potency[3].

At any rate, it has been demonstrated that the introduction of an ortho hydroxyl group into each ring of bis-4-hydroxyphenyl disulfide to form bis-2, 4-dihydroxyphenyl disulfide (IV) increases the estrogenic potency to a great extent, but it has not yet been determined in any other way whether a chelation really exists.

Experimental Part[12]

6-Hydroxy-1, 3-benzoxathiolone-(2) (II).—To a solution of 22 g. of resorcinol and 100 g. of crystalline copper sulfate in 500 ml. of water, 62 g. of ammonium thiocyanate dissolved in 100 ml. of water were added with stirring. A black precipitate appeared and turned gray in color. After standing for one hour with occasional stirring, the precipitate was removed, and the orange-red filtrate was heated on a waterbath and left to stand to complete the precipitation of a yellow substance. The yellow precipitate was collected on a filter and recrystallized three times from water-alcohol. Pale yellow needles, m. p. 154.5–155°. Yield, 12 g. (36% of the theory).

Anal. Found: C, 49.83; H, 2.36; S, 18.90. Calcd. for $C_7H_4O_3S$: C, 49.99; H, 2.40; S, 19.07%.

2, 4-Dihydroxythiophenol (III).—In the stream of nitrogen 100 ml. of 2 N caustic soda was added gradually to 10 g. of 6-hydroxy-1, 3-benzoxathiolone-(2) (II) contained in an Erlenmeyer flask. The mixture was gently heated to complete dissolution, left to cool down to the room temperature, acidified to acid reaction to Congo Red with 2 N hydrochloric acid, and extracted with ether. The white residue from the ethereal extract was recrystallized twice from benzene. A white crystalline powder, m. p. 110–111°. Yield, 6.5 g. (79% of the theory).

Anal. Found: C, 50.90; H, 4.37; S, 22.49. Calcd. for $C_6H_6O_2S$: C, 50.68; H, 4.25; S, 22.55%.

Bis-2, 4-dihydroxyphenyl Disulfide (IV).—A solution of 6 g. of the thiophenol (III) in 40–60 ml. (as little as possible) of water was cooled below 10°, about 4 ml. of 35% hydrogen peroxide was added gradually with stirring at a temperature not exceeding 15°, and the mixture was left to stand with cooling. The white crystalline substance was collected on a filter and recrystallized twice from water. A white crystalline powder,

8) U.S. Patent, 2,332,418; *Chem. Abstr.*, **38**, 1889 (1944).

9) *J. Am. Chem. Soc.*, **55**, 2080 (1933).

10) E. Hirota and Y. Morino, private communication. Cf. also S. Mizushima, "Structure of Molecules and Internal Rotation," Academic Press, New York (1954), p. 93.

11) E. Bergmann and M. Tschudnowsky, *Z. physik. Chem.*, B, **17**, 107 (1932).

12) Melting points uncorrected.

m. p. 170–171°, Yield, 4 g. (67% of the theory).

Anal. Found: C, 51.14; H, 3.42; S, 22.27. Calcd. for $C_{12}H_{10}O_4S_2$: C, 51.05; H, 3.57; S, 22.72%.

Bis-2, 4-dimethoxyphenyl Disulfide (V).—2, 4-Dimethoxythiophenol, prepared by the method of C. M. Suter and H. L. Hansen[9], was treated with a slight excess of iodine in alcoholic solution. The precipitate was recrystallized from alcohol. Colorless needles, m. p. 113–115°. Yield, quantitative.

Anal. Found: C, 56.59; H, 5.19; S, 18.79. Calcd. for $C_{16}H_{18}O_4S_2$: C, 56.78; H, 5.36; S, 18.91%.

Bis-2, 4-dihydroxyphenyl disulfide (IV), dissolved in caustic soda, and dimethyl sulfate gave a white crystalline product. Recrystallized from alcohol, it showed a melting point 109.5–112.5° and no depression of the melting point was observed in admixture with the bis-2, 4-dimethoxyphenyl disulfide described above.

Attempted methylation of 2, 4-dihydroxythiophenol (III) to the known methyl 2, 4-dimethoxyphenyl sulfide, $C_6H_3(SCH_3)(OCH_3)_2$ (1, 2, 4), was accompanied by oxidation and resulted in the formation of 2, 4-dimethoxyphenyl disulfide (V).

Department of Chemistry, Faculty of Science, The University of Tokyo
Tokyo

Spectrochemical Study of Microscopic Crystals. XI.[1] *The Structure and Polarized Absorption Spectra of Some Metallic Compounds with Remarkable Interaction between Metal Atoms through Anions*

By Shoichiro YAMADA and Ryutaro TSUCHIDA

(Received January 9, 1956)

These several years the present authors have been particularly interested in those inorganic compounds which display in the crystalline state much deeper colours than would be expected from the colours of their components in solution. In one type of the compounds, the metal-to-metal interaction was concluded to exist, causing the unusual deepening of the colour[2]. In the compounds of another type, there was supposed to be interaction between metal atoms through anions[3]. In the study of the above compounds, the measurement of polarized absorption spectra has proved to be a feasible means, since the interaction was found to cause enormous changes in the direction along which the interaction was known to exist between the metal atoms. We have taken up those compounds in which there would be expected to be infinite chains of metal atoms connected with anions as bridging groups. In the present work, polarized absorption spectra of $Pd(NH_3)_2Cl_3$, Pt (en)Cl_3[4] and $(NH_4)_3AgAuCl_7$ have been quantitatively determined and the results have been discussed with relation to the structure of the compounds.

Experimental

Materials.—Trans-$[Pd(NH_3)_2Cl_2]$ was prepared in orange crystals of moderate size by spontaneous evaporation of an aqueous solution of $[Pd(NH_3)_4]Cl_2$[5]. The crystals show a straight extinction. They appear yellow with the electric vector along the *c*-axis, and orange with the electric vector normal to the *c*-axis. The measurement was made along the two directions. The X-ray study of the crystal structure[5] indicates that the *c*- and *a*-absorption denote absorption with the electric vector along and normal to the complex molecules, respectively.

$[Pd(NH_3)_2Cl_2][Pd(NH_3)_2Cl_4]$ was prepared according to the method of Cohen et al.[6] The crystals obtained in black needles belong to the orthorhombic system, showing a straight extinction and a remarkable dichroism. They appear quite dark with the electric vector along the *c*-axis, and yellow with the electric vector normal to the *c*-axis. There were sometimes grown crystals with a different habit, which exhibited a dichroism different from the above. The dichroism measurement was made with the crystals of the former type.

$[Pt(en)Cl_2]$ was prepared in yellow powder according to the method of Basolo[7]. Crystals of

1) Part X of this series, S. Yamada and R. Tsuchida, This Bulletin, 29, 289 (1956).

2) S. Yamada and R. Tsuchida, *J. Chem. Soc. Japan*, 70, 142 (1949); S. Yamada, *J. Am. Chem. Soc.*, 73, 1579 (1951); This Bulletin, 24, 125 (1951); S. Yamada and R. Tsuchida, *J. Am. Chem. Soc.*, 75, 6351 (1953); This Bulletin, 27, 156 (1954).

3) S. Yamada, Y. Shimura and R. Tsuchida, This Bulletin, 26, 72 (1953); R. Tsuchida and S. Yamada, *Nature*, 174, 1064 (1954).

4) The notation, en, denotes a molecule of ethylenediamine.

5) F.G. Mann, D. Crowfoot, D.C. Gattiker and N. Wooster, *J. Chem. Soc.*, 1935, 1642.

6) A.J. Cohen and N. Davidson, *J. Am. Chem. Soc.*, 73, 1955 (1951).

7) F. Basolo, ibid., 72, 2433 (1950).

a moderate size suitable for the absorption measurement could not be obtained. Its absorption spectrum was determined in the aqueous solution with a Beckman DU spectrophotometer.

$[Pt(en)Cl_4]$ was prepared in pale yellow powder by the method of Basolo[7]. The measurement of the polarized absorption spectra with the crystals could not be made, since the crystals large enough for the measurement were not available. Its absorption spectrum was determined using the aqueous solution.

$Pt(en)Cl_3$ was prepared by oxidizing $[Pt(en)Cl_2]$ with ammonium persulphate according to the method of Tschugaeff et al.[8] or by allowing to cool a hot, mixed solution of $[Pt(en)Cl_2]$ and $[Pt(en)Cl_4]$. Red, plate-like crystals thus obtained were strongly dichroic; purplish-red and pale yellow with the electric vector along and normal to the *c*-axis, respectively. The measurement of the polarized absorption spectra was performed along the above two directions. The *a*- and *c*-absorption have the same meaning as the above.

$Cs[AuCl_4]$ was prepared in yellow prisms from tetrachloro-auric acid and caesium chloride, which were purified by repeated recrystallization from water. A slight dichroism was observed with the crystals under the microscope. The measurement of the dichroism was made along the directions parallel and normal to the prism axis. The C- and A- absorption denote absorption with the electric vector along and normal to the prism axis, respectively. Measurement of absorption spectra was also made with the aqueous solution containing CsCl.

$Cs_2AgAuCl_6$ was obtained in black microcrystals by the method of Wells[9]. To an aqueous solution of tetrachloro-auric acid acidified with hydrochloric acid was added silver nitrate and caesium chloride, followed by warming on a water bath. The precipitate of silver chloride, which was formed at first, again entered into solution, from which the black crystals sparated out. The crystals of a larger size suitable for the absorption measurement could not be obtained. The visual observation, however, could be made with some of them under the microscope. The crystals showing a straight extinction were strongly dichroic. They appear almost black with the electric vector along the *c*-axis, and yellow with the electric vector normal to the *c*-axis.

$(NH_4)_3AgAuCl_7$ was prepared in very dark crystals follwing the same procedure as that with the above caesium compound, except that ammonium chloride was used instead of caesium chloride[10]. The reaction also proceeded in a way very similar to the case of the corresponding caesium compound. The needles of the compound, which belong to the orthorhombic system, showed a marked dichroism. They appeared quite dark along the *c*-axis, and yellow in the direction normal to the *c*-axis. The dichroism measurement was made with reference to the above two directions.

Measurement.—Quantitative dichroism measurements were made by Tsuchida-Kobayashi's microscopic method[11] with polarized light in the regions covering 2400 to 8000 Å. The notations used are the same as those in the previous papers of this series[1].

Results and Discussion

In 1948, Brosset[12] studied the crystal structure of $Pt(NH_3)_2Br_3$. The crystal analysis indicates that the crystal of the compound, which should be formulated as $[Pt(NH_3)_2Br_2][Pt(NH_3)_2Br_4]$, consists of infinite chains, each containing alternate planes of $[Pt(NH_3)_2Br_2]$ and octahedra of $[Pt(NH_3)_2Br_4]$, as illustrated in Fig. 1. From visual observation of the crystals under the microscope and examination of their magnetic property, Cohen et al.[6] supposed that the crystal of $Pd(NH_3)_2Cl_3$, which could be represented by $[Pd(NH_3)_2Cl_2][Pd(NH_3)_2Cl_4]$, would possess the same structure as that of $[Pt(NH_3)_2Br_2][Pt(NH_3)_2Br_4]$. This was confirmed later by the X-ray analysis of the crystal[13].

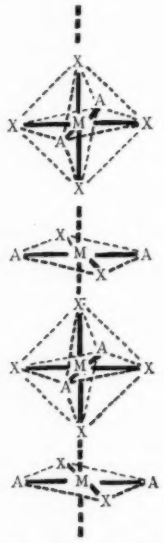

M: Pd or Pt A: ammonia or amine
X: halide or hydroxyl group

Fig. 1. Chain structure in the crystals of the compounds having the empirical formula, MA_2X_3.

8) L. Tschugaeff and J. Tschernyaeff, *Z. anorg. allgem. Chem.*, **182**, 159 (1929).
9) H. L. Wells, *Amer. J. Sci. Silliman*, (5) **3**, 257 (1920); *Chem. Zentr.*, **1922**, 239.
10) W.B. Pollard, *J. Chem. Soc.*, **117**, 99 (1920).
11) R. Tsuchida and M. Kobayashi, This Bulletin, **13**, 619 (1938); "The Colours and the Structures of Metallic Compounds", Zoshindo, Osaka, Japan (1944), p. 180.
12) C. Brosset, *Arkiv Kemi Mineral. Geol.*, **25A**, No. 19 (1948).
13) E. W. Hughes, unpublished; private communication from Dr. A.J. Cohen; C.S. Adams, M.S. thesis, University of Sydney, 1952.

The result of the present measurement is shown in Fig. 2. Polarized absorption spectra of one component, *trans*-$[Pd(NH_3)_2Cl_2]$, are also given in Fig. 2. The other component,

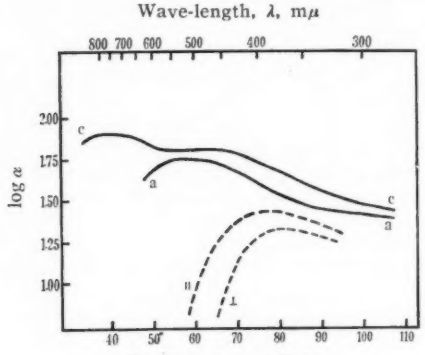

Fig. 2. Absorption spectra of $[Pd(NH_3)_2Cl_2][Pd(NH_3)_2Cl_4]$ (——) and *trans*-$[Pd(NH_3)_2Cl_2][Pd(NH_3)_2Cl_4]$ (- - - -), both in crystalline state.

$[Pd(NH_3)_2Cl_4]$, is too unstable to be isolated in crystals. Its solution, however, is orange in colour. The crystal of $[Pd(NH_3)_2Cl_2][Pd(NH_3)_2Cl_4]$, therefore, is seen to show its absorption at much longer wavelength than would be expected from the absorption spectra of the components. This suggests that the component complexes would undergo specific effects in the crystal of $[Pd(NH_3)_2Cl_2][Pd(NH_3)_2Cl_4]$. Moreover, the present measurement shows that absorption is much more bathochromic with the electric vector along the chains, - - -Cl—Pd^{IV}—Cl- - - Pd^{II}- -Cl—Pd^{IV}—Cl- - -, than that normal to the chain. This relation is seen to be reverse to that with the crystal of *trans*-$[Pd(NH_3)_2Cl_2]$. ***It may be presumed from the above relations that in the crystals of*** $[Pd(NH_3)_2Cl_2][Pd(NH_3)_2Cl_4]$ ***there would be strong interaction between the metal atoms in different oxidation states through the anions.*** Thus with the electric vector along the chain, absorption was observed at $30\text{–}45\times10^{13}$/sec., whereas the absorption in this region was not observed with the electric vector normal to the above chain. This absorption might be assumed to be a charge-transfer band[14] due to the chain, - - -Cl—Pd^{IV}—Cl- - -Pd^{II}- - -Cl—Pd^{IV}—Cl- - -.

The compound, $Pt(en)Cl_3$, may be considered as a compound of a similar type. Thus the compound can be prepared from a mixed aqueous solution of $[Pt(en)Cl_2]$ and $[Pt(en)Cl_4]$. Further, magnetic examination[15] indicates that this compound is diamagnetic, involving no platinum in tervalent state. The above facts seem to show that the compound should be formulated as $[Pt(en)Cl_2][Pt(en)Cl_4]$.

The compound, $[Pt(en)Cl_2][Pt(en)Cl_4]$, in the crystalline state has much deeper colour than either of the component complexes; $[Pt(en)Cl_2]$ is pale yellow, and $[Pt(en)Cl_4]$ is also yellow. Thus the compound, $[Pt(en)Cl_2][Pt(en)Cl_4]$ dissolves in hot water to give a yellow solution, from which its red crystals separated. As may be expected from the colours, $[Pt(en)Cl_2][Pt(en)Cl_4]$ in the crystalline state is found to show its absorption at far longer wave-length than either of the component complexes (Fig. 3). This shows

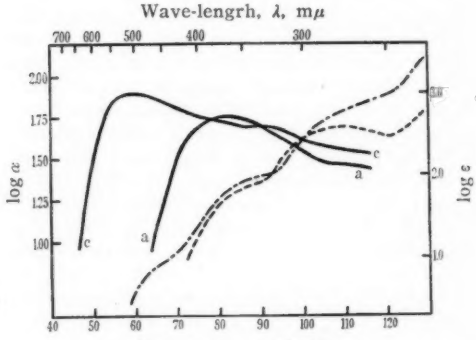

Fig. 3. Absorption spectra of $[Pt(en)Cl_2][Pt(en)Cl_4]$ (——), $[Pt(en)Cl_2]$ (- - - -) and $Pt(en)Cl_4$ (—·—·—).

that the complexes are under remarkable effect in the crystalline state. The nature of the effect may be judged from the results of the dichroism measurement. The dichroism of the above compound, as given in Fig. 3, may be well understood, assuming that the red compound involves infinite chains similar to those in the crystal of $[Pd(NH_3)_2Cl_2][Pd(NH_3)_2Cl_4]$. That is, assuming the *c*-absorption to be the absorption along the infinite chains, - - -Cl—Pt^{IV}—Cl- - -Pt^{II}- - -Cl—Pt^{IV}—Cl - - -, and the *a*-absorption to be the absorption normal to the chain, then the absorption is seen to be much more bathochromic with the electric vector along the above chains than the absorption normal to the chains. This relation on the dichroism is found to be quite similar to that of $[Pd(NH_3)_2Cl_2][Pd(NH_3)_2Cl_4]$, and may be best understood in the same way as with the above palladium compound. ***It is most likely that the crystal of*** $[Pt(en)Cl_2][Pt(en)Cl_4]$ ***involves the infinite chains along the c-axis, as assumed above.*** The absorption at $50\text{-}65\times10^{13}$/sec.,

14) See, for example, R.S. Mulliken, *J. Am. Chem. Soc.*, **72**, 605 (1950), etc.

15) Y.K. Syrkin and V.I. Belova, *Zhur. Fiz. Khim.*, **23**, 664 (1949); *C.A.*, **43** 7277 (1949).

which is not observed with the electric vector normal to the chains, is observed with the electric vector along the chains. This absorption may be a charge transfer band due to the chains, $\cdots Cl—Pt^{IV}—Cl\cdots Pt^{II}\cdots Cl—Pt^{IV}—Cl\cdots$.

Besides the compounds described above, another type of compounds is known in which similar interaction may be found between metal atoms through anions. One of the compounds may be $Cs_2AgAuCl_5$. This crystal is very dark, almost black in colour. Elliott et al.[16] studied the crystal structure of the above compound, showing that the crystal of this compound involves infinite chains along the *c*-axis, each containing alternate planes of $[AuCl_4]^-$ and linear ions of $[Cl–Ag–Cl]^-$. The crystals of $Cs_2AgAuCl_5$ which we obtained were too small to be used for the dichroism measurement. We, however, could observe visually some of the crystals under the microscope. The observation showed that the crystals appeared almost black with the electric vector along the *c*-axis, and yellow with the electric vector normal to the *c*-axis. This fact seems to suggest that absorption with the electric vector along the infinite chains lies at much longer wave-length than that with the electric vector normal to the chains. Thus, it may be supposed that the crystal of $Cs_2AgAuCl_5$ exhibits dichroism of a type similar to that of $[Pd(NH_3)_2Cl_2][Pd(NH_3)_2Cl_4]$. The absorption at the longer wave-length, which would be allowed only with the electric vector along the infinite chains, $\cdots Au^{III}(Cl_4)\cdots Cl—Ag^{I}—Cl\cdots Au^{III}(Cl_4)\cdots$, may be a charge transfer band, characteristic of the above chains. This may be considered as showing that there would be a strong interaction between the metal atoms through the chlorine atoms.

By following the same procedure as in the preparation of $Cs_2AgAuCl_5$ except that ammonium chloride was used instead of caesium chloride, a dark-coloured compound, $(NH_4)_3AgAuCl_7$, was obtained. The reaction proceeded in quite the same way as in the caesium compound. The crystal structure of $(NH_4)_3AgAuCl_7$ has not been determined as yet. But similarity to the corresponding caesium compound in the method of preparation and in the reaction of its formation seems to indicate that the crystals of $(NH_4)_3AgAuCl_7$ involve components similar to those of the corresponding caesium compound; that is, $[Cl–Ag–Cl]^-$ and $[AuCl_4]^-$ ions. The crystals of this compound are found to absorb in much longer wave-length than would be expected for the component complexes (Figs. 4 and 5). This indicates

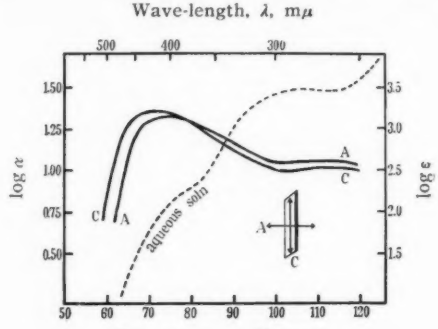

Fig. 4. Absorption spectra of $Cs[AuCl_4]$.

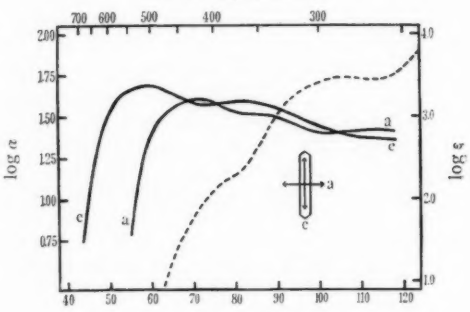

Fig. 5. Absorption spectra of $(NH_4)_3AgAuCl_7$ (——) and $Cs[AuCl_4]$ (- - - -).

that the component complexes undergo some effects in the crystalline state.

It has also been found that the *c*-absorption is much more bathochromic and somewhat more hyperchromic than the *a*-absorption. These relations, which are similar to those with the crystals of $Pd(NH_3)_2Cl_2$, $Pt(en)Cl_2$ and $Cs_2AgAuCl_5$, seem to agree with the assumption that *the crystals of* $(NH_4)_3AgAuCl_7$ *may contain infinite chains of* $\cdots Au^{III}(Cl_4)\cdots Cl—Ag^{I}—Cl\cdots Au^{III}(Cl_4)\cdots$ *along the c-axis.* Thus the absorption at 55×10^{13}/sec. for the *c*-absorption, which is not observed for the *a*-absorption, may be assigned to a kind of charge transfer band due to the above chains.

General Discussion

Surveying the above results, the following generalization may be induced. *Those compounds having infinite chains such as* $\cdots X—M^{m}—X\cdots M^{n}\cdots X—M^{m}—X\cdots$, *M and X being metal and halogen atoms, show at the*

16) N. Elliott and L. Pauling, *J. Am. Chem. Soc.*, 60, 1846 (1938).

longer wave-length a new absorption band, characteristic of the infinite chains and polarized along the chains. The new band may be interpreted as due to a charge transfer between the two components.

This may be taken as showing that *in those crystals there would exist some interaction between metal atoms through anions.* In the above instances, the halogen atoms are supposed to act as bridges, facilitating the electron transfer between the metal atoms. Assuming the picture of the electron transfer between metal atoms, the interaction would be stronger between atoms in different oxidation states of the same or similar elements than between atoms of different elements. The interaction between the metal atoms in the above compounds, however, seems to be slightly different from the interaction between metal atoms in μ-peroxo-dicobalt-compounds, magnetite or prussian blue[17]. That is, in the groups of the latter compounds all the metal atoms are almost or completely equivalent and undistinguishable, while in the former there are involved two kinds of the metal atoms which are clearly unequivalent. The electronic migration between the two metal atoms would occur much more readily in the compounds of the latter type than in those of the former.

It is to be noted that the complex, $[Pd(NH_3)_2Cl_4]$, is rather stable in the crystal of $[Pd(NH_3)_2Cl_2][Pd(NH_3)_2Cl_4]$, although the former has never been isolated in solid under any ordinary condition. In the same way, the $[Cl-Ag-Cl]^-$ anion seems to be much more stable in the crystal of $Cs_2AgAuCl_7$ and $(NH_4)_3AgAuCl_7$ than in other compounds of an ordinary type involving the anions. The remarkably enhanced stability of the above complexes in the present compounds may be closely associated with the interaction between the metal atoms through the anions.

It is suggested that a number of compounds having platinum or palladium in apparently tervalent state would involve similar chains. Thus, in the crystals of $Pt(NH_3)_2(OH)Cl_2$ there would be similar chains, in which the atom of bivalent platinum would be connected with the atoms of quadrivalent platinum through OH^- or Cl^- ions. In fact, according to Bokii et al., the crystals of $Pt(NH_3)_2(OH)Cl_2$ appears black with polarized light having its electric vector along the needle axis, and very pale with the electric vector normal to the needle axis[18]. This seems to indicate that the compound in the crystalline state displays in the visible region an absorption band which would be polarized in the direction of the needle axis. It is most probable that the band at the longer wave-length may be a charge transfer band due to the possible chains, $\cdots X-Pt^{IV}-X\cdots Pt^{II}\cdots X-Pt^{IV}-X\cdots$, indicating the interaction between the bivalent and quadrivalent platinum atoms through negative ions such as OH^- or Cl^- ions (Fig. 1).

The so-called copper-coloured oxalato-platinum compounds[19] and the Wolffram's compound[20], $Pt(NH_2\cdot C_2H_5)_4Cl_3\cdot 2H_2O$, also are believed to belong to the same type of compounds involving similar chains. Polarized absorption spectra which were determined lately[21,22] are found to support the above presumption. The detailed reports on those compounds will be submitted later.

Summary

Polarized absorption spectra of $[Pd(NH_3)_2Cl_2][Pd(NH_3)_2Cl_4]$, $Pt(en)Cl_3$ and $(NH_4)_3AgAuCl_7$ in the crystalline state have been determined by Tsuchida-Kobayashi's microscopic method in the regions betwen 2400 and 8000 Å.

The crystals of the above compounds which are supposed to involve infinite chains of a type, $\cdots X-M^m-X\cdots M^n\cdots X-M^m-X\cdots$, have been found to display absorption at longer wave-length than any of the respective component complexes. This absorption at the longer wave-length has been shown to be completely polarized along the direction of the supposed chains in the crystals.

The above results show that in these crystals there would be rather strong interaction between the metal atoms through the anions along the infinite chains.

The work reported here was supported by the grant in aid of the Ministry of Education.

Department of Chemistry, Facutly of Science, Osaka University, Osaka

17) S. Yamada, Y. Shimura and R. Tsuchida, This Bulletin, 26, 72 (1953); P.E. Fielding and D.P. Mellor, *J. Chem. Physics*, 22, 1155 (1954), etc.

18) G.B. Bokii and G.I. Distler, *Doklady Akad. Nauk S.S.S.R.*, 56, 923 (1947).

19) A. Werner and E. Grebe, *Z. anorg. Chem.*, 21, 381, 387 (1899), etc.

20) H. Wolffram, Dissertation, Königsberg, 1900.

21) R. Tsuchida and S. Yamada, read before the annual meeting of the Chemical Society of Japan, Kyoto, April, 1953.

22) To be submitted later.

*Studies on Phosphonitrile Chlorides by their Pure Quadrupole Spectra**

By Hisao NEGITA and Sumio SATOU

(Received December 20, 1955)

A group of phosphonitrile chlorides $(PNCl_2)_n$ have been known so far[1], where n is the degree of polymerization and is three or above. Of these, the trimer is the most ordinary compound and has been thought to form a plane ring[2], composing of nitrogen and phosphorus atoms alternatively. On the contrary, the tetramer has been shown to have a puckered ring and two kinds of chlorine atoms attached to the same phosphorus atom[3].

Trimer

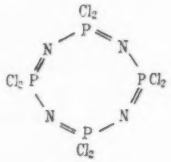

Tetramer

We therefore examined the pure quadrupole spectra due to Cl^{35} of these two compounds and considered the states of their chlorine atoms, comparing the resonance absorption frequencies or absorption lines with each other.

Experimental

Preparation of Samples.—Phosphonitril chlorides were prepared by heating phosphorus pentachloride and ammonium chloride in *sym*-tetrachloroethane[4]. After the product was freed from ammonium chloride, solvent, and rubber-like residue, it was fractionally distilled at about 13 mmHg. The most part of the product was distilled off at about 127°C and this fraction was used as the sample of the trimer (m.p. 114°C). The fraction at 185–190°C was about one-tenth of the trimer, showing m.p. of 121–124°C. Thus it was used as the tetramer (m.p. 123.5°C), for a small content of impurities does not affect the absorption frequency, though they make the line width broader.

Apparatus.—To measure the absorption frequencies, we used the spectrometer reported in the previous paper[5], which was improved on a few points. For instance, a variable condenser of small capacity was connected parallel to the tank circuit of the main oscillator for the purpose of band spread, and its graduations were corrected every time by the crystal oscillator. By this method, the absorption frequency of potassium chlorate $KClO_3$ was found to be 28.147 Mc. at 14°C, which was in good agreement with the value of Wang et al.[6], taking the temperature effect into consideration.

Results and Considerations

The absorption frequencies of phosphonitrile chlorides were found at room temperature as shown in Table I. The experimental error was assumed to be several kc. in each case.

TABLE I

THE RESONANCE ABSORPTION FREQUENCIES DUE TO Cl^{35} IN PHOSPHONITRILE CHLORIDES $(PNCl_2)_n$ (287°K)

Compound	$(PNCl_2)_3$	$(PNCl_2)_4$
Frequency (Mc./sec.)	27.630	27.265
	27.704	28.124
	27.834	28.182
	27.903	28.616

It is noticed that both compounds show four kinds of frequencies. This fact seems to be curious in the case of the trimer $(PNCl_2)_3$, for six chlorine atoms of this molecule might be equivalent in the solid as well as in the vapor phase[2], and only one absorption frequency is to be expected. Otherwise, two or six kinds of frequencies may reasonably be expected, assuming slight distortion of P-Cl bonds or of the ring.

In the same way, two, four, and eight kinds may be probable in the case of the tetramer $(PNCl_2)_4$, for there are at least two kinds of chlorine atoms; that is, two chlorine atoms attached to the same phosphorus atom are at distances of 1.97 Å and 2.01 Å, respectively, according to the X-ray analysis[3].

The patterns of the spectra are illustrated in Fig. 1, where the intensity of each line is estimated roughly from the ratio of signal to noise. It is seen from this figure that

* A part of this research was reported at the 8th meeting of the Chemical Society of Japan, on April 2, 1955.

1) L.F. Audrieth, R.S. Steinman and A.D.F. Toy, *Chem. Rev.*, 32, 109 (1943).

2) L.O. Brockway and W.M. Bright, *J. Am. Chem. Soc.*, 65, 1551 (1943).

3) J.A.A. Ketelaar and T.A. de Vries, *Rec. trav. chim.*, 58, 1081 (1939).

4) R. Schneck and G. Römer, *Ber.*, 57, 1343 (1924).

5) H. Negita, H. Yamamura and H. Shiba, This Bulletin, 28, 271 (1955).

6) T.C. Wang, C.H. Townes, A.L. Schawlow and A.N. Holder, *Phys. Rev.*, 86, 810 (1952).

four lines of the trimer are characterized by two kinds, the stronger and the weaker, whereas those of the tetramer are all of the same order. Consequently, it may be concluded that the stronger of the trimer and all of the tetramer are caused by two equivalent chlorine atoms in their molecules, and the weaker by only one. Thus, the four lines in each spectrum are concerned with the numbers of chlorine atoms in the corresponding molecules as 2+1+1+2=6 and 2+2+2+2=8, respectively.

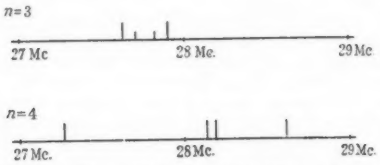

Fig. 1. The relative intensities of the absorption lines in $(PNCl_2)_n$.

However, it must be borne in mind that the intensity of the line in the pure quadrupole spectra is not always proportional to the amounts of the corresponding atoms, because it is affected also by the spin-lattice relaxation time and other factors[7].

The ionic character α of P-Cl bond may be assumed[8] by the relation $\alpha=1-\nu/\nu_0$, where ν is the measured absorption frequency of the compound and ν_0 is the absolute value of the coupling constant of atomic chlorine[9], 54.87 Mc.. Accordingly, the smaller is the frequency, the larger is the ionicity of the bond.

Several compounds which have P-Cl bonds and whose absorption frequences have been known are listed in Table II. From this table and Table I, it is seen easily that the ionicity of P-Cl bonds in phosphonitrile chlorides are closest to those of phosphorus oxychloride, taking account of frequancy increases, which presumably amount to several hundreds kc. at 77°K.

TABLE II

THE RESONANCE ABSORPTION FREQUENCIES OF SEVERAL COMPOUNDS WHICH HAVE P-Cl BONDS (77°K)

Compound	m.p. (°C)	Frequency (Mc./sec.)
PCl_3	−92	26.202[10]
		26.107
$POCl_3$	1.4	28.9378[11]
		28.9835
PCl_5	163	32.282[12]
		32.384
		32.63

Furthermore, two chlorine atoms in the trimer, corresponing to the absorption frequenty 27.630 Mc., are regarded as the most ionic of the six chlorine atoms, and they are to be replaced together to yield disubstituted compounds in place of monosubstituted compounds. In this way, the fact can be explained without difficulty that hydrolysis of the trimer gives triphosphonitrile dihydroxytetrachloride $P_3N_3(OH)_2Cl_4$ as a main product[13]. Trimeric phosphonitrilic acid $P_3N_2(OH)_6$ is unstable, whereas tetrameric phosphonitrilic acid $P_4N_4(OH)_8\cdot 2H_2O$ is so stable that various hydrolytic intermediates have not been obtained[1]. However, these are likely to be isolated by controlled hydrolysis, for the absorption lines of the tetramer are widely spaced. Studies on the chemical behaviour of the phosphonitrile chlorides and their derivatives are now in progress, in connection with the results of the pure quadrupole spectra.

In conclusion, the authors wish to express their sincere thanks to Prof. T. Ichikawa and Dr. H. Yamamura for their encouragement and useful discussions throughout this research, and also to Messers. M. Miyashita and Z. Hirano for their able assistance of this work. This research was supported by the research grant from the Ministry of Education.

Chemical Department, Faculty of Science, Hiroshima University, Hiroshima
and
Chemical Laboratory, Faculty of Education, Kagawa University, Kagawa

7) J. Hatton and B.V. Rollin, *Trans. Faraday Soc.*, 50, 398 (1954).
8) W. Gordy, W. V. Smith and R. F. Trambarulo, "Microwave Spectroscopy", John Wiley & Sons Inc., New York (1953) p. 284.
9) V. Jaccarino and J.G. King, *Phys. Rev.*, 83, 471 (1951).
10) R. Livingston, *J. Phys. Chem.*, 57, 496 (1953).
11) R. Livingston, *Phys. Rev.*, 82, 289 (1951).
12) D.W. McCall and H.S. Guttowsky, *J. Chem. Phys.*, 21, 1300 (1953).
13) H.N. Stokes, *Am. Chem. J.*, 17, 275 (1895); *Ber.*, 28, 437 (1895).

Studies on Crystals of Metallic Tris-ethylenediamine-complexes. I. The Crystal Structure of DL-*Tris-ethylenediamine-cobalt (III) Chloride Trihydrate,* $[Co\ en_3]Cl_3 \cdot 3H_2O$

By Kazumi NAKATSU, Yoshihiko SAITO and Hisao KUROYA

(Received January 1, 1956)

Introduction

No complete structure determination of a complex salt containing the $[Co\ en_3]^{3+}$ ion has yet been reported, although determination of a complex salt containing the $[Ni\ en_3]^{2+}$ ion has been carried out by Watanabé and Atoji[1].

The present work on the familiar crystals of the complex salt $[Co\ en_3]Cl_3 \cdot 3H_2O$ was undertaken mainly to determine the shape and size of the complex ion in the course of our studies on metallic tris-ethylenediamine complex compounds. Ter Berg[2] has reported the unit cell dimensions, space group and other crystallographic data of this substance together with several related compounds. In this work his results were indeed verified.

Experimental

Tris-ethylenediamine-cobalt (III) chloride trihydrate was prepared according to the method described by Jörgensen[3]. Jaeger[4] reported that the crystals belong to ditrigonal scalenohedral class with $a:c=1:0.6667$. Crystals grown for this work by slow evaporation of saturated aqueous solution at room temperatures were hexagonal prisma. Cylindrical specimens of about 0.3 mm. in diameter parallel to all principal axes were prepared. All the equatorial reflections were recorded by using Fe K radiation ($K\alpha$, $\lambda=1.937$ Å).

The unit cell dimensions were obtained from high order ($hki0$) and ($h0\bar{h}l$) reflections on the equatorial lines of oscillation photographs. The results are: $a=11.50\pm0.02$, $c=15.52\pm0.04$ Å, giving the axial ratio $2a:c=1:0.668$, in agreement with that reported by Jaeger.

From the density 1.504 g./cc. obtained by the pyknometer method at 17°C, one finds that the unit cell contains four formula units of $[Co\ en_3]Cl_3 \cdot 3H_2O$. Laue symmetry was found to be D_{3d}-$3m$. The systematic absences are: ($000l$) present only with l=even, and ($h0\bar{h}l$) present only with l=even. Hence the space group is either C_{3v}^3-$P3c1$ or D_{3d}^1-$P\bar{3}c1$. No piezoelectric effect was observed*, so that the space group is probably D_{4h}^1-$P\bar{3}c1$. This space group has 12-fold general positions; accordingly the four cobalt atoms have to be placed in some special positions**.

Usual multiple film technique was used and the intensities of reflections were obtained visually by comparison with a calibrated standard. The usual correction factors were applied by means of the chart given by Cochran[5]. No correction for absorption was made. Observed structure amplitudes were later placed on an absolute scale by comparison with the calculated values.

Determination of the Structure

At the outset of the analysis it was found that reflections ($hki0$) are generally rather strong when $h-k=3n$ and, moreover, odd-layer lines of oscillation photographs about the c-crystal axis are weaker than even-layer lines. These characteristics of reflections, combined with the results of Patterson projections $P(U, V)$ and $P(U, W)$, suggested that the cobalt atoms are on the 4-fold special positions; 4 d, 1/3, 2/3, z, etc. with $z\fallingdotseq1/8$.

All the large peaks in $P(U, V)$ except those due to Co–Co interatomic vectors were mainly interpreted in terms of Co–Cl and Co–N vectors. The Co–N peaks were readily identified, if an approximate octahedral coordination of six nitrogen atoms of ethylenediamine molecules was assumed. First an electron-density projection $\rho(X, Y)$ was prepared using all the observed $F(hki0)$ values, whose signs were calculated from the arrangement of Co, Cl and N atoms only. The resulting distribution showed heavy cobalt and

TABLE I

FRACTIONAL ATOMIC COORDINATES

atom	x	y	z
Co	1/3	2/3	0.125
Cl	0.097	0.493	0.372
O	0.087	0.225	0.873
C_1	0.180	0.397	0.077
C_2	0.215	0.397	0.173
N_1	0.192	0.525	0.050
N_2	0.333	0.525	0.200

1) T. Watanabé and M. Atoji, *Kagaku*, **21**, 301 (1951).
2) J. Ter Berg, *Diss. Univ. Groningen*, (1937).
3) S.M. Jörgensen, *J. pr. Ch.*, **2**, 39, 546 (1898).
4) F.M. Jaeger, *Z. Krist.*, **38**, 546 (1904).
* We are grateful to Mr. Y. Iidaka of the Mineralogical Institute, University of Tokyo, for piezoelectric test of the crystals.

** The unit cell, space group and the assignment of the positions of the cobalt atoms are in agreement with the results obtained by Ter Berg.
5) W. Cochran, *J. Sci. Instruments*, **25**, 253 (1949).

chlorine atoms clearly resolved, together with faint outlines of the remaining atoms. Successive refinements with $(Fo-Fc)$ syntheses[6] led to the final projection shown in Fig. 1, which can be interpreted with the aid of Fig. 2. From this electron-density map x- and y-parameters of all the atoms were fixed. The z-parameters of each atom were deduced from $P(U, W)$, taking of complex ions and Cl^- ions into consideration. Successive Fourier syntheses, $\rho(X, Z)$ were carried out and the final electron-density map is shown

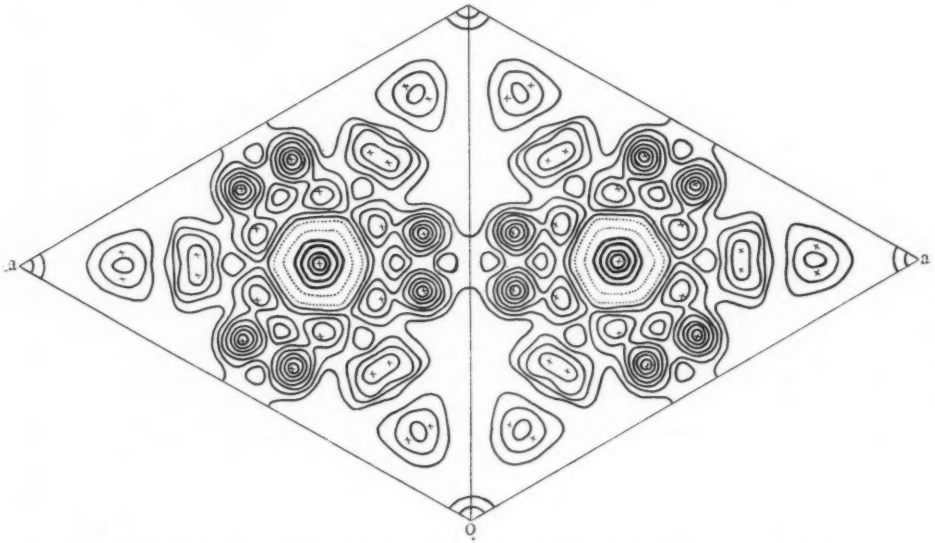

Fig. 1. Electron-density map of $[Co\ en_3]Cl_3 \cdot 3H_2O$ projected on (0001) (Contours are drawn at intervals of 4 e. Å^{-2}, the zero contour line being broken. The heavy lines of the Co peak are drawn at intervals of 20 e. Å^{-2}).

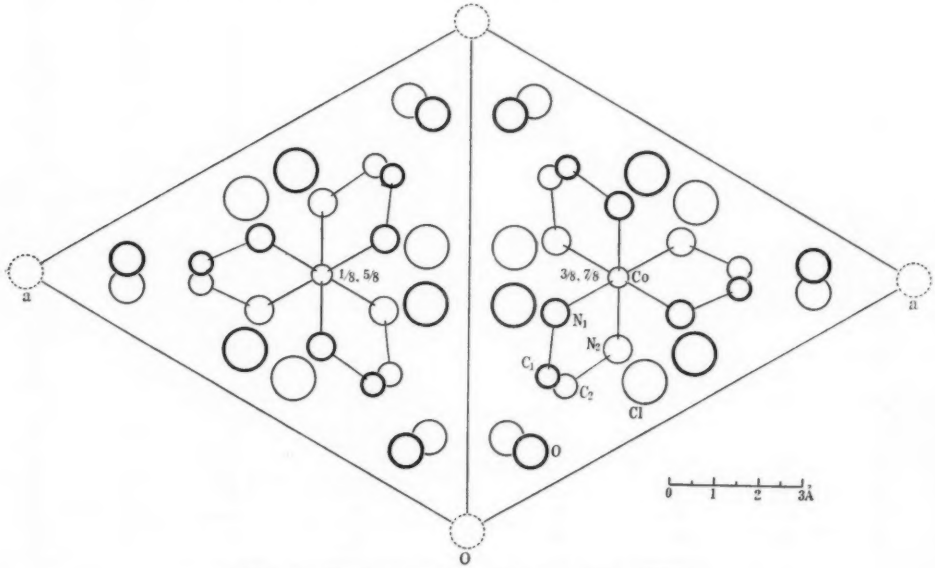

Fig. 2. Projection of the structure upon (0001).

6) W. Cochran, *Acta Cryst.*, **4**, 408 (1951).

TABLE II

OBSERVED AND CALCULATED STRUCTURE AMPLITUDES

*h*0.0	*Fo*	*Fc*	10.*l*	*Fo*	*Fc*	40.*l*	*Fo*	*Fc*
1	134	−134	2	104	−104	6	41	−44
2	11	−26	4	55	35	8	44	−50
3	51	−55	6	62	−57	10	34	32
4	69	−71	8	—	−8	12	22	25
5	44	−33	10	24	11	14	1	−13
6	66	58	12	40	28	50.*l*		
7	84	−93	14	12	14	2	43	32
8	12	1	2	97	102	4	59	49
9	15	20	4	60	45	6	26	−21
10	40	42	6	70	54	8	60	−68
			8	—	−19	10	6	20
*h*1.0			10	17	−6	12	54	52
1	84	95	12	46	40	2	35	−29
2	17	−28	14	25	−19	4	51	46
3	—	−13				6	24	14
4	91	94	20.*l*			8	60	−68
5	18	−23	2	39	74	10	9	−12
6	35	−34	4	13	−16	12	61	50
7	85	74	6	82	−77	61.*l*		
8	30	−26	8	45	34	2	—	−15
9	31	−38	10	71	72	4	13	−6
			12	25	−20	6	23	1
*h*2.0			14	32	−35	8	—	−4
2	72	62	2	80	−53	12	—	7
3	20	−20	4	8	−13	14	18	−24
4	56	−52	6	92	85	2	—	17
5	48	33	8	52	30	4	17	−5
6	32	−28	10	82	−85	6	18	−6
7	19	−21	12	20	−16	8	—	−5
8	50	51	14	33	47	10	1	−1
9	—	−11				12	16	−24
			30.*l*			70.*l*		
*h*3.0			2	177	178	2	129	−125
3	105	110	4	25	−14	4	48	52
4	50	47	6	66	−92	6	54	51
5	49	−53	8	48	42	8	29	−27
6	71	51	10	42	44	10	50	−38
7	54	−41	12	—	−20	2	124	127
8	14	−4	14	29	−34	4	42	44
			2	174	−172	6	41	−57
*h*5.0			4	20	2	8	21	−16
4	—	−22	6	72	82	10	35	45
5	10	−8	8	54	21	80.*l*		
6	13	−20	10	46	−34	2	46	62
7	27	30	12	—	−7	4	16	−20
			14	23	25	6	8	−8
*h*5.0						8	19	25
5	19	15	40.*l*			2	46	−64
6	—	2	2	27	6	4	16	−19
			4	84	64	6	—	15
00.*l*			6	40	38	8	17	24
2	—	−11	8	32	−45	90.*l*		
4	315	−313	10	41	−25	2	15	22
6	—	18	12	22	21	4	19	−9
8	84	103	14	1	8	6	11	29
10	19	−19	2	17	−4	2	12	22
12	109	−121	4	74	68	4	15	13
14	25	15				6	11	−25
						100.*l*		
						2	19	−22
						2	15	19

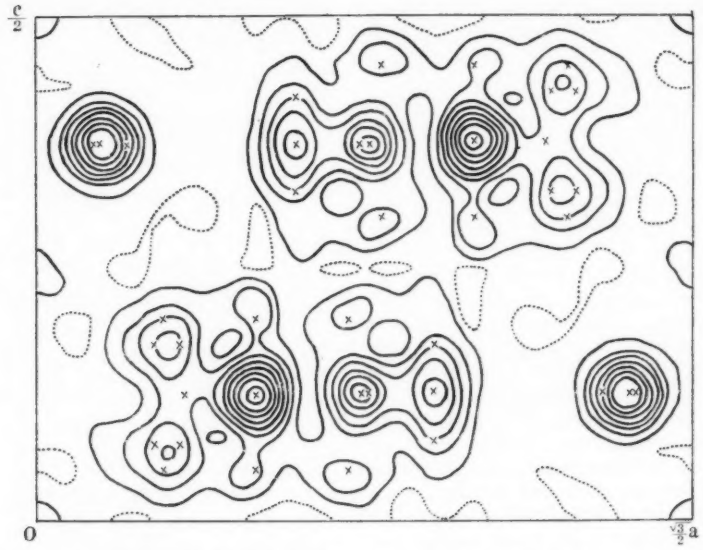

Fig. 3. Electron-density map projected on a plane perpendicular to the *a*-axis (Contours are drawn in the same manner as Fig. 1.

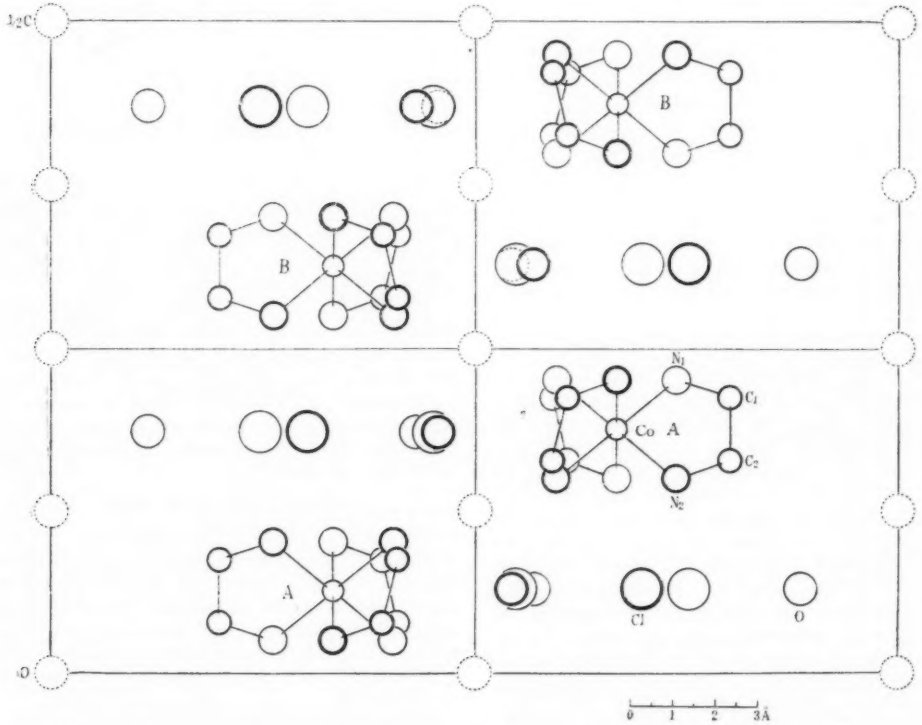

Fig. 4. Projection of the structure upon a plane perpendicular to the *a*-axis (The figure represents an elevation of the structure shown in Fig. 2, and does not correspond to $\rho(X, Z)$ in Fig.3.)

in Fig. 3. Since the resolution of the atoms on $\rho(X, Z)$ was not very good, the z-parameters deduced from $\rho(X, Z)$ were further refined by the method of least squares. The final set of coordinates thus obtained is shown in Table I, and the observed and calculated structure amplitudes are given in Table II. The atomic scattering factors used for the calculation of the structure factors were those listed in the International Tables. Temperature corrections of the form exp $-B(\sin\theta/\lambda)^2$ were used, where B was given the value 2.5 Å^2 for ($hki0$) zone and 3.0 Å^2 for ($h0hl$) zone respectively. The values of B and the scale factor were estimated by plotting the values of log Fc/Fo versus $(\sin\theta)^2$ at the final stage. The discrepancy factors $R = \sum| |Fo|-|Fc| |/\sum|Fo|$, are 0.140 for ($hki0$) reflections and 0.202 for ($h0\bar{h}l$) reflections respectively, with a weighted mean value of 0.186, where all the observed reflections up to $\sin\theta=0.98$ are included. The calculated interatomic distances and bond angles are recorded in Table III.

TABLE III

CALCULATED INTERATOMIC DISTANCES AND BOND ANGLES

$Co-N_1$	2.00 Å	$Cl\cdots N_1$	3.13 Å
N_2	2.00		3.26
N_1-C_1	1.47	$Cl\cdots N_2$	3.18
C_1-C_2	1.51		3.41
C_2-N_2	1.47	$Cl\cdots O$	3.34
		$Cl\cdots C_1$	3.30
$Co-N_1-C_1$	105.4°	C_2	3.67
$N_1-C_1-C_2$	112.6°	$O\cdots C_1$	3.36
$N_2-C_2-C_1$	112.6°	C_2	3.12
$Co-N_2-C_2$	105.4°		

Description of the Structure

The final electron-density map shown in Fig. 3 gives the arrangement of atoms shown in Fig. 4, which represents an elevation of the structure in Fig. 2. The shape and size of a complex ion $[Co\ en_3]^{3+}$ as it exists in the crystal is illustrated in Fig. 5. This figure shows one of the two stereo-isomeric ions, which are present in equal numbers in the structure. The complex ion is required by the space group to have trigonal symmetry. However, within the errors of experiment it possesses the symmetry D_3–32. Six nitrogen atoms of three ethylenediamine molecules form a slightly distorted octahedron around the central cobalt atom. The five-membered ethylenediamine cobalt rings are not planar, that is, the ethylenediamine ligands take so-called "gauche" forms. Arrangement of atoms about C_1-C_2 bond is illustrated in Fig. 6.

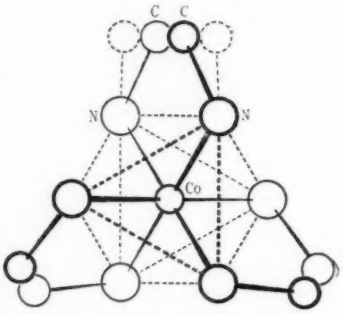

Fig. 5. The complex ion $[Co\ en_3]^{3+}$.

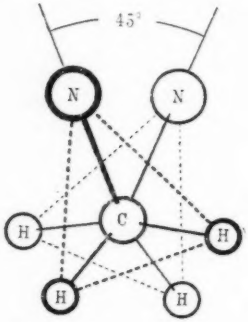

Fig. 6. Arrangement of atoms around C_1-C_2 bond.

The Co–N distances of 2.00 Å as well as the shape and size of the ethylene diamine molecules may be compared with those perviously described by Nakahara and two of us[7] for the complex ion $[Co\ en_2Cl_2]^+$.

The gauche configuration of ethylenediamine has a mirror image non-superposable, which we shall denote as d and l. Then ethylenediamine molecules may enter into combination with a cobalt atom in its d- or l-form. The possibilities of isomerism are, therefore, greatly increased and the following cases should arise:[8,9]

Dddd, Dddl, Ddll, Dlll,
Llll, Llld, Lldd, Ldddd,

where D or L indicates the configuration of the whole complex ion, i.e. the way in which the three ligands coordinate to a central cobalt atom. Nevertheless, our X-ray evidence showed that the complex ion possesses trigonal symmetry. Thus the representation for the

7) A. Nakahara, Y. Saito and H. Kuroya, This Bulletin, 25, 331 (1952).
8) M. Kobayashi, *J. Chem. Soc. Japan*, 64, 652 (1943).
9) J. V. Quagliano and S. Mizushima, *J. Am. Chem. Soc.*, 75, 6084 (1953).

complex ion in the crystal should be one of the following sets: (*Dddd, Llll*) and (*Dlll, Lddd*). The projections of the carbon atoms in Fig. 4 will change as indicated by dotted circles, if the other antipode of the ethylenediamine ligands coodinates to the central cobalt atom, keeping the configuration of the whole complex ion as before. However, final electron-density projection $\rho(X, Y)$ excludes this latter possibility, so that only one definite configuration is possible for each stereoisomeric complex ion in the crystal. By no means, should the presence of various stereoisomers in solution be excluded by our *X*-ray evidence. At this stage, however, it is impossible to decide whether the complex ion illustrated in Fig. 4 corresponds to dextro or laevo rotatory. Recently the determination of the absolute configuration of this complex ion has been carried out in our laboratory and a brief account has been published already[10].

The way in which the complex ions form bonds in the structure is best described by referring to Figs. 1 and 4. A complex ion is surrounded by nine Cl ions. Six of them are at the apices of a distorted trigonal prism, being 3.18 Å and 3.26 Å apart form N atoms. The other three form an equilateral triangle, being nearly on the same level as a cobalt atom. These N···Cl distances are 3.13 Å and 3.41 Å. The former distance of 3.13 Å suggests a hydrogen bond of the type N–H···Cl between N_1 and Cl. All these N···Cl distances are in good agreement with those reported by various authors[11,12,13,14,15]. Fig. 4 also indicates the packing of the formula units in the structure. Starting with any complex ion denoted by A, another complex ion denoted by B follows by the operation of the glide plane "*c*" or center of symmetry.

Remarks on the Water of Crystallization

Together with Cl^- ions the complex ions form structure with hollow channels along the *c*-crystal axis, in which water molecules are enclosed. They are on a set of general positions 12 *g*. A water molecule is associated to Cl^- ions with a distance of 3.34 Å. Other environmets of an oxygen atom are as follows: O···C_1=3.36 Å, O···C_2=3.12 Å, O···O=3.90 Å, 4.19 Å and 4.54 Å.

It seems to be an unlikely occurrance that water molecules are held together with such long O···O distances in the hollow channel. On the other hand, it was found that small peaks on electron-density maps, corresponding to the sets of 2-fold positions 2 *a* (000); (00$\frac{1}{2}$) and 2 *b* (00$\frac{1}{4}$); (00$\frac{3}{4}$), could by no means be eliminated even at the final stage of refinement. These positions are indicated by dotted circles in Figs. 2 and 4. This fact led us to assume that water molecules are randomly distributed on these positions as well as the above-mentioned general positions. Such a random arrangement of water molecules gives rise to a sequence of oxygen atoms with reasonable distances of 2.96 Å and 3.00 Å in the channel. Calculation of the structure amplitudes based on this model gave a lower value of *R* by about 0.02. From this fact only, one cannot decide whether such random distribution of water molecules is realized or not in the crystal.

It is to be noted here that water content of the crystal varies appreciably according to its history. Careful measurements of the density and analyses of the water of crystallization revealed that the crystal contains about 3.5 mol. of water of crystallization, when freshly prepared, and it gradually loses part of its water of crystallization on standing in the air, and the chemical formula tends to [Co en_3] $Cl_3 \cdot 3H_2O$. These excessive water molecules may be randomly distributed on the sets of special positions 2 *a* and 2 *b*. It was observed that a single crystal can be completely dehydrated by gently heating at 120°C, without bringing about any remarkable change in its appearance except a loss of transparency. A single crystal oscillation photograph was obtained even after complete dehydration, and furthermore, practically no change was found in its cell dimensions. These observations seem to support such a weak bonding of water molecules in the crystal. Further studies on the behaviour of this water of crystallization, including thermal analysis, are now going on. The results will be published soon.

Summary

The crystal structure of [Co en_3]$Cl_3 \cdot 3H_2O$ has been determined by *X*-ray methods. It is trigonal D_{3d}^4–$P\bar{3}c1$ with four formula units in a cell of dimensions: a=11.50±0.02, c=15.52±0.04 Å. The configuration of the two stereoisomeric complex ions $[Co\ en_3]^{3+}$ is described. The three ethylenediamine molecules in a complex ion assume "gauche" forms; their nitrogen atoms form a slightly distorted

10) Y. Saito, K. Nakatsu, M. Shiro and H. Kuroya, *Acta Cryst.*, 8, 729 (1955).
11) W.P. Binnie and J.M. Robertson, *Acta Cryst.*, 2, 180 (1949).
12) J.M. Bloomhead, *Acta Cryst.*, 1, 324 (1948).
13) W. Cochran, *Acta Cryst.*, 4, 81 (1951).
14) D.C. Phillips, *Acta Cryst.*, 7, 159 (1954).
15) J. Trommel and J.M. Bijvoet, *Acta Cryst.*, 7, 703 (1954).

octahedron around a central cobalt atom. It is shown that ionic bonds essentially link the complex ions in the structure. The water molecules are weakly associated to chlorine ions. It is found that a single crystal can be completely dehydrated by gently heating at 120°C, without bringing about any remarkable change in its appearance, except a loss of transparency. A single crystal oscillation photograph was obtained even after complete dehydration.

The authors wish to thank Professors I. Nitta, T. Watanabé and R. Tsuchida of the Osaka University for their kind advice and encouragement throughout this work. This research was aided by a fund from the Scientific Research Expenditure of the Ministry of Education to which the authors' thanks are due.

Institute of Polytechnics, Osaka City University, Osaka

Infrared Spectra of Charoninsulfuric Acid, Chondroitinsulfuric Acid, and Some Related Polysaccharides

By Koji NAKANISHI, Noriko TAKAHASHI and Fujio EGAMI

(Received January 1, 1956)

As reported in a recent publication[1], charoninsulfuric acid isolated from the mucus of *Charonia lampas*, has been fractionated into F-1, F-3, F-A, and F-B, and the respective fractions identified as shown in Chart 1; it was also shown that the anomeric cellulose and amylose structures were not contained merely as mixtures, but that they constituted a compound charonin, which was decomposed by the action of Schweitzer's reagent.

Chart 1. Fractionation of charoninsulfuric acid.

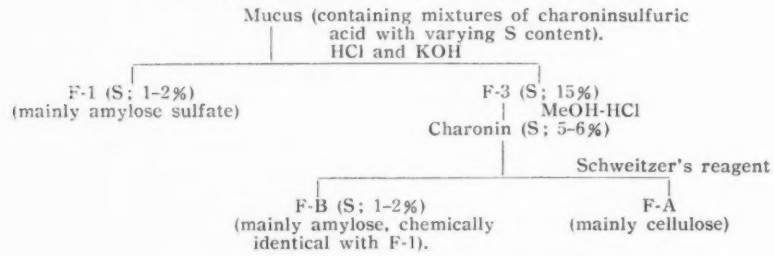

Barker, et al.[2,3] have analysed the complicated infrared spectra of D-pyranoses and its derivatives (O-methyl, O-acetyl) in the 730–960 cm^{-1} region, and have shown that the method renders possible the assignment of the derivatives to either the α- or the β-series, no matter whether they are reducing sugars, acetates, or polysaccharides; α-anomers absorb at 844±8 and β-anomers at 891 ±7 cm^{-1} (type 2a and 2b band). The method has been applied to the present series of fractions from *Charonia lampas* and extended to several related sulfates. The data fully substantiate the chemical findings; in addition, an assumption, though tentative, as regards the distribution of sulfate groups in the glucose units is forwarded. The results are summarised in Table I. The spectrum of chondroitinsulfuric acid from shark cartilage has also been measured and has been shown to be identical with "chondroitinsulfuric acid B" obtained from bovine nuclei pulpose[4].

Experimental

Materials.—The various fractions of charoninsulfuric acid are those reported in a previous communication[1]. The other materials were obtained as follows.

1) F. Egami, T. Asahi, N. Takahashi, S. Suzuki, S. Shikata and K. Nisizawa, This Bulletin, 28, 685 (1955).
2) S.A. Barker, E.J. Bourne, M. Stacey and D.H. Whiffen, *J. Chem. Soc.*, **1954**, 171.
3) S.A. Barker, E.J. Bourne, R. Stephens and D.H. Whiffen, ibid., **1954**, 3468.
4) S. F. D. Orr, *Biochim. Biophys. Acta*, **14**, 173 (1954).

Cellulose: Whatman, ashless powder for chromatography.

Amylose: Potato amylose prepared through Schoch's butanol precipitation method. An aqueous solution of the precipitate was filtered through a glass filter and dried-frozen.

Dextran: From *Leuconostoc mesenteroides*.

Cellulose sulfate (Na): Prepared from filter paper.

Potato starch sulfate (Na), and Dextran sulfate (Na): Prepared according to conventional methods.

Chondroitinsulfuric acid: Prepared from shark cartilage and freed from protein by kaolin adsorption and by Sevag's chloroform-gel method. $[\alpha]_D^{11°}$ of Na-salt, $-15.4°$.

Infrared Spectra.—These were measured with a Hilger H 800 spectrometer, sodium chloride optics, by the Nujol mull method. The wavelength was callibrated against a polystyrene film. The sulfates easily gave satisfactory mulls, but for the free polysaccharides thorough grinding in ether and subsequent drying was necessary. Absorptions arising from Nujol are marked with small circles in Figs. 1–5.

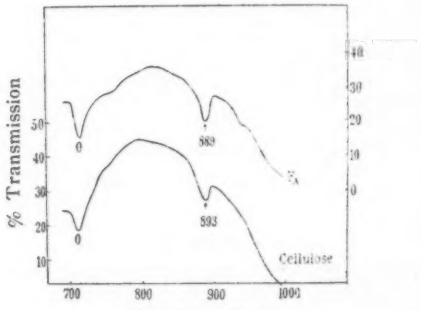

Fig. 1. F-A and cellulose.

TABLE I

INFRARED ABSORPTION OF SOME POLYSACCHARIDES

Compounds		Principal type of glycosidic linkage	Type 1[2] (ring vibr.)	Type 2[2] (C-H Deform.) 2a	Type 2[2] (C-H Deform.) 2b	Type 3[2] (ring-breathing)	Sulfate[4]	Others
α-D-Glucopyranose			912 s	835 s		765 s		
Cellobiose		β 1 : 4			896, 889 s			835, 738 m***
Dextran		α 1 : 6, α 1 : 4 branches	912 s	848 m		758 m		
Fig. 1	Cellulose	β 1 : 4	**		893 m	**		
	F-A	β 1 : 4			899 m			
Fig. 2	Amylose	α 1 : 4	932 m	860, 846 m	893* vw	758 m		
	F-1	α 1 : 4	931 m	856, 847 m	888 vw	759 m	803 w	
	F-B	α 1 : 4	929 m	854, 841 m	896 vw	755 m	802 w	781 w
Fig. 3	Charonin (F_3)	Compd. of F-A & F-B	935, 919 m**	855 w	900 w	769 m	812 m	
Sulfate of Dextran (Na-salt)		α 1 : 6, α 1 : 4 branches	939 w	845 w		740 m	809, 826 w	
Fig. 4	Cellulose (Na-salt)	β 1 : 4	937 m		895 vw	767 m, 731 vw	800, 815 w	
	Potato starch (Na-salt)	α 1 : 4, α 1 : 6 branches	937 m			740 vw	823 m br	
	F-3 (K-salt)	Compd. of F-A & F-B	935 m		887 vw	760, 730 vw	806 m br	

Remark: Abbreviations, s (strong), m (medium), w (weak), vw (very weak), br (broad).

* Since the possibility that this small but evident band which is not seen in the spectrum given by Barker, et al.[2] could have arisen from contaminating cellulose (filter paper), glass filters were used throughout the purification procedure. However, the 893 cm^{-1} band became even more evident with the disolved, filtered, and dried-frozen samples. Hence, this 893 cm^{-1} band seems to be inherent to amylose, rather than being due to an impurity.

** Barker, et al.[2] give 914 w br, 933 w br (type 1), 894 w (type 2b), 766 vw (type 3) for cellulose, and the bands of charonin (935, 919) may corespond to the first set of bands, which, however, was not observed by us.

*** Also observed in Sadtler's curve (# 1020).

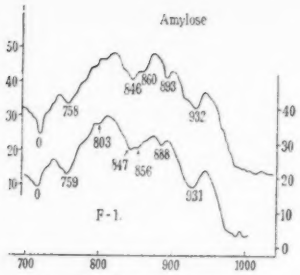

Fig. 2. F-1 and amylose.

Discussion

Charoninsulfuric Acid.—The closes similarity of the absorptions displayed by cellulose and F-A (Fig. 1), and by amylose, F-1, and F-B (Fig. 2; F-B not shown in figure), provide convincing evidence of the results obtained chemically. Since F-1 is presumed as being a slightly sulfated compound of amylose and cellulose, in which the former is predominant, the weak type 2b band (β-anomers) at 888 cm^{-1} and sulfate band[4] at 803 cm^{-1} is not unexpected. F-B shows no difference with F-1 in its chemical behavior[1] and this is also supported from infrared data; the presence of minor cellulose* (type 2b band at 896 cm^{-1}) and sulfate structures (band at 802 cm^{-1}) may be explained by the incomplete desulfation and decomposition by HCl-MeOH and Schweitzer's reagent, respectively. The curve of

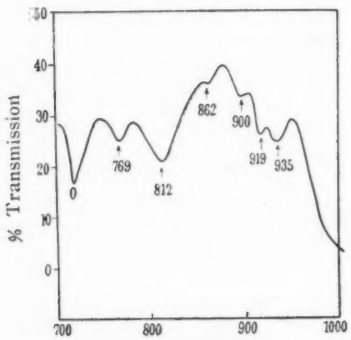

Fig. 3. Charonin.

charonin (Fig. 3) may not precisely be compared with the composite of F-A and F-B owing to the still relatively high sulfur content (5–6%; also evidenced by distinct sulfate band at 812 cm^{-1}); however, as might be expected, both type 2a and 2b bands may be observed. At present, differentiation between a compound and a mere mixture is probably not possible in this case, owing to the high molecular weight of the two constituents; chemical evidences point to a compound formation[1].

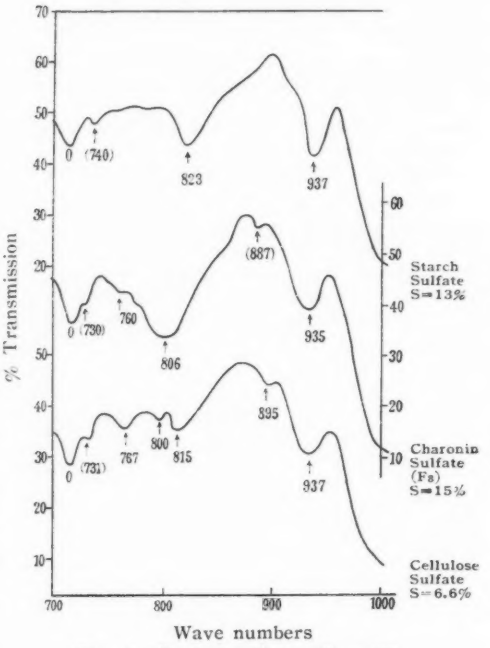

Fig. 4. Typical sulfates (Na-salt).

The spectra of the sulfates may be summarised as follows. Type 1 band appeared at 937–939 cm^{-1} with no difference between α- and β-series. Type 2 bands were generally weak or overlaid by the stronger nearby sulfate absorption at 810 cm^{-1} and though the results of Barker, et al. seem to be equally applicable for diagnosing anomeric polysaccharide sulfates, more data are necessary. As noted by Barker, et al.[3] the bathochromic shift of type 3 bands acompanying conversion of glucose to its tetra- or penta-acetate, i. e., 770→740 cm^{-1}, may be satisfactorily correlated with its assignment to a ring breathing frequency of the tetrahydropyran nuclei, the extra weight of the substituents being responsible for the shift (for tetrahydropyran, the corresponding band is at 813 cm^{-1},[8]). It may be seen (Fig. 4 and Table I) that two sets of bands, i) 765 cm^{-1} ii) 735 cm^{-1},[8]), falling in the range of type 3 bands are present in the polysaccharide sulfates, and it may also be noted that cellulose sulfate having the

* cf. Foot note *) of Table I.

8) S.C. Burket and R.M. Badger, *J. Am. Chem. Soc.*, 72, 4397 (1950).

lowest sulfur content, shows the strongest relative intensity of the 3-i band. It would be tempting to assign 3-i and 3-ii bands to the ring breathing frequencies of the unsulfated and heavily sulfated glucose residues, respectively. And from this, the assumption that the sulfate groups have a tendency to be crowed into certain glucose units rather than to be evenly distributed may be made. However, the assumption is based on a very limited amount of data, and furteer work in this line is certainly necessary to test its validity.

Chondroitinsulfuric Acid.—Orr[4] has been able to characterize two isomers of chondroitinsulfuric acid, designated A and B, from the infrared absorption and has discussed the hexuronic acid to hexosamine ratio and the stereochemistry of the sulfate groups (i. e., axial or equatorial). The B isomer has been found alone in samples from bovine nuclei pulposi, but both isomers have been found together in samples from bovine articular cartilage and trachea. The spectrum of Fig. 5 the present sample from shark cartilage

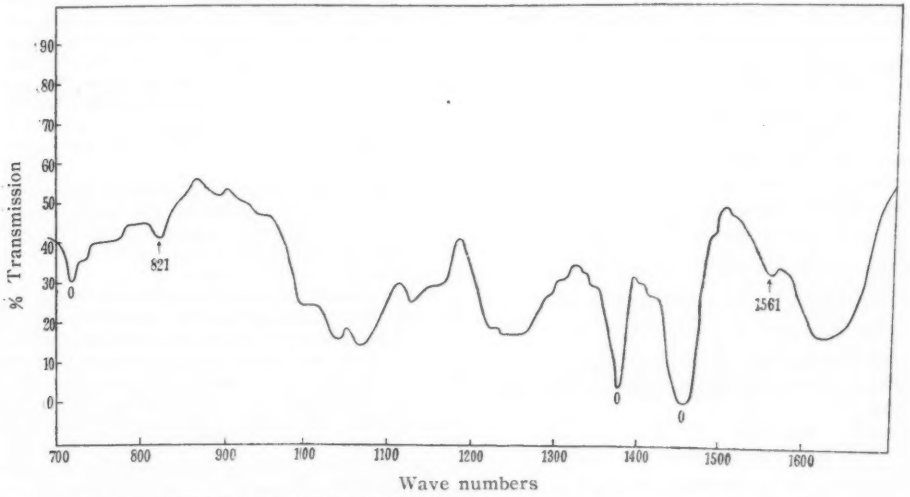

Fig. 5. Chondroitinsulfuric acid-Na (Nujol).
~1615 (carboxylate and amide I band, 1561 (amide II band), ~1240 (sulfate), ~1050 (O-H and C-O-C), 821 cm^{-1} (sulfate)

shown in Fig. 5 is identical with the B isomer and not with the A ismer. Hence, if the conclusions brought forth by Orr be accepted, the same apply to the present sample. Namely, the ratio of hexuronic acid residue to hexosamine residue is 25% less than that in hyaluronic acid, and the sulfate groups are attached to equatorial hydroxyl groups. Orr's conculusions were based on i) assigning a 820 cm^{-1} band observed in sulfates to "vibrational modes involving stretching within the C-O-S system" similar to the 1240 cm^{-1} acetate band, and ii) extending the stereochemical correlation between the acetate band and its conformation (splitting of 1240 cm^{-1} acetate band occurs in axial acetates[5]) to the sulfate band of polysaccharides. Assignment of the band at 820 cm^{-1} seems to warrant further investigation, especially since the frequency remains unaltered when passing from the free form to the salt form of polysulfated hyaluronic acid. In this connection, it may be mentioned that the 1250 cm^{-1} band in trichloroacetic acid assigned to a C-O stretching vibration (coupled with the OH bending vibration) is shifted to 1350 cm^{-1} upon conversion into the salt[6]. In addition, notwithstanding several known instances of the splitting of the C-O stretching frequency[7], in which the phenomena were correlated with stereochemistry after the conformations had been established via chemical methods, the origin of this splitting is still not clarified. Accordingly, it appears that the interesting deductions of Orr should be accepted with some reserve.

5) R.N. Jones, P. Humphries, F. Herling and K. Dopriner, *J. Am. Chem. Soc.*, **73**, 3215 (1951). A.R.H. Cole, R.N. Jones and K. Dobriner, ibid., **74**, 5571 (1952).
6) K. Kuratani, *J. Chem. Soc. Japan*, **73**, 758 (1952).
7) A.R.H. Cole, *J. Chem. Soc.*, **1952**, 4969. W.G. Dauben and N.K. Freeman, *J. Am. Chem. Soc.*, **74**, 5206 (1952). A. Stoll, Th. Petrzilka, J. Rutschmann, A. Hofmann and Hs. H. Günthard, *Helv.*, **37**, 2039 (1954). J.R. Lewis and C.W.S. Shoppee, *J. Chem. Soc.*, **1955**, 1375. C. R. Eddy, M. Barnes and F.S. Fenske, *Anal. Chem.*, **27**, 1067 (1955).

Summary

The infrared spectra of charoninsulfuric acid and related carbohydrates have been measured and the results support previous chemical evidences. The work has been extended to a few polysaccharide sulfates, and a tentative assumption as to the distribution of the sulfate groups within the polysaccharide chain is presented.

Chondroitinsulfuric acid from shark cartilage has been shown to be identical with the chondroitinsulfuric acid from bovine nuclei pulposi; a comment on the 820 cm^{-1} sulfate band is made.

Chemical Institute, Faculty of Science
Nagoya University, Nagaya

SHORT COMMUNICATION

Synthesis of Ethylenediamine labeled with Carbon-14

By Kunihiko KIGOSHI and Shizuko OKAMOTO

(Received December 15, 1955)

Studies on the isotopic exchange of ethylenediamine with ethylenediamine complex have been initiated in this laboratory. In these studies, the synthesis of ethylenediamine labeled with isotopic carbon is required. Since radiocarbon is available in the form of barium carbonate, it is necessary to examine the procedures of preparation of ethylenediamine starting with the carbonate. The procedure which is employed in this laboratory is based on the following scheme.

$$Ba\overset{*}{C}O_3 \rightarrow K\overset{*}{C}N \rightarrow CH_2\overset{*}{C}N \rightarrow CH_3\overset{*}{C}H_2NH_2 \rightarrow$$
$$CH_3\overset{*}{C}H_2OH \rightarrow CH_2\overset{*}{C}H_2 \rightarrow CH_2BrC\overset{*}{H}_2\,Br \rightarrow$$
$$NH_2CH_2\overset{*}{C}H_2NH_2$$

By these steps the overall yield was about 20% of the theoretical value, based on barium carbonate.

Experimental

The methods of preparation of alkali cyanide from radioactive barium carbonate have been described by a number of authors; among those we adopted the method proposed by O. Simamura et al.[1] by which these authors obtained the highest yield up to 100%. Also, in our experiments the yield of the cyanide above 90% of the theory was confirmed. Radioactive silver cyanide was precipitated by adding the calculated amount of silver nitrate to the alkali cyanide solution which was obtained by the distillation of crude potassium cyanide in sufuric acid solution as usual.

About 200 mg. of radioactive silver cyanide was dissolved in a solution of 7.8 g. of inactive sodium cyanide in 12 ml. water. The solution was shaken at room temperature with 25 g. of methyl iodide in order to prepare acetonitrile. After about twenty to thirty hours' shaking the solution became homogeneous, and then the solution was slowly distilled, of which a fraction of 76–100°C was collected as crude acetonitrile. Hydrogenation was carried out at room temperature and atmospheric pressure with 50 ml. solution containing crude acetonitrile and 8 g. of Raney's nickel. The process adopted here to obtain ethylamine from sodium cyanide is similar to that performed by Kilmer and duVigneaud[2]. The filtered solution containing ethylamine was acidified and the yield of ethylamine was estimated by titrating with acid. Ethyl alcohol was obtained by the action of the calculated amount of sodium nitrite on the acid solution.

The dilute ethyl alcohol obtained by distillation of this solution was redistilled with calcium oxide by which ethyl alcohol was concentrated 80–90%. The yield of ethyl alcohol from sodium cyanide was about 60% of the theory.

The procedure of catalytic dehydration of ethyl alcohol consists in passing the vaporized alcohol through a tube which is packed with granules of alumina and maintained at the temperature of 360°C in an electric furnace. The reaction products were condensed in a trap cooled with liquid oxygen, and the whole system was evacuated to a few mmHg. After the dehydration process the trap containing ethylene was connected to a bromination apparatus. The bromination and the purification of the resulting ethylene dibromide were carried out in the usual way. The preparation of ethylenediamine from ethylene dibromide was made by the action of ammonia in a sealed tube. Five grams of the ethylene dibromide and 40 g. of concentrated ammonia (containing 35% NH_3 in weight) was sealed in the glass tube. By shaking the tube at the temperature of 50°C for seven hours the solution was made homogeneous, and then it was kept at the temperature of 50°C for twenty hours. The content of the tube was evaporated to dryness and distilled with alkali as usual to obtain ethylenediamine hydrate. Because of the scarcity

of the product, we cannot make an accurate measurement on the physical properties of the ethylenediamine monohydrate. However the obtained product was roughly identified by chlorine analysis on nhe ethylenediamine hydrochloride precipitated from the alcoholic solution.

Anal. Found: Cl, 54. Calcd. for $NH_2CH_2CH_2NH_2 \cdot 2HCl$: Cl, 53.4%.

The purity of the product was also certified by cation exchange resin, using 0.1 f. caustic soda eluant. The elution curve taken from the activity of the product just correspounds to the curve for the ordinary reagent of ethylenediamine. The yield of ethylenediamine from ethyl alcohol was 30% of the theory.

Department of Physics and Chemistry
Gakushuin University, Mejiro
Tokyo

1) M. Hasegawa, N. Inamoto and O. Simamura, This Bulletin, 28, 445 (1955).
2) G.W. Kilmer and V. duVigneaud, *J. Biol. Chem.*, 154, 247 (1944).

N-Dialkylaniline as a Solvent of Polyvinyl Chloride

By Teiji TSURUTA and Junji FURUKAWA

(Received December 28, 1955)

It has been found that polyvinyl chloride (PVC) is soluble in N-dialkylaniline, but is practically insoluble in unsubstituted aniline. In this paper, some properties of the dialkylaniline solution of PVC are reported.

Materials.—Geon 101 ($\bar{P} \fallingdotseq 1400$) was washed with methanol and hot water and dried at 60°C in an air oven for twenty hours. N-Dimethylaniline was treated with acetic anhydride, distilled at reduced pressure; the distillate was washed with water, dried on anhydrous sodium sulfate and was distilled under nitrogen at reduced pressure. N-Diethylaniline was purified in a similar way. C.P. aniline and nitrobenzene were purified by distillation.

Solubility.—A mixture of PVC and 50 ml. of the aniline was heated at 95°C in a steam bath under a reflux condenser for four hours. The solution was filtered by sintered glass at 15°C. To 10 ml. of the filtrate, methanol (about 100 ml.) was added and powdery precipitates separated from the solution were collected, washed with methanol, dried at 60°C, and were weighed. The results are shown in Table I.

TABLE I

SOLUBILITY OF GEON 101 ($\bar{P} \fallingdotseq 1400$) IN THREE ANILINES AT 15°C

Solvent	Solubility (g./100 ml.)
Aniline	0.00
Dimethylaniline	2.25
Diethylaniline	0.68

Viscosity.—The viscosity of PVC in the N-alkylaniline and in nitrobenzene was measured by the Ostwald viscometer at 30°C. The results are shown in Fig. 1.

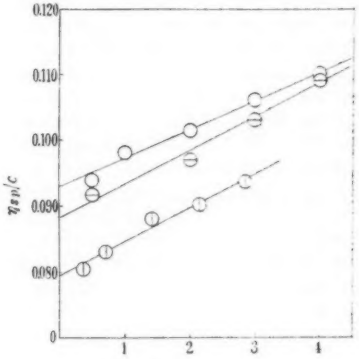

Fig. 1. Viscosity of polyvinyl chloride in three solvents: ○, in nitrobenzene; ⊖, in dimethylaniline; ◯, in diethylaniline.

From the table and the figure, it is seen that dimethylaniline is a better solvent for PVC than the other two anilines are. The property of the N-dimethyl derivative may be noted in connection with that of dimethylformamide as a unique solvent for polyacrylonitrile. The lack in the dissolving power in unsubstituted aniline seems to be partly interpreted in terms of the hydrogen bonding between aniline molecules themselves.

The authors are grateful to Dr. M.L. Huggins for advice and to the Japanese Geon Co. Ltd. for donating the sample.

Institute for Chemical Research
Kyoto University, Takatsuki
Osaka

A Theoretical Relation between Bond-order and Bond-length in Conjugated Systems using Morse-type Potential Function

By Toshinobu ANNO, Mitsuo ITO, Ryoichi SHIMADA, Akira SADÔ and Wataru MIZUSHIMA

(Received December 12, 1955)

It has been well known that there exists a definite relation between bond-order and bond-length in conjugated systems[1]. For C-C bonds Coulson[2] derived a theoretical formula explaining the relation between bond-lengths and bond-orders calculated by MO approximation. Anno and Sado[3] showed that a similar formula applies also to C-Cl bonds in conjugated systems. In deriving their formula, they used a method originally due to Lennard-Jones[4], who used Hooke-type stretching potential functions of bonds in reference molecules. For this reason, their formulae combined with the empirical values of parameters do not explain completely the order-length relationships for C-C and C-N bonds, where the bond-orders and bond-lengths change widely from molecule to molecule. One way of removing this difficulty may be to use the Morse-type function instead of the Hooke-type one. This idea was first suggested by Lennard-Jones[4] and used by Coulson[2] in qualitative explanation of the correction to the empirical parameters for fitting the theoretical order-length curve to an empirical one. However, the quantitative study of the theoretical order-length relationship using Morse-type function has not been undertaken.

In the present communication, a theoretical equation for order-length relation will be proposed taking this idea into account. The results for applications to C-C and C-N bonds will also be given.

The energy difference between pure single and triple bonds may be considered to be mainly due to π-electrons. Then the following equation holds:

$$4\beta = E_t^0 - E_s^0 + V_t(x-x_t) - V_s(x-x_s) \qquad (1)$$

where β is the resonance integral, and E_s^0 and E_t^0 denote the bond energy in pure single and triple bonds at their equilibrium values x_s and x_t, respectively. $V_s(x-x_s)$ and $V_t(x-x_t)$ are the potential energies of single and triple bonds when the internuclear distances are x. Instead of assuming the Hooke-type function, the following forms of the Morse-type function may be assumed:

$$\begin{aligned} V_s(x-x_s) &= D_s[1-\exp\{-a_s(x-x_s)\}]^2 \\ V_t(x-x_t) &= D_t[1-\exp\{-a_t(x-x_t)\}]^2 \end{aligned} \qquad (2)$$

where D is the bond strength and a is given by

$$a = \sqrt{\frac{k}{2D}}$$

in which k is the bond stretching force constant.

On the other hand, the total bond energy F which allows for the compression of the σ-bond is given by

$$F = V_s(x-x_s) + 2p\beta \qquad (3)$$

where p is the mobile bond-order. By a method similar to that used by Coulson[2], and using Eqs. (1), (2) and (3), it follows that

$$p = \frac{2}{1 - \frac{a_t D_t}{a_s D_s}\left[\frac{\exp\{-a_t(x-x_t)\} - \exp\{-2a_t(x-x_t)\}}{\exp\{-a_s(x-x_s)\} - \exp\{-2a_s(x-x_s)\}}\right]}. \qquad (4)$$

Taking reasonable values of constants, which will be discussed in subsequent articles, curves shown in Figs. 1 and 2 are obtained. Figs. 1 and 2 refer to C-C and C-N bonds, respectively. As can be seen in these figures

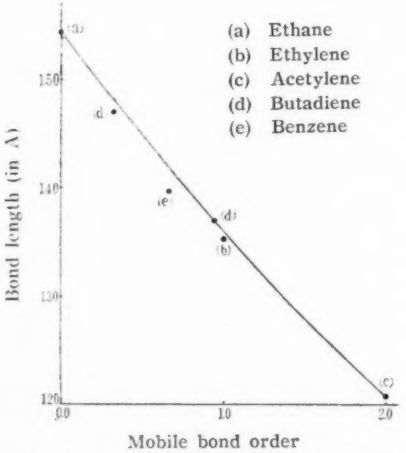

Fig. 1. The relation between bond-order and bond-length for C-C bonds

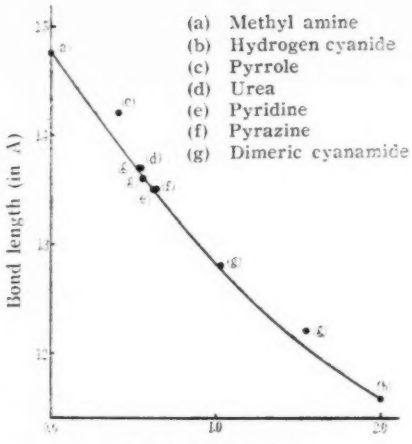

Fig. 2. The relation between bond-order and bond-length for C-N bonds.

the theoretical curves explain the empirical data in fair approximation.

The equation (4) can also be used to calculate the force canstants if it is combined with the considerations similar to those due to Coulson and Longuet-Higgins[5].

Full account of this communication will be published in the near future.

The authors express their hearty thanks to Professor S. Imanishi for his encouragement throughout this work and for reading this manuscript.

Department of Chemistry, Faculty of Science
Kyushu University, Fukuoka

1) See, for example, E.G. Cox and G.A. Jeffery, *Proc. Roy. Soc.* (London), **A 207**, 110 (1951).
2) C.A. Coulson, *Proc. Roy. Soc.* (London), **A 169**, 413 (1939).
3) T. Anno and A. Sado, This Bulletin, **28**, 350 (1955).
4) J. E. Lennard-Jones, *Proc. Roy. Soc.* (London), **A 158**, 280 (1937).
5) C.A. Coulson and H.C. Longuet-Higgins, *Proc. Roy. Soc.* (London), **A 193**, 456 (1948).